Alpha (α) – Crystallins as Protectors in Oxidative Stress and Photochemical Damage of the Retina

Thesis submitted to Cardiff University for the degree of Doctor of Philosophy

Melissa E. Trego

School of Optometry and Institute of Vision Science

Visual Neuroscience and Molecular Biology Division

Cardiff University

September 2008

ProQuest LLC
789 East Eisenhower Parkway
P.O. Box 1346
Ann Arbor, MI 48106-1346

DECLARATION

This work has not previously been accepted in substance for any degree and is not concurrently submitted in candidature for any degree.

Signed ..... (candidate) Date 10/6/09

STATEMENT 1

This thesis is being submitted in partial fulfillment of the requirements for the degree of PhD

Signed ..... (candidate) Date 10/6/09

STATEMENT 2

This thesis is the result of my own independent work/investigation, except where otherwise stated. Other sources are acknowledged by explicit references.

Signed ..... (candidate) Date 10/6/09

STATEMENT 3

I hereby give consent for my thesis, if accepted, to be available for photocopying and for inter-library loan, and for the title and summary to be made available to outside organisations.

Signed ..... (candidate) Date 10/6/09

Acknowledgements

I would first like to extend my thanks and appreciation to my supervisors Professor Mike Boulton and Dr. Mike Wride – the both of you have kept me balanced and focused, either in person or thousands of miles away. Additional thanks to my very savvy advisor, Jon Erichsen – your American Thanksgiving is still the best! Thank you all for your continued support and encouragement.

My thanks and appreciation to the Pennsylvania College of Optometry at Salus University, for their support and belief in my ability to complete this program. I would also like to thank Jim Wood for his animal expertise and advice, and Lydia Parke for her continued assistance and helping hand with research at PCO.

Dr. Alexander Dizhoor – your mind amazes me – thank you for all of your support, help and advice. I continue to be inspired by you. Dr. Elena Olshevskaya – your help and assistance was more than I could ask for – thank you! Thank you for your expertise, thank you for your patience and thank you for your friendship.

To Rhonda and Magdalena at Thomas Jefferson – your assistance and help with histological work was greatly appreciated.

To my colleagues and friends at the Eye Institute, Drs. Connie Chronister, Helene Kaiser, Gwenn Amos, Andy Gurwood, Jean Marie Pagani, Jeff and Neal Nyman, Kelly Malloy, Bernie Blaustein, Chris Reinhart and of course, Marilyn, Aliceann and Cathie – thank you for your support, advice, ears, and smiles! Your clinical expertise and mentorship has been invaluable to me – do not forget that ALL OF YOU make PCO what it is.

Thanks, gratitude and of course lots of love to Linda, Jen/Dave, Debs, Tina, Llinos, Matt, Miguel, Jack, Aihua, Yadan and Stuart. In August of 2004, I stepped onto UK soil as an ignorant, Eastender/Corontation Street lacking, malt vinegar virgin American and left with some of the best mates I have ever had. You all have made me feel welcomed, loved, supported and inspired. I am proud to call you my colleagues,

but more than that, I am proud to call you friends (Especially since you clarified that 'Delilah' was ***not*** the Welsh national anthem)!

Additional thanks and love to my family (Aurands', Kusins', Brosious', Bowns' and Patels') – for some reason, you still love me regardless of my adventures or insane ideas – thank you for loving me and supporting me.

Dr. Beth Schultz – my thanks and gratitude to you for your support, friendship and encouragement. May we one day share a workplace where hanging off of your office wall in a climbing harness is nothing unsual!

Dr. J Brûlé – WHOA! the times we have shared...thank you for keeping me sane and reminding me what matters the most....***good friends, a FANTASTIC bottle of Riesling, a mystery menu and lots of laughter*** – your friendship means so much – thank you for putting a smile on my face whenever Cher comes on the radio – I look forward to our adventures!

Raj – I love you – even though you steal underware and eat dirt, you will always be my boy!

And finally, I have saved the very best for last....thanks....thanks a million to Drs. Felix and Pierrette Barker. The both of you have been more than supervisors, you have been mentors, coaches, colleagues and parents to me – you believed in me when I could not even believe in myself. This whole process would not have been possible without the both of you – from the very bottom of my heart, thank you.

Dedicated to my grandparents, John and Eileen Aurand....love you!

Abstract

Alpha (α) – crystallins (αA- and αB-) once thought to be exclusive to the lens, have been discovered in the sensory retina and may act as molecular chaperones against cellular stresses. The premise of this work examined the potential protective role of α-crystallins in both the retinal pigment epithelium (RPE) and retina *in-vitro* and *in-vivo* respectively during oxidative stress or photochemical damage.

Initial *in-vitro* work compared growth characteristics of wild-type (WT) and αA-crystallin knock-out (K/O) mice RPE to their human counterparts revealing strong similarities. Mitochondrial viability of all cell types treated with hydrogen peroxide (H_2O_2) or *tert*-butylhydroperoxide (*t*-BOOH) for 24hrs revealed that RPE lacking αA-crystallin yielded highly significant decreased cell viability, indicating a possible protection in the presence of αA-.

To further investigate the *in-vivo* protective role of α-crystallins in the retina, in particular αA-, WT mice and αA-crystallin K/O mice were exposed to moderate levels of continuous blue light daily up to 7 days. Visual function was assessed with electroretinography (ERG) on all animals before exposure, immediately after exposure, and after a 10 day recovery period. Retinal morphology was examined immediately after and after a 10 day recovery period from light exposure. Although both strains revealed continual decline in their visual function with little morphological changes, αA- K/O mice degenerated significantly faster during their 10 day recovery period, both functionally and morphologically.

Protein analysis revealed that WT mice exhibited statistically significant upregulation of the α-crystallins during their recovery period, while αB-crystallin expression in αA-K/O mice was not significantly upregulated at any time point. Therefore the absence of αA- may effect expression and potency of αB-crystallin in response to stress-related conditions.

Results presented will demonstrate that the presence of α-crystallins, in particular, αA-, may play a protective role in oxidative stress to the RPE and photochemical damage of the retina.

Table of Contents

Abbreviations

α	Alpha
β	Beta
γ	Gamma
µg	Microgram
µl	Microliters
µm	Micrometer
µM	Micromole
°C	Degrees Centigrade
°F	Degrees Fahrenheit
AGE	Advanced Glycosylation End Products
AMD	Age-related Macular Degeneration
ARM	Age-related Maculopathy
ATP	Adenosine Triphosphate
bp	Base Pairs
BSA	Bovine Serum Albumin
cAMP	Cyclic Adenosine Monophosphate
CNV	Choroidal Neovascularization
CRALBP	Cellular Retinaldeyhde-Binding Protein
CRYAA	AlphaA-Crystallin
CRYAB	AlphaB-Crystallin
DNA	Deoxyribonucleic Acid
ECL	Enhanced Chemiluminescence
EDTA	Ethylenediaminetetracetic Acid

ERG	Electroretinography
ETC	Electron Transport Chain
FCS	Fetal Calf Serum
g	Gram
GAPDH	Glyceraldehyde-3-phosphate dehydrogenase
GSH	Glutathione
GPX	Glutathione Peroxidase
HCl	Hydrochloric Acid
Hr/hrs	Hour/Hours
H_2O_2	Hydrogen Peroxide
$HO_2\cdot$	Hydrogen Peroxyl Radical
HSP	Heat Shock Protein
Mins	Minutes
ml	Milliliters
mM	Millimolar
mRNA	Messenger RNA
mtDNA	Mitochondrial DNA
NADH	Nicotinamide Adenine Dinucleotide
ng	Nanogram
nm	Nanometer
O_2	Oxygen
$^1O_2$	Singlet Oxygen
$O_2^{-}\cdot$	Superoxide Anion

OH·	Hydroxyl Free Radical
PAGE	Polyacrylamide Gel Electrophoresis
PBS	Phosphate Buffered Saline
PCD	Programmed Cell Death
PCR	Polymerase Chain Reaction
PDGF	Platelet Derived Growth Factor
PEDF	Pigment Epithelial-Derived Factor
PTM	Post-Translational Modifications
PUFA	Polyunsaturated Fatty Acid
RNA	Ribonucleic Acid
ROO·	Lipid Peroxyl Radical
ROS	Reactive Oxygen Species
RPE	Retinal Pigment Epithelium
RT-PCR	Reverse-Transcriptase PCR
SDS	Sodium Dodecyl Sulphate
sHSP	Small Heat Shock Protein
SOD	Superoxide Dismutase
TBE	Tris-Borate-EDTA
t-BOOH	*tert*-butylhydroperoxide
UV	Ultra-violet
v/v	volume/volume
VEGF	Vascular Endothelial Growth Factor
WT	wild-type

Chapter 1.0:
General Introduction

1.0 Introduction

The retina is the innermost layer of the eye which contains a number of neuronal cells and processes which are vital to the perception of our visual world. It shares an intimate, yet vital, relationship with a monolayer of cells known as the retinal pigment epithelium (RPE). Together, these two tissues undergo a myriad of local and environmental stressors which persist throughout the lifetime of an organism.

The α-crystallins, members of the small heat shock protein (sHSP) family, are expressed in the retina and have been suggested to play a role in protection of the photoreceptors through their molecular chaperone properties. In particular, α-crystallins appear to be upregulated in intense light exposure of the retina (Sakaguchi *et al.*, 2003).

The purpose for this introduction is to provide background on the anatomy and physiology of the sensory retina and RPE, as well as the molecular changes which can occur through routine cellular metabolism, physiological ageing and a lifetime of exposure to visible light. Additionally, it will provide an overview of the α-crystallins, both in lens and non-lens tissues.

1.1 Anatomy and Physiology of the Sensory Retina

The sensory retina is a compact, highly differentiated, metabolically active, neuroectodermal derived tissue, which is approximately 100-500μm thick and consists of two distinct regions: the central retina (macula; which is further subdivided into the fovea and the foveola) and the peripheral retina. The retina is composed of nine sensory layers; 3 layers of cell bodies, 2 layers of synapses, the photoreceptor layer, internal and external limiting membranes and the nerve fiber layer (Fig.1)

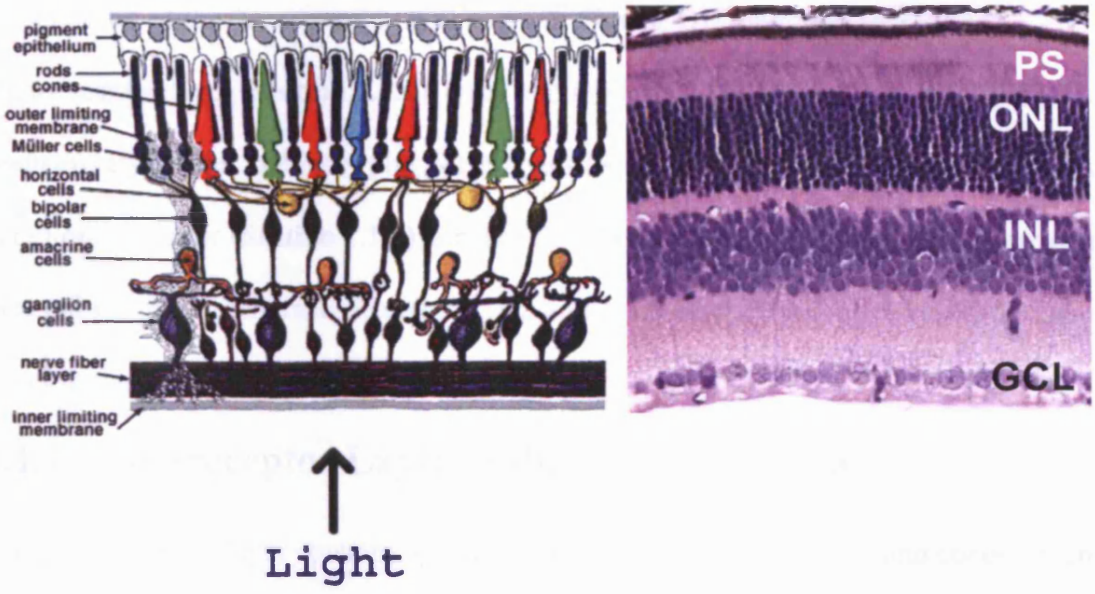

Figure 1.1: A schematic diagram of the retinal layers. The cartoon shown in the left was taken from Bonnel et al., 2003and describes individual cells within the retinal structure. The figure shown on the right is a histological section from mouse retina revealing the three layers of cell bodies (ONL – outer nuclear layer, INL – inner nuclear layer, GCL – ganglion cell layer), two layers of synapses (OPL – outer plexiform layer, IPL – inner plexiform, and photoreceptor segments (PS).

As stated above, the retina is from neurorectoderm origin and is derived from the optic cup, which is a continuous outgrowth from the fore-brain (Wolff, 1955). During its course of ocular morphogenesis, primitive sensory retina is formed from the inner layer of the developing optic cup, while the outer layer of the optic cup develops into future retinal pigment epithelium (**Section 1.2**)(Wolff, 1955). In the adult, both the sensory retina and RPE

are the site of transformation of light energy into a neural signal, also known as phototransduction (**see Section 1.2.3).**The space between the inner and outer layers of the developing optic cup, the optic ventricular space, will become the future subsensory retinal space (SSRS) in the adult. The SSRS plays a vital role in the maintenance and sustenance of the outer retina and RPE.

The day to day functions of the sensory retina and RPE are pivotal in the maintenance and preservation of the visual world. As shown in **Figure 1.1,** the retina consists of a photoreceptor layer (**Section 1.1.1**), outer and inner nuclear layers (**Section 1.1.3 and 1.1.5, respectively**), outer and inner plexiform layers (**Sections 1.1.4 and 1.1.6, respectively),** a ganglion cell layer **(Section 1.1.7),** a nerve fiber layer (**Section 1.1.8**) and the internal and external limiting membranes (**Section 1.1.2 and 1.1.9 respectively**), which are discussed in detail in the following sections.

1.1.1 Photoreceptor Layer of the Sensory Retina

The photoreceptor layer contains special sense cells known as the rods and cones which contain photopigments that absorb incoming photons of light (Wolff 1955, Remington 2005). Rods are specialized for low-light or dim vision, while the cones are specialized for well-lit, brighter conditions. Photoreceptors of mice are very similar to primate photoreceptors in physical dimensions (Fu and Yau 2007). In the murine retina, rods constitute approximately 97% of mouse retinal photoreceptors, while cones account for the remaining 3% (Carter-Dawson and LaVail 1979, Szel *et al.,* 1992, Fu and Yau 2007,). Due to this scarcity and fragility of cones in the murine retina, phototransduction of the rods has been investigated more extensively than cone phototransduction (Lem and Makino 1996, Hurley and Chen 2001, Wenzel *et al.,* 2005, Fu and Yau 2007, Imai *et al.,* 2007, Lee and Flannery 2007, Krishnan *et al.,* 2008, Pawar *et al.,* 2008,).

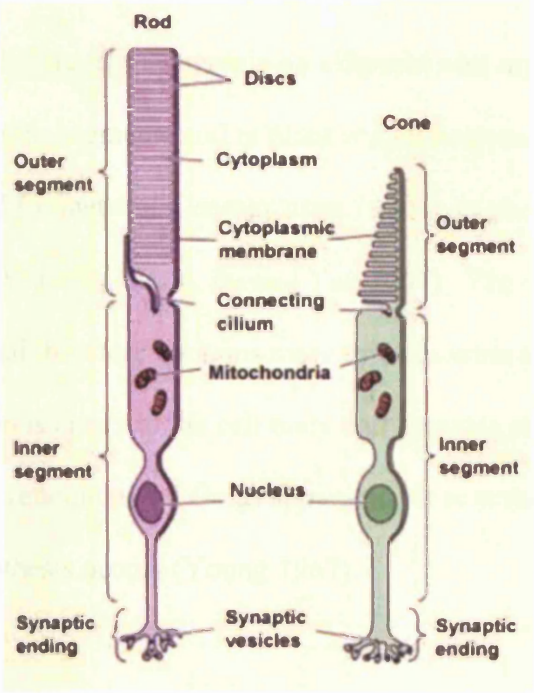

Figure 1.2 Structural and functional regions of the photoreceptor cells. Both rods and cones contain an outer segment, inner segment, cell body and synaptic terminal. A notable difference between the two cells are their outer segment composition. Rod discs are completely internalized and separate from the plasma membrane, while cone discs remain as foldings of the plasma membrane. Source: http://thebrain.mcgill.ca/flash/d/d_02/d_02_m/d_02_m_vis/d_02_m_vis_1a.jpg

As shown above, rods and cones consist of outer/inner segments, cell bodies and synaptic terminals. The outer segments of the photoreceptors are filled with stacks of membranous discs filled with visual pigment (**see Section 1.5.6)** and other phototransduction components (Wolff 1955, Remington 2005, Fu and Yau 2007). Outer segment rod discs are separated from the plasmalemma, or plasma membrane, forming sacs that are closed at both ends and are free of attachment to adjacent discs (Anderson *et al.,* 1978, Arikawa *et al.,* 1992, Cohen, 1992). Discs in the outer segment of the cones are continuous with the plasmalemma and are not easily separated from each other (Anderson *et al.,* 1978). Outer segments of the rods and cones share an intimate relationship with RPE which is vital to the shedding and renewal of discs, as well as the process of phototransduction (**see Section 1.2.3**)

The inner segments of photoreceptors contain an **ellipsoid and myoid region**. The ellipsoid portion is closer to the outer segments and is filled with numerous mitochondria, which help to meet the high demand for metabolic energy associated with phototransduction (Wolter 1959, Remington 2005, Wu *et al.*, 2006, Fu and Yau 2007). The ellipsoid area of the cone contain is much wider and therefore contains more mitochondria than the rod (Hogan *et al.*, 1971). The myoid region is closer to the cell body and contains other necessary organelles such as the endoplasmic reticulum and Golgi apparatus. It is in the myoid region of the inner segment that protein synthesis occurs (Young 1967).

The cell body portion of the photoreceptors contains the nucleus and the synaptic terminal of both receptors release the neurotransmitter, glutamate (Kolb and Famiglietti 1976). The synaptic terminals differ between rods and cones, with rods containing a **spherule** and cones contain a **pedicle.** Spherules contain an internal, invaginated surface that forms a synaptic complex that contains bipolar dendrites and horizontal cell processes (Wolter 1959, Kolb and Famiglietti 1976, Migdale *et al.*, 2003). Pedicules are broad, flattened terminals which contains several invaginated areas and exhibit triad contacts, bipolar contacts and gap junctions that assist in facilitating electrical communication between adjacent rods or cones (Wolter 1959, Raviola and Gilula 1975, Cohen 1992).

1.1.2 External Limiting Membrane

Although not a true membrane, not external and limits nothing, the external limiting membrane separates photoreceptor nuclei (outer nuclear layer, **see Section 1.1.3**) from the inner and outer segments of the photoreceptors (Smith 2001).

1.1.3 Outer Nuclear Layer

The outer nuclear layer contains the rod and cone cell bodies. In mice, the outer nuclear layer is 10 – 12 nuclei thick with very little perinuclear cytoplasm. Nuclei of the rods appear densely basophilic with unevenly distributed nucleoplasm, while nuclei of cones are slightly larger and less basophilic (Smith 2001). Photoreceptor nuclei are separated from the inner and outer segments by the external limiting membrane (**Section 1.1.2**).

1.1.4 Outer Plexiform Layer

The outer plexiform layer, which is also known as the outer synaptic layer, is a layer of synapses located between photoreceptors and neural cells of the inner nuclear layer (**Section 1.1.5**). As stated above in **Section 1.1.1**, rods contain spherule synaptic terminals and cones contain pedicle synaptic terminals. These photoreceptor synaptic terminals synapse with bipolar and horizontal cells (second order neurons), which are located in the inner nuclear layer.

1.1.5 Inner Nuclear Layer

The inner nuclear layer contains the cell bodies of the bipolar cells, horizontal cells, amacrine cells, Müller cells and some displaced ganglion cells (Remington 2005). In mice, the inner nuclear layer is a dense layer that is six to nine cells thick in peripapillary retina (Smith 2001). The cells most abundant in this layer are the bipolar cells, which relay information from the photoreceptors to horizontal, amacrine, and ganglion cells and receive synaptic feedback from amacrine cells (Ayoub and Matthews, 1992, Remington 2005). Eleven types of bipolar cells exist based on their morphology, physiology, and dendritic contacts and of those, the rod bipolar cell is the only bipolar cell not associated with cones (Kolb *et al.*, 1992).

Horizontal cells are responsible for transferring information in a horizontal direction which is parallel to the retinal surface. Horizontal cells synapse with photoreceptors, bipolar and other horizontal cells, all occurring in the outer plexiform layer. It has also been shown that these cells release an inhibitory transmitter, possibly playing a role in the process of visual integration (Hart 1992, Witkorsky 1994). Although horizontal cells connect the cone pedicules and rod spherules in a complex pattern, they are able to provide inhibitory feedback to photoreceptors or inhibitory feed forward to bipolar cells (Smith 2001, Kolb *et al.*, 2003). It has been reported that horizontals can modulate the response of the cones, but not of the rods (Bloomfield and Dacheux 2001, Kolb *et al.*, 2003).

Amacrine cells play an important role in modulating information that eventually reaches the ganglion cells (Witkorsky 1994). Amacrine cells have both dendritic and axonal characteristics which contain the inhibitory neurotransmitter gamma-aminobutyric acid (GABA). Additionally, they carry information horizontally, and form complex synapses with bipolar axons, dendrites and soma of ganglion cells (Dowling and Boycott 1965, Hogan *et al.*, 1971, Kolb 1997, Sharma and Ehinger 2003, Remington 2005).

Müller cells extend throughout a large portion of the retina with cytoplasmic processes extending from the retinal surface to villous processes just beyond the external limiting membrane (Smith 2001). Müller cells play an important role in the retina by providing glucose and glycogen, and helping to maintain retinal structure integrity by filling retinal space unoccupied by neurons (Wolter 1959, Smith 2001). One of the most important functions of these cells is their ability to remove glutamate from the extracellular space, which may critical for survival of other retinal neurons (Carter-Dawson *et al.*, 1998).

1.1.6 Inner Plexiform Layer

The inner plexiform layer, also known as the inner synaptic layer, consists of synaptic connections between ganglion, bipolar and amacrine cells. Since this layer consists of synapses, it is usually nuclei free, however displaced nuclei from the inner nuclear or ganglion cell layers may occur sporadically (Smith 2001).

1.1.7 Ganglion Cell Layer

The ganglion cell layer contains the ganglion cells of the retina. In humans this layer is generally a single layer thick except near the macula, where it can range from 8-10 cell layers thick (Wolff 1955). In addition to containing the ganglion cells, this layer may also contain glial processes from Müller cells, other neuroglia and branches of retinal vessels (Cohen 1992, Ramírez *et al.*, 1996). In normal mouse retina, ganglion cells are closely aligned as a single layer, but may increase to two to three cell layers thick in the peripapillary area (Smith 2001).

1.1.8 Nerve Fiber Layer

The nerve fiber layer is formed from the axons of the ganglion cells. Axons of the ganglion cells are unmyelinated and do not become myelinated until reaching the retrolaminar division of the optic nerve. These unmyelinated axons are surrounded by cells processes of astrocytes, which help to form these axons into bundles before entering the lamina cribrosa, and Müller cells (Wolff 1955).

1.1.9 Internal Limiting Membrane

The internal limiting membrane assists in forming the innermost boundary of the retina. It is formed by the basal lamina of Müller cells and lies directly internal to the nerve fiber layer (Smith 2001). Additionally, the internal limiting membrane shares an intimate relationship

with surrounding vitreous through attached collagen fibers from cortical vitreous (Hogan *et al.*, 1971).

1.2 Anatomy and Physiology of the Retinal Pigment Epithelium (RPE)

Although the RPE has no photoreceptive or neural function like the retina, it is essential to the support and viability of the photoreceptor cells. The RPE is a monolayer of differentiated, hexagonal, neuroepithelium, which lies between the photoreceptors and the choriocapillaris and spans the retina from the margin of the optic disk anteriorly to the ora serrata (Berman, 1991b; Marmor, 1998). Photoreceptor segments of the sensory retina form a functional unit with the RPE.

As illustrated in **Figure 1.3, t**he RPE is split into two distinct regions: the *apical surface* and the *basal surface*. The apical surface (towards the photoreceptors) has numerous microvilli, which partially envelop the outer segments and assists in their phagocytosis. Microfilaments, microtubules and melanin compose the cytoplasm of the apical region and the central region of the RPE cell contains the nucleus and necessary organelles for vitality. Tight junctions (zonula occludens) in the apical region assist in forming part of the blood-retinal barrier, while junctional complexes and gap junctions assist in RPE cell-to-cell connection and communication. The basal surface (towards choriocapillaris) contains multiple infoldings to increase its surface area for absorption and secretion activities (Berman, 1991b; Marmor, 1998).

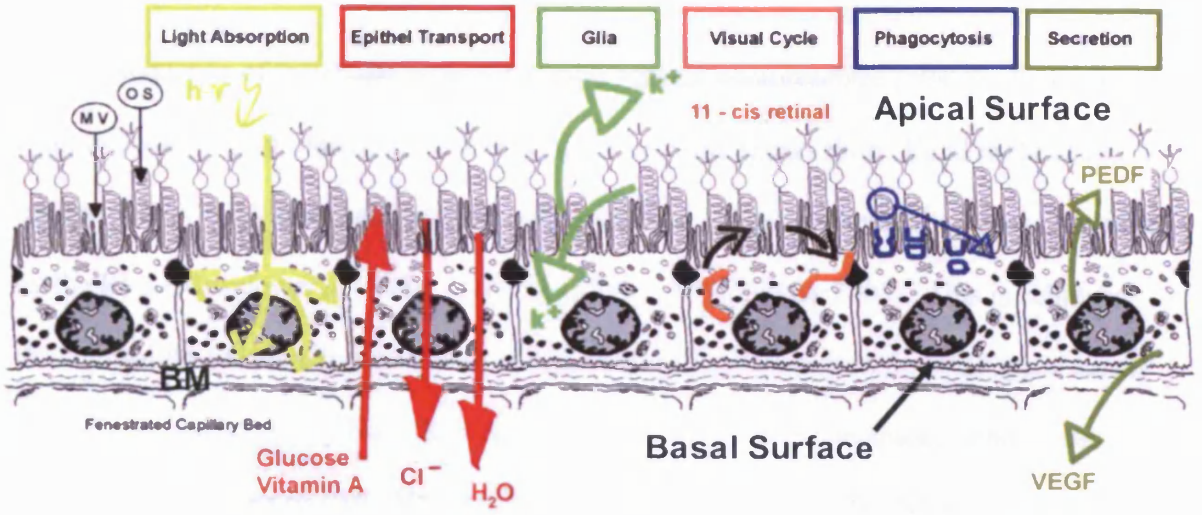

Figure 1.3 Summary of the numerous functions of the RPE that are ultimately responsible for the support and function of our visual world. As shown, the apical portion of the RPE is towards the photoreceptors, while the basal portion shares an intimate relationship with Bruch's Membrane (BM) and the choriocapillaris. (hν denotes an incoming photon of light, PEDF – pigment epitheliumt derived-factor, VEGF – vascular endothelial growth factor, MV – microvilli, OS – outer segments). Figure was taken and adapted from an elegant review on the RPE from Strauss 2005.

As shown, the RPE plays a pivotal role in the survival and sustenance of both the photoreceptors and the choriocapillaris (**see sections 1.2.1 – 1.2.4**).

1.2.1 Environmental Responsibilities

The surrounding physiological responsibilities of the RPE include forming part of the blood-retinal-barrier, transporting nutrients and ions, synthesizing necessary growth factors and interacting with a number of endocrine, vascular and proliferative factors (Marmor, 1998). The blood –retinal-barrier is formed by the tight junctions located at the cell's apical surface. These tight junctions exhibit control by blocking the free passage of water and ions and inhibit the exchange of potentially toxic substances between the choroidal circulation and the neural retina (Berman, 1991b).

Transportation of necessary nutrients and ions also plays a key role in the environmental responsibilities of the RPE. Due to the high amount of water produced in the retina and RPE

as a consequence of metabolic turnover of neurons and photoreceptor cells, the RPE must be equipped with transportation mechanisms to remove this excess fluid. Fluid in the retina is transported by the Müller cells into the subsensory retina space where it becomes eliminated by the RPE (Moseley *et al.*, 1984, Nagelhus *et al.*, 1999, Strauss 2005). This is achieved through solute-linked active transport of dissolved solutes from the subretinal space across the RPE to the choroid by Na^+ - K^+ - ATPase pumps located on the apical membranes (Ostwald and Steinberg 1980, Berman 1991b, Gundersen *et al.*, 1991, Marmorstein 2001, Rizzolo 1991, Marmorstein *et al.*, 1998, Strauss 2005). In addition to removing excess fluid from the retina and RPE, this active pumping force also helps to generate the normal adhesion between the neural retina and the RPE, which if compromised, can lead to retinal detachments and subsequent vision loss (Kita and Marmor 1992, Marmor 1998).

The RPE also has the ability to secrete growth factors for itself and for other cells (Bryan and Campochiaro., 1986). Examples of growth factors expressed in the RPE both *in vitro* and *in vivo* include: **platelet derived growth factor (PDGF)** (involved in the regulation of cell growth and differentiation during development) (Campochiaro 1998), **vascular endothelial growth factor (VEGF)** (stimulates angiogenesis *in vivo* and its expression is increased by hypoxia) (Adamis *et al.*, 1993, Kuroki *et al.*, 1996, Nagineni *et al.*, 2003), **fibroblast growth factor (FGF)** (has numerous activities ranging from angiogenesis, stimulation of chemotaxis and epithelial differentiation) (Bost *et al.*, 1992, Ishigooka *et al.*, 1993, Bost *et al.*, 1994, Dunn *et al.*, 1998,), **transforming growth factor β (TGF-β)** (the function of which is unknown in the retina and choroids, but it may exhibit neuroprotection and prevent vascular invasion)(Kvanta 1994, Khaliq *et al.*, 1995), and **insulin and insulin-like growth factors (IGF)** (may play a role in retinal development) (Campochiaro 1998, Eichler *et al*, 2008).

Recent studies have found **interferon beta (INF-β)** expression in human RPE cells may play a role in protecting the retina from excessive inflammation (Hooks *et al.*, 2008).

Of the many growth factors secreted, there is a tight balance between healthy and unhealthy expression of particular growth factors, especially PEDF and VEGF when describing advanced retinal disease of the eye. Under healthy conditions, PEDF is secreted at the apical portion of the RPE acting as a neuroprotector against glutamate-induced or hypoxic conditions (Dawson *et al.*, 1999, King and Suzuma 2000, Cao *et al.*, 2001, Ogata *et al.*, 2001). PEDF has also been shown to function as an antiangiogenic factor inhibiting endothelial cell proliferation (Dawson *et al.*, 1999, King and Suzuma 2000, Ogata *et al.*, 2001) and playing a role in protecting the eye from light damage (Cao *et al.*, 2001). VEGF, during healthy conditions, is secreted on the basal side of the RPE, where in low concentrations, it can prevent endothelial cell apoptosis, is essential for an intact endothelium of the choriocapillaris, and can act as a permeability factor to stabilize the fenestrations of the endothelium (Adamis *et al.*, 1993, Witmer *et al.*, 2003). If at any point there is an imbalance in the unhealthy secretion of these particular growth factors, or those mentioned prior, havoc can result in the eye, with angiogenesis and neovascular membranes which can irreversibly affect vision (Reviewed in Andreoli and Miller 2007, Lotery and Trump 2007, Grisanti and Tatar 2008).

1.2.2 Outer Segment Phagocytosis

One of the crucial roles of RPE function is the ingestion of the photoreceptor outer segments. To maintain the excitability of photoreceptors, the photoreceptor outer segments (POS) undergo a constant renewal process (Young 1967, Young and Droz 1968, Hall *et al.,* 1969, Young and Bok 1969, Bok and Hall 1971, Young 1976, Steinberg 1985, Bok 1993) and this phenomenon is due to the ingestion of the outer segments of the photoreceptors by RPE cells. Essentially there are two steps to this vital process: the ingestion of the outer segments by the RPE and the subsequent digestion of these segments. Outer segments of the photoreceptors that are being ingested contain the highest concentration of radicals, photo-damaged proteins, and lipids (Strauss 2005). Photoreceptors (high in polyunsaturated fatty acids and vitamin A) shed their discs approximately every 10 days, and the RPE has developed a unique catabolic process known as the phagolysosomal system (Feeney, 1973). As shown in **Figure 1.4,** initially, the outer segment is recognized and then bound to the RPE.

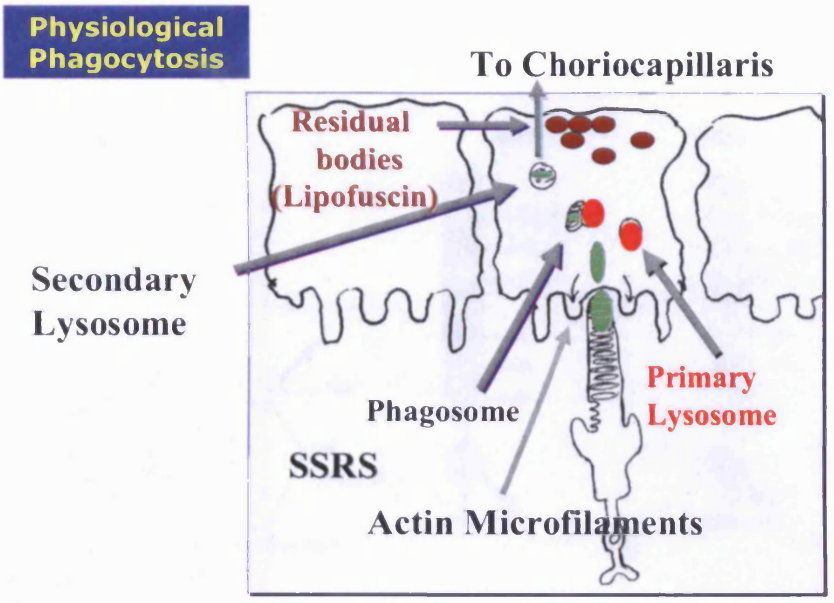

Figure 1.4 Illustration of physiological phagocytosis of the photoreceptor outer segments by the RPE. As shown the apical portion of the RPE recognizes the outer segment of the photoreceptor, ingests the outermost portion and primary lysosomes bind with the ingested outer segment and phagosome to form a secondary lysosome. Secondary lysosomes contain hydrolytic enzymes responsible for breaking down the ingested material, however physiological phagocytosis can become pathological and result in the formation of lipofuscin. Illustration was modified from Neuroanatomy Lecture of Lorraine Lombardi, PhD.

Complete ingestion of the outer segment into the RPE occurs and the ingested segments become surrounded by phagosomes. Phagosomes then fuse with primary lysosomes to form secondary lysosomes. Secondary lysosomes contain a number of hydrolytic enzymes, which further facilitate the digestion of these outer segments (Berman 1991b, Besharse and Derfoe, 1998, Marmor 1998a). A by-product of RPE phagocytosis is lipofuscin, which is one of the aging markers in the retina. Lipofuscin is an autofluorescent, phototoxic, undigestable lipid and protein complex resulting from the phagocytosis of the photoreceptor outer segments (Feeney 1978, Boulton and Dayhaw-Barker, 2001a, Bonnel *et al.*, 2003, Wolf 2003,). Lipofuscin is a photoinducible generator of ROS (**see section 1.4.1**) (Boulton *et al.*, 1993, Terman *et al.*, 2006, Biesemeier *et al.*, 2008, Ng *et al.*, 2008) and may play a role in the degeneration of the photoreceptor segments and RPE (Bonnell *et al.*, 2003, Vives-Bauza *et al.*, 2008).

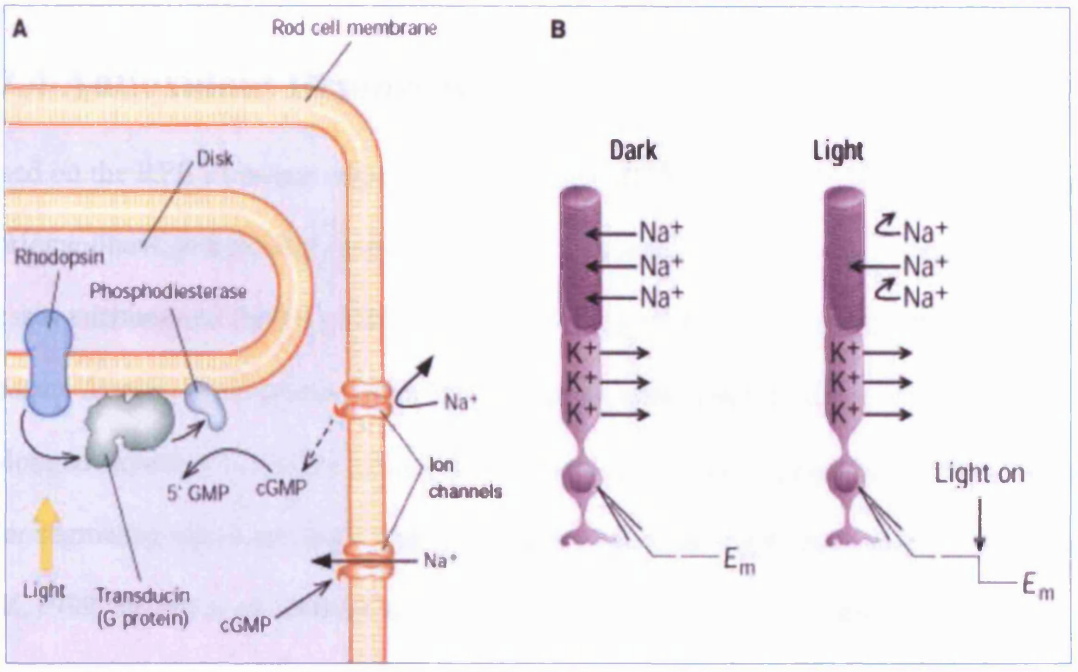

Figure 1.5Illustration of rod phototransduction. As shown, during dark conditions, cGMP gated channels remain open, allowing an influx of Na+ keeping the photoreceptor cell depolarized. Once a photon is absorbed from incoming light, a series of events occur ultimately hyperpolarizing the membrane through the closure of the cGMP gated channels. Photo adapted from Hargrave, 2001.

As described above, photoreceptors utilize the highly photosensitive vitamin A analog, 11-*cis*-retinal, for light absorption and signal transduction initiation (Thompson and Gal, 2003). The visual pigment cycle within the RPE converts vitamin A (all-*trans*-retinol) from dietary intake to 11-*cis*-retinal. All-*trans*-retinol is transported to the retina via the circulation where it moves into the RPE cells. Once in the RPE, the all-*trans*-retinol is esterified to form a retinyl ester, which is the storage form. Retinyl esters can be hydrolyzed and isomerized to form 11-*cis*-retinol when needed. 11-*cis*-retinol can be oxidized to form 11-*cis*-retinal, which is transported to the rod photoreceptor cells and binds to opsin to form the visual pigment rhodopsin. Absorption of a photon of light catalyzes the isomerization of 11-*cis* retinal to all-*trans* retinal and results in its release (Berman 1991b, Chader *et al.,* 1998, Thompson and Gal, 2003). Once released, all-*trans* retinal is converted to all-*trans* retinol, and is transported across the interphotoreceptor matrix to the retinal epithelial cell to complete the visual cycle.

1.2.4 Antioxidant Resources

Based on the RPE's various responsibilities in the maintenance of the photoreceptors and choriocapillaris, antioxidant resources must be available to it to counteract the diverse stresses encountered during its lifetime. The RPE is subjected to a number of oxidative stressors from several sources including its high oxygen concentration environment, prolonged exposure to visible light, and the phagocytosis and degradation of photoreceptor outer segments, which are high in polyunsaturated fatty acids (Winkler *et al.,* 1996, Winkler *et al.,*1999, Beatty *et al.,* 2000, Cai *et al.,* 2000, Strunnikova *et al.,* 2004).

To cope with these oxidative stressors, the RPE is rich in antioxidants such as Vitamin E, superoxide dismutase, catalase, glutathione-S-transferase, glutathione and ascorbate (Newsome *et al.,* 1990, Beatty *et al.,* 2000). Recent studies have reported the antioxidant capacity of melatonin (Reiter *et al.,* 2000) and its ability to directly scavenge a variety of ROS (Liang *et al.,* 2004). Melatonin an endogenous neurohormone which is naturally produced by the pineal gland and retina in mammals, was also found to enhance the activity of antioxidative enzymes such as glutathione peroxidase, superoxide dismutase and glutathione-S-transferase (Antolin *et al.,* 1996, Urata *et al.,* 1999, Okatani *et al.,* 2002). *In vitro*, melatonin is more efficient in scavenging hydroxyl and peroxyl radicals in comparison to conventional antioxidants such as Vitamin C and E (Martin *et al.,* 2000).

1.3 Progression of Ageing in the Sensory Retina/RPE

Ageing of the retina/RPE is inevitable due to the constant amount of environmental stressors which accumulate over time. Because of their postmitotic nature, both the retina and the RPE are equipped with a number of cellular defenses and antioxidant capacities, but unfortunately

with ageing, these tissues cannot avoid damaging physiological alterations (**see sections 1.3.1 – 1.3.3**).

1.3.1 Intracellular and Extracellular Deposits

Advanced glycosylation end products (AGEs) may contribute to RPE dysfunction and represent a component of lipofuscin (Boulton and Dayhaw-Barker, 2001a, Howes *et al.*, 2004, Glenn *et al.*, 2008,). Lipofuscin is one of the major intracellular ageing markers of the sensory retina and RPE. As described earlier, lipofuscin is an autofluorescent, phototoxic, undigestable lipid and protein complex resulting from the phagocytosis of the photoreceptor outer segments (Boulton and Dayhaw-Barker, 2001a, Bonnel *et al.*, 2003, Wolf 2003). Lipofuscin is located in the RPE where it is continually exposed to high O_2 tensions (70 mmHg) and visible light (400-700nm), setting up the prime environment for the generation of ROS (**see Section 1.4.1**) (Boulton *et al.*, 1993, Bonnel *et al.*, 2003, Ng *et al.*, 2008, Spaide 2008). As a photoinducible generator of ROS, it has the potential to damage cellular proteins and lipid membranes. In addition, A2E, a lipofuscin fluorophore, mediates blue-light induced apoptosis of RPE cells through membrane disruption and the inhibition of lysosomal degradation (Schutt *et al.*, 2000, Sparrow *et al.*, 2000, Gaillard *et al.*, 2004, Lamb and Simon, 2004, Iriyama *et al.*, 2008, Kim *et al.*, 2008, Sparrow *et al.*, 2008, Vives-Bauza *et al.*, 2008). Vitamin A may also assist in the photoreactivity of lipofuscin (Eldred and Lasky, 1993).

Extracellular deposits include drusen, which accumulate between the RPE basal lamina and the inner collagenous layer of the Bruch's membrane. Drusen, can be classified as *hard* or *soft* and are risk factors in the development of age-related macular degeneration (AMD) (Crabb *et al.*, 2002, Ambati *et al.*, 2003). A proteome analysis of drusen performed by Crabb *et al*, (2002) supported the hypothesis of oxidative stress as a contributor to AMD pathogenesis.

1.3.2 Structural Alterations

Most of the structural alterations that occur in the ageing retina include a decrease in the neuronal cell populations including ganglion cells (Curcio and Drucker, 1993a), and rods (Gao and Hollyfield, 1992, Curcio *et al.*, 1993b). In addition to the decrease in cell numbers, astrocytes display increased levels of glial fibrillary acidic protein, the function of which is not well understood, but it may be involved in controlling the shape and movement of astrocytes and cytoplasmic organelles (Ramirez *et al.*, 2001).

Changes in RPE cell density appear contradictory in a number of studies (Boulton and Dayhaw-Barker, 2001a), yet there is sufficient evidence in the loss of cell shape, atrophy and pigmentary changes (Feeney-Burns *et al.*, 1984). Melanin content also appears to be affected in the ageing visual system. There is a decrease in melanin granules in all regions of the retina (centrally and peripherally) after 40 years of age (Feeney-Burns *et al.*, 1984; Boulton 1998) and this decline may be due to the role of melanin photooxidation (Sarna *et al.*, 2003).

1.3.3 Cellular Modifications

Cellular modifications in the ageing retina/RPE include damage to mitochondrial DNA (Barron *et al.*, 2001; Liang and Godley, 2003; Navarro 2004), decrease in antioxidant capacity (Liles *et al.*, 1991, Friedrichson *et al.*, 1995, Boulton and Dayhaw-Barker, 2001a), protein cross-linking and lipid peroxidation (Boulton and Dayhaw-Barker, 2001a, Bonnel *et al.*, 2003). A strong association exists between ageing and damage to mitochondrial DNA due to the role of the mitochondria as the pacemakers of tissue aging due to continuous production of ROS and nitrogen species (Navarro, 2004).

1.4 Oxidative Stress in the Sensory Retina/RPE

As discussed previously, in addition to retina and RPE's high metabolic activity and photoreceptor turnover, the RPE and retina are also exposed to constant levels of light throughout its lifetime (see **Section 1.5**). This leads to an accumulation of photo-damaged proteins and lipids as well as the self-generation of photo-oxidative radicals from accumulated oxidative stress (Beatty *et al.*, 2000).

Oxidative stress was defined by Sies in 1991, as "a disturbance in the prooxidant-antioxidant balance in favor of the prooxidant, leading to potential damage" (Sies, 1991). In other words, oxidative stress occurs when the production of damaging free radicals (prooxidants), and other oxidative molecules, exceeds the capacity of the body's antioxidant defenses to detoxify them. *Prooxidant* species include ROS (**see section 1.4.1**) and *antioxidant* species include a number of antioxidant enzymes (superoxide dismutase, catalase, glutathione peroxidase, glutathione reductase, and glutathione), vitamins C, E and certain carotenoids. In addition, the visual system contains metal binding proteins, which include albumin, ceruloplasmin, metallothionein and transferrin (Newsome *et al.*, 1990).

Oxygen is a necessity for biochemical cycles, yet as a by-product of its metabolism, it produces highly toxic ROS, which, in excessive amounts, can be toxic to cells. A number of diseases that accompany ageing have oxidative stress as one of the major determinants (Harman 1981, Andersen 2004, Junqueira *et al.*, 2004, Navarro 2004, Toler 2004). Oxidation of biomolecules is related to susceptibility to diseases such as cancer and heart disease, as well as being associated with the process of aging (Junguiera *et al.*, 2004).

Oxidative stress is not only responsible for accidental cell damage, but it may also actively trigger intracellular signaling pathways that lead to cellular demise, also known as apoptosis or programmed cell death (PCD) (Alge *et al.,* 2002, Andersen 2004, Junqueira *et al.,* 2004).

In addition to the oxidative stress on the various systemic organs, oxidative stress is also believed to contribute to the pathogenesis of many ocular diseases associated with ageing, including AMD (Winkler et al., 1999; Beatty et al., 2000; Cai et al., 2000; Liang and Godley, 2003, Roth *et al.,* 2004, Zarbin 2004).

A number of cellular mechanisms and components become altered or damaged (**see section 1.4.2**) due to the presence of ROS (**see Section 1.4.1)** which are generated from a number of factors both endogenously (**see section 1.4.1.a**) and exogenously (**see section 1.4.1.b**).

1.4.1 Reactive Oxygen Species (ROS)

ROS are defined as molecular entities that react with cellular components, resulting in detrimental effects on their function (Andersen 2004). ROS include free radicals such as superoxide anion ($O_2^{-}\cdot$), hydrogen peroxyl radicals ($HO_2\cdot$), hydroxyl free radical ($OH\cdot$) and lipid peroxyl radicals ($ROO\cdot$) (Halliwell 1991, Beatty *et al.,* 2000). Free radicals contain an odd (unpaired) number of electrons and can be formed when oxygen interacts with certain molecules. Additional ROS include singlet oxygen ($^1O_2$) and hydrogen peroxide (H_2O_2), which are in an unstable state even with their full complement of electrons. Due to the instability of free radicals, they often react quickly with other compounds by trying to capture the necessary electron to reach stability. Often free radicals steal an electron from the nearest stable molecule. When an electron is lost from the attacked molecule, the attacked molecule now becomes a free radical, beginning a chain reaction. Once initiated, the process can

cascade, resulting in the disruption of a living cell, its components and associated metabolic cycles (Bergamini *et al.*, 2004).

The generation of ROS is due to a number of factors both endogenously (**see section 1.4.1.a**) and exogenously (**see section 1.4.1.b).** Effects of ROS can lead to considerable damage to DNA, proteins and lipids, which ultimately can lead to apoptosis or necrosis of living cells (Cai *et al.*, 1999).

1.4.1.a Endogenous ROS

Mitochondria are prime contributors in the generation of endogenous ROS (Chance *et al.*, 1979, Barron *et al.*, 2001, Liang and Godley, 2003, Alexeyev *et al.*, 2004, McLennan and Degli Esposti, 2004, Melov 2004, Navarro 2004). Mitochondria are intracellular organelles whose main function is the synthesis of adenosine triphosphate (ATP) through oxidative phosphorylation (Hauptmann and Cadenas, 1997). Electrons leaking from the electron transport chain (ETC) reduce molecular oxygen to form $O2^{-}\cdot$, which then generates ROS through both enzymatic and non-enzymatic reactions (Alexeyev *et al.*, 2004). Damage to ETC components and mitochondrial DNA (mtDNA) results, promoting additional ROS and subsequent damage. McLennan and Degli Esposti, 2004 found that out of the 5 protein complexes associated with the ETC, complex I (NADH-ubiquinone reductase) and complex II (succinate-ubiquinone reductase) are the predominant generators of ROS during prolonged respiration under uncoupled conditions. By-products produced from the ETC include hydrogen peroxide, superoxide and hydroxyl radicals (Beckman and Ames, 1997). Approximately 90% of total O_2 consumption is due to the ETC (Beatty *et al.*, 2000).

Besides contribution from the mitochondria in endogenous ROS generation, peroxisomal fatty acid oxidation (Ames *et al.*, 1993), reduced coupling of the cytochrome P450 catalytic

cycle (Zangar *et al.*, 2004) and outer segment phagocytosis in the RPE (Ueda *et al.*, 1996; Beatty *et al.*, 2000) (**see section 1.4.3**) also play a role in ROS production.

1.4.1.b Exogenous ROS

A number of environmental factors contribute to the exogenous generation of ROS. These factors include smoking (Cai *et al.*, 2000), dietary intake (Ames *et al.*, 1993, Junqueira *et al.*, 2004, Li *et al.*, 2004), UV-light damage (Bergamini *et al.*, 2004, Davies 2004a), blue-light exposure (; Rozanowska *et al.*, 1995, Boulton *et al.*, 2001b, King *et al.*, 2004) (**see section 1.5.3**), and metal ions (Davies 2004a).

1.4.2 Cellular Damage

Effects of ROS can lead to considerable damage to DNA, proteins and lipids, which ultimately can lead to apoptosis or necrosis of living cells (Cai *et al.*, 1999). DNA damage includes both nuclear DNA and mitochondrial DNA (mtDNA). As revealed in **Section 1.4.1.a**, the mitochondria are the main intracellular components in the generation of ROS. The ensuing state of oxidative stress results in damage to ETC components and mtDNA (mitochondrial DNA), thus increasing further the production of ROS (Melov, 2004). Production of ATP is dependent on mitochondrial respiration and, therefore, any damage to the mitochondria, as a result of O_2 stress, would ultimately lead to reduced ATP (energy) and comprise overall cell function (Barron *et al.*, 2001, Liang and Godley, 2003, Godley *et al.*, 2005). mtDNA is more susceptible to oxidative damage than nuclear DNA.

1.4.3 Retina/RPE Susceptibility to Oxidative Stress

The RPE is subjected to a number of oxidative stressors from several sources including its high oxygen concentration environment, prolonged exposure to visible light, and the phagocytosis and degradation of photoreceptor outer segments, which are high in

polyunsaturated fatty acids (Winkler *et al.*, 1996, Winkler *et al.*,1999, Beatty *et al.*, 2000, Cai *et al.*, 2000, Strunnikova *et al.*, 2004).

Strong evidence suggests oxidative stress as a contributing factor in RPE apoptosis (Winkler *et al.*, 1999, Cai *et al.*, 2000, Liang and Godley, 2003). Previous studies have shown that stress induced by H_2O_2 (generated physiologically during phagocytosis outer segments), causes mtDNA dysfunction, and induces apoptosis (Ballinger *et al.*, 1999, Jin *et al.*, 2001). Bonnel *et al.* (2003) suggests that damage to mtDNA may play a possible role in RPE degeneration and subsequently, AMD (see **Figure 1.6**).

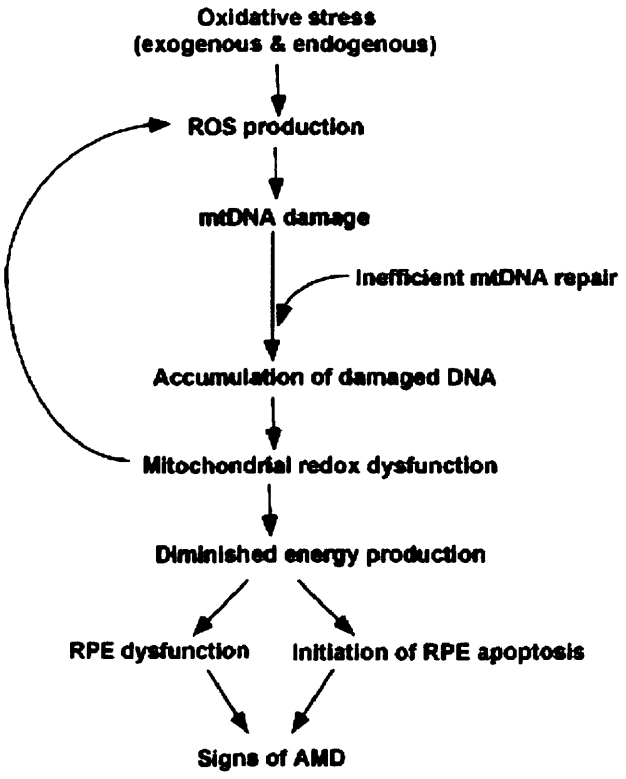

Figure 1.6: Mitochondrial Reactive Oxygen Species (ROS) model for Age-Related Macular Degeneration (AMD) Development (Source: Bonnel et al., 2003).

Oxidative stress has also been shown to disrupt RPE cell junctions and barrier integrity (Bailey *et al.*, 2004). The disruption of these cell junctions may contribute to the pathogenesis of diseases associated with the RPE through disruption of the blood-

retinal barrier. Stress from hydrogen peroxide treatment has also been shown to result in decreased expression of the RPE markers, RPE-65 and cellular retinaldehyde-binding protein (CRALBP) (Alizadeh *et al.*, 2001, Bailey *et al.*, 2004).

1.5 Retinal Light Damage

The universal effect of light on the retina is to generate the visual signal. However, with time and constant exposure, light, which is necessary for perception of the visual world, can also promote damage at a molecular level, which ultimately can threaten sight.

The *photoelectric effect* states that light is transmitted in quanta of energy particles known as photons and when these photons strike an atom, a quantum of energy proportional to the frequency and inversely the wavelength of the light, is absorbed (Algvere *et al.*, 2006, Siu *et al.*, 2008). The amount of energy absorbed from the incident light depends on the transparency of the tissue and the wavelength of the incident light (Wu *et al.*, 2006).

Although the eye is exposed to a range of wavelengths of incoming light, surrounding ocular structures are well equipped to filter out particular wavelengths of light which can be severely damaging to the retina.

Remé *et al,* (1998), describes the action spectrum as "the light dose that is required to obtain the same biological effect at different wavelengths." The electromagnetic spectrum, which ranges from the shortest ionizing waves to the longest radiowaves, is the distribution of electromagnetic radiation according to energy. The spectrum of the retina and the RPE is dependent on the absorption characteristics of the cornea and lens, which can vary according to age, species, absorption and transmission factors. For the visual system, the cornea absorbs wavelengths less than 295nm and the lens absorbs light in the long UV-B range (300-

315nm) and full UV-A range (315-400nm) (Boulton *et al.*, 2001b; Algvere *et al.*, 2006). The vitreous absorbs light greater than 1400nm, therefore the wavelength of light which reaches the retina falls into the "visible region". Visible light (400-700nm) represents a small portion (1%) of the electromagnetic spectrum (Miller and Burns, 2004a; Algvere *et al.*, 2006; Siu *et al.*, 2008). Therefore the effect of UV light (see **Section 1.5.2)** on the retina and RPE is minimal and the focus of retinal photodamage appears to be with the 'visible component' (see **Section 1.5.3**) (Taylor *et al.*, 1992, Organisciak and Winkler, 1994, Remé *et al.*, 1998, Boulton *et al.*, 2001b, Taylor *et al.*, 1992, Wenzel *et al.*, 2005, Wu *et al.*, 2006, Siu *et al.*, 2008).

Optical radiation that reaches the retina may be absorbed by a number of retinal chromophores, such as the visual pigments (**see Section 1.5.5)** as well as melanin, macular pigments and other proteins. Melanin, in particular, appears to protect the photoreceptors from scattered light and converts the absorbed photons into heat (Boulton *et al.*, 2001b). The 'pigmented' color of the RPE can be attributed to its melanin, which is abundant in both the apical and midportion regions of the cells of the RPE. In addition to its role impinging light scattering, melanin can also act as a neutral density filter, bind chemicals, act as a free radical scavenger or generator, and can absorb energy in the visible or UV range (Boulton 1998).

1.5.1 Classification of Retinal Light Damage

Light damage to a cellular system is classified into three categories: **photomechanical, photothermal** and **photochemical**. The effects of damage are determined by: irradiance from the light source, the wavelength of incident light, the duration of exposure and the absorption of target tissue (Mainster *et al.*, 1983).

Photomechanical injury results from high irradiance with short duration exposure, stripping electrons from molecules and disintegrating the target tissue into a collection of ions and electrons (Mainster *et al.*, 1983, Boulton *et al.*, 2001b, Miller and Scott, 2004b). The rate of delivery and extent of absorbed energy are dominant factors which determine damage in photomechanical damage; wavelength does play a major role (Marshall 1970, Lund and Beatrice 1979, Wu *et al.*, 2006). During photomechanical injury in the RPE, energy is absorbed so rapidly by the melanin granules that heat dissipation cannot take place, in turn generating irreparable damage to the RPE and photoreceptors (Cleary and Hamwrick 1969, Ham *et al.*, 1974, Goldman *et al.*, 1977).

Photothermal injury results from moderate irradiance with trapped or absorbed energy in a substrate molecule resulting in an elevation of temperature. The quoted temperature rise for the retina is 10°C or more (Mainster *et al.*, 1983). The amount of energy required to elicit damage increases for longer exposure times because heat dissipates with exposure (Wu *et al.*, 2006). Photothermal energy produces protein denaturation and enzyme inactivation, which results in coagulation, cellular necrosis and hemostasis of the target tissue (White *et al.*, 1971, Priebe *et al.*, 1975, Boulton *et al.*, 2001b). Macromolecular systems are susceptible to thermal damage due to disruption of their tertiary structure by breaking hydrogen bonds and hydrophobic/hydrophilic bonds (Wu *et al.*, 2006).

Photochemical or **phototoxic** effects occur with low to moderate irradiances below coagulation thresholds and with short wavelengths, in particular UV and visible blue wavelengths (Mainster *et al.*, 1983). Absorption of a photon by outer electrons causes a photoexcited singlet state, which undergoes intersystem crossing to form a transient excited triplet state (Boulton *et al.*, 2001b). This transient excited triplet state is quite durable and

can interact with surrounding molecules to form ROS. Tissues with a large concentration of cell membranes (like the photoreceptor outer segments PUFA's) are severely damaged to due to subsequent lipid peroxidation leading to a breakdown of the cell membrane structure (Foote 1968, Pryor *et al.*, 1976). Photochemical damage to cellular components occurs at temperatures too low to cause thermal destruction, and therefore may account for a delay of 24-48 hours before the appearance of possible damage (Foote 1968, Spikes and Macknight 1972, Boulton *et al.*, 2001b, Miller and Scott, 2004b). The majority of the damage which affects the retina falls into the photochemical or phototoxic category.

In 1980, Noell originally classified photochemical light damage as primary or secondary manifestations. He claimed that primary damage resulted from light affecting the photoreactive molecules within a damaged cell while secondary damage occurs subsequent to the primary event (Noell 1980, Organisciak and Winkler 1994). He further classified secondary damage into Type I or Type II. Type I damage results from extensive rhodopsin bleaching over short periods of time, with hyperthermia, dark rearing and intermittent light exposure (Organisciak and Winkler 1994). Type I damage is characterized by massive visual cell loss with loss of adjacent RPE cells. Type II damage results from long duration exposure with low intensity light, and also appears to be rhodopsin mediated (Noell 1980, Organsciak and Winkler 1994). Type II damage is characterized by widespread photoreceptor loss with little to no RPE damage.

Nine years later, according to Kremers and van Norren (1989), photochemical damage of the retina can be classified as Class I or Class II. Class I damage has an action spectrum which is identical to the absorption spectrum of the visual pigments (Organisciak and Winkler 1994, Wu *et al.*, 2006). It consists of exposures at low irradiances below 1 mW/cm^2 for several

hours to weeks with initial damage occurring in the photoreceptors (Kremers and van Norren 1989). Class II's action spectrum peaks at short wavelengths and occurs at higher irradiances above 10 mW/cm^2 (Kremers and van Norren 1989). Class II damage primarily occurs in the RPE. Due to similarities between Kremers, van Norren and Noell, it has been suggested that Type I and II damage described by Noell may be subsets of Class I damage (Organisciak and Winkler 1994).

1.5.2 Retinal UV Light Exposure

Although previous studies suggest that the RPE and the sensory retina may be damaged by UV light exposure (Noell *et al.*, 1966), the effect of UV light appears to be minimal.

In studies where patients lacked UV filters with their intraocular lenses, there was an increase in cystoid macular edema (Kraff *et al.*, 1985) and decreased sensitivity in the blue-cone region (Werner *et al.*, 1989).

1.5.3 Retinal Blue Light Exposure

Blue light exposure falls into the 'visible spectrum,' which ranges from (400-700nm). It has been described as the "most hazardous component of the visual spectrum and has the greatest potential for photoxicity" (Ham *et al.*, 1976). Studies support blue light damage as a possible inducer in the degeneration of the RPE and photoreceptors in age related disease (King *et al.*, 2004, Margrain *et al.*, 2004, Godley *et al.*, 2005, Algvere *et al.*, 2006, Chu *et al.*, 2006, Wu *et al.*, 2006, Thomas *et al.*, 2007, Siu *et al.*, 2008). Blue light induced lesions appear to be mediated by rhodopsin (Grimm *et al.*, 2000, Grimm *et al.*, 2001, Algvere *et al.*, 2006, Wu *et al.*, 2006, Tanito *et al.*, 2007, Thomas *et al.*, 2007). Two types of photochemical damage occur with blue light: short (less than 12 hours), intense exposures at the RPE level and long

(12-48 hours), less intense exposures at the photoreceptor level (Noell *et al.*, 1966, Ham *et al.*, 1978, Margrain *et al.*, 2004).

Chromophores have been designated as one of the primary causes in blue light induced photoreceptor damage (**see section 1.5.6**).

1.5.4 Green Light Exposure

Green light, or diffuse white light, exposure mimics outdoor exposure (Remé *et al.*, 1998). Its effect on retinal photodamage appears to be less than that of blue light exposure. A study conducted by Rapp *et al.*, 1992, examined damage from both long (green) and short (360nm) wavelengths of light. They found that shorter wavelengths were 50-80 times more capable of causing light damage. Green light did not have an effect on the retina, even with increased energy levels (Rapp and Smith, 1992). With exposure, green light bleaches all of the available rhodopsin, leaving no excitable chromophores, unlike blue light, which is absorbed less efficiently and can lead to rhodopsin degeneration (Boulton *et al.*, 2001b).

1.5.5 Chromophores

Chromophores are the visual pigments that absorb light in the sensory retina and RPE. Numerous studies have shown that chromophores in both rods and cones may play a role in photodamage of the retina (Noell *et al.*, 1966; Gorn and Kuwabara, 1967; Williams and Howell, 1983). Chromophores of the retina include rhodopsin, flavins, melanin, lipofuscin, macular pigments, hemoglobin and porphyrin proteins (Boulton *et al.*, 2001b).

The main chromophores responsible for light-induced damage are the visual pigments. Photodamage of rhodopsin may occur during extended rhodopsin activation in the meta-II state, resulting in a decrease in the concentration of calcium and initiates apoptosis (Boulton

et al., 2001b). Additionally, damage may occur with the release of toxic photobleaching products, including retinal (Boulton *et al.*, 2001b).

The role of flavins and porphyrins remains poorly understood, while the role of melanin and macular pigments appear to play a protective, possible antioxidant role (Boulton *et al.*, 2001b; Davies and Morland, 2004b). However, lipofuscin appears to be a generator of ROS and is largely responsible for the "blue light" damage (Rozanowska *et al.*, 1995). The supporting factors for lipofuscin's role in damage to the retina and RPE can be attributed to its accumulation with age and the changing absorption properties of the ageing lens (Delori *et al.*, 2001).

1.5.6 Cellular/Molecular Damage Effects from Light Damage of the Retina/RPE

The ability for light to cause significant damage to the retina/RPE not only depends on exposure duration, temperature and wavelength of the inducing light, but also on the chromophore concentrations, environmental conditions and absorption of other ocular tissues (Organisciak and Winkler, 1994). Intense light initiates damage and then a cascade of cellular events occur, which ultimately lead to photoreceptor necrosis or apoptosis (Gordon *et al.*, 2002). A number of morphologic changes have been documented in the photoreceptors, including vesiculation of the discs, mitochondrial swelling, dense cytoplasm and nuclear pyknosis signifying DNA loss and death of the cell (Noell 1958, Moriya *et al.*, 1986, Gordon *et al.*, 2002).

ROS, generated due to intense light exposure and in combination with lipid mediators have also been shown to induce retinal damage (Remé *et al.*, 1998). Lipid mediators and oxidative

stress can initiate a number of different inter or intracellular pathways, which can activate cytokines and initiate apoptosis or activate macrophages which lead to inflammation, cell proliferation and cell death (Remé *et al.,* 1998).

1.6 α- Crystallins

The α-crystallin gene family consists of: αA (see **Section 1.6.1**) and αB (see **Section 1.6.1**) with 4 major 20kDa subunits: αA, αA1, αB, and αB1. In their native state, α-crystallins are the largest of the lens crystallins with molecular masses ranging from 600-900kDa. Both αA and αB-crystallin share a 57% amino acid sequence homology and exhibit a 3:1 molar ratio of αA:αB subunits (Berman 1991a, Horwitz 1993, Horwitz *et al.,* 1999, Andley *et al.,* 2000, Horwitz 2003). Post-translational modifications of these peptides gives rise to other α-crystallin subunits (Bloemendal *et al.,* 2004; Boulton and Saxby, 2004).

In addition, the α-crystallins belong to the family of small heat shock proteins (see **Section 1.7**) and can act as molecular chaperones (Horwitz 1992, Boyle and Takemoto, 1994, Wang *et al.,* 1995, Andley *et al.,* 1996, Derham and Harding,1999, Horwitz 2000, Derham and Harding, 2002, Horwitz 2003, Thiagarajan *et al.,* 2004 Cheng *et al.,* 2008, Ecroyd and Carver, 2008, Ghosh *et al.,* 2008, Tanaka *et al.,* 2008).

1.6.1 αA- and αB-Crystallins

The αA-crystallin gene, a member of the small heat shock protein family, exhibits chaperone activity (**see Section 1.6.2**), is found on chromosome 21, and encodes for a 173 amino acid protein. αA-crystallin chains are synthesized and phosphorylated mainly, if not entirely, in the differentiating lens fiber cells (Berman 1991). Initially thought to be lens-specific (see **Section 1.6.3**) , αA- expression has also been found in the spleen, thymus, brain, and retina

(**see Section 1.6.4**) (Bhat *et al.*, 1991, Kato *et al.*, 1991, Horwitz 1992, Srinivasan *et al.*, 1992, Deretic *et al.*, 1994). The promoter region of αA-crystallin has four areas that are highly conserved between the mouse, human and chicken (Boulton and Saxby, 2004). Although highly conserved, the function of αA-crystallin is varied between the different species.

The αB-crystallin gene is found on chromosome 11 and encodes for a 175 amino acid protein. αB-crystallin is also a member of the sHSP superfamily and functions as a molecular chaperone. Due to its role as a member of the sHSPs, expression of αB-crystallin is universal in stressed biological systems and abundant in cells with minimal mitotic capacity (Groenen PTJA, *et al.*, 1994; Alge *et al.*, 2002). Besides being expressed in the lens, ocular expression of α-B has also been found in rat retinal pigmented epithelium (RPE) (Nishikawa *et al.*, 1994), ciliary body and iris (Iwaki *et al.*, 1990) and retina (Iwaki *et al.*, 1990, Xi *et al.*, 2003a). In addition, mRNA levels of αB have been detected in the following murine tissues: RPE, iris, ciliary body, cornea and optic nerve (Robinson and Overbeek, 1996).

1.6.2 α-Crystallins as Molecular Chaperones

Molecular chaperones belong to a class of proteins that performs a number of cellular duties including: stabilization of native protein conformations, protein folding, and the correct oligomeric assembly of proteins; protection of other proteins from heat denaturation or other cellular stresses, and finally translocation of proteins (; Ellis and van der Vies, 1991, Horwitz 1992). α-crystallin was initially classified as a molecular chaperone by Horwitz in 1992, based on its *in vitro* ability to prevent the heat-induced aggregation of proteins and enzymes in the lens (Horwitz 1992). α-crystallin traps unfolded or denatured proteins and suppresses

their non-specific irreversible aggregation of these proteins (Derham and Harding, 1999), although it does not participate in the refolding of these denatured proteins (Jakob *et al.*, 1993; Das and Surewicz, 1995). The function of α-crystallin in suppressing protein aggregation is important in the maintenance of lens transparency (Bloemendal *et al.*, 2004).

1.6.3 Lenticular Role of α-Crystallins

The lenticular roles of α-crystallins include maintaining the refractive index (Tardieu 1998) and lens transparency, protecting lens enzymes from inactivation due to glycation, steroids or cyanate insults (Derham and Harding, 1999) and interacting with the lens cytoskeletal elements (Fitzgerald and Graham, 1991). In addition, the α-crystallins exhibit their role as molecular chaperones in the lens by serving as a one-way 'sink' by binding and controlling the unavoidable denaturation of proteins associated with aging. Since there is no turnover of proteins or repair mechanisms in the lens fiber cells, α-crystallin binds the denatured proteins, to avoid aggregation, which would ultimately lead to light scattering and cataracts (Horwitz *et al.*, 1999).

The expression of αA-crystallin is necessary not only for the maintenance of lens transparency, but also for controlling the solubility of other crystallins in the lens (Brady *et al.*, 1997; Xi *et al.*, 2003a). The role of αA-crystallin is easily demonstrated in gene knockout studies. In 1997, Brady *et al.*, produced an αA-crystallin knock out mouse, which resulted in cataract development starting in the nuclear area with progression involving the entire lens. In addition to the development of a cataract, dense inclusion bodies were also discovered, consisting of αB-crystallin (Brady *et al.*, 1997) as well as γ-crystallin (Horwitz, 2003). This study concluded that αA-crystallin was not only important in the maintenance of lens transparency, but also played a role in controlling the solubility of other crystallins. Xi *et al.*

(2003b) also found that with the absence of αA-crystallin there was an increase of cell death *in vivo* during the mitotic phase.

Genomic stability may be maintained by the presence of αB-crystallin (Andley *et al.*, 2001). αB- mouse knockout studies revealed that the presence of αB is not necessary for normal lens development (Brady *et al.*, 2001). However, a surprising finding was the decreased life span of the knockout mice compared to the wild-type mice with the αB-crystallin gene. Knockout mice lost weight, developed degenerative osteoarthritis and died prematurely (Brady *et al.*, 2001). An additional finding from Andley *et al.* (2001), found that cells lacking the αB gene had a tendency to hyperproliferate.

1.6.4 α-Crystallins in the Retina

Once thought to be exclusive to the lens, α-crystallins are also expressed in the sensory retina and the RPE. Low levels of α-crystallin have been detected in frog retinal photoreceptors (in post-Golgi membranes) suggesting a role in rhodopsin trafficking (Deretic *et al.*, 1994). Furthermore and both αA- and αB-crystallin have been shown to prevent apoptosis through the inhibition of caspases (Kamradt *et al.*, 2001, Alge *et al.*, 2002). Increased expression of crystallins in light damaged photoreceptors and the decreased expression of αA-crystallin in the retinal dystrophic rat suggests a possible role for crystallins in protecting the photoreceptors from light damage (Crabb *et al.*, 2002; Sakaguchi *et al.*, 2003). In addition, crystallins were identified as components of retinal drusen in patients with macular degeneration (Crabb *et al.*, 2002). A recent study done by Rao *et al* (2008) revealed that αA-crystallin protected photoreceptors in experimentally induced uveitis and was upregulated in the diabetic retina of rats (Wang *et al.*, 2007).

Xi *et al.* (2003a) localized expression of αA and αB-crystallins to distinct retinal layers in the mouse retina. αA was distributed in the ganglion cell layer nuclei, and the inner and outer photoreceptor nuclear layers, but was undetectable in the photoreceptor inner and outer segments. αB was detected in the same retinal layers as αA, but was additionally found in the inner segments of the photoreceptors (Xi *et al.*, 2003a).

Alge *et al.* (2002) examined the expression of α-B crystallin in human RPE and found a greater baseline expression of αB-crystallin from the macular area compared to the peripheral area. Increased expression of αB-crystallin occurred with heat shock treatment and oxidative stress and αB- crystallin functioned as a stress-inducible anti-apoptotic protein in human RPE cells (Alge *et al.*, 2002).

Although the expression of the α-crystallins has been demonstrated in the retina, their specific roles remain a mystery. Expression in the retina of the α-crystallins could represent an adventitious form of expression, perhaps representing rudiments of early interactions between the developing lens and the optic vesicle (Jones *et al.*, 1999).

1.7 Small Heat Shock Protein Classification

Heat shock proteins (HSPs), originally identified on the basis of their increased synthesis after cellular exposure to high temperature (Lindquist 1986), are ubiquitously expressed in multiple tissues. They are classified into families according to their molecular weight. The four most common groups of HSPs are: **HSP70, HSP60, HSP40** and **sHSPs.** The sHSPs are the lowest molecular weight family, having subunits less than 35kDa (Derham and Harding, 1999).

Initial classification of the α-crystallins as a sHSP and molecular chaperones (**see section 1.6.1**) was in 1983 when Craig *et al.* discovered a 55% nucleotide sequence homology between the *Drosophila* sHSPs and α-crystallin. Most sHSPs exert strong cytoprotective effects (Alge *et al.*, 2002), act as molecular chaperones, and have been identified in the RPE (Wong and Lin, 1989).

The role of αB-crystallin as a member of the sHSP family was shown through induction by heat stress (Klemenz *et al.*, 1991) and hypertonic stress (Dasgupta *et al.*, 1992).

1.8 Transgenic Mice

Animal models of retinal degeneration have provided a better understanding of disease pathogenesis and have led to the development of novel therapeutic strategies (Delyfer et al., 2004). Recent construction of the α-crystallin knock-out mice has been useful in examination of the lenticular and non-lenticular roles that α-crystallins may play in the eye. Of interest to this study is the αA-crystallin gene knock-out mice created on 129SvJae_129SvEv (Brady *et al.*, 1997, Brady *et al.*, 2001) (Please see **Section 1.6.3)**

1.8 Aims of this Study

The following chapters will examine an *in-vitro* and *in-vivo* investigation into the possible protective role of the α-crystallins in the murine retina. Initially, it will examine the mitochondrial viability of the primary RPE cultures from wild-type and αA-crystallin knock-out mice in response to two well known oxidative agents, hydrogen peroxide (H_2O_2) and *tert*-butylhydroperoxide (t-BOOH) (**Chapter 3**).

Chapters 4, 5, and 6 will provide an insight into the *in-vivo* mechanisms involved in moderate intensity, continuous blue light exposure in a non-pigmented model and two pigmented strains, wild-type mice and αA-crystallin knock-out mice. **Chapter 4** utilizes an albino model, BALB/cBYJ model to confirm the potential for damage from the designed light apparatus, while **Chapters 5 and 6** examine the effect of continuous exposure in pigmented mice that have the αA-crystallin protein (**Chapter 5, Wild-Type)** and those that lack αA-crystallin (**Chapter 6, Knock-Out).** *In-vivo* mechanisms will be analyzed on a morphological and functional level by examining retinal histology and electroretinography respectively.

These chapters will provide insight and a better understanding of retinal α-crystallins and examine the hypothesis that ***αA-crystallin acts as a molecular chaperone and demonstrates protective roles in the RPE and retina in response to oxidative stress and moderate photochemical retinal damage.***

Chapter 2.0:
General Methods

2.1 Tissue Culture

2.1.1 Cell Culture Media and Supplements

Ham's F10 Nutrient Medium, and DMEM cell culture medium for the maintenance of RPE cells, was purchased from Invitrogen, UK or Invitrogen USA. Supplemental cell culture components, glutamine, streptomycin, MEM, kanamycin and penicillin were purchased from Sigma, UK or Sigma, USA; fungizone and fetal calf serum (FCS) were purchased from Invitrogen, UK or Invitrogen USA.

2.1.2 Isolation, Growth & Maintenance of Human Primary RPE Cell Cultures

Human donor eyes were obtained from the Bristol Eye Bank or the National Disease Research Interchange (NDRI, Philadelphia, PA) within 48 hours of post-mortem. The donors ranged in age between 18 and 93 years. None of the donors had a known history of eye disease (*all tissue received in the UK had prior permission for utilization in research purposes as well as those received in the US; see* ***Appendix 1***).

Human RPE cells were harvested as described previously (Boulton *et al.,* 1983) with minor adaptations. In brief, for the isolation of the RPE cells, the anterior segment of the eye was separated by circumferential incision, just posterior to the ora serrata. The vitreous was gently removed and the neuroretina was detached from the underlying RPE layer by dissection at the optic nerve. The remaining eyecup was washed with fresh, sterile phosphate-buffered saline (PBS) and then treated with 0.25% trypsin/0.02% EDTA solution (Sigma UK or Sigma USA). The eyecup was placed in a humidified 5% CO_2 / 95% air incubator at 37°C for 1 hr to allow the RPE cells to sufficiently detach from Bruch's membrane. After 1 hr, detached

RPE cells were gently collected by mixing growth medium consisting of Ham's F10 nutrient medium supplemented with 20% v/v FCS, 2mM glutamine, and antibiotics (100μg/ml streptomycin, 100μg/ml kanamycin and 60μg/ml penicillin) and then plated in a 6-welled plate (Triple Red, UK or Fisher Scientific, USA). After vigorous break up of the RPE cells, 1000μL of supernatant containing growth medium and cells was plated into 4 wells of a 6-welled plated. The 6-welled plate was examined daily through light microscopy, confirming cell attachment and growth (Cell attachment and growth characteristics of RPE cells can be found in 3.4.1 – 3.4.3) (From this point forward, **growth medium** will be referring to Ham's F10 nutrient medium supplemented with the above-mentioned components).

The newly isolated RPE cells were maintained at 37°C in a humidified 5% CO_2 / 95% air incubator with the growth medium being changed every 3-4 days until the cells had become confluent, as visualized by inverted light microscopy (Olympus 1X70 or Nikon DS). Typical times to confluency averaged 20 – 24 days. Confluency was measured by coverage of 95% - 100% of coverage on the bottom of the 6-welled plate. Once the primary RPE cells reached confluency, they were sub cultured by gently removing the growth medium and washing with sterile, ice cold PBS. After removal of the PBS, 0.25% trypsin/0.02% EDTA solution was added and incubated at 37°C for approximately 1-2min. After the detachment of the RPE monolayer, ~1ml of growth medium was added to neutralize the action of the trypsin. The RPE cells were pelleted by centrifugation at 700*g* for 5min at 4°C. The supernatant was discarded while the pellet was resuspended in pre-warmed growth medium and added to a 25cm^2 cell culture flask.

This newly sub cultured RPE primary culture was maintained at 37°C in a humidified 5% CO_2 / 95% air incubator with the growth medium being changed every 3-4 days until the cells

had become confluent. At this point the RPE cultures were either used for experimentation, were spilt at a ratio of 1:3 for further cell culturing or stored in liquid nitrogen for future use.

2.1.3 Growth and Maintenance ARPE-19 Human Cell Line

ARPE-19 is a spontaneously arising RPE cell line derived from the normal eyes of a 19-year-old male donor. Cells form stable monolayers, which exhibit morphological and functional polarity (Dunn *et al.*, 1996).

The human RPE cell line ARPE-19 (CRL-2302, American Type Culture Collection, Rockville, MD) was grown and maintained at 37°C in a humidified 5% CO_2 / 95% air incubator with the growth medium being changed every 3-4 days until the cells had become confluent. Once the ARPE19 cells had reached confluence, as observed with inverted light microscopy, (Olympus 1X70 or Nikon DS), cells were either used for experimentation, were spilt at a ratio of 1:3 for further cell culturing or stored in liquid nitrogen for future use.

2.1.4 Isolation, Growth and Maintenance of Primary Wild-Type or αA-crystallin Knock-Out Mice RPE Cell Cultures

Mice eyes (both 129Sv wild-type and αA-crystallin knock-out) were obtained from the animal colony at the Comparative Medical Center located at Salus University. Originally, 129Sv wild-type mice were purchased from Taconic Animal Facilities (Rockville, MD) and αA-crystallin knock-out mice were a generous gift from Eric Wawrousek, PhD at the Transgenics and Genome Manipulation Division of the National Eye Institute (NIH, Bethesda, MD). All animals were treated according to the regulations in the ARVO Statement for the Use of Animals in Ophthalmic and Vision Research and regulations of the Institutional Animal Care and Use Committee (IACUC) at Salus University (*please refer to the **Appendix 1** for colony maintenance protocols and certifications).*

Mice RPE cells were harvested as described previously (Gibbs and Williams, 2003) with minor adaptations. Optimal age for RPE isolation occurred between 10-14 days post natal due to the lack of photoreceptors fully reaching the apical surface of the RPE, creating a cleaner detachment of the neuroretina from the underlying RPE. Isolation of RPE cells occurred in lots of 10 (i.e. 5 mice were euthanized per isolation yielding a total of 10 eyes).

Eyes were gently removed with fine curved forceps and then washed in serum-free DMEM supplemented with 1X MEM non-essential amino acids and penicillin/streptomycin. Washed eyes were then transferred to a 2% dispase solution in DMEM and incubated at 37°C for 45 minutes with gentle agitation every 15-20 minutes. After designated incubation, eyes were washed twice with serum supplemented DMEM and transferred to a Petri dish of serum supplemented DMEM buffered with 20mM HEPES. Under a tungsten Stereomaster dissection microscope (Fisher Scientific, USA), all surrounding extraocular muscles, hair and connective tissue were removed, leaving a solid, clean globe. A circumferential incision was made at the corneal limbus and the anterior segment was gently removed and discarded. Since the murine lens occupies about 75% of the intraocular space (Zinn and Mockel-Pohl, 1973; Marshall *et al.*, 1982), extreme care was used to remove the lens so there was no disruption of the anterior/posterior lens capsule, resulting in lysis of lens fiber cells and possible false detection of the α-crystallins in the RPE and/or neural retina (RPE cells were only gathered from eyes with isolated, intact, murine lens to avoid this false detection).

Posterior eye cups only containing neural retina, underlying RPE and choroid were then incubated for 20 minutes at 37°C in a humidified 5% CO_2 / 95% air incubator in serum supplemented DMEM. After incubation, neural retina was gently peeled away from the underlying RPE and choroid. Remaining posterior eye cups were inverted and gently

agitated from side to side breaking off sheets of RPE cells. All sheets of RPE cells were pulled into a 15ml conical tube containing sterile serum supplemented DMEM and centrifuged at 1500rpms for 3 minutes at 4°C. After centrifugation, cells were resuspended in 0.05% trypsin solution, gently pipetted up and down to break up cells and then incubated at room temperature for 3-4 minutes. Sterile, serum supplemented DMEM was added to neutralize the trypsin solution and cells were then centrifuged at 1500rpms for 5 minutes at 4°C. Medium was removed and cells were washed again with serum supplemented DMEM and then centrifuged at 1500rpms for 3.5 minutes at 4°C. Medium was removed and pellet was resuspended in 20% fetal calf serum supplemented DMEM and plated into 2 or 3 wells of a sterile 24-welled plate.

This newly sub cultured RPE primary culture was maintained at 37°C in a humidified 5% CO_2 / 95% air incubator with the growth medium being changed every 3-4 days until the cells had become confluent. At this point the RPE cultures were either used for experimentation, were spilt at a ratio of 1:3 for further cell culturing or stored in liquid nitrogen for future use.

2.1.5 Determination of Human Primary RPE and Mouse RPE Cell Purity with Cytokeratin

To determine the purity of the isolated human primary RPE cells, immunostaining for cytokeratin, as previously described by McKechnie et al (1988), was performed on RPE cells at passages 2 or 3. Primary cells were plated onto sterile coverslips in a 24-welled plate (Triple Red, UK or Fisher Scientific, USA) with growth medium and grown for 1-2 days until nearly confluent. The medium was aspirated and the cells were washed 3 times with sterile PBS for 5 mins. The cells were fixed by immersion in 70% ethanol for 5min and then the ethanol was removed and cells were washed twice with PBS for 5min. Cells were permeabilized with 0.1% Triton X-100 (Sigma, UK or Sigma, USA) (v/v PBS) for 10

minutes and then washed three times with PBS for 5 mins. The primary monoclonal antibody, anti-cytokeratin peptide 18–FITC (Sigma, UK or Sigma, USA) was diluted 1:100 in PBS and for nuclear labeling, 3µl of Hoechst (1mg/ml) (Sigma, UK or Sigma, USA) was added per ml of antibody solution (i.e. anti-cytokertatin and PBS); a final volume of 250µl of antibody solution per well. The 24-welled plate was covered in aluminum foil and incubated at room temperature for 2 hrs. Cells were washed 5 times with PBS and mounted on microscope slides using Hydromount (DiaMed, Canada). The cells were observed through an upright microscope (Leica DMRA2) using a FITC/DAPI filters and analyzed using Leica Q-Fluro Software (Leica Microsystems Ltd., UK). Cells that did not stain positive for cytokeratin were discarded and not used for experimentation.

2.1.6 Storage of Cell Cultures in Liquid Nitrogen

Cells to be utilized in the future were stored in cryotubes (Triple Red, UK) in a liquid nitrogen refrigeration chamber. Briefly, after trypsinization for 1-2min, detached cells were pelleted by centrifugation at 5000*g* for 7min at 4°C. The supernatant was discarded and the pellet was resuspended in 10% v/v dimethylsulphoxide (DMSO) (Sigma, UK or Sigma, USA) prepared in pre-warmed FCS (Invitrogen, UK or Invitrogen USA).

2.1.7 Analysis of Cell Morphology

Primary human RPE and ARPE-19 cell growth was observed with an inverted light microscope (Olympus 1X70) and photodocumented using an image analysis system (Image-Pro Plus, Version 4.1, Media Cybernetics, MD, USA).

Primary wild-type and αA-crystallin knock-out mice RPE cell growth was observed with a Nikon Phase Contrast Microscope (Nikon DS-Fi1 digital camera) and photodocumented using an image analysis system (NIS-Elements F2.30).

2.2 α-Crystallin Expression in Primary Human RPE and the ARPE-19

Initial studies investigated the *in-vitro* expression of α-crystallins in primary Human RPE and ARPE-19 cells. mRNA and protein expression was performed with Reverse Transcriptase Polymerase Chain Reaction (RT-PCR) and Western Blotting, respectively.

2.2.1 Total RNA Isolation

Total RNA was isolated with TRIzol reagent (Invitrogen, UK) from ARPE19 and primary human RPE cells using the manufacturer's protocol. Initially, cells were washed with PBS and then lysed by adding 1ml of TRIzol reagent to the monolayer. Cells were incubated at room temperature for 5min and the monolayer was disrupted with a cell scraper to allow the complete dissociation of nucleoprotein complexes. Chloroform was added (0.2ml) to the solution, shaken vigorously, allowed to sit at room temperature for 3 minutes, and centrifuged at 12,000*g* for 15 minutes at 4°C. Following centrifugation, the mixture formed three phases; the lower red, phenol-chloroform phase, an interphase and an upper aqueous phase. The phenol-chloroform phase contained proteins, the inter-phase contained DNA and the upper aqueous phase contained the RNA. The aqueous phase was collected and transferred to an RNase-free eppendorf tube. The RNA was precipitated with 0.5 mL isopropyl alcohol overnight at -20°C.

After overnight precipitation, RNA was centrifuged at 12,000*g* for 10 minutes at 4°C, forming a gel-like pellet on the sides and bottom of the eppendorf tube. The supernatant was removed; the RNA pellet was washed with 75% ethanol, vortexed and centrifuged at 7500*g*

for 5min at 4°C. Ethanol was removed and the pellet was air-dried for approx 15 min. The air-dried RNA pellet was dissolved in 50µl of RNase-free water.

The concentrations and purity of the RNA were determined by ultraviolet spectroscopy (Gene-Quant II, Pharmacia-Biotech, Cambridge, UK) and by UV visualization on a denaturing formaldehyde-agarose gel (see **section 2.2.2**). The newly extracted RNA was either used immediately for RT-PCR analysis (see **section 2.2.6**) or frozen at -20°C.

2.2.2 RNA Formaldehyde Denaturing Gel and UV Transillumination

The quality of the isolated RNA samples was assessed via electrophoresis on a denaturing formaldehyde-agarose gel. Because RNA is single-stranded and able to form secondary structures by intramolecular base pairing, it must be electrophoresed under denaturing conditions. The facilitation of a denaturing environment is achieved by the addition of formaldehyde. For a 1.5% final formaldehyde-agarose gel concentration, 1.5g of agarose was heated in 72ml of RNase-free water and cooled to 60°C. After sufficient cooling, 10ml of 10X MOPS buffer (0.04M MOPS (Sigma, UK), pH 7.0, 0.01M Sodium Acetate (Sigma, UK), 0.001M EDTA (Sigma, UK)) and 18ml of 37% formaldehyde (Fisher Bio-Reagents, UK) were added and the gel was allowed to solidify.

A denaturation reaction, consisting of 4.5µL of isolated RNA in 2.0µl 10X MOPS, 3.5µl of 37% formaldehyde, 10.0µl of formamide (Fisher Bio-Reagents, UK), and 0.5µL of ethidium bromide, was heated at 55°C for 15min. Reactions were chilled on ice for 1 minute and then mixed with loading dye (Promega, UK) in a 6:1 ratio.

Approximately 20µl of the denaturing RNA reaction was loaded to the gel and underwent electrophoresis with a running buffer consisting of double-autoclaved water, 10X MOPS and 37% formaldehyde. Gel was run at 60V for 45 minutes. After electrophoresis, the gel was visualized and digitally photographed on a UV transilluminator (UVIdoc Gel Documentation System, Jencons, UK).

2.2.3 Protein Isolation

Proteins were isolated from ARPE19 and primary human RPE cells using RIPA Lysis Buffer (0.5M Tris-HCl, pH 7.4, 1.5M NaCl, 2.5% deoxycholic acid, 10% NP-40, 10mM EDTA) (Upstate, USA) with additive protease inhibitor cocktail (Sigma, UK). Briefly, cells were washed twice with ice cold PBS and then incubated on ice with 1ml of RIPA Lysis Buffer and protease inhibitor cocktail (1ml of cocktail solution for every 100ml of lysis buffer). After 45 minutes of incubation, the monolayer of cells was disrupted with a cell scraper, breaking up cells and releasing proteins. Cells were centrifuged at 12000*g* for 30 minutes at 4°C. After centrifugation, the supernatant was transferred to fresh eppendorf tubes and stored at -20°C for future use. The protein content was measured by the bicinchoninic acid (BCA) protein assay (Pierce, Rockford, IL, USA) (see section **2.2.4**).

2.2.4 Determination of Protein Concentration

Protein concentration levels were measured using the BCA protein assay kit (Pierce Chemical Co., Rockford, IL, USA) according to the manufacturer's protocol. Briefly, an aliquot (25µl) of the unknown sample or bovine serum albumin (BSA) standard was transferred into a microplate well (Triple Red, UK). The working reagent was added (200µl) and thoroughly mixed with the protein sample at room temperature for 30 seconds. The microplate was covered and then incubated at 37°C for 30min. After incubation, the microplate was cooled to room temperature and the absorbance was read using a microplate reader with a 590-nm filter

(Labsystems, Multiskan Ascent, UK). The concentration of protein was determined from a standard curve of known BSA standards (0, 25, 125, 250, 500, 750, 1000, 1500 and 2000µg/ml). (For SDS-PAGE electophoresis and Western Blotting, see **Sections 2.5.3 and 2.5.5,** respectively).

2.2.5 PCR Primers for Human αA-, and αB-Crystallin

Primers for each human α-crystallin gene (αA- and αB-) were described by Hawse et al. 2003 (please **see Table 2.1**). These oligonucleotide gene-specific primers (OPERON Biotechnologies, Germany) were used in PCR reactions (**see 2.2.7**) for examining mRNA expression.

Gene	Sequence (5'→3')	Amplicon Size (bp)	Annealing Temp (°C)
CRYAA	CCACCTCGGCTCCCTCGTCCTAAG (Sense) CCATGTCCCCAAGAGCGGCACTAC (Anti-)	492	64
CRYAB	AGCCGCCTCTTTGACCAGTTCTTC (Sense) GCGGTGACAGCAGGCTTCTCTTC (Anti-)	452	60

Table 2.1 Human αA-, αB-crystallin and Gene Specific Primers

2.2.6 Reverse Transcriptase – Polymerase Chain Reaction (RT-PCR)

After confirming the structural integrity of the isolated RNA samples by electrophoresis, Total RNA was used to synthesize cDNA according to the manufacturer's protocol provided with the Reverse-iT™ 1st Strand Synthesis Kit (AB gene, UK). All reactions were performed in a thermocycler (DNA Engine, DYAD, UK). In a sterile eppendorf tube, 1.5µg of Total RNA was combined with 1µl of anchored oligo dT (500ng) and double-autoclaved water to give a final volume of 12µl. The combined components were heated at 70°C for 5min to remove any secondary structures and then placed on ice. The first strand cDNA synthesis reaction was performed in 20µl reactions composed of 4µl of 5X first strand synthesis buffer, 2µl of dNTP mix (5mM), 1µl of DTT (100mM) and 1µl of *Reverse*-iT™ RTase (negative

controls of cDNA synthesis were carried out under the same experimental conditions, but in the absence of *Reverse*-iT™ RTase Blend). The reactions were incubated at 47°C for 50min and then terminated at 75°C for 10min to inactivate the *Reverse*-iT™ RTase Blend. The newly synthesized cDNA was either used immediately for PCR analysis or frozen at -20°C.

2.2.7 PCR Amplification of α-crystallin in Primary RPE and ARPE19 Cells

PCR amplification of the cDNA was performed according to the manufacturer's protocol provided with GeneAmp® XL PCR (Applied BioSystems, UK) in a DNA thermocycler (DNA Engine, DYAD, UK). PCR amplifications were performed in a total reaction volume of 100µl with 500ng of cDNA, 200µM dNTPs, 10µM of primers, 3.3XL PCR Buffer II (50mM Tris-HCL (pH 8.0), 100mM NaCl, 0.1mM EDTA, 1mM DTT, 50% glycerol and 1% Triton X-100), 1.5mM $MgCl_2$ and 1 unit of XL r*Tth* Polymerase. PCR reactions were initially incubated at 94°C for 30 secs to completely denature the template and activate the *Taq* polymerase enzyme. This was then followed by 30 cycles of denaturation at 94°C for 30secs, primer annealing from 60-64°C (depending on the gene of interest, see Table 2.3) for 30 secs and primer extension at 72°C for 40 secs. PCR amplification products were separated by agarose gel electrophoresis and stained with ethidium bromide for visualization (**section 2.2.8**). PCR performed on each sample of RNA that had not been reverse transcribed to cDNA was used as a negative control and showed no amplified product.

2.2.8 Agarose Gel Electrophoresis and UV Transillumination

Aliquots of the PCR product were mixed with blue/orange loading dye (Promega, UK) in a 6:1 ratio and loaded onto a 1.5% agarose gel stained with 0.01% of ethidium bromide (10mg/ml). Agarose gel was run at 80V for 40min in 1x TBE running buffer. After

electrophoresis, the gel was visualized and digitally photographed on a UV transilluminator (UVIdoc Gel Documentation System, Jencons, UK).

2.2.9 Exposure of the ARPE19, Primary Human RPE, WT and αA K/O RPE to Oxidative Stressors Hydrogen Peroxide (H_2O_2) and *tert*-butylhydroperoxide (*t*-BOOH)

All RPE cell types were plated into 6-welled plates (Triple Red, UK); 3 wells of cells corresponded to each concentration of the oxidative stressors (0μM, 100μM and 200μM) for 24hrs. Immediately prior to the experiment, oxidative stressors were diluted in serum-free Ham's F10 to achieve the desired final concentration. Prior to exposure, growth medium was removed and the cell cultures were washed once with sterile, ice cold PBS. PBS was removed and the oxidative stressors were added to the cells for 24hrs. During the exposure to the oxidative stressors, all cells were maintained at 37°C with 5%CO_2 / 95% air in a humidified incubator.

After the indicated oxidative exposure, cells were again washed twice with PBS and the 3-(4,5-dimethylthiazol-2-yl)-2,5-diphenyl tetrazolium bromide (MTT) cell viability assay was performed (**see Section 2.2.10**). The control cell monolayers were treated with cell culture medium without additive FCS.

2.2.10 3-(4,5-dimethylthiazol-2-yl)-2,5-diphenyl tetrazolium bromide (MTT) Cell Viability Assay

Cell viability can be determined by dehydrogenase activity, which indicates the activity of mitochondria. Dehydrogenase converts (3-[4,5-dimethylthiazol-2-yl]-2,5-diphenyl tetrazolium bromide (MTT) into purple MTT formazan, causing a colorimetric change that can be monitored photometrically. Cell viabilities of the treated and untreated RPE cells were measured by the ability of succinate dehydrogenase to convert into visible formazan crystals. The MTT assay was performed as described by Mosmann (1983) with some modifications. In

brief, after complete removal of the oxidative stressor medium, all cells were washed twice with sterile PBS and 0.5mg/ml of MTT was added to each flask. ARPE-19 cells were then incubated at 37°C for 3 hrs in a 5%CO_2 / 95% air humidified incubator. After incubation, the MTT solution was removed and acidified isopropanol containing 0.04M of HCl was added to dissolve the resultant formazan crystals. Aliquots (125µl) were transferred 96-welled plated (Company, UK) and absorbance at 590nm was measured on a microplate reader (Labsystems, Multiskan Ascent, UK). The number of attached living cells was proportional to the absorbance of MTT at 590 nm. Samples were run in triplicate and the cell viability was determined using the MTT reduction values for the treated samples, which were expressed as a percentage of the non-treated normalized control samples.

2.3 Exposure of Mice to Blue Light

2.3.1 Mice

129Sv wild-type mice, αA-crystallin knock-out mice (129Sv:CRYA1) and BALB/cBYJ albino mice were maintained at the Comparative Medical Center at Salus University. Originally, 129Sv wild-type mice and BALB/cBYJ were purchased from Taconic Animal Facilities (Rockville, MD) and αA-crystallin knock-out mice were a generous gift from Eric Wawrousek, PhD at the Transgenics and Genome Manipulation Division of the National Eye Institute (NIH, Bethesda, MD). All animals were treated according to the regulations in the ARVO Statement for the Use of Animals in Ophthalmic and Vision Research and regulations of the Institutional Animal Care and Use Committee (IACUC) at Salus University.

2.3.2 Animal Colony Maintenance (*Please refer to the **Appendix** for colony maintenance protocols and certifications).*

All mice (BALB/cBYJ, 129Sv, 129Sv:CRYA1) were maintained at the Comparative Medical Center at Salus University. All animals were housed in Poly acrylic cages (19x20x13cm)

under hygienic conditions at normal room temperature (74–76 °F) on a 12-h light (300 lux)/dark cycle (50 lux). Maximum amount of animals per cage never exceeded 4. Mice were fed with Rodent 5001 commercial pellet diet (PMI Nutrition®, Henderson, CO, USA) (no supplemental antioxidants in food) and had free access to water at all times.

In order to maintain mice of the same genetic background to be used for experiments, breeding was necessary to maintain the homozygous transgenic lines. On average, between 20 and 30 breeding pairs of 129SV and 129Sv:CRYA1 mice were used yearly (all BALB/cBYJ mice purchased from Jackson Laboratories were female and no breeding occurred with this particular strain). During breeding conditions, each cage held one pair of a homozygous female and male. Gestation periods for all mice were 21days and males were separated from females after 19-20 days. Once separated, females were given a nesting pad and carefully checked on a daily basis until pups were delivered. Newly born pups were closely observed to assure that the mother was nursing. Three weeks after birth, progeny mice were ear tagged (see **Appendix 3**) and tails were clipped for future genotyping (see **Section 2.3.3**). Immediately after tagging and tail clipping females and males from the progeny were housed in separate cages, 4 mice per cage until used in experiment or for further breeding as described above.

*2.3.3 Genotyping of Mice (minor **Code A** procedure)*

Genotyping of all mice strains (129Sv, 129Sv:CRYA1, and BALB/cBYJ) was performed in order to determine the presence or absence of the αA-crystallin gene. This common technique has been previously described by Hogan *et al.*, (1994). In brief, mice 3 weeks of age were labeled with a small identification ear tag number (National Band and Tag Co., Newport, KY) (*please refer to the **Appendix 3** for the ear tag key used in experiments).* At the time of ear tagging, a small piece (~ **3-5** mm long) of the tip of the tail (wiped with 70%

ethanol just before the cutting) was clipped using a sterile razor blade wiped with ethanol. Various protocols use 0.5ml/L Isoflurane for anesthesia, but young mice such as the ones used, do not experience pain/distress during this minor procedure so the tail clipping for 3-weeks without anesthesia is widely used and commonly accepted practice (NIH Guidelines for the Genotyping of Rodents; Ren *et al.*, 2001; Campbell and Hess, 1997). In mice at <21 days, tissue near the tip of the tail is soft and the bones have not completely mineralized, therefore, removing of the tail tip of a young mouse yields minimal, momentary pain for the animal (NIH Guidelines for the Genotyping of Rodents). Short-term minor bleeding after the tail clipping was common and no special further treatment was required, however, before the animals were placed back into the cage, the bleeding was stopped by pressing on and holding with an aseptic glove at the end of the tail until the clot is completely formed. Tails were carefully placed into a sterile, labeled Eppendorf tube and stored at -20°C until DNA digestion could be performed.

Before PCR of the tails could be performed, digestion of DNA from the acquired tails was necessary. Tails were removed from the -20°C freezer and 500µl of nuclei lysis buffer (Promega, USA) and 20µl of Proteinase K (Invitrogen, US) was added and tails were incubated in a 55°C shaker for 3-5 days (the longer the tail, the longer the incubation).

After designated incubation with nuclear and protein lysis buffers, Eppendorf tubes containing the digested tails were cooled to room temperature. Protein precipitate solution (Invitrogen, US) was added to each tube, vigorously vortexed and incubated on ice for 5 minutes. Tubes were then centrifuged (x16000*g*) for 10 minutes) and 450 µl of the supernatant was transferred to a newly labeled Eppendorf tube containing 550µl of isopropanol (2-propanol) (Sigma, US). Eppendorf tubes were inverted multiple times,

centrifuged (x16000*g* for 10 minutes) and the supernatant was discarded. In order to make sure the supernatant was completely discarded, tubes were re-centrifuged at x16000*g* for 30 secs and remaining supernatant was gently removed. Remaining pellets were dissolved with 200µl of distilled H_2O and incubated for 20 minutes at 55°C. After incubation at 55°C, Eppendorf tubes were cooled to room temperature and 400µL of 300mM Sodium Acetate in 90% Ethanol (Sigma, US) was added and tubes incubated at room temperature for an additional 5-10minutes. Tubes were then centrifuged (x16000*g* for 10 minutes), supernatant was removed and tubes were re-centrifuged (x16000*g* for 30secs) to assure all supernatant was properly discarded. Remaining pellets were air-dried for 20 minutes and then re-suspended in 200µl of distilled water. DNA was either used immediately for PCR reactions or stored at -20°C.

In order to assure that the mice contained or lacked the αA-crystallin gene, primers were designed for the αA-crystallin K/O mice (**Table 2.2**), including the first exon between restriction enzymes sites, AatII and XhoI. Expected PCR product with the PGK neo insert was 3570bps (**Figure 2.1**).

	Sequence (5'→3')	Length	Tm
Forward Primer	TGGGAAATCCCTTAATTCCTCCATTCT	27	66
Reverse Primer	CTGATGGGAGGAAAAGACAGCAGTC	25	65

***Table 2.2** Forward and reverse primer design for the detection of αA-crystallin's presence or absence in 129Sv wild-type, αA-crystallin knock-out or BALB/cBYJ albino mice. Primers were purchased from Invitrogen.*

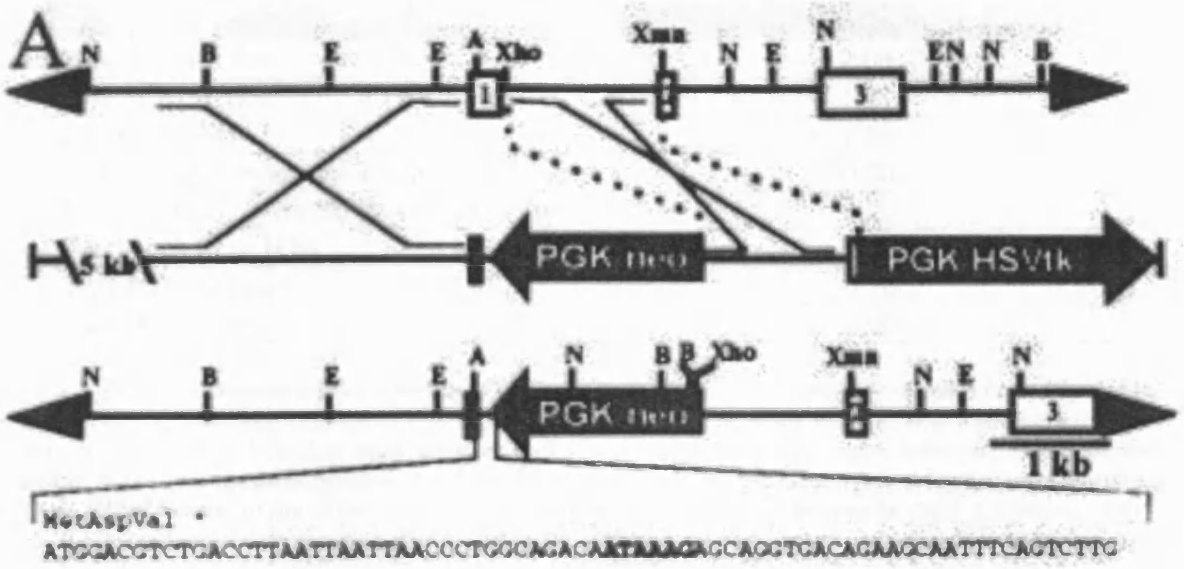

Figure 2.1 Shown above is the targeted disruption of the mouse αA-crystallin gene. (Top) Normal αA locus. (Middle) Targeting vector. (Bottom) Disrupted αA locus. The sequence of an oligonucleotide inserted between the 5ι αA sequences and PGK/neo containing multiple stop codons in all three reading frames and a polyadenylylation signal (enclosed in box) is shown beneath a diagram of the targeted allele. Depicted restriction sites include NcoI (N), BglI (B), EcoRI (E), AatII (A), XhoI, and XmnI. HSVtk, herpes simplex virus thymidine kinase. (Figure was taken directly from Brady et al. 1997 to illustrate area of target for the generation of the αA-crystallin knock-out transgenic mouse.

In order to determine the presence or absence of the αA-crystallin gene for experimental purposes, DNA obtained from the tail digestion underwent PCR reactions with αA-crystallin specific primers (see **Table 2.2**). PCR components (see **Table 2.3**) and parameters (see **Table 2.4**) are shown below. All PCR reactions were performed on the Robocycler Gradient 96 (Stratagene, US).

PCR Component	Volume of PCR Components (µL)
10X Taq Buffer	2.00
25mM MgCl2	1.21
2.5mM dNTP	1.60
100µM αA-Crystallin Forward Primer*	0.20
100µM αA-Crystallin Reverse Primer*	0.20
Nuclease-Free H20	12.80
Taq Polymerase	0.10
Sample DNA*	2.00

Table 2.3 *PCR components and volumes used for each individual DNA sample from mice tails. Depending on the number of reactions (including controls), a stock solution was made with the above components (except for *) and then 17.6µL of stock solution was added to individual Eppendorf tubes incubating on ice. *Denotes individual volumes added to the final stock solution. For control samples 2.00µl of nuclease-free H_20 was added instead of the DNA sample. Parameters of reactions can be seen in Table 2.3 below. αA-crystallin primer sequences can be found in Table 2.1. All components were purchased from (Invitrogen, US).*

PCR Step	Temperature	Time	Cycle Number
Initial Denaturation	95°C	3 min	1
Denaturation	95°C	1 min	27
Annealing	61°C	1 min 30 sec	
Extension	72°C	1 min 30 sec	
Final Extension	73°C	5 min	1
Soak	6°C	Indef.	1

Table 2.4 *Long-Range PCR Parameters for amplified DNA samples for the αA-crystallin gene. All reactions were performed on the Stratagene Robocycler Gradient 96. Each DNA sample was extracted from mice tails and underwent long-range PCR to determine the absence or presence of the αA-crystallin gene.*

A stock solution was made of all PCR components except for the forward and reverse primers, as well as the individual DNA sample (see **Table 2.3**). After the PCR reaction components were complete, all samples were topped with mineral oil prior to undergoing PCR to avoid any evaporation during the PCR reaction. Once samples were finished undergoing PCR, 10µl of sample and 10µL of nuclease-free H20 were added to pre-made 2% E-gels (Invitrogen, USA) and ran for 15 minutes. Bands were visualized with Ultra Lūm UV Transilluminator (Dual Wave, USA) and photographed with Photodocumentation Camera/Hood, FB-PDC-34 (Fisher Biotech, USA). The expected band, corresponding to the αA-crystallin gene, was present at 531bp.

2.3.4 Experimental Blue Light Apparatus

Pigmented (129Sv, and αA-crystallin knock-out), and non-pigmented (BALB/cBYJ albino) mice were exposed to blue light (400-480nm) at energy levels that do not produce immediate tissue response for periods of 24 - 168 hrs (1 – 7 days) to assess the location and degree of retinal damage (Seiler et al., 2000, Davies et al., 2001, Ham et al., 1980, Farrer et al., 1970).

The blue light apparatus caging consisted of 6 mounted, stainless steel fluorescent light holders bolted together, creating an enclosed box open at both ends. Each stainless steel mount held 2, 48" fluorescent bulbs (Philips Natural Sunshine, 40 watts; T12, Philips Lighting Company, Somerset, NJ, USA), therefore there were 4 on top, 2 on both sides and 4 on the bottom for a total of 12 lights (**see Figure 2.2A**). The radiant exposure produced by the 12 Phillips fluorescent tubes was filtered by blue gel filter material (Lee #197 Zenith Blue) that was wrapped around the caging inside the boxed fluorescent tubes (**see Figure**

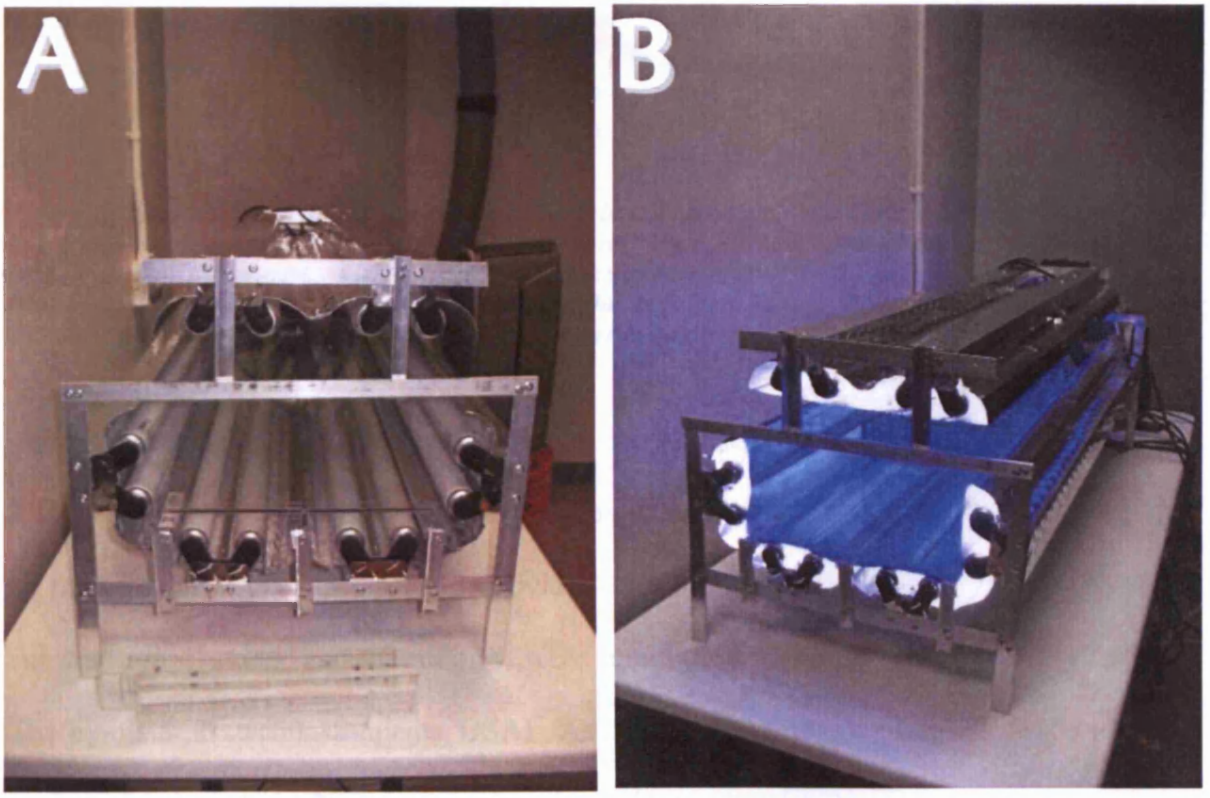

***Figure 2.2**: Shown in 'A' is the blue light apparatus caging consisting of 6 mounted, stainless steel fluorescent light holders bolted together, creating an enclosed box open at both ends. At one end of the apparatus is a fan and the other end is opened for un-interrupted airflow. Shown in the far right is an air-conditioner run during exposure to maintain acceptable temperature levels. Shown in 'B' is the apparatus with LEE Filter #197 Zenith Blue.*

This arrangement resulted in a net spectral exposure which was a close approximation of the Blue Light Hazard Function (BLHF) (**see Figure 2.3**), but which includes a small long wavelength window which has been seen typically in other experiments and is not considered to be significant to the photic damage outcomes (Seiler et al., 2000).

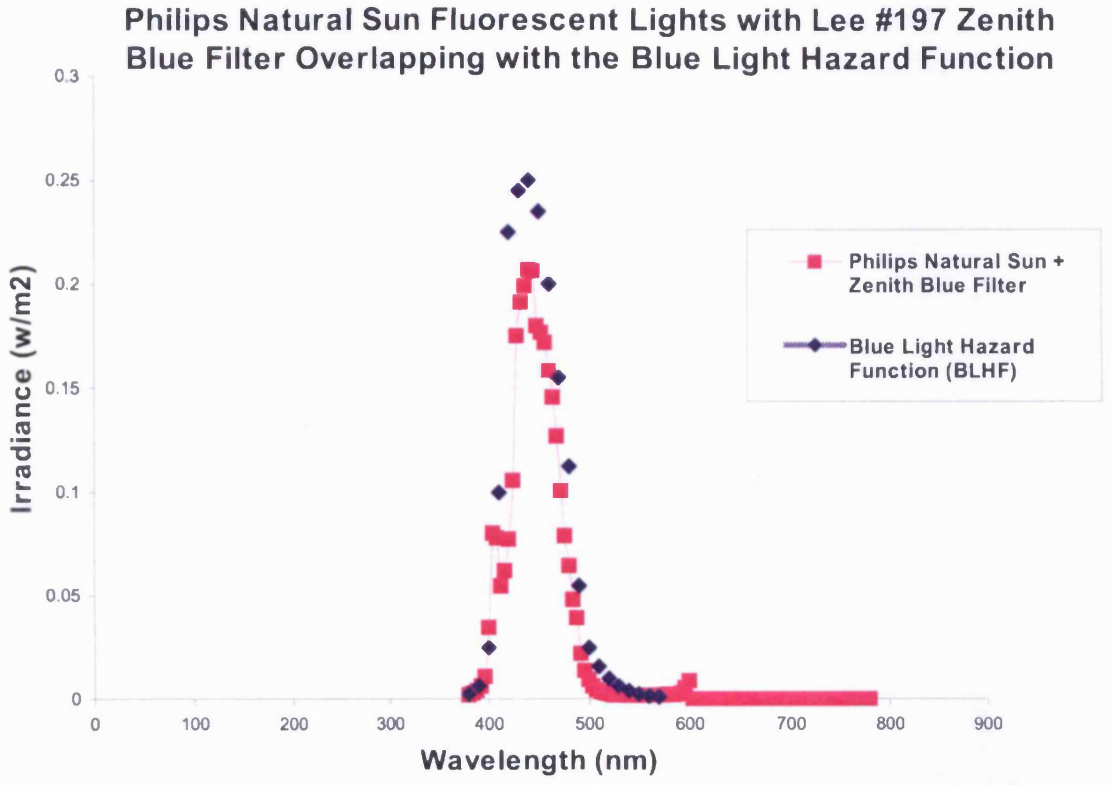

***Figure 2.3** Spectral range of light exposed to animals in the blue light apparatus. As shown, Philips Natural Sun Bulbs overlayed with #197 Zenith Blue Filter (Lee Filters, USA) creates a range of light in the BLHF (shown as blue diamonds). Visible light has a spectral range of 400–750 nm, however the high-energy (short-wavelength) part of the spectrum responsible for blue light hazard function (excitation peak around 440 nm) (Algvere et al., 2006) is reached with this experimental setup.*

The apparatus held 6 individual stainless steel cages measuring 5"Hx6"Wx11"L (**see Figures 2.4 C-F**). Caging temperature was kept low by using fans and an air conditioner to circulate air through the whole apparatus and individual cages. Additionally maximum, minimum and current temperatures and humidities were monitored twice a day (Big Digit Hygro-Thermometer, Extech Instruments, USA). As constructed, this apparatus was nearly identical to that of Seiler et al , 2000 and produced an illumination level (600 lux bottom – 1200lux

top) in the same range as that research group. Lux levels were measured at three points during the experiment (Day 1, 4 and 7) (Traceable Nist Calibrator, Fisher Scientific, USA).

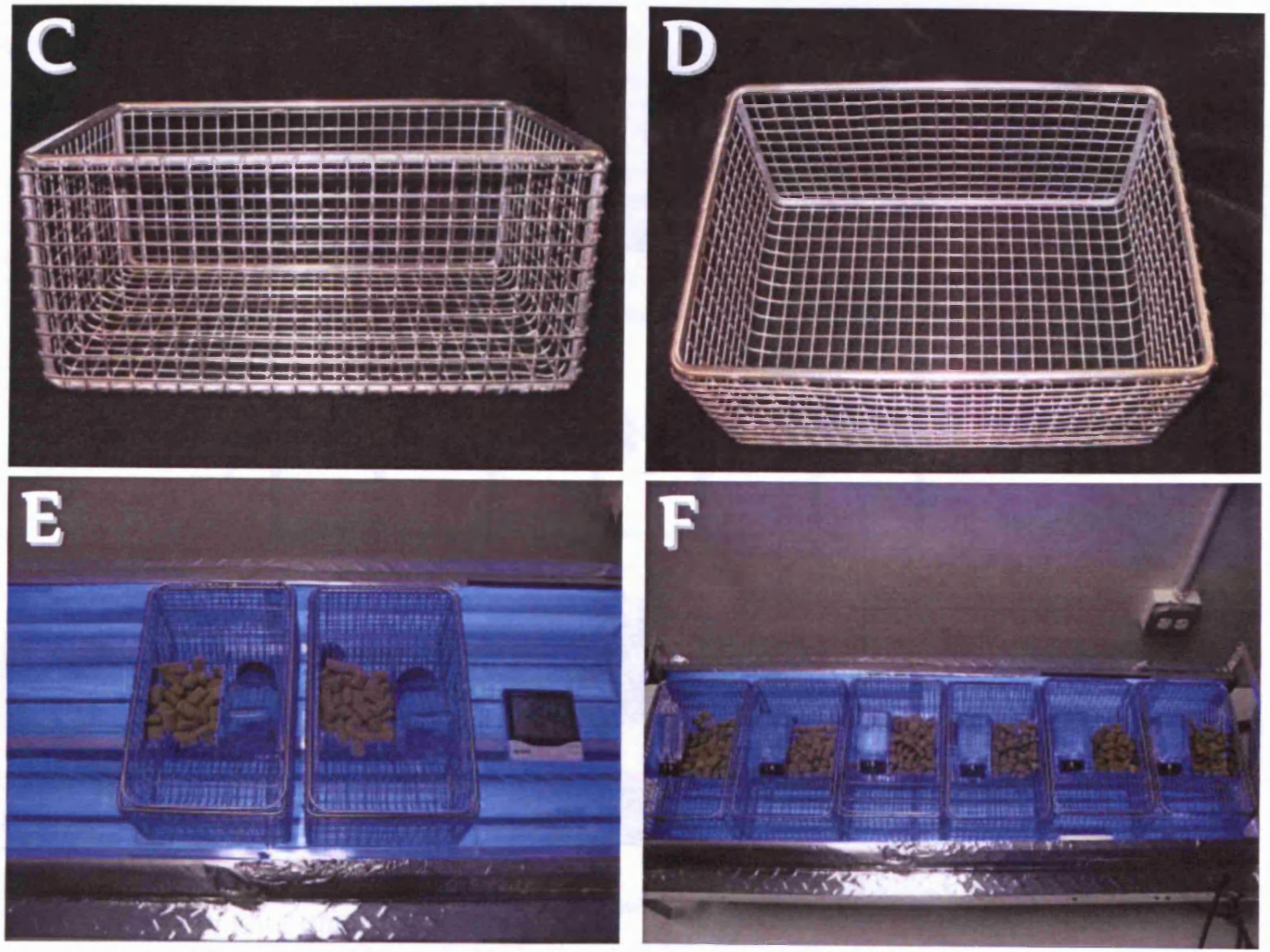

Figure 2.4: 'C' and 'D' show the side view and top view of the stainless steel cage respectively. Caging dimensions are 5"Hx6"Wx11"L and each individual cage holds up to 3 mice. 'E' illustrates two cages with food and water; to the right of the cages is the maximum/minimum temperature and humidity monitor, which was checked twice a day. 'F' shows the apparatus with all 6 stainless steel cages equipped with food and water without the top set of lights.

2.3.5 Blue Light Exposure Experimental Design (Please refer to flowchart below)

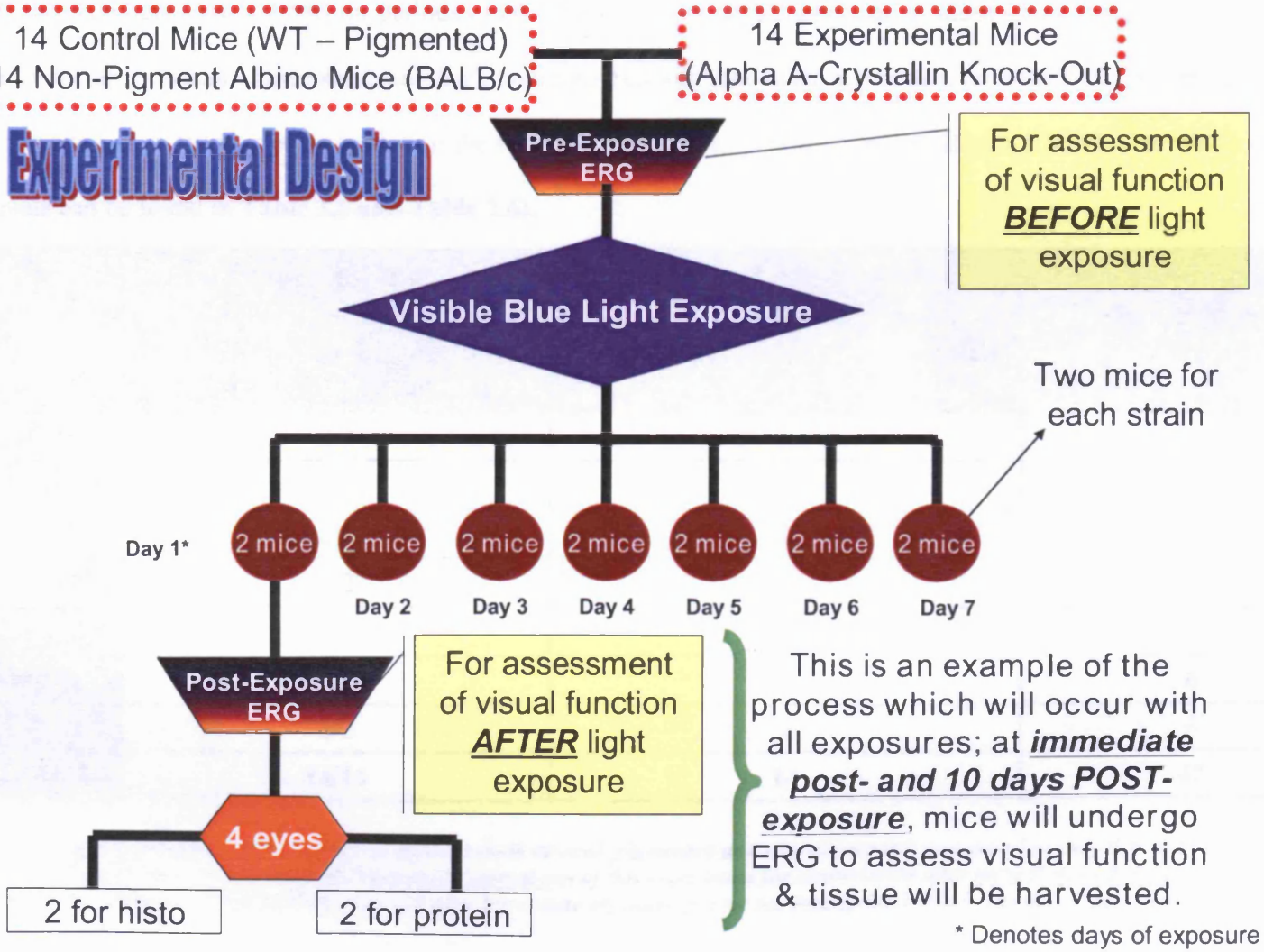

When referring to the above mentioned flowchart, for each trial of individual mice, sixteen wild-type, αA-crystallin knock-out or BALB/cBYJ mice were exposed to blue light (400-480nm) for periods of 24 - 168 hrs (1 – 7 days). Fourteen of those sixteen mice were exposed to blue light up to 7 days (2 mice for each day; one was examined after immediate exposure, the other mouse was returned to normal cyclic conditions (12hrs on/12hrs off) and examined at 10-days post-exposure); the remaining two mice were used as NO BLUE LIGHT controls (Individual numbers and usage of animals can be found in **Table 2.5 and Table 2.6)**.

Day of Exposure	Number of Wild-Type Mice (Pigmented Controls (129Sv)/Non-Pigmented Controls (BALB/cByJ))	Number of αA-crystallin Knock-Out Mice (129Sv:CryA1)(Experimental)	Total Number of Mice Exposed
Day 1 (24hrs)	2/2	2	6
Day 2 (48hrs)	2/2	2	6
Day 3 (72hrs)	2/2	2	6
Day 4 (96hrs)	2/2	2	6
Day 5 (120 hrs)	2/2	2	6
Day 6 (144hrs)	2/2	2	6
Day 7 (168hrs)	2/2	2	6
Total	**14/14**	**14**	**42**

***Table 2.5**: The table shown above illustrates the number of animals (both control (pigmented and non-pigmented) and experimental) that will be used for exposure to visible light. As shown, a total of 14 animals will be used per experimental run of this experiment for examination after immediate and 10 days post-exposure. An additional examination of the changes will be initially observed after immediate exposure (please see description below). Details of their significance can be seen in FLOWCHART 1.*

Experimental Runs	Number of Wild-Type Mice (Pigmented Controls (129Sv)/Non-Pigmented Controls (BALB/cByJ))	Number of αA-crystallin Knock-Out Mice (129Sv:CryA1)(Experimental)	Total Number of Mice Exposed
1¥	16/16	16	48
2¥	16/16	16	48
3¥	16/16	16	48
4**	16/16	16	48
Total	**64/64**	**64**	**192**

***Table 2.6:** The table shown above illustrates the number of animals (both control and experimental) that will be used for each experimental run for exposure to visible light .As shown, a total of 16 animals will be used per experimental run of this experiment per strain (¥) (When referring to Table 2.5, only 14 are exposed; the additional 2 mice will serve as NO-LIGHT pigmented/or non-pigmented controls). Details of the animals significance can be seen in the EXPERIMENTAL FLOWCHART.*

Mice were weighed at three points during the experiment; before exposure, immediately after exposure and at their 10-day post designated exposure time. Before exposure, mice were dark-adapted for 12-16 hours in a standard cage supplied with food and water and then underwent a *pre-ERG* initial assessment of visual function (**see Section 2.4.1**). During ERG recordings, mice pupils were dilated once with 1% atropine sulfate, which kept the pupils fully open for maximum exposure for 7 days. Animals were not sedated with standard anesthesia for blue light exposure experiments. This treatment does not comply with the Guide For the Care and Use of Laboratory Animals (NRC 1996) for light period, but then this is the purpose of the study, namely to produce the well known effect of retinal degeneration due to constant light.

Previous studies have examined continuous blue light exposure up to freely moving, unsedated animals (Noell *et al.*, 1966, Rapp and Williams, 1979, Seiler *et al.*, 2000). For these experiments, animals were closely monitored twice a day for any behavioral evidence of pain and distress **(see Figure 2.5 G-H)**. If any pain or distress was noted, sedation would be administered. At no point during trials of this experiment was any pain or distress noted.

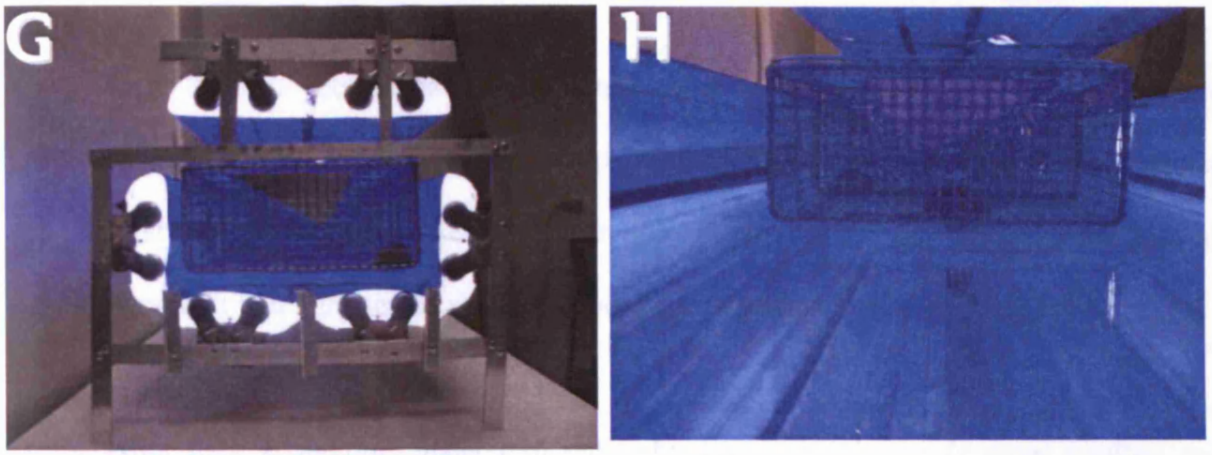

***Figure 2.5*: 'G' and 'H' show the blue light apparatus with the mice being exposed. As shown in both figures, mice are free to roam and are constantly surrounded and being exposed to blue light.**

Photophobia can be encountered in typical bright, full-spectrum light; but with the blue light restriction, there was a natural dimming of the perceived brightness which lowered the chance of photophobia in the animals. After light exposure, some animals were euthanized immediately and tissue was harvested **(see Section 2.5.1)**. Mice not euthanized immediately were returned to normally cyclic conditions (12hrs on/12 hrs off) and post-ERG analysis and subsequent euthanasia occurred at 10 days post-exposure.

2.4 Retinal Function Analysis of Mice Exposed to Continuous Blue Light

2.4.1 Electroretinography (ERG) of Mice

This procedure was used to evaluate the impact of the αA-crystallin knockout on retinal function. ERGs were performed prior to light exposure, immediately after designated exposure (1 – 7 days) and at 10-days post-exposure, right before euthanasia and tissue

harvesting (see **Section 2.5.1**). Full-field ERGs were recorded under dark-adapted conditions from both eyes of all blue light exposed mice (21 129Sv, 21 129Sv:CRYA1, and 8 BALB/cBYJ). Additionally, ERGs were also performed on 3 129Sv, 3 129Sv:CRYA1, and 2 BALB/cBYJ control mice not exposed to the blue light.

Prior to ERG recordings, animals were administered 1 drop of 1% atropine ophthalmic solution in both eyes to maintain full pupil dilation for ERG recordings and designated blue light exposure time. After administration of the 1% atropine, mice were dark adapted overnight in a light-sealed ventilated room and provided with food and water.

After dark adaptation, under dim red light illumination, animals were weighed and then sedated with 150 mg/kg ketamine (IP) and 10 mg/kg xylazine (IP) for the duration of recordings (approx. 1.5 hour), to minimize discomfort from application of electrodes on their cornea, eyelid and skin and to prevent movements during the recordings. A small contact electrode was applied to the corneas of the sedated mice with a drop of water in it to serve as the *active recording* electrode. Both the *reference* and *grounding* channel for both eyes were applied via the single platinum wire electrode upon which the upper palate of the mouth was rested. A Ganzfeld dome surrounded the animal and ERGs were elicited with 10 μs-flashes of white light (112 lux) presented at intervals of 5s. Five consecutive responses were amplified and averaged using a 1902 signal conditioner/1401 laboratory interface. DOS based ERG software analyzed recordings from the light damaged mice as cornea negative ("a-wave) and cornea negative to cornea-positive ("b-wave") amplitudes for comparison with responses from the no light control mice. The a-wave amplitude was measured from the baseline to the peak of the a-wave response and the b-wave amplitude was measured from the trough of the a-wave to the peak of the b-wave (***please refer to Figure 2.6)***.

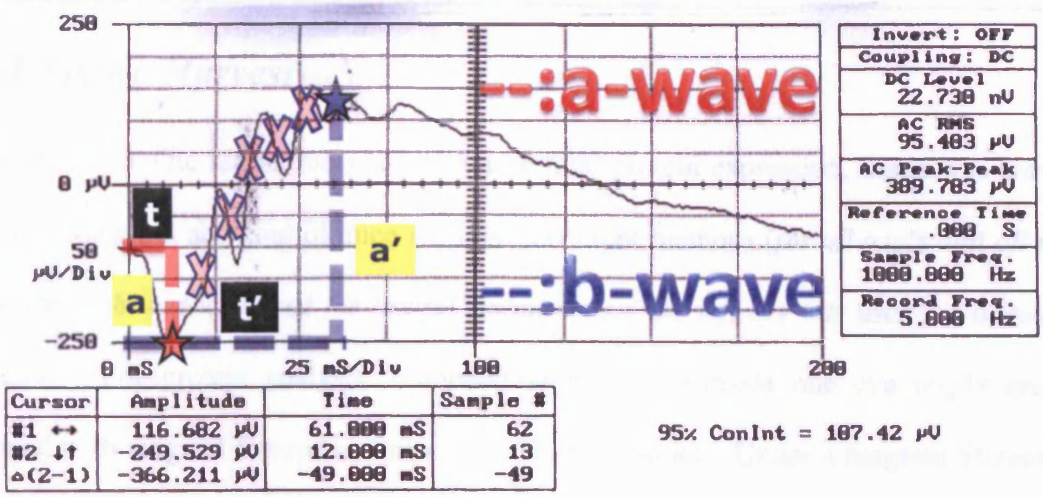

Figure 2.6 Shown above is a representative ERG depicting the principle measurement points (amplitude and latency) of the a- and b-waves. The 'x's' represent measurement of the best fit curve. The amplitudes of the a- and b-wave were measured from the baseline to the negative trough of the a-wave (a), and from the trough of the a-wave to the following peak of the b-wave (a'). Latencies of the a- and b-waves were measured from flash onset to the trough of the a-wave (t) and the time (t') from flash onset to the peak of the b-wave. In the example shown above, the amplitude of the a-wave was -249µV at a latency of 12mS; the b-wave amplitude was 373µV at a latency of 63mS.

After the *pre*-ERG recordings mice were either returned to normal cyclic conditions (12hrs on/12 hrs off) until their designated exposure, or placed into the blue light exposure apparatus. *Immediate* ERGs were performed directly after mice underwent their designated exposure to blue light (with 1 hour of dark-adaptation) and were then returned to normal cyclic conditions until the 10 day post-exposure ERG analysis. *Post*-ERG analysis and subsequent euthanasia occurred with an overdose of ketamine/xylazine with secondary cervical dislocation. Tissue harvest was performed (see **Section 2.5.1**) for future histology (see **Section 2.6.2**) and protein analysis (see **Section 2.5**).

2.5 Protein Analysis of Mice Exposed to Continuous Blue Light

2.5.1 Tissue Harvest

In order to examine retinal morphology and retinal protein expression, tissue was harvested from experimental and control mice with two different methods (***for all trials and all mouse types, the right eye was used for retinal isolation and the left eye was used for histological analysis)***. For protein analysis, immediately after euthanasia one eye (***right eye***) was removed with surgical forceps and placed in 1X PBS on ice. Under a tungsten Stereomaster dissection microscope (Fisher Scientific, USA), all surrounding extraocular muscles, hair and connective tissue were removed, leaving a solid, clean globe. A circumferential incision was made at the corneal limbus and the anterior segment was gently removed and discarded. Since the murine lens occupies about 75% of the intraocular space (Zinn and Mockel-Pohl, 1973; Marshall *et al.*, 1982), extreme care was used to remove the lens so there was no disruption of the anterior/posterior lens capsule, resulting in lysis of lens fiber cells and possible false detection of the α-crystallins in the RPE and/or neural retina. After careful dissection, the retina was gently removed from the underlying RPE and choroid and immediately placed in RIPA Lysis Buffer (0.5M Tris-HCl, pH 7.4, 1.5M NaCl, 2.5% deoxycholic acid, 10% NP-40, 10mM EDTA) (Upstate, USA) with additive protease inhibitor cocktail (Sigma, US) (see **Section 2.5.2**)

2.5.2 Retinal Protein Isolation

Retinae from exposed and non-exposed mice from all strain were isolated carefully under a dissection microscope. To isolate proteins, RIPA Lysis Buffer (0.5M Tris-HCl, pH 7.4, 1.5M NaCl, 2.5% deoxycholic acid, 10% NP-40, 10mM EDTA) (Upstate, USA) with additive protease inhibitor cocktail (Sigma, UK) was used. Briefly, 1 retina/animal was incubated on ice with 500μL of RIPA Lysis Buffer and protease inhibitor cocktail (1ml of cocktail solution for every 100ml of lysis buffer). After 45 minutes of incubation, the tissue was homogenized breaking up cells and releasing proteins. Cells were centrifuged at 12000*g* for 30 minutes at

4°C. After centrifugation, the supernatant was transferred to fresh Eppendorf tubes and stored at -20°C for future use. The protein content was measured by the bicinchoninic acid (BCA) protein assay (Pierce, Rockford, IL, USA) (see **Section 2.2.4**).

2.5.3 Sodium Dodecyl Sulphate – Polyacrylamide Gel Electrophoresis (SDS-PAGE)

SDS-PAGE is an electrophoretic technique which separates proteins into their individual polypeptides according to their molecular weights (MW). SDS, an anionic detergent, disrupts hydrogen bonds, blocks hydrophobic interactions, and partially unfolds the protein molecules, minimizing differences in molecular form by eliminating the tertiary and secondary structures.

Denatured proteins (10μg), mixed with an equal volume of 2X Laemmli Sample Buffer (Bio-Rad Laboratories, UK), were incubated at 95°C - 100°C for 1-2 min and then separated under reducing conditions by electrophoresis with a 5% SDS-PAGE stacking gel and a 10% SDS-PAGE or 8% SDS-PAGE resolving gel depending on the protein of interest (**see Table 2.7**). Two different layers of acrylamide are necessary for proper separation of protein samples. The stacking gel composition compresses the protein samples into thin bands for better resolution while migrating through the resolving gel, which actually separates the polypeptides by their size. Samples (10μg of protein), representing equal loading, and Precision Plus Protein Standard (Bio-Rad Laboratories, US) (5μl) were added to the polyacrylamide gel submerged in a 1X Tris/Glycine/SDS Running Buffer (Bio-Rad Laboratories, US) and samples were run with a 4W electric current until the standard dye approached the bottom of the gel (approximately 1hr). The applied electric current causes the negatively charged proteins to migrate across the gel, resulting in smaller proteins migrating the farthest.

Following electrophoresis, the gel was either stained with Coomassie Brilliant Blue (**see 2.5.4**) allowing visualization of the separated proteins, or used for Western immunoblotting with protein specific antibodies (**see 2.5.5**).

SDS-PAGE Components	10% Resolving Gel Composition (µl)	8% Resolving Gel Composition (µl)	5% Stacking Gel Composition (µl)
Distilled H_2O	5800	6800	2100
30% Acrylamide:Bis Mix	5000	4000	500
1.5M Tris/HCl (pH 8.8)	9400	9400	--
1.0M Tris/HCl (pH 6.8)	-	-	380
10% SDS	250	250	30
10% APS	625	625	30
TEMED	6.25	6.25	3

***Table 2.7** Composition and Volume of 10% or 5% Resolving and 5% Stacking SDS-PAGE: 30% Acrylamide:Bis Mix (Bio-Rad Laboratories, US), TEMED (Sigma, US). For protein analyis of αA-, αB-crystallins and actin, 10% resolving gel was used. For protein analysis of Hsp70 and NF-κB, 8% resolving gel was used. All protein analysis utilized the 5% stacking gel.*

2.5.4 Coomassie Brilliant Blue Staining

Coomassie Brilliant Blue staining binds nonspecifically to virtually all proteins and is the most commonly used stain in protein visualization post-electrophoresis (Deutscher, 1990). After electrophoresis, the SDS-PAGE gel was soaked in ~15ml of Coomassie Brilliant Blue R-250 Staining Solution (Bio-Rad Laboratories, US) for 30 minutes at room temperature with mild agitation. After 30 minutes, the Coomassie stain was removed and the gel was washed 3-4X with distilled water and destained overnight with distilled water. Any dye that is not bound to protein diffuses out of the gel during the destaining steps. Protein bands were visualized and photographed using an EPSON Expression 1680 Pro Scanner.

2.5.5 Western Blotting

Immunoblotting, or Western Blotting, is a widely-used and powerful technique for the detection and identification of proteins using antibodies (Burnette, 1981). The process involves the separation of proteins by SDS-PAGE, followed by the transfer of the separated proteins from the gel onto a nitrocellulose membrane. The membrane binds and immobilizes

the proteins in the same pattern as in the original gel. The membrane is blocked and then exposed to a solution containing antibodies that recognize and bind to the specific protein of interest. The antibodies bound to the membrane are detected by any of a variety of techniques, usually involving treatment with a secondary antibody coupled with horseradish peroxidase (HRP) (**see Section 2.5.6**).

Denatured proteins (5µg) were separated under reducing conditions by electrophoresis with a 5% SDS-PAGE stacking gel and a 10% or 8% SDS-PAGE resolving gel (**see Table 2.7**). Proteins were then transferred from the gel to a nitrocellulose membrane (Amersham-Biosciences, US) in 1X Tris/CAPS Transfer Buffer (Bio-Rad Laboratories, US) at 16V overnight (approximately 16hrs). To assure complete transfer, the nitrocellulose membrane was stained briefly with Ponceau S Staining Buffer (Sigma, US) to visualize bands and then destained with distilled water.

Nonspecific binding sites on the nitrocellulose membrane were blocked for 30 minutes at room temperature with Blocking Buffer with Tween-20 (PBST) (1X PBS, 50mM NaF (Sigma, UK), 5% Milk Powder (Sigma, UK) and 0.05% Tween-20 (Sigma, UK)). Membrane was then incubated overnight at 4°C with primary antibodies of interest (**see Table 2.8**).

Primary Antibody	Catalog Number	Dilution Used
αA-crystallin (G-20)	sc – 22743	1:50
αB-crystallin (K-20)	sc – 22744	1:100
NF-κB p65 (F-6)	sc – 372	1:250
Actin (I-19)	sc – 1616	1:200

Table 2.8 Primary antibodies used in Western Blotting of mouse retinas. All antibodies were purchased from Santa Cruz Biotechnology (California, US). Visualization of protein bands were performed with subsequent binding with secondary antibodies (please refer to Table 2.8 below).

After overnight incubation, membrane was washed 5X for 5 minutes each with PBST and then incubated with secondary antibodies conjugated with horseradish peroxidase (Santa Cruz Biotechnology, US) (see **Table 2.8**) for 2 hrs at room temperature. Membrane was

washed 3X with PBST and then 2X with PBST without the 5% milk powder. Immunoreactive bands were visualized with enhanced chemiluminescence (**see Section 2.5.6**) detection.

Secondary Antibody	Catalog Number	Dilution	Primary Antibody
Anti-Goat IgG HRP	sc – 2020	1:2000	Actin
Anti-Rabbit IgG HRP	sc – 2040	1:2000	αA-, αB-crystallin, NF-κB

***Table 2.9** Secondary antibodies used in Western Blotting of mouse retinas. All antibodies were purchased from Santa Cruz Biotechnology (California, US).*

2.5.6 Enhanced Chemiluminescence (ECL) Detection

Enhanced chemiluminescence (ECL) detection was performed according to the manufacturer's protocol (Amersham-Biosciences, US). Briefly, after the membrane was washed with PBST without milk powder, equal volumes of Detection Solution 1 and Detection Solution 2 were mixed and incubated with the membrane for 1 min at room temperature. Excess buffer was drained from the membranes and then membrane was placed **protein side up** on Sarah Wrap™ in an X-ray film cassette (Amersham-Biosciences, US). Two sheets of Hyperfilm ECL were placed on top of the membrane and exposed for 15 minutes. Films were developed manually in standard solutions (Sigma, US).

2.5.7 Analysis of the Western Blotting Results

Exposed films were scanned using an imaging densitometer (Model GS-700 Imaging Densitometer, Bio-Rad Laboratories, USA). Images were then imported into Multi-Analyst Imaging Software (Version 1.0.1 PPC, Bio-Rad Laboratories, 1997) for densitometry analysis. Optical density values were obtained and imported into Microsoft® Excel and normalized to actin densitometry readings. Comparison to actin was done to ensure that any differences noted were true differences in expression, rather than varying quantities of proteins during each exposure day. Mean normalized band intensity and standard error of the mean were calculated for αA-crystallin, αB-crystallin, and NF-κB for each exposure day,

immediate and after a 10 day recovery to blue light. Statistical analysis identified any significant changes in expression (one-way ANOVA with Tukey's post-hoc test)

2.6 Retinal Morphology Analysis of Mice Exposed to Continuous Blue Light

2.6.1 Tissue Harvest

The remaining eye (***left eye)*** was used for histological evaluation of retina morphology. After the first eye was removed, the mouse was perfused with 1XPBS with subsequent fixation with 2.5% Paraformaldehyde/Glutaraldehyde mixture in 0.1M Sodium Cacodylate Buffer, pH 7.4 (Electron Microscopy Services, Hatifield, PA, USA) under a fume hood (Labconco, Kansas City, Missouri, USA). After successful perfusion/fixation, surrounding extraocular tissue was removed and the optic nerve was severed as close to the optic chiasm as possible. The fixated eye was carefully removed from the orbit, surrounding extraocular muscles and connective tissue was removed and the eye was placed in 2.5% Paraformaldehyde/Glutaraldehyde mixture at 4°C overnight. After 24hrs of incubation in the mixture, fixated eyes were washed 3 times with 1XPBS for 30 minutes and then stored for future dehydration and subsequent sectioning. All tissues were dehydrated and sectioned with the assistance of the Kimmel Cancer Center's Core Pathology/Research Facility at Thomas Jefferson University (Philadelphia, PA).

2.6.2 Dehydration and Sectioning of Tissue

Whole eyes were removed from 1XPBS and dehydrated in graded alcohols from 70% through 100% ethanol (70% for 1hr, 90% for 5 hours and 100% for 3hrs). Tissues were then cleared in xylene, and infiltrated with paraffin. After this process, tissues were embedded into paraffin blocks and sectioned at 4μm onto positively-charged slides.

Tissue slides were then deparaffinized in xylene and rehydrated in graded alcohols from 100% through 70% ETOH, and rinsed in tap water. Next, slides were stained in hematoxylin for 4 minutes; differentiated in acid alcohol, and rinsed in tap water. Slides were further differentiated in bluing solution, rinsed in tap water and placed in 95% ETOH. Slides were next stained in eosin for 1 minute, and dehydrated from 95% to 100% ETOH. After complete dehydration, tissues were cleared in xylene and coverslipped, prior to viewing under a light microscope. Photographs of the histological sections were captured and morphometric analysis measurements was performed (see **Section 2.6.3)**

2.6.3 Retinal Morphometrics

After histological sections were captured, they were imported into Adobe® Photoshop® CS2 Version 9.0.2. During all trials of mice (both pigmented and non-pigmented), histological changes occurred in the posterior pole, in particular around the optic nerve. All eyes were sectioned at the level of the optic nerve, and the area of measurement occurred 0.10mm to 0.25mm superior and inferior to the optic nerve.

Using the measuring tool from Adobe® Photoshop®, whole retinal thickness, outer and inner nuclear layer thickness was measured at 20X. Whole retinal thickness was defined from the basal portion of the RPE to the ganglion cell layer. Thickness of the photoreceptor segments occurred at 40X and was defined from the apical portion of the RPE to the external limiting membrane.

For each animal, at each exposure time, a minimum of 4 sections were analyzed per eye. In each section, six measurements were made and then all values were averaged together. Mean thickness values and standard error of the mean were calculated and statistical analysis

identified any significant changes in thickness compared to the control expression (one-way ANOVA with Dunnett's post-hoc test)

2.7 Statistical Analysis

Statistical analyses were performed using GraphPad Prism M (GraphPad Software, La Jolla, USA) and SAS Proc GLM procedure (SAS version 9.1, SAS Institute, Cary, NC). Different statistical strategies of multiple comparisons were used to test the differences among experimental groups. Specifically, multiple comparisons were performed on MTT data, retinal morphometrics with Tukey tests. All other data were analyzed using Dunnett's tests. For all samples, mean and standard error of the mean were calculated. Means were then analyzed using a one-way ANOVA with post-hoc tests of Dunnett's (comparing experimental samples to the control) or Tukey's (comparing samples to each other). Accepted level of significance for all tests was $p<0.05$.

Chapter 3.0:

In-vitro examination of mitochondrial viability in Wild-Type and αA-crystallin knock-out RPE

3.1 Chapter Introduction

Based on the anatomical location and function of the RPE, it is no stranger to a highly oxidative environment (Beatty *et al.*, 2000; Cai *et al.*, 2000; Winkler *et al.*, 1999). Oxidative stress refers to cumulative oxidative injury at the molecular and cellular level caused by reactive oxygen species (ROS) including free radicals, hydrogen peroxide, hydroxyl radicals, and superoxide anion (Halliwell and Cross, 1994; Cai *et al.*, 2000). Oxidative metabolism, the reduction of oxygen to water in the mitochondria to produce ATP, results in production of superoxide radicals that generate these ROS which can lead to mitochondrial damage and leakage into the cytosol to damage other organelles (Ames et al., 1995; Lu *et al.*, 2006).

The RPE has developed a number of antioxidant defense mechanisms to combat this constantly 'stressed' environment (Li *et al.*, 2002) however with time, these defenses can become compromised leading to dysfunction of the RPE and ultimately irreversible blindness (Winkler *et al.*, 1999). Due to the post-mitotic nature of the RPE and its highly stressed environment, it was essential to investigate any prospective protective factors which may contribute to the sustainability and efficiency of these versatile cells. As discussed in **Chapter 1,** the α-crystallins (αA- and αB-) are members of the small heat shock protein family and are considered molecular chaperones. This association of α-crystallins to act as molecular chaperones without the consumption of ATP and their sHSP association makes them an efficient defense mechanism against the many cellular compromises associated with aging and environmental stressors (Wong and Lin 1989; Horwitz 1992; Sax and Piatigorsky 1994). Additionally, their stabilized presence in cells with minimal mitotic activity further supports their longevity throughout the lifetime of the organism (Piatigorsky 1989; Iwaki *et al.*, 1990; Sax and Piatigorsky 1994; Horwitz 2000).

The presence and expression of these α-crystallins in the RPE are exceptionally important, since sHSP, like αA- and αB-, are shown to enable the adaptation of cells to gradual, chronic changes in their surrounding environment, often being able to survive lethal conditions. Therefore it was essential to determine the presence of α-crystallins in the RPE and neural retina and monitor any change of expression when encountering environmental stressors. A number of studies have examined the presence and induction of sHSP expression in the RPE and neural retina in response to oxidative agents (Wong and Lin 1989; Kerendian *et al.,* 1992; Wakakura and Foulds 1993; Strunnikova *et al.,* 2001; Alge *et al.,* 2002).

In this study, the oxidative agents chosen to examine stress of the RPE were hydrogen peroxide (H_2O_2) and *tert*-butylhydroperoxide (*t*-BOOH). H_2O_2, a well-known *in vivo* by-product of routine cellular metabolism, has been shown to cause significant mitochondrial and genomic DNA damage in the RPE (Ballinger *et al.,* 1999; Liang and Godley, 2003; Lu *et al.,* 2006). In some cases, high concentrations of H_2O_2 have also been shown to cause apoptosis and necrosis in the RPE (Kim *et al.,* 2003). *t*-BOOH is a well-known oxidant used to study the effects of lipid peroxidation in the RPE and has been shown to result in a wide variety of oxidative damage to DNA, lipids, mitochondrial membranes and proteins (Cai *et al.,* 1999; Honda *et al.,* 2004; Jiang *et al.,* 2005; Miceli and Jazwinski 2005). Numerous studies support the use of these oxidative inducing stressors in the RPE, thus making them suitable for our study (Ballinger *et al.,* 1999; Cai *et al.,* 1999; Liang and Godley, 2003; Honda *et al.,* 2004; Jiang *et al.,* 2005; Miceli and Jazwinski 2005; Lu *et al.,* 2006).

This chapter will provide an overview of the *in-vitro* α-crystallin expression in human RPE and retina, and highlight the growth characteristics between human RPE and mouse RPE,

including cells from αA-crystallin knock-out mice. Additionally, it will examine the mitochondrial viability in all cell types after 24hrs of oxidative stress.

3.2 Chapter Aims

For this *in-vitro* study, we will examine four different RPE cell types: primary human RPE, the well established ARPE-19 cell line, wild-type (WT) RPE, and αA-crystallin knock-out (K/O) RPE. Initial studies will examine the *in-vitro* growth characteristics of all cell types, and expression of the α-crystallins will be examined at a gene and protein level in human RPE and retina. Once cell lines have been established, all RPE cells will be exposed to H_2O_2 and *t*-BOOH for 24hrs to assess mitochondrial viability under stressed conditions. This will be accomplished by the following aims:

> 3.2a.) Examine *in-vitro* growth characteristics of primary human RPE cells, the ARPE-19, wild-type RPE, and αA-crystallin knock-out RPE and highlight any notable differences between the species
>
> 3.2b.) Examine the presence of the α-crystallins in human RPE and neural retina
>
> 3.2c.) Expose all cell types to the oxidative stressors, H_2O_2 and *t*-BOOH for 24hrs and determine mitochondrial viability

3.3 Experimental Design (Detailed descriptions of the methods can be found in Chapter 2.0)

Human RPE cells were isolated from human donor eyes (Bristol Eye Bank or the National Disease Research Interchange (NDRI, Philadelphia, PA) within 48 hours of post-mortem. The ARPE-19 cell line was purchased from American Type Culture Collection, Rockville, MD (CRL-2302). The technique for isolation of RPE cells from mice (both WT and K/O), was taught by Dr. Daniel Gibbs at the University of California at San Diego School of Medicine.

In brief, once all cells had been isolated, their growth characteristics were documented and compared. Additionally, for both the primary human RPE and the ARPE-19, RNA and proteins were extracted for the presence of the α-crystallin gene and protein, respectively.

Once cell lines were maintained, oxidative stressors were added for 24hrs and then mitochondrial cell viability was assessed by the MTT assay. Since the RPE is exposed to constant oxidative stressors either via reactive oxygen species or oxidation of the polyunsaturated fatty acids (PUFAs), two physiological oxidative agents, hydrogen peroxide (H_2O_2) and *tert*-butylhydroperoxide (*t*-BOOH) were chosen. These choices were due to their ability to induce direct oxidative stress (H_2O_2) or by the oxidative stress induced by the peroxidation of lipids (*t*-BOOH).

3.4 Chapter Results

3.4.1 Growth Characteristics of Human Primary RPE Cells

Cells were initially isolated into 3 wells of a 6-welled plate. Isolated cells began to attach to the surface of the sterile wells within 2 to 4 days post-isolation. At initial stages, the cells were highly pigmented with a clear, central nuclear region and exhibited a rounded, flat structure (**Figure 3.4.1A**). Between 5-14 days, cells, which were non-dividing, retained their pigmentation (**Figure 3.4.1B**), while cells, which underwent cell division, became depigmented (**Figure 3.4.1C**). The cells formed a confluent depigmented culture within 21 days, leaving just a few pigmented cells interspersed (**Figure 3.4.1D**). Cells were used at early passages (P1-P6) due to the pigmentary changes which occur *in vitro.*

3.4.2 Growth Characteristics of ARPE-19 Cells

The ARPE-19 cell line is a spontaneously arising human cell line purified by selective trypsinization of primary RPE cell culture. Growth characteristics include defined cell borders, a flattened, cobblestone appearance and dome formation, which confirms their ability to pump ions *in vitro* (**Figure 3.4.2**).

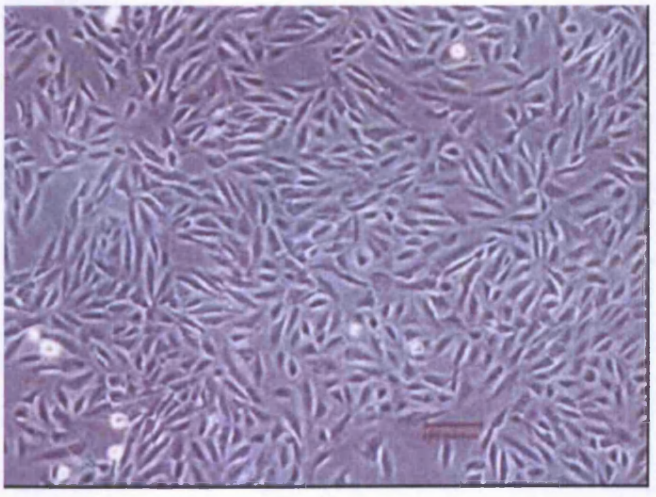

Figure 3.4.2 Typical Growth Characteristics of the ARPE-19 Cell Line. Cells were purchased from ATCC, maintained in growth medium (Passage 5), and exhibited a confluent, monolayer culture (Bar = 100μm).

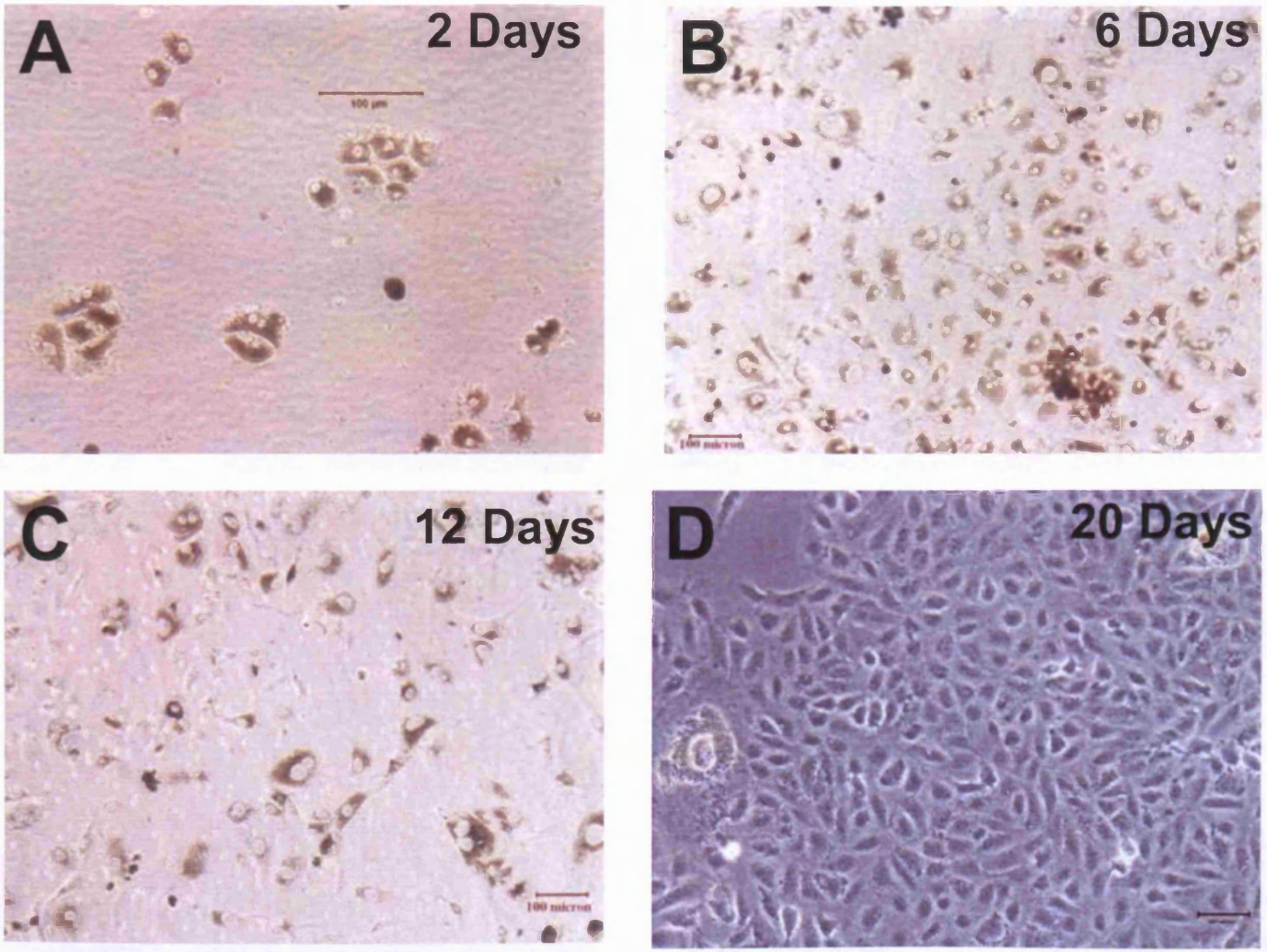

Figure 3.4.1 Typical growth characteristics of Isolated Primary Human RPE Cells: The RPE cells were isolated from an 83-year-old female. A) 2 days after isolation; B) 6 days after isolation; C) 12 days and D) 20 days after isolation displaying a confluent monolayer with pigmented cells interdispersed (Bar = 100µm).

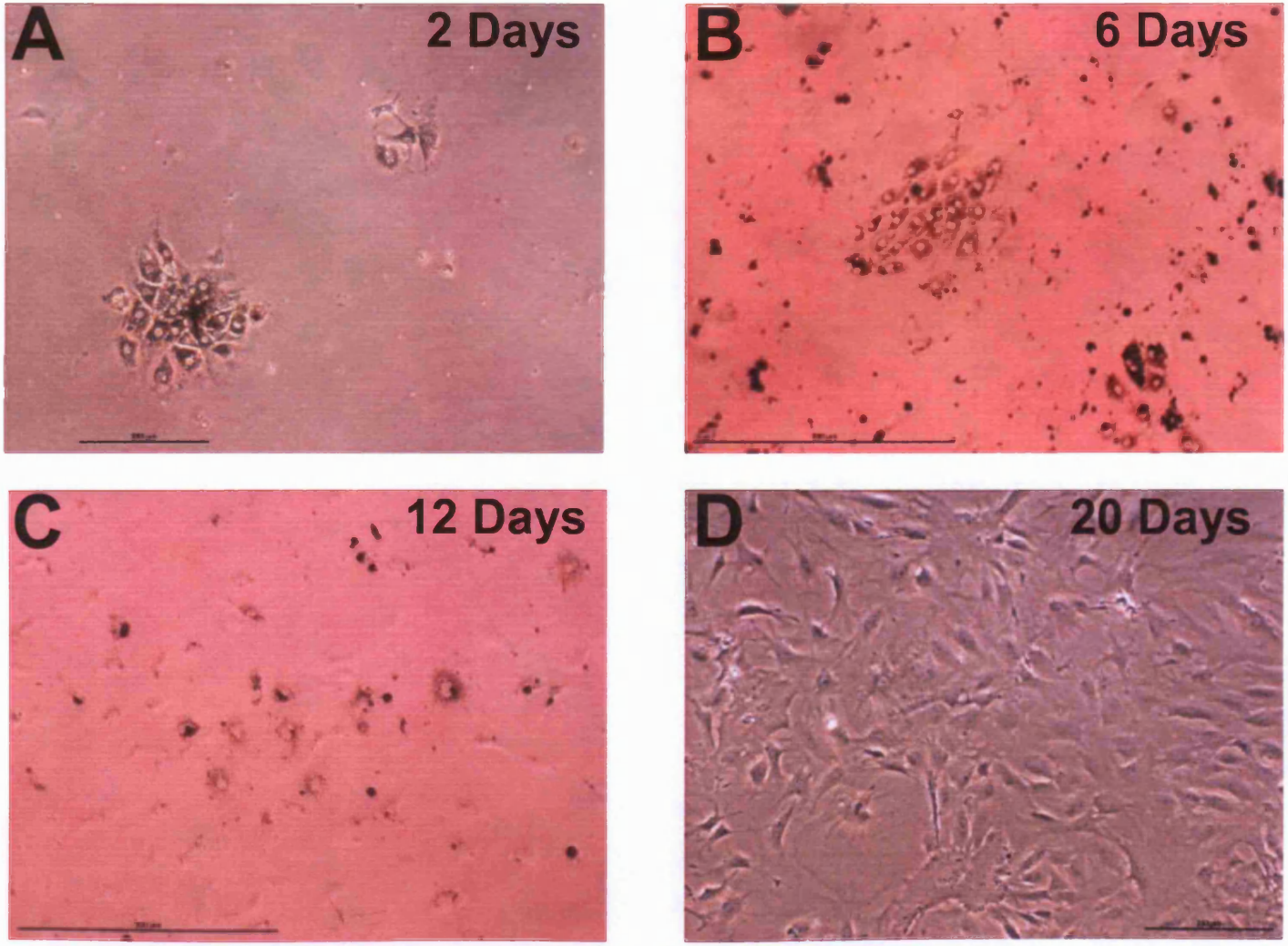

Figure 3.4.3 Typical growth characteristics of Isolated Primary Wild-Type Mouse RPE Cells (RPE cells were isolated from 10-14 day old mice). A) 2 days after isolation; B) 6 days after isolation; C) 12 days and D) 20 days after isolation displaying a confluent monolayer with pigmented cells interdispersed (Bar = 200μm).

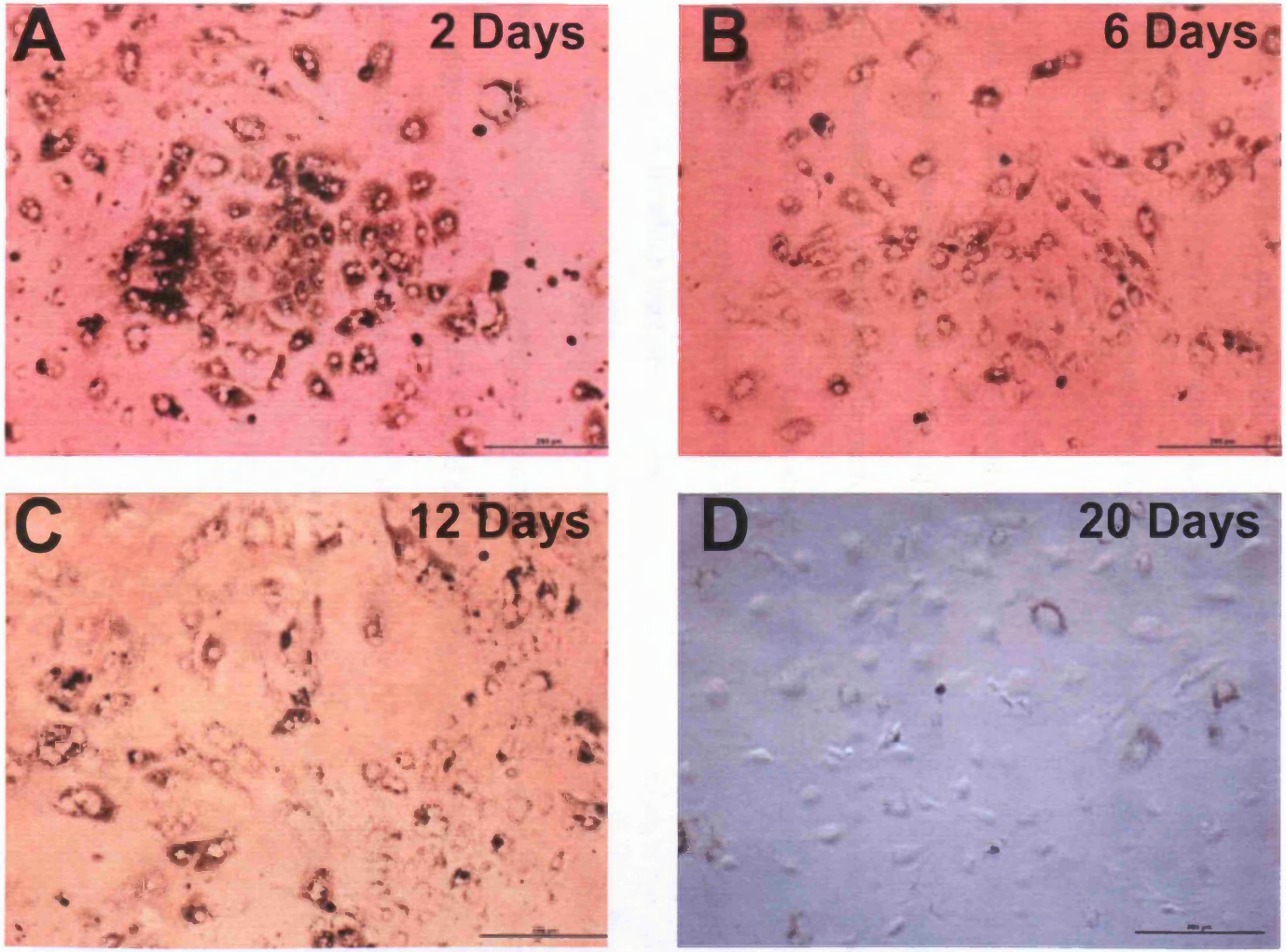

Figure 3.4.4 Typical growth characteristics of Isolated Primary αA-crystallin Knock-Out Mouse RPE Cells (RPE cells were isolated from 10-14 day old mice). A) 2 days after isolation; B) 6 days after isolation; C) 12 days and D) 20 days after isolation displaying a confluent monolayer with pigmented cells interdispersed (Bar = 200μm).

3.4.3 Growth Characteristics of Primary Wild-Type RPE and αA-crystallin Knock-Out RPE

When examining gross growth characteristics between the wild-type and αA-crystallin knock-out RPE, there are strikingly identical components of attachment, growth and length of confluencey (**see Figures 3.4.3 and 3.4.4).** Additionally, both cell lines share similar characteristics to primary human RPE cell growth (**see Section 3.4.1**).

Cells were initially isolated into 3 wells of a 24-welled plate. Upon immediate isolation, some cells remained attached, exhibiting monolayer patches of hexagonally shaped RPE cells. Isolated and grouped cells began to attach to the surface of the sterile wells within 2 to 4 days post-isolation. At initial stages, the cells were highly pigmented with a clear, central nuclear region and exhibited a rounded, flat structure (**Figures 3.4.3A and 3.4.4A**). Between 5-14 days, cells which were non-dividing, retained their pigmentation, while cells which underwent cell division, became depigmented (**Figure 3.4.3B and C, Figure 3.4.4B and C**). Similar to their human counterparts, mice RPE loss their pigmentation as cells continued to undergo cell division. The cells formed a confluent depigmented culture within 20 days, leaving just a few pigmented cells interspersed (**Figures 3.4.3D and 3.4.4D**). Cells were used at P0 or at very early passages (P1-P2) due to the pigmentary changes which occur *in vitro* and poor cell growth with increasing passages.

3.4.4 Cytokeratin Staining of Isolated Human Primary RPE Cells, the ARPE-19, Primary Wild-Type Mice RPE, and Primary αA-Crystallin Knock-Out Mice RPE

Isolated primary human RPE cells (**Figure 3.4.5A**), ARPE-19 cells (**Figure 3.4.5B**), wild-type primary mice RPE (**Figure 3.4.5C**) and αA-crystallin knock-out primary mice RPE (**Figure 3.4.5D**) stained positive for the epithelial cell marker, cytokeratin, confirming their identity in epithelial origin. Nuclei of the RPE stained with Hoechst fluoresced blue, while the cytokeratin (distributed in the cytoplasm and staining the cytoskeletal elements of the RPE cells) fluoresced green. Isolated cells that stained positive were used for future experiments, while negative staining cells possibly infiltrated with fibroblasts or melanocytes, were discarded.

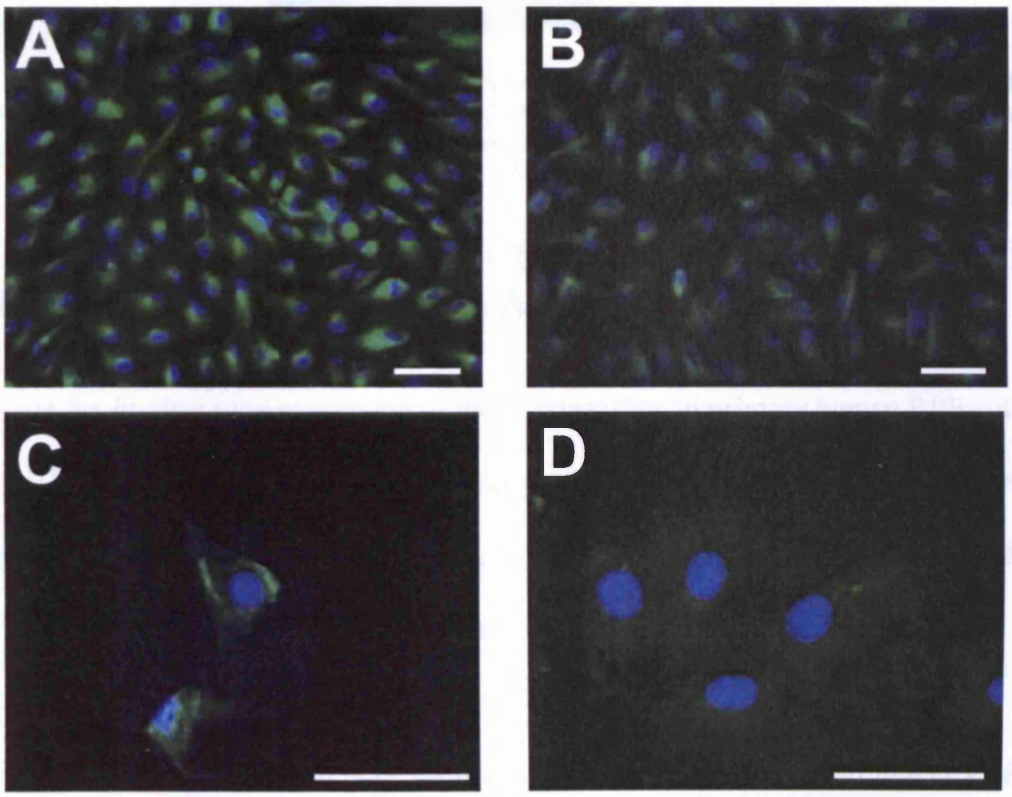

***Figure 3.4.5** Positive Cytokeratin Staining of Isolated Primary RPE Cells (Human and Mouse) and the ARPE-19 Cell Line: A) Isolated primary human RPE at P1; B) ARPE-19 cell line at P7; C) Magnified view of wild-type RPE at P1; and D) Magnified view of αA-crystallin knock-out RPE at P1 (Bar = 100μm)*

3.4.5 Confirmation of RNA Integrity

Figure 3.4.6 shows a representative formaldehyde-denaturing gel revealing the confirmation of RNA integrity. RNA of good quality will reveal the 18S and 28S ribosomal RNA (rRNA) bands. If these bands are discrete, with no significant smearing and the 28S rRNA band is approximately twice as intense as the 18S rRNA band, then the sample quality is good. Additionally, RNA concentration and purity was further assessed by A_{260}/A_{280} absorption. Only intact and good quality RNA was used for future experiments.

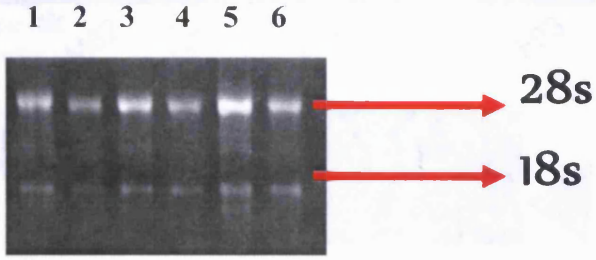

Figure 3.4.6 Representative 1.5% Formaldehyde/Agarose RNA Denaturing Gel of Intact RNA Extracted from cultured Human RPE cells. Lanes 1: ARPE19, 2: Male, 62yrs, 3: Male, 78yrs, 4: Female, 83yrs, 5: Male, 84yrs, and 6:Female, 93yrs (Each lane contains 1μg of RNA).

3.4.6 *In-Vitro* Gene Expression of the α-crystallins (αA- and αB-) in Primary Human RPE and the ARPE-19 Cells

To examine the *in-vitro* gene expression of the α-crystallins in primary human RPE cultures and the ARPE-19 human cell line, RT-PCR was performed with α-crystallin specific primers (**see Chapter 2**). As shown in **Figure 3.4.7**, a PCR band at 452-bp indicates αB-crystallin mRNA is present in both primary RPE cells and the ARPE-19 cell line. Also shown in **Figure 3.4.7** is the absence of αA-crystallin gene expression in both the ARPE-19 and primary human RPE. To adequately determine whether or not there is a definite lack of αA-crystallin mRNA expression in human RPE, the use of a positive control is necessary. The human lens epithelial cell line, SRA 01/04, a generous gift from Dr. Venkat Reddy, was used

as a positive control. SRA 01/04 expresses αA-crystallin mRNA in both early and late cell passage numbers (Ibaraki *et al.*, 1998).

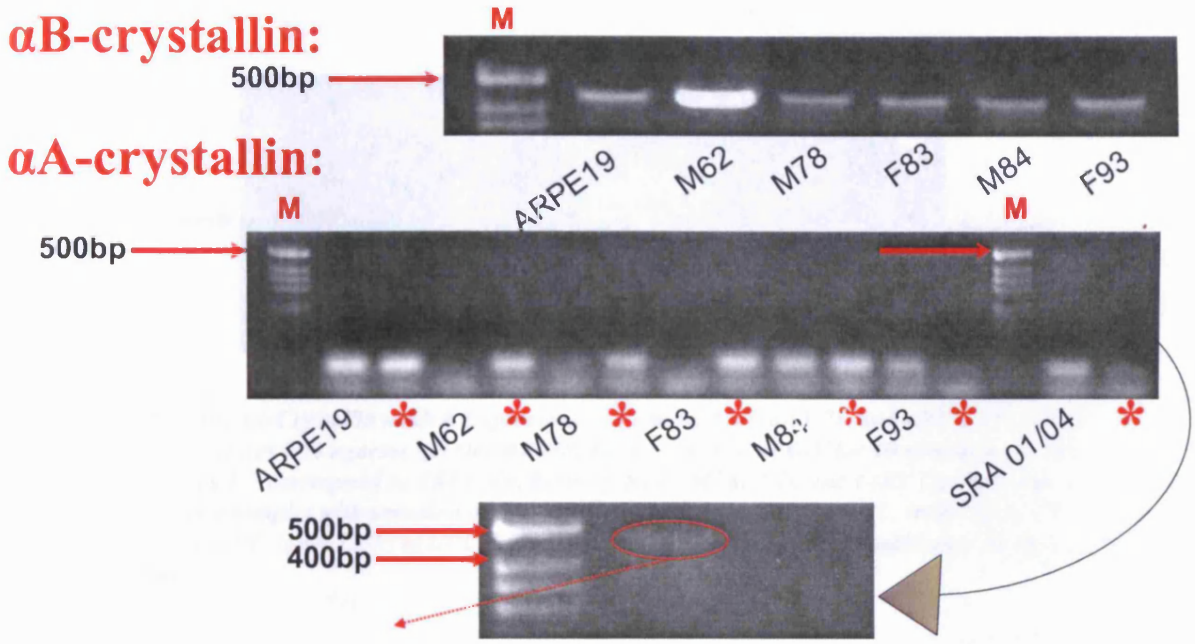

Figure 3.4.7 In-Vitro αA- and αB-Crystallin mRNA Expression in Primary Human RPE and the ARPE-19 Cell Line. cDNA from RPE cells was amplified with αA- and αB-crystallin gene specific primers for 30 cycles at an annealing temperature of 64˚C and 60˚C, respectively, on a thermocycler (DNA Engine, DYAD, UK). The αB-crystallin band corresponds to 452bp (PCR performed on the negative control, when reverse transcriptase was omitted, was negative) (data not shown). αA-crystallin mRNA expression was not detected in the ARPE19 and human RPE. An in-vitro positive control, cell line SRA 01/04, was utilized to assure that primers, cycle numbers and annealing temperatures were correct. As shown a band at 492bp with the SRA 01/04 corresponds to αA-crystallin (2.0% Agarose gels stained with EtBr; M = DNA standard lane (1Kb) is shown to the left of each gel.

Additional troubleshooting for the lack of αA-crystallin expression included varying the annealing temperatures (see **Figure 3.4.8)** and cycle numbers (see **Figure 3.4.9)**. As shown in **Figure 3.4.8**, the PCR reactions were repeated at varying annealing temperatures from 61-70˚C, keeping the cycle numbers constant at 30. Only primer dimers, no bands, which would correspond to 492-bp were found when the reactions were analyzed on an agarose gel stained with EtBr. The next attempt was to keep an annealing temperature of 64˚C, per Hawse *et al.*, 2003, and vary the cycle numbers to 20, 25 and 40. Again, only primer dimmers were detected; no bands corresponding to 492bp (**see Figure 3.4.9**). Additionally, when the reactions were performed with varying cycle numbers, αB-crystallin was also amplified as a

positive control, assuring that the problem was not technique, machine malfunction, or kit degradation.

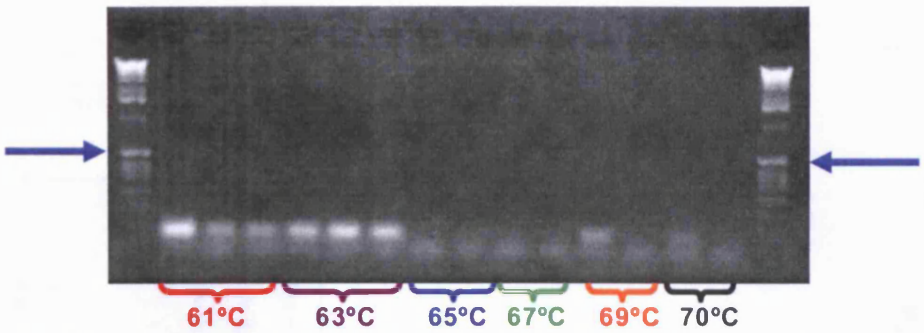

Figure 3.4.8 In-vitro αA-Crystallin mRNA Expression in Primary Human RPE and ARPE-19 at Different Annealing Temperatures (2% agarose gel stained with EtBr – Gel ran at 80V for 40 minutes). Lanes 1: DNA Ladder, 1Kb. Lanes 2-7 correspond to ARPE-19, Primary RPE (M78)(P4), and (-)RT Control, respectively. Lanes 8-15 contain the same samples with omission of the (-) RT control. Lanes 2-4 at 61°C, lanes 5-7 at 63°C, lanes 8-9 at 65°, lanes 10-11 at 67°C, lanes 12-13 at 69°C, lanes 14-15 at 70°C – all reactions underwent 30 cycles) Blue arrow indicates 500bp.

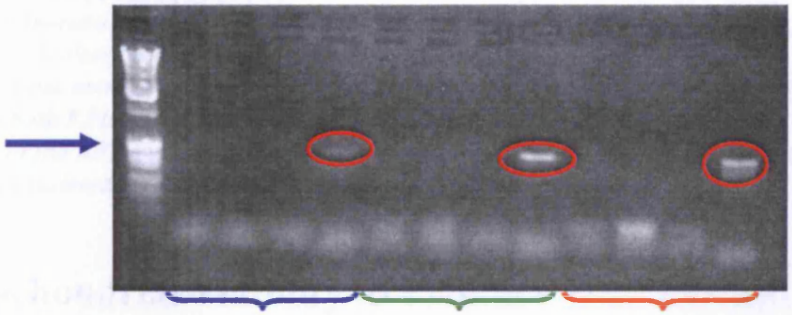

Figure 3.4.9 In-vitro αA-Crystallin mRNA Expression in Primary RPE and ARPE-19 at Different Cycle Numbers (2% agarose gel stained with EtBr – Gel ran at 80V for 40 minutes). Lanes 1: DNA Ladder, 1Kb 2,6,10: ARPE-19, 3,7,11: Primary RPE (M78)(P4), 4,8,12: (-)RT Control 5,9,13: ARPE-19 – with αB-crystallin Blue arrow indicates 500bp (Lanes 2-5 at 20 cycles, lanes 6-9 at 25 cycles and lanes 10-13 at 40 cycles – all reactions had an annealing temperature of 64°C – red circles correspond to αB-crystallin at 452bp)

3.4.7 *In-Vitro* Protein Expression of the α-crystallins (αA- and αB-) in Primary Human RPE, the ARPE-19 Cells and Retina

Proteins were isolated either from cell culture flasks (25cm^2, Triple Red, UK) or from fresh tissue from human donor eyes. As shown in **Figure 3.4.10**, αB-crystallin expression was

detected in all *in-vitro* RPE cultures, as well as in the retina. αA-crystallin was detected in fresh retina, but not in any of the *in-vitro* RPE cultures or in fresh RPE.

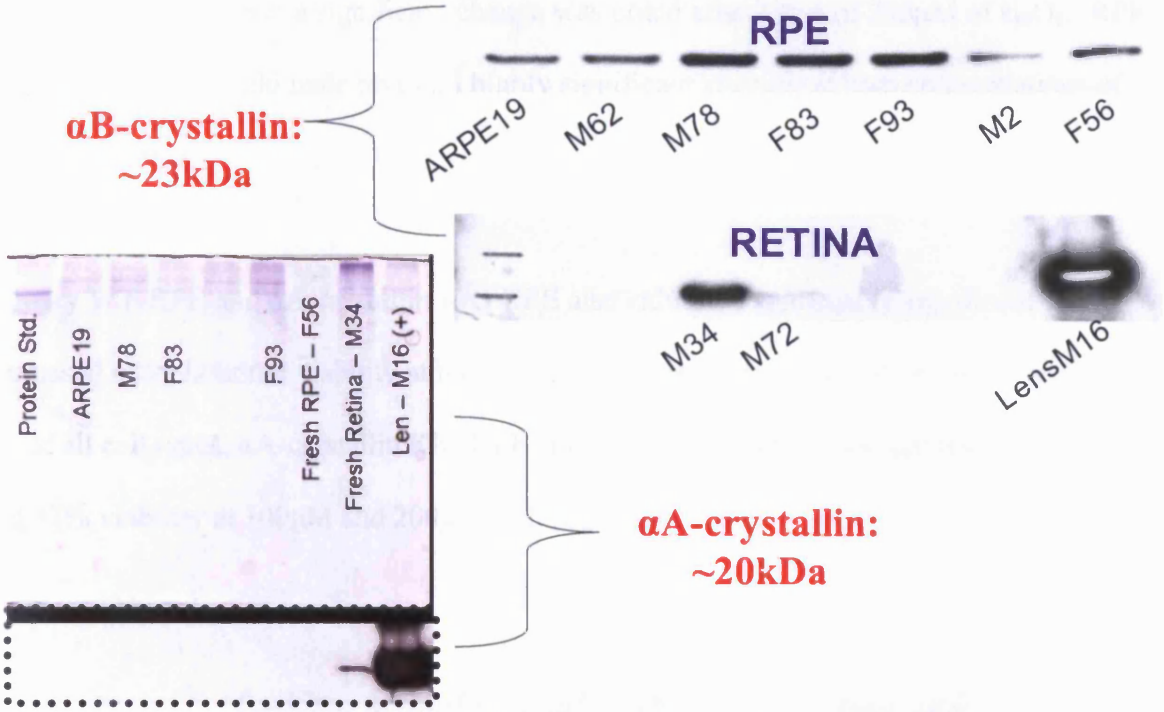

***Figure 3.4.10** In-vitro protein expression of the α-crystallins in fresh human retina, fresh RPE and cultured RPE. Isolated proteins were separated under reducing conditions by SDS-PAGE, transferred to a nitrocellulose membrane and blocked with α-crystallin specific antibodies. As shown, αB is expressed in both RPE and retina (represented as a band at 23kDa), while αA-crystallin expression was not detected in the RPE but was found to be expressed in the retina (represented as a band at 20kDa). A human lens isolated from a 16 year old male was used as a positive control.*

3.4.8 Mitochondrial Viability in Primary Human RPE, ARPE-19 and Primary Wild-Type RPE and αA-Crystallin Knock-Out RPE Exposed to Hydrogen Peroxide (H_2O_2) for 24hrs

Exposures of all cell types to H_2O_2 for 24hrs were photodocumented and can be seen in **Figures 3.4.11 and 3.4.12.** As shown, there were no visible morphological changes associated with 100 and 200μM of H_2O_2 exposure for 24hrs. Cell viability was determined by dehydrogenase activity, which indicates the activity of mitochondria. Therefore cell survival was measured as the percentage of mitochondrial viability, the greater the mitochondrial activity, the greater the chances of cell survival.

Figure 3.4.13 illustrates that all cell types exhibited statistically significant changes after 24hrs of H_2O_2 exposure. The ARPE-19 exhibited the greatest cell survival at both concentrations; however a significant change was noted after 24hrs of 200μM of H_2O_2. RPE isolated from a 79yr old male revealed highly significant changes at both concentrations of H_2O_2 after 24hrs.

Primary WT-RPE and αA-crystallin K/O RPE also exhibited statistically significant decreased mitochondrial viability at both concentrations after 24hrs of exposure. However, out of all cell types, αA-crystallin K/O RPE appeared to be affected the greatest, with 38% and 37% viability at 100μM and 200μM of H_2O_2, respectively.

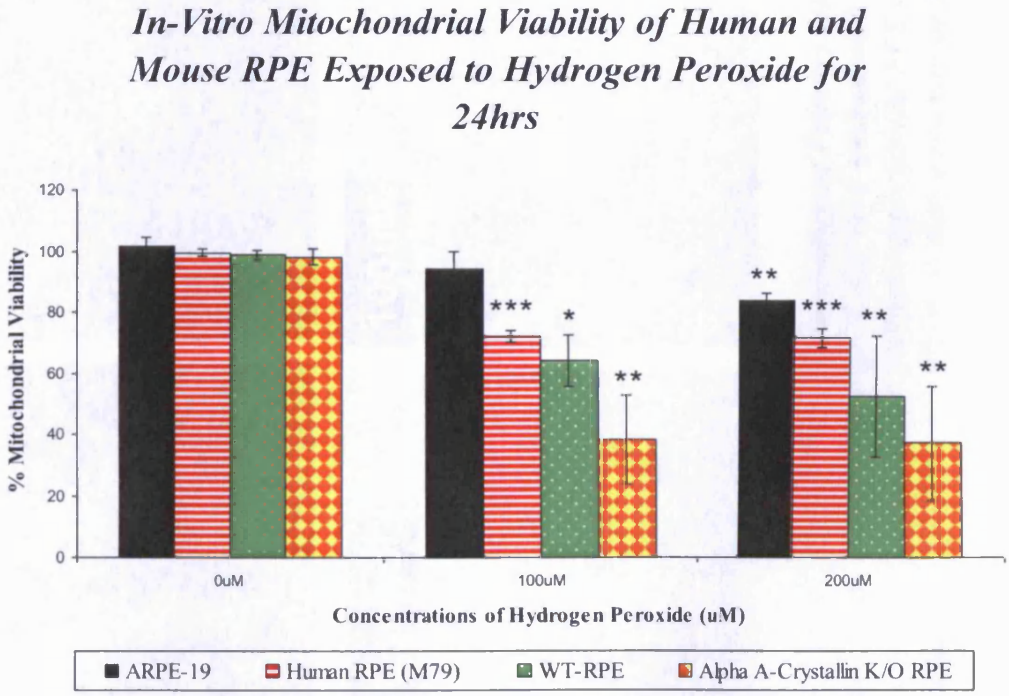

***Figure 3.4.13** Mitochondrial viability in the ARPE-19, Primary Human RPE (M79), WT-RPE and αA-crystallin K/O RPE after 24hrs of Exposure to Hydrogen Peroxide. The x-axis corresponds to the concentration of H_2O_2 used and the y-axis corresponds to the percentage of mitochondrial viability measured by the MTT assay. Data are expressed as mean ±S.D. and statistical significance was assessed with a one-way ANOVA followed by Dunnett's multiple comparison test. A $p < 0.05$ was considered statistically significant compared to the control (* $p<0.05$, ** $p<0.01$, *** $p<0.001$). Experiment was performed a minimum of three times.*

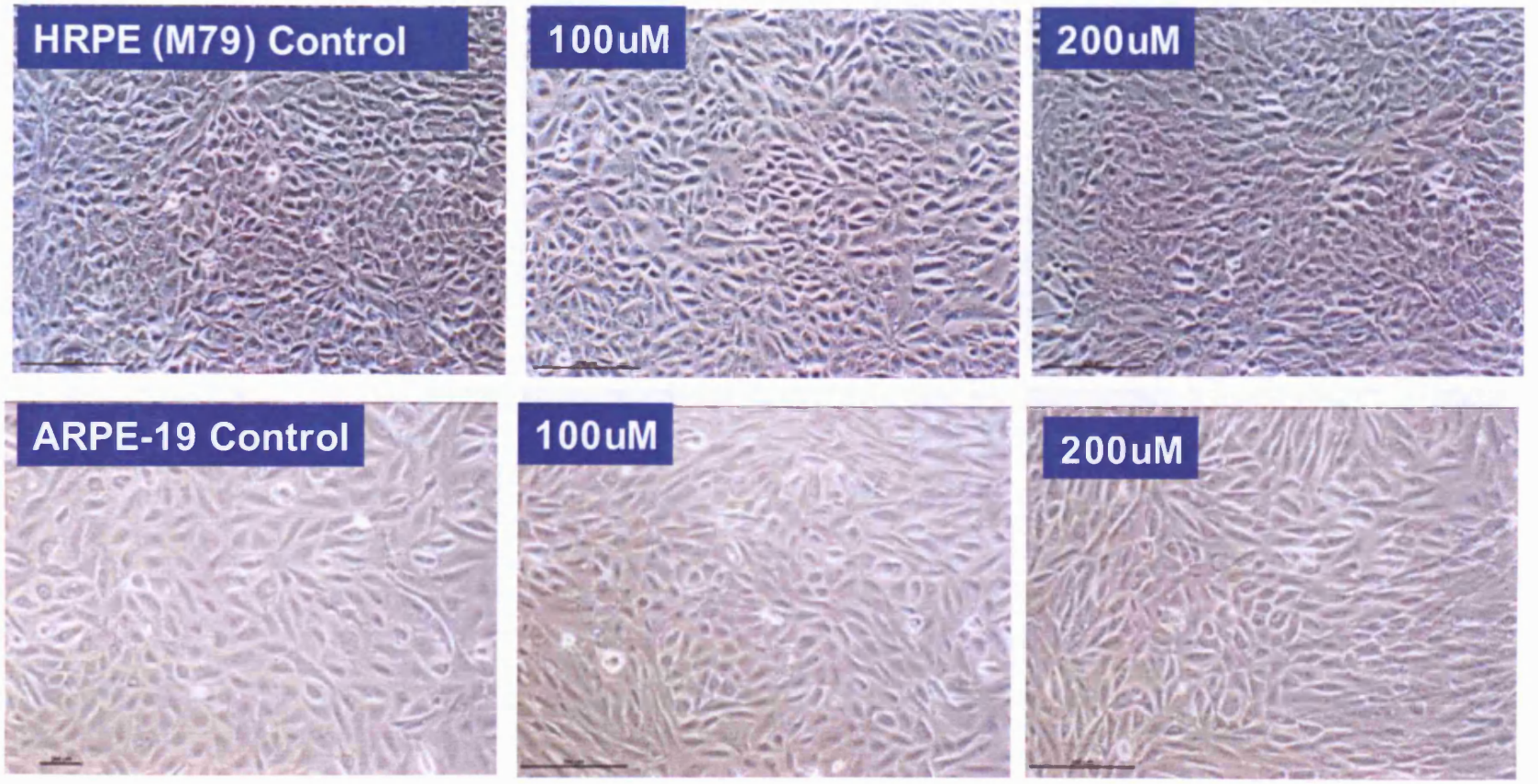

Figure 3.4.11 Representative Photodocumentation of Primary Human RPE (M79) and the ARPE-19 after 24hrs of Exposure to Hydrogen Peroxide (H_2O_2). Cells were washed with 1XPBS and then incubated with the oxidative stressor diluted in Hams F-10 media without supplemental FCS to achieve desired concentrations. Control cells were mock treated with Hams F-10 with no oxidative stressor or FCS (Scale bar = 200μm)

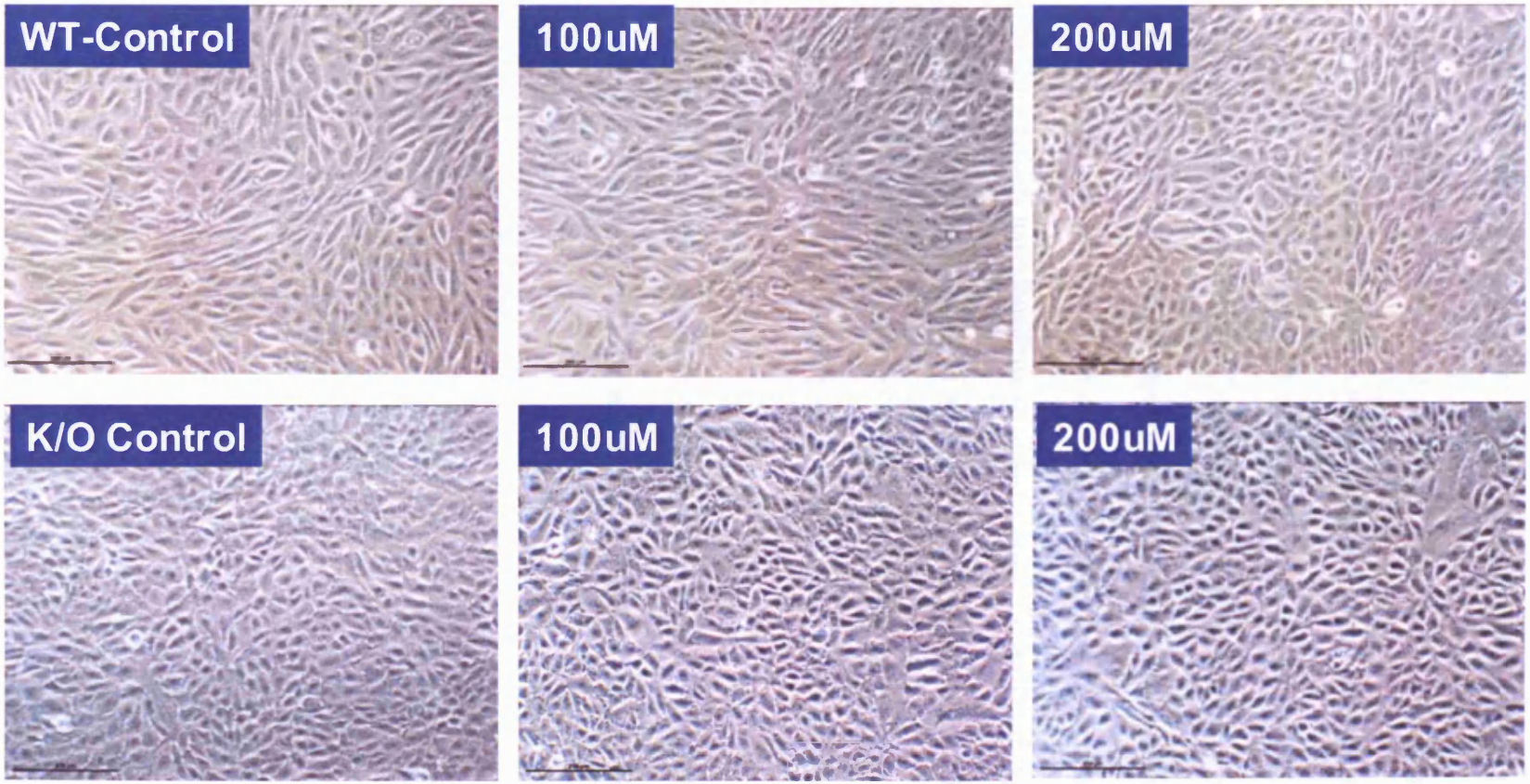

Figure 3.4.12 ***Representative Photodocumentation of Primary Wild-Type RPE and αA-crystallin Knock-Out RPE after 24hrs of Exposure to Hydrogen Peroxide (H_2O_2). Cells were washed with 1XPBS and then incubated with the oxidative stressor diluted in Hams F-10 media without supplemental FCS to achieve desired concentrations. Control cells were mock treated with Hams F-10 with no oxidative stressor or FCS (Scale bar = 200μm)***

3.4.9 Mitochondrial Viability in Primary Human RPE, ARPE-19 and Primary Wild-Type RPE and αA-Crystallin Knock-Out RPE Exposed to *tert*-butylhydroperoxide (*t*-BOOH) for 24hrs

Exposures of all cell types to *t*-BOOH for 24hrs were photodocumented and can be seen in **Figures 3.4.14 and 3.4.15.** No visible morphological changes associated with 100 and 200μM of *t*-BOOH exposure for 24hrs were noted in human RPE, the ARPE-19 and WT-RPE. K/O RPE did exhibit visible changes at both concentrations. Exposure with 100μM revealed a loss of cell to cell attachments and an increased concentration at 200μM resulted in a loss of the cobblestone appearance and cells took on a more rounded, swollen shape. Previous reports have found that oxidative stress induces phenotypic changes in cultured cells which may include dissociation from neighboring cells, a rounded appearance and an extension of cellular processes (Parrish *et al.*, 1999; Bailey *et al.*, 2004; Zareba *et al.*, 2006). These phenotypic signs are evident in the K/O RPE at both concentrations.

Figure 3.4.16 reveals significant changes in mitochondrial viabilities of all cell types, with the K/O RPE showing the most significant decrease in viability with increasing concentrations.

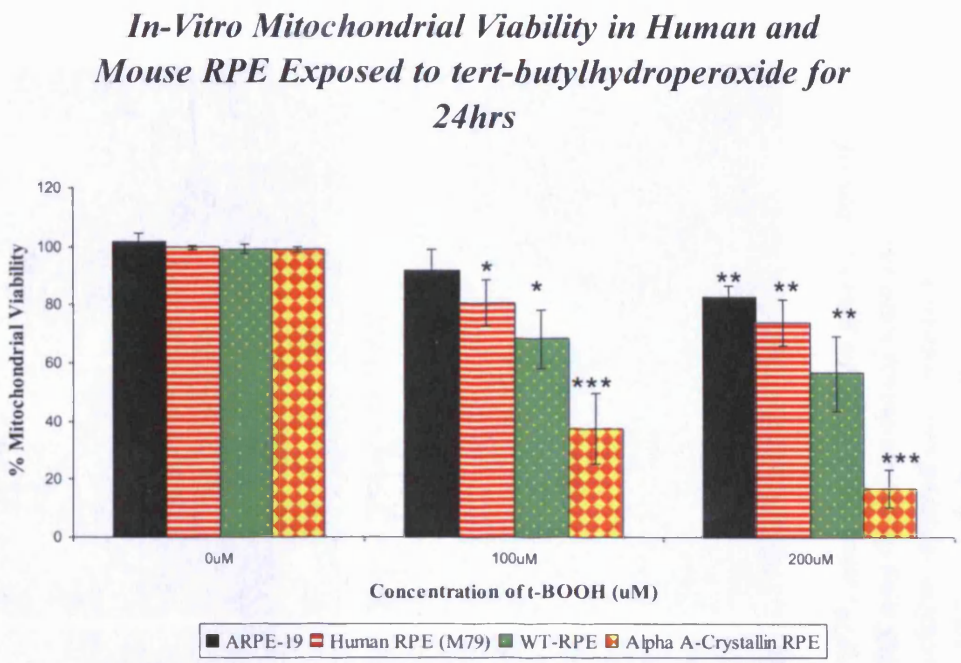

***Figure 3.4.16** Mitochondrial viability in the ARPE-19, Primary Human RPE (M79), WT-RPE and αA-crystallin K/O RPE after 24hrs of Exposure to tert-butylhydroperoxide (t-BOOH). The x-axis corresponds to the concentration of t-BOOH used and the y-axis corresponds to the percentage of mitochondrial viability measured by the MTT assay. Data are expressed as mean ±S.D. and statistical significance was assessed with a one-way ANOVA followed by Dunnett's multiple comparison test. A $p < 0.05$ was considered statistically significant compared to the control (* $p<0.05$, ** $p<0.01$, *** $p<0.001$). Experiment was performed a minimum of three times.*

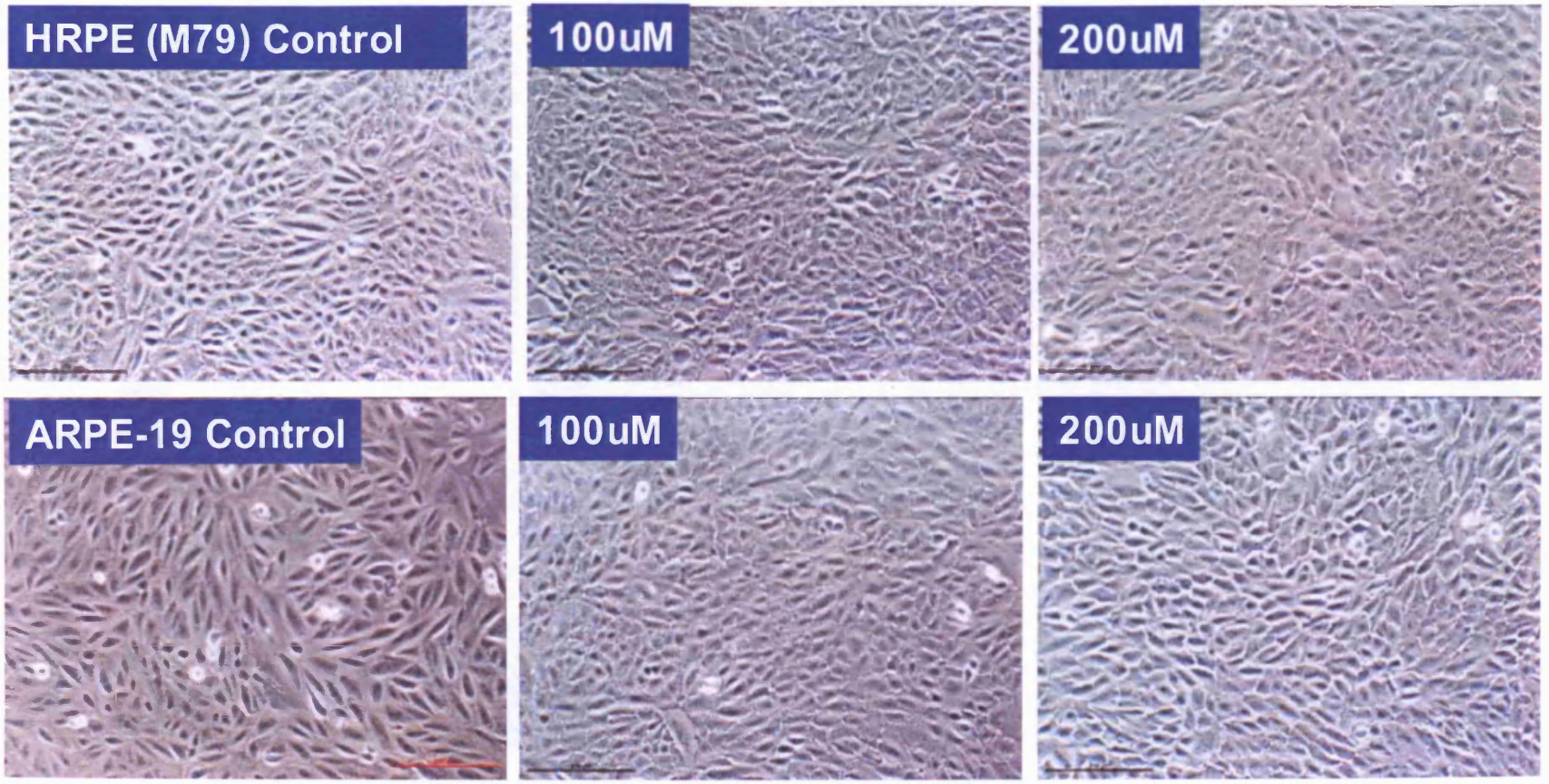

Figure 3.4.14 Representative Photodocumentation of Primary Human RPE (M79) and the ARPE-19 after 24hrs of Exposure to tert-butylhydroperoxide (t-BOOH). Cells were washed with 1XPBS and then incubated with the oxidative stressor diluted in Hams F-10 media without supplemental FCS to achieve desired concentrations. Control cells were mock treated with Hams F-10 with no oxidative stressor or FCS (Scale bar = 200μm)

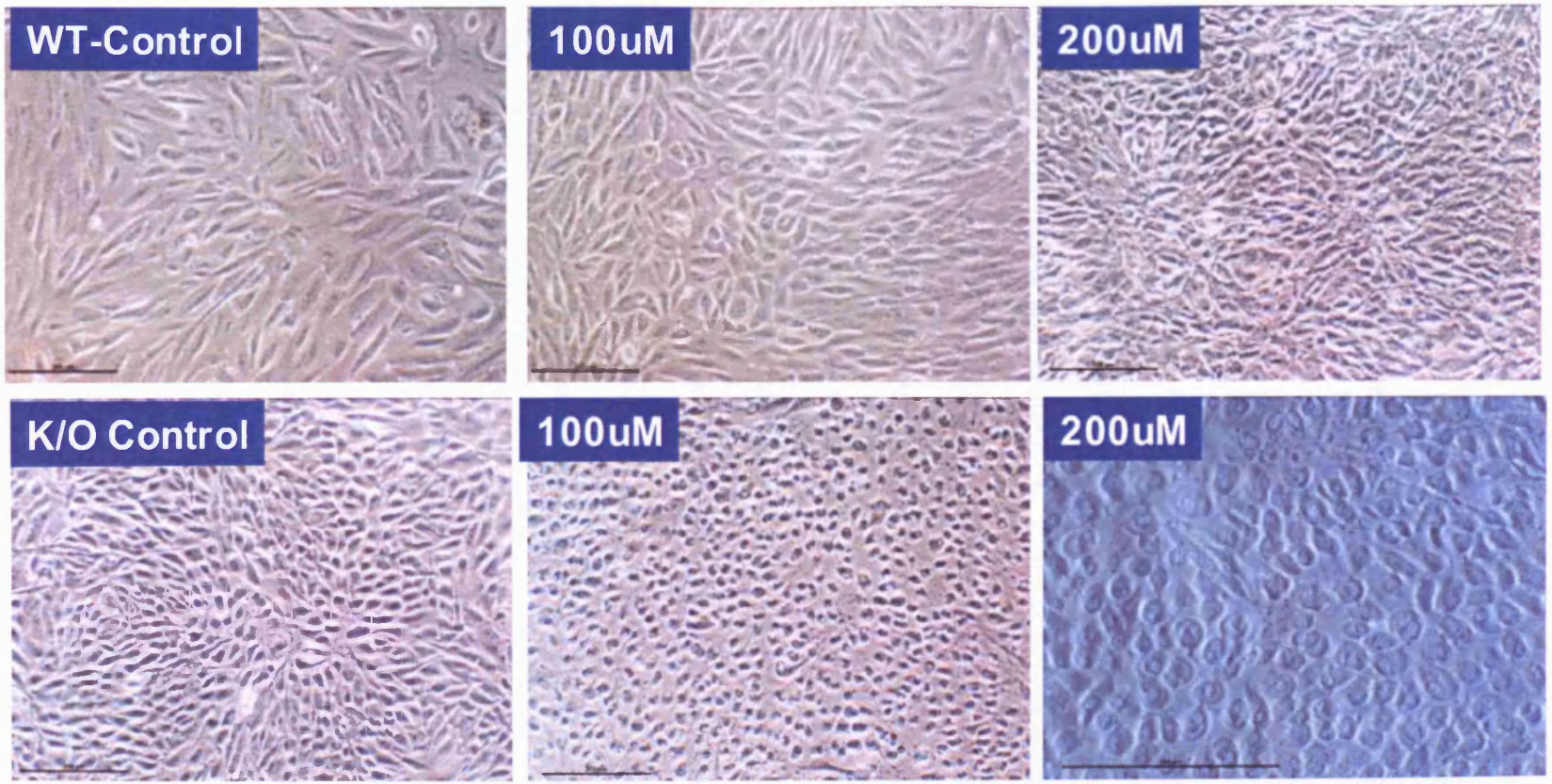

Figure 3.4.15 Representative Photodocumentation of Primary Wild-Type RPE and αA-crystallin Knock-Out RPE after 24hrs of Exposure to tert-butylhydroperoxide (t-BOOH). Cells were washed with 1XPBS and then incubated with the oxidative stressor diluted in Hams F-10 media without supplemental FCS to achieve desired concentrations. Control cells were mock treated with Hams F-10 with no oxidative stressor or FCS (Scale bar = 200μm)

3.5 Chapter Discussion

This work revealed preliminary studies on *in vitro* α-crystallin expression in two RPE cell types; isolated primary RPE cells and the well-established, non-transformed human ARPE-19 cell line, as well as in the neural retina. Primary *in vitro* human RPE cell culture is well documented (Edwards, 1981; Boulton *et al.,* 1983; Edwards, 1983; Boulton, 1990; Pfeffer, 1991) and provides the isolation of a pure cell population, highly controllable conditions allowing measurements on a cell-by-cell basis, time course flexibility and the examination of mechanisms in ocular pathogenesis (Boulton, 1990; Seigel, 1999). When comparing RPE cells *in vitro* with their *in vivo* counterparts, there are numerous morphological similarities including apical microvilli, junctional complexes, basal nuclei, and cytoplasmic organelles (Boulton, 1990). Additionally, cultured RPE can ingest and phagocytose rod outer segments (Boulton *et al.,* 1984), synthesize and secrete glycosaminoglycans (Edwards, 1983), produce an extracellular matrix (Campochairo *et al.,* 1986) and if fed with rod outer segments for an extended time, develop intracellular inclusion bodies (Boulton *et al.,* 1989). It is important to note that although many similarities exist between RPE *in vitro* versus *in vivo,* disadvantages of RPE cell culture can include the selective loss of specific cell phenotypes/functions, modifications of tissue architecture, and the absence of stimuli from surrounding cells types (Boulton, 1990; Seigel, 1999). Specifically, disadvantages of cultured RPE include the loss of melanin pigmentation with progressive cell division and various degrees of dedifferentiation (Boulton and Marshall, 1985). In this present work and in future studies, using the isolated cells at early passage numbers can conquer these mild disadvantages and if necessary, depigmented RPE cells can be 'artificially' repigmented as previously described (Boulton and Marshall, 1985).

The ARPE-19 retains many important RPE characteristics such as outer segment phagocytic activity, cell polarity, and expression of key RPE cell markers (Dunn *et al.,* 1996). As described, isolated primary RPE cells and the ARPE-19 retain many of their normal *in vivo* properties during cell culture conditions and thus are suitable for our study (Boulton and Marshall, 1985; da Cruz et al., 1998; Hu and Bok, 2001; Haruta et al., 2004). However, it is important to note that when comparing between primary RPE and the ARPE-19, one should use caution. Cai and Del Priore (2006) performed DNA microarray analysis on both cell types and found that although there are similarities between the two cell types, there are also significant differences in their gene expression profiles.

For our particular study, it was important to use primary human RPE as a comparison between both the ARPE-19 and primary murine RPE, with regards to characteristics of *in-vitro* growth. As reported in this chapter, similarities between primary human and the ARPE-19 are strikingly similar with regards to attachment, division and confluency. The only notable difference between human and mouse RPE isolation was simply the volume of cells isolated. Based on the size difference between the human eye and the mouse eye, more eyes were needed from the mouse to obtain enough cells to form a confluent culture.

Additionally, the presence of the α-crystallins was examined in human RPE and retina. As shown, αB-crystallin was detected in both the human RPE (primary RPE and the ARPE-19) and retina at gene and protein levels. This finding is further supported by previous studies that also examined αB-crystallin expression in human RPE cells (Lin *et al.,* 1993; Alge *et al.,* 2003; Mao *et al.,* 2004; Yaung *et al.,* 2007) and retina (Xi *et al.,* 2003; Joachim *et al.,* 2007; Kim *et al.,* 2007; Whiston *et al.,* 2008).

It is important to note that αA-crystallin expression was not found in either the primary human RPE or the ARPE-19, but was found in the retina. Retinal expression of αA-crystallin has previously been examined in mice (Xi *et al.,* 2003; Rao *et al.,* 2008), rats (Kapphahn *et al.,* 2003; Sakaguchi *et al.,* 2003; Wang *et al.,* 2007; Miyara *et al.,* 2008), horses (Hauck *et al.,* 2007), and frogs (Deretic *et al.,* 1994).

The lack of αA-crystallin expression in the RPE is not consistent with a recent study done by Yaung *et al.,* 2007, that found αA-crystallin was present in the human RPE at both a gene and protein level. It was a surprising finding since a number of troubleshooting techniques were utilized. Possible errors in gene expression could include incorrect primer sequences, low PCR cycle numbers, and incorrect annealing temperatures. All of these possible problems were ruled out and in addition, a positive control, the lens epithelial cell line, SRA 01/04, was used yielding a band corresponding to αA-crystallin. Additionally, it is important to note αA-crystallin expression in the RPE is much lower than αB-crystallin expression (Yaung *et al.,* 2007). Detection of αA-crystallin through RT-PCR was not successful in our study, however Yaung *et al.,* 2007 used real time PCR amplification, therefore it may be useful to consider this technique for future studies.

RPE protein expression of αA-crystallin was also discovered by Yaung *et al.,* 2007. Perhaps our protein samples were not concentrated enough to detect αA-crystallin or the expression of αA-crystallin was so low that our method of detection was unsuccessful. Future studies could make the proteins more concentrated and utilize the use of a species-specific biotinylated secondary antibody with streptavidin peroxidase to amplify the protein signal.

The final component of our study examined the mitochondrial viability of human RPE, the ARPE-19 and mouse RPE (WT and αA-crystallin K/O) with two well documented oxidative stressors, H_2O_2 and *t*-BOOH. These two oxidative stressors are biologically relevant, especially for the RPE. H_2O_2 has been found in ocular tissues in vivo (Halliwell *et al.,* 2000) and is produced by the RPE as a reactive oxygen intermediate during photoreceptor outer segment phagocytosis (Tate *et al.,* 1995). *t*-BOOH is a compound of early intermediates of lipid peroxidation and is relevant because it is able to initiate lipid peroxidation (Halliwell and Gutteridge 1999). Results of induced oxidative stress in cultured RPE cells include DNA damage (Matsui *et al.,* 2001) changes in patterns of gene expression (Alizadeh *et al.,* 2001, Weigel *et al.,* 2002), apoptosis (Jiang *et al.,* 2000, Jin *et al.,* 2001), and damage to chloride channels (Wills *et al.,* 2000, Wang *et al.,* 2002). These and other biological effects of oxidative stress result in reduced cell viability that can be measured by assays that detect leaky membranes (Matsui *et al.,* 2001; Alge *et al.,* 2002; Bailey *et al.,* 2004).

For our particular analysis, we examined mitochondrial activity as an indicator of cell viability. The mitochondrion is the main organelle in which oxygen metabolism occurs, and stress from H_2O_2 treatment increases ROS generation in human RPE (Kannan *et a.,* 2004, Yaung *et al.,* 2007). However, it is important to note that performing an MTT assay alone cannot localize mitochondrial dysfunction. Other useful measurements of oxidative stress and associated cell death include trypan blue (Matsui *et al.,* 2001, Bailey *et al.,* 2004), propidium iodide (Nieminen *et al.,* 1992, Alge *et al.,* 2002) caspase-3 activation (Yaung *et al.,* 2007) and mitochondrial membrane permeability transition (Yaung *et al.,* 2007).

In our mitochondrial viability studies, we found that the ARPE-19 cell line was the most resistant to both oxidative stressors while the αA-crystallin K/O was the most affected,

especially with *t*-BOOH. This significant decrease in cell viability is further supported by Yaung *et al.*, 2007 who also found that RPE from α-crystallin K/O animals were more susceptible to oxidative damage than their WT counterparts.

The presence of α-crystallins in post-mitotic tissues like the RPE and neural retina may help contribute to their viability and longevity. As shown, α-crystallins were detected in human RPE and retina. *In-vitro* growth characteristics were similar between human and mice RPE and the presence of the α-crystallins may contribute to protecting the RPE and retina from oxidative stress.

In summary this chapter demonstrated that:

- *In-vitro* culturing of human RPE is similar to both wild-type and αA-crystallin knock-out RPE
- Human *in-vitro* expression of the α-crystallins were found in the RPE and neural retina
- The lack of αA-crystallin may make the RPE more susceptible to oxidative stress

Chapter 4.0:

In-vivo morphological and functional analysis of non-pigmented mice exposed to continuous blue light up to 7 days

4.1 Chapter Introduction

To investigate the potential protective role of α-crystallins in Noell's photochemical Type II damage of the retina, it was crucial to use an experimental design of light damage which exposed unsedated animals to continuous levels of light at low intensities (Noell *et al.*, 1966; Rapp and Williams 1979; Seiler *et al.*, 2000). As discussed previously (**Chapter 1**), in 1980 Noell classified non-thermal damage Type I or Type II based on the multifaceted dysfunction of the retina under light damaged conditions. Type I damage is characterized by massive photoreceptor loss with subsequent damage of the overlying RPE, precipitated by extensive bleaching of rhodopsin through short, intermittent light exposures in dark-reared animals (Noell 1980a, Organisciak and Winkler 1994). On the other hand, Type II damage is characterized by widespread photoreceptor loss with little or no damage to the RPE with long duration exposures with low intensity light (Noell 1980). Similar to Type I, Type II damage is also mediated by rhodopsin. Type II photochemical damage of the retina is the most commonly studied form of retinal light damage (Organisciak and Winkler, 1994).

Retinal blue light exposure has been described as one of the "most hazardous components of the visual spectrum with the greatest potential for photoxicity" (Ham *et al.*, 1976). Studies support blue light damage as a possible inducer in the degeneration of the RPE and photoreceptors in age related disease (King *et al.*, 2004, Margrain *et al.*, 2004, Godley *et al.*, 2005, Algvere *et al.*, 2006, Chu *et al.*, 2006, Wu *et al.*, 2006, Thomas *et al.*, 2007, Siu *et al.*, 2008) by inducing damage which appears

mediated by the visual pigment, rhodopsin (Grimm *et al.*, 2000, Grimm *et al.*, 2001, Wu *et al.*, 2006, Wu *et al.*, 2006, Tanito *et al.*, 2007a, Thomas *et al.*, 2007)).

Therefore, one of the main purposes for this particular chapter was to determine if the constructed blue light apparatus had the potential to elicit damage in albino (non-pigmented) mice. Numerous experimental models of light damage that examine photochemical injury to the neural retina make use of albino rodents (Grignolo *et al.*, 1969, Cicerone 1976, Rapp and Williams 1979, Oraedu *et al.*, 1980, Rapp and Williams 1980, Li *et al.*, 2001, Wasowicz *et al.*, 2002, Danciger *et al.*, 2005, Tanito *et al.*, 2007a, Tanito *et al.*, 2007b,Tanito *et al.*, 2008)). Albino rodents have a defect in the enzyme tyrosinase, which catalyzes reactions that are responsible for the synthesis of the ocular pigment, melanin (Barsh, 1996). Melanin appears to protect the photoreceptors from scattered light and converts potentially absorbed photons into a mild thermal rise (Ginsberg and LaVail 1985, LaVail and Gorren 1987, Boulton *et al.*, 2001b). The 'pigmented' colors of the RPE and choroid can be attributed to its melanin, which is abundant in both the apical and midportion regions of the cells of the RPE and throughout the choroidal stroma. Importantly, in addition to its role of reducing the effects of light scattering, melanin can also act as a neutral density filter, bind chemicals, act as a free radical scavenger or generator, and can absorb energy in the visible or UV range (Boulton 1998).

The construction and experimental paradigm for continuous blue light exposure was based on an experiment previously conducted by Magdalene Seiler's group at the University of Louisville (Seiler *et al.*, 2000). In brief, Seiler's group developed a

model of photoreceptor degeneration (Type II) with selective photoreceptor loss and RPE sparing in unsedated albino rats exposed to continuous blue light.

Although Seiler's groups utilized albino Sprague-Dawley rats, this study examined the effects of continuous light exposure in the BALB/cBYJ of albino mice at 1, 3, 5 and 7 days of exposure. The BALB/cBYJ strain of albino mice are shown to be more susceptible to light damage due to identified allelic polymorphisms in the retinal pigment epithelium-specific gene, *Rpe65*, that modify retinal light damage (Danciger *et al.* 2000). For the BALB/cBYJ strain, an allele encoding a leucine at amino acid 450 (Leu450) of the *RPE65* protein was associated with this greater sensitivity to light damage (Danciger *et al.*, 2004). RPE65 is a protein which plays a vital role in the regeneration of rhodopsin kinetics and light damage susceptibility in mice (Wenzel *et al.*, 2005).

An additional focus for this chapter was to examine the expression of nuclear factor-kappa beta (NF-κB) in photochemical damage of the retina. NF-κB is a ubiquitous transcriptional factor that regulates a broad range of genes and plays a pivotal role in cell death and survival (Van Antwerp *et al.*, 1996, Ghosh *et al.*, 1998, Yang *et al.*, 2007). NF-κB has been linked to the α-crystallins in the area of inflammation (Masilamoni *et al.*, 2006, Ousman *et al.*, 2007). In particular, *in-vivo* and *in-vitro* studies found that αB-crystallin prevents cell death of astrocytes by inhibiting caspase-3 activation, and suppresses the inflammatory role of NF-kB (Ousman *et al.*, 2007). Additionally, it was shown that if cells were pre-treated with α-crystallins, NF-κB activity was suppressed, therefore downregulating the expression of proinflammatory cytokines (Masilamoni *et al.*, 2006).

Activation of NF-κB has been linked to microglia activation and production of proinflammatory molecules (Pawate *et al.*, 2004) and has also been shown to play a role in retinal degeneration (Zeng *et al.*, 2008) and photoreceptor apoptosis (Krishnamoorthy *et al.*, 1999, Masilamoni *et al.*, 2006, Yang *et al.*, 2007, Zeng *et al.*, 2008). Signaling of NF-κB begins with phosphorylation and degradation of IκB, a key component of the cytoplasmic NF-κB complex (Viatour *et al.*, 2005), and releases p50 and p65 subunits that translocate to the nucleus and promote transcription of proinflammatory genes (Chan and Murphy, 2003). Due to its connection to microglial activation, there are significant increases in the activity of NF-κB in many neurodegenerative diseases (Terai *et al.*, 1996, Hunot *et al.*, 1997, Kaltschmidt *et al.*, 1997).

This chapter not only will provide evidence that the designed apparatus has been constructed properly for future experiments, but it will also offer insight into morphological and functional changes associated with continuous blue light exposure in a non-pigmented rodent strain as well as the activity of NF-κB in photochemical damage of the retina (please refer to **Section 4.2 Chapter Aims**).

4.2 Chapter Aims

As stated above, Chapter 4 will investigate the ability for the blue light apparatus to elicit damage in a non-pigmented rodent strain. In order to accomplish this, the following aims will be addressed:

4.1a.) Analysis of any retinal morphological changes associated with sub-threshold, continuous blue light exposure in the BALB/cBYJ mouse strain

4.1b.) Assessment of visual function before blue light exposure and after a 10 day recovery period from initial exposure

4.1c.) Activity of NF-κB in photochemical damage of the albino retina

These aims were carried out by methods briefly discussed below (**Section 4.3**).

4.3 Experimental Design (*Detailed descriptions of the methods can be found in Chapter 2.0)*

The particular strain of albino mice used for this particular experiment were the BALB/c BYJ. As stated previously, Seiler's group used albino Sprague-Dawley rats that were exposed continuously to blue light for 1-7 days. Since remaining chapters examined pigmented mice on the 129 background, it was important to be consistent in the rodent model. Therefore an albino mouse strain was chosen instead of an albino rat strain.

Mice were obtained from Taconic Animals Facilities (Rockville, MD) in limited numbers due to vendor and space problems. At the time of purchase, the number of albino mice available at the requested age (6-8wks) was *fifteen*, therefore when referring to the experimental design flow chart (see **Section 2.3.5)** exposure of the mice would occur over **1, 3, 5 and 7 days and not 1-7 days** due to limited animal numbers.

Limited animal numbers resulted in limited trials; therefore for analysis of BALB/cBYJ mice, one trial was used for immediate analysis (histological and protein) and two trials were used for the 10 day recovery analysis (ERG, histological and protein). All mice were examined with ERG prior to light exposure.

Detailed descriptions of the experimental blue light apparatus (see **Section 2.3.4),** blue light experimental design (see **Section 2.3.5**), ERG testing (see **Section 2.4**), histology (see **Section 2.6**) and protein analysis (see **Section 2.5**) can be found in **Chapter 2**.

4.4 Chapter Results

4.4.1 Daily Humidity and Temperature Readings of BALB/cBYJ Mice Exposed to Continuous Blue Light

During all trials of blue light exposure, parameters were monitored twice a day. These parameters included maximum, minimum, and average temperature and humidity, checked every 12hrs while during experimental exposure, All temperature/humidity readings were taken with (Big Digit Hygro-Thermometer, Extech Instruments, USA). **Figure 4.4.1** illustrates the average values of both trials together and shows the standard mean and deviation overall of temperature readings during the all trials of BALB/cBYJ albino mice.

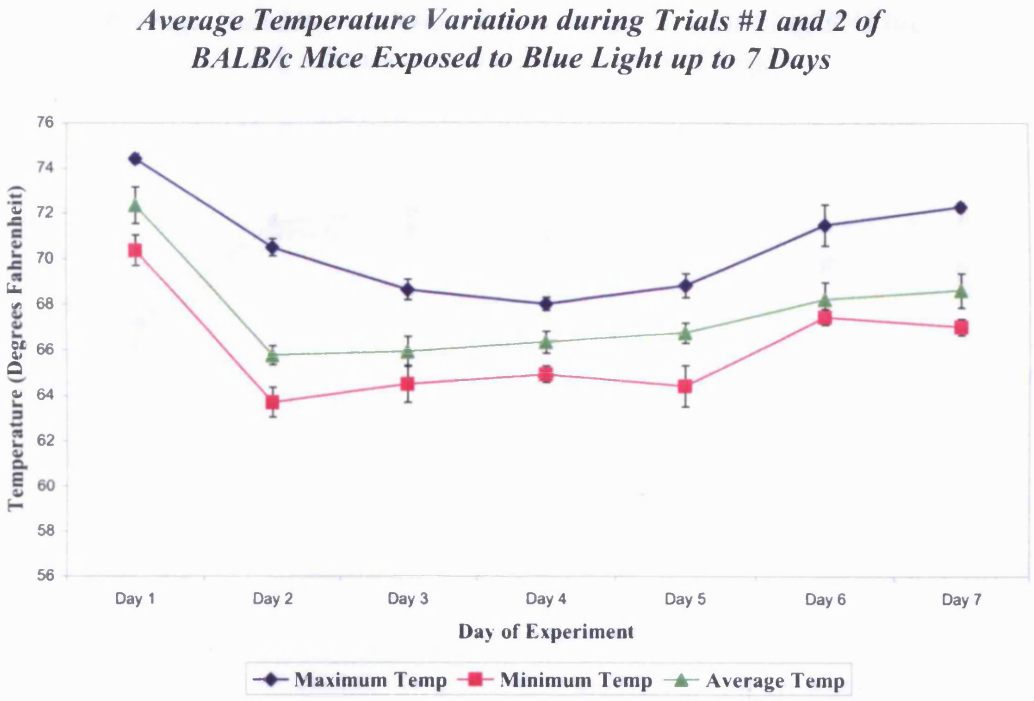

***Figure 4.4.1** Shown above are the maximum, minimum and average temperature readings taken during Trials #1 and 2 of BALB/cBYJ albino mice exposed to blue light up to 7 days. The x-axis corresponds to the day of the experiment and the y-axis refers to the temperature in degrees Fahrenheit. Individual readings at maximum, minimum and average were taken twice a day (every 12hrs) and recorded to assure that the overall temperature of the apparatus did not exceed 80˚F, which could cause extreme distress to the animals being exposed. Vertical bars represent the standard error of the mean.*

Figure 4.4.2 illustrates the average humidity values of both trials together and shows the standard mean and deviation overall of humidity readings during the two trials of BALB/cBYJ albino mice.

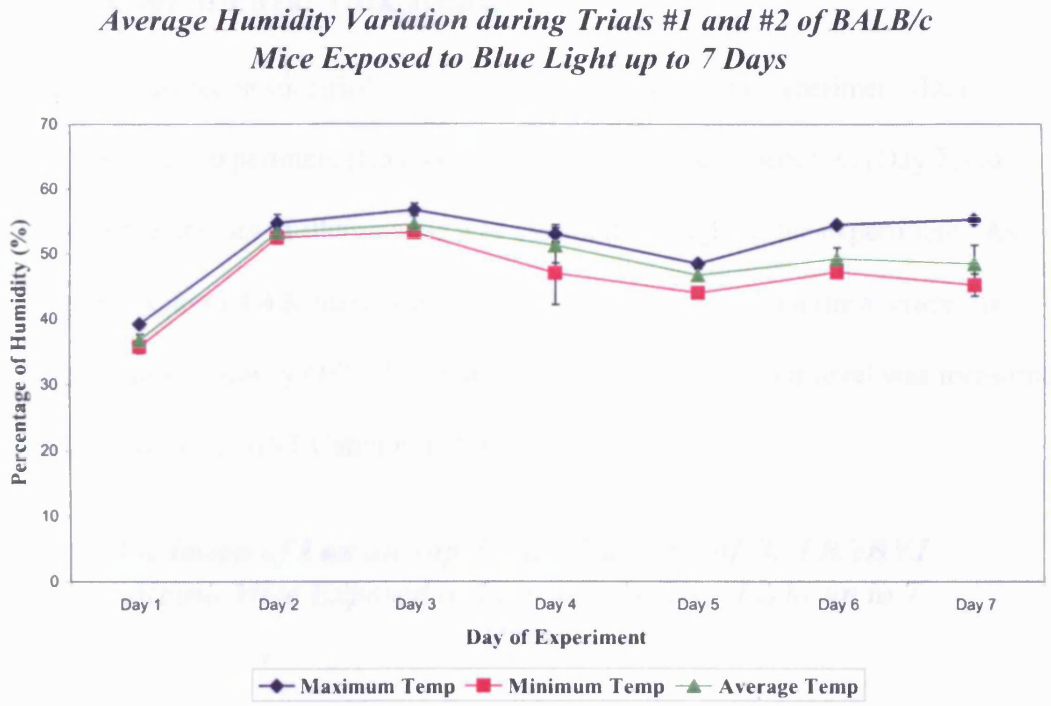

Figure 4.4.2 Shown above are the maximum, minimum and average humidity readings taken during Trials #1 and 2 of BALB/cBYJ albino mice exposed to blue light up to 7 days. The x-axis corresponds to the day of the experiment and the y-axis refers to the percentage of humidity. Individual readings at maximum, minimum and average were taken twice a day (every 12hrs) and recorded to assure that the overall humidity fell within the required 30-70% range. Vertical bars represent the standard error of the mean.

When referring to the overall average readings of both the temperature and humidity (**Figures 4.4.1 and 4.4.2** respectively), at no point does the maximum limit of temperature or humidity result. Based on the NIH Guide for the Care and Use of Laboratory Animals, a maximum temperature of 80˚F is considered dangerous to the animal and the range of humidity percentage must fall between 30 – 70%. As shown in both of these figures, the temperatures and humidity's fell within required ranges which were not dangerous to the exposed animals.

4.4.2 Experimental Lux Readings

Lux were measured at specified points (at the very start of the experiment (Day 1), in the middle of the experiment (Day 4) and at the end of the experiment (Day 7)) to assure that the amount of illuminance was constant throughout the experiment. As revealed in **Figures 4.4.3,** there was no significant deviation from the average lux reading of approximately 600. Illuminance (lux) at the cage floor level was measured using the Traceable NIST Calibrator (Fisher Scientific, USA).

Variation of Lux during Trials#1 and #2 of BALB/cBYJ Albino Mice Exposed to Continuous Blue Light up to 7 Days

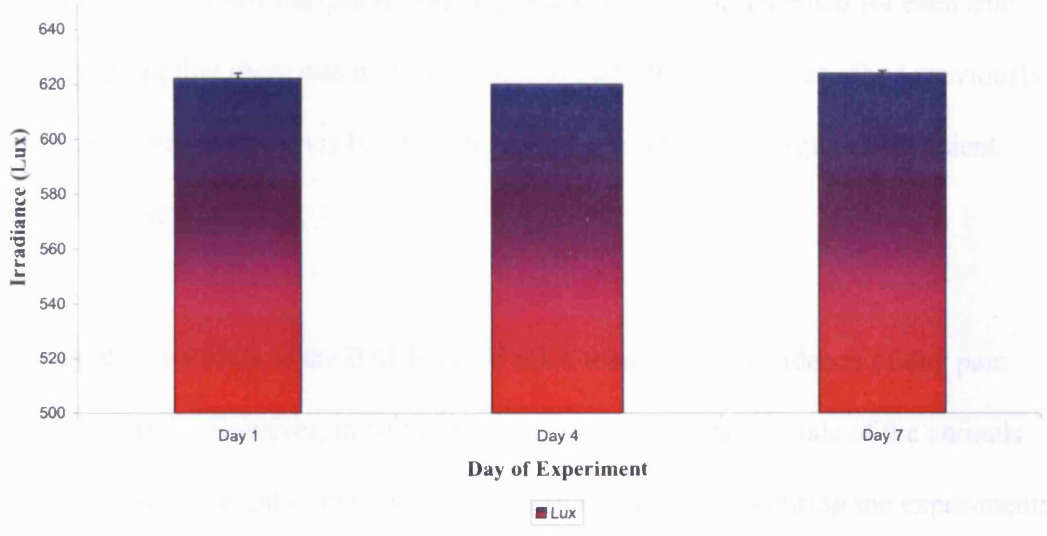

***Figure 4.4.3:** Shown above are lux measurements of the experimental blue light apparatus at Day 1, 4 and 7 of the experiment during Trials #1 and #2. The x-axis corresponds to the day of the experiment and the y-axis refers to the lux. Data represents the mean ± S.D.*

4.4.3 Behavioral Patterns of Exposed and Non-Exposed BALB/cBYJ Albino Mice

Based on approved animal protocols (*please see **Appendix 1),*** animals were required to be checked every 12hrs to assure that there was no pain or distress while being exposed to the continuous blue light. According to the NIH Guide for the Care and

Use of Laboratory Animals, "The recognition of pain and pain-induced distress, in animals is ethically necessary for proper clinical management of animals to ensure their well-being and to reduce research variability." Distinct signs and symptoms noted in laboratory rodents include: decreased activity, piloerection, and excessive licking and scratching, which can progress to selfmutilation (NIH Guide for the Care and Use of Laboratory Animals). In addition, respiration can be rapid and shallow and mice may vocalize and become unusually aggressive. For the particular strain used in these experiments (albino) an important sign of pain or distress are porphyrin ("red tears") secretion which can be seen around the eyes and nose.

A standard check-off list (*please see **Appendix 3)*** was implemented for each trial, documenting that there was no visible sign of pain/distress (as described previously), no ocular abnormalities visible with the naked eye, intact ear tags and sufficient food/water levels.

During the two trials of the BALB/cBYJ mice there was no evidence of any pain and/or distress. However, in addition to monitoring the daily vitals of the animals being exposed, weight of the mice were taken at three points during the experiment; before exposure to blue light, immediately after exposure to blue light and 10 days of recovery post-blue light exposure. Results from weight from Trial #1 and Trial #2 can be found in **Figure 4.4.4.**

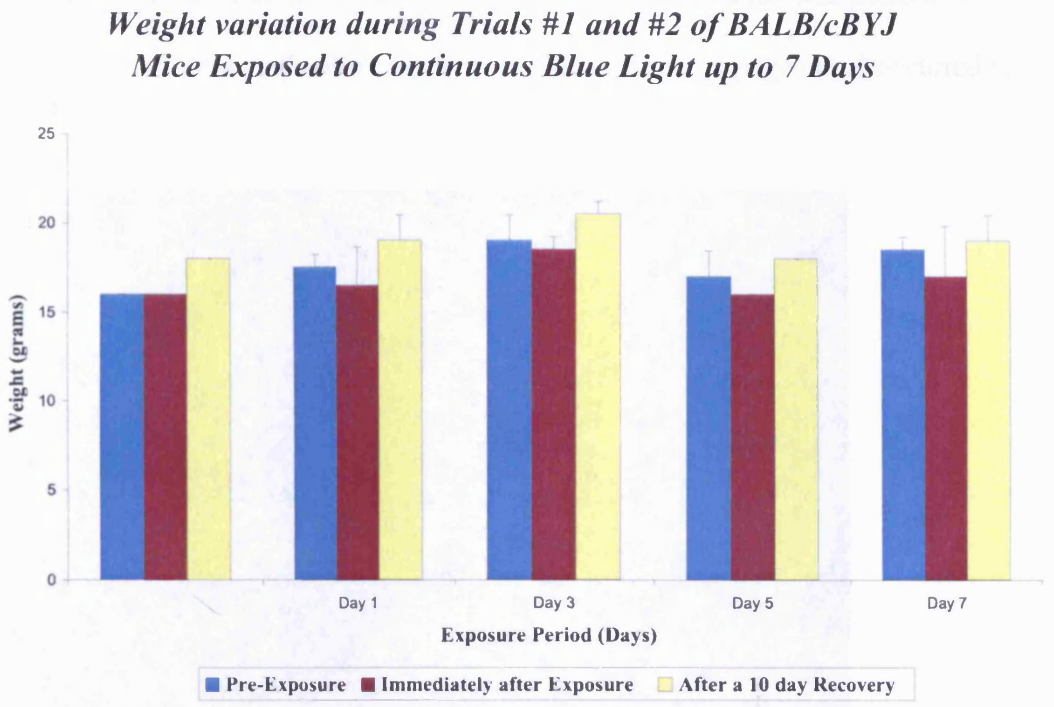

***Figure 4.4.4**: Shown above are the weight measurements of individual BALB/cBYJ mice exposed to blue light for 1, 3, 5 or 7 days in Trials #1 and #2. Shown on the x-axis is the exposure period of the animal (days) and the y-axis corresponds to the weight measured in grams. Measurements were performed before blue light exposure (pre-experimental), immediately after exposure (interim) and after a 10 day recovery from blue light exposure (10-days post experiment). Day 0 refers to the control animal (no blue light exposure). Data presented represents the mean ± S.D.*

Overall there was no statistically significant effect on the weights of albino mice exposed to continuous blue light up to 7 days. During both trials of the experiment, animals were supplied with fresh food and water. Although some animals exhibited a slight decrease in their weight immediately after exposure, all animals regained their original weight during the 10 day recovery period.

4.4.4 Histological Analysis of the BALB/cBYJ Retina Immediately after and after a 10 day recovery from Exposure to Continuous Blue Light

Retinal histology of albino mice exposed to continuous blue light for 1, 3, 5, or 7 days was examined immediately after their designated exposure. **Figure 4.4.5** illustrates area of capture for analysis of the whole sections of central retina. All eyes were

sectioned at the level of the optic nerve and photodocumentation was performed 0.10 – 0.25mm from either side of the optic disc. Most of the damage noted occurred in this region.

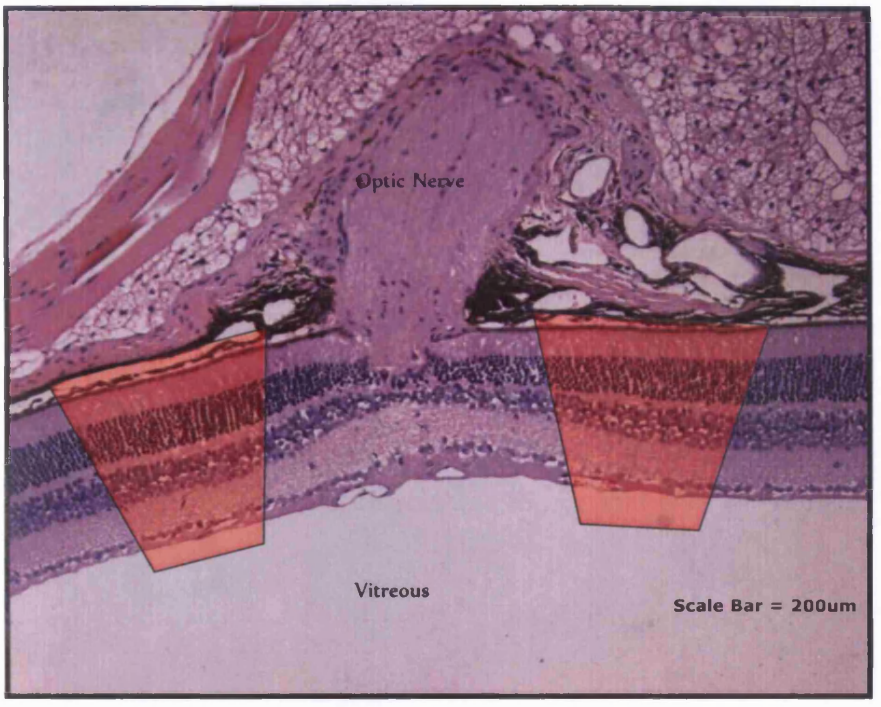

***Figure 4.4.5** Shown above is an example of the measured areas of total retina for histological analysis (this section is actually from a pigmented, 129Sv mouse). All eyes were sectioned at the level of the optic nerve and the area of analysis (note red shaded areas) was 0.10mm to 0.25mm on either side of the optic disc. Sections were stained with haematoxylin and eosin to visualize retinal structure. Scale bar represents 200µm.*

In order to analyze any photochemical damage which may have occurred during exposure, histological sections of mouse retina were analyzed to determine any cellular loss

Due to limited number of available animals, only 1 trial examined the effects of continuous blue light exposure immediately after the designated exposure period. **Figure 4.4.6** contains whole sections of retina as well as a magnified view of the outer and inner segments of the photoreceptors. As shown, **Day 0 (no blue light control)** and **Day 1 (24hrs)** contain normal rows of photoreceptor nuclei (8-10 rows)

with a tight, uniform structure to the inner and outer photoreceptor segments. Both **Day 0 and Day 1** exhibited an RPE cell layer which appears to be intact with no presence of any surrounding macrophages in the subretinal space.

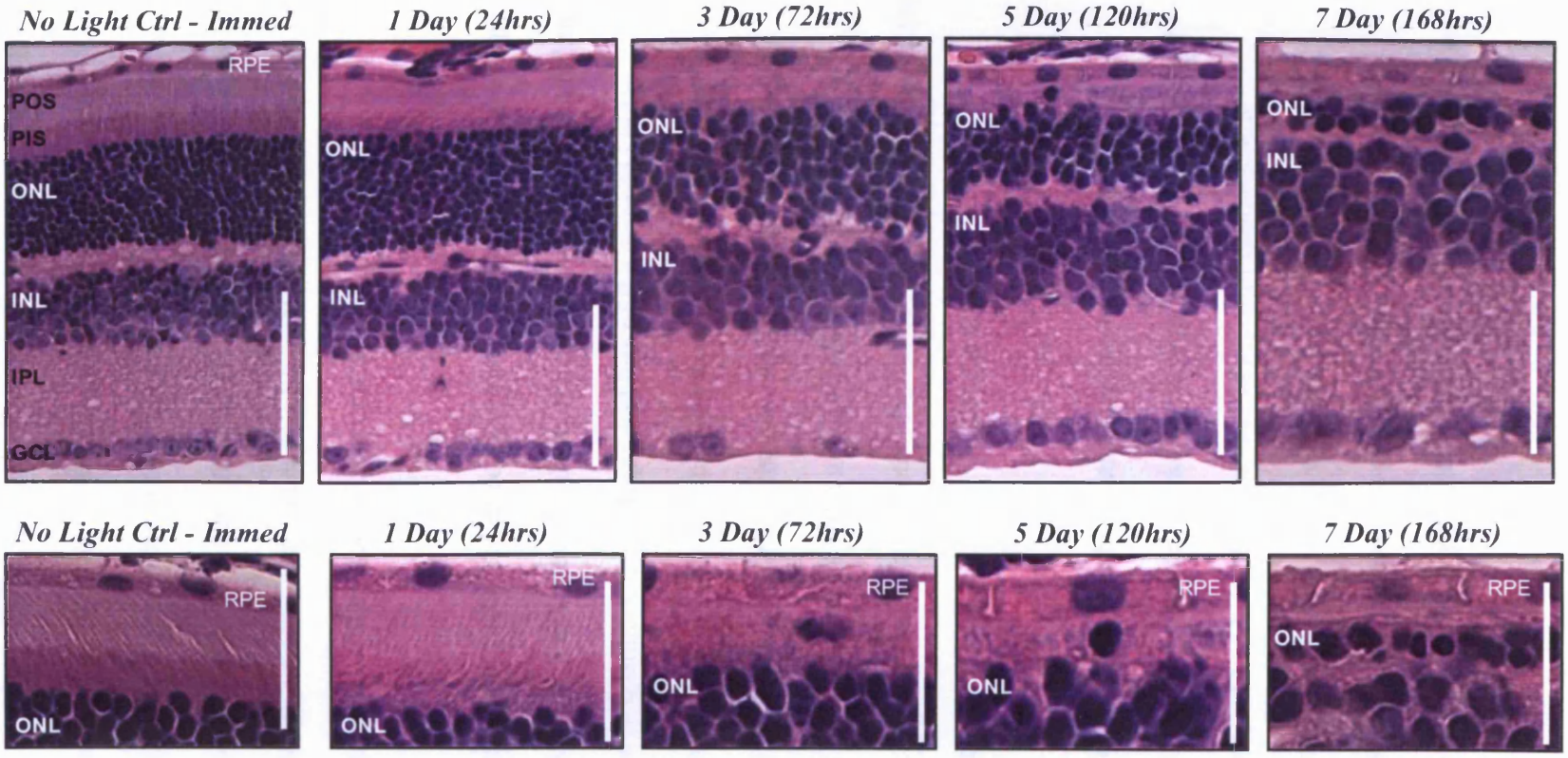

Figure 4.4.6 Immediate whole retinal histological of inner/outer photoreceptor segment analysis of albino mice exposed to continuous blue light for 1, 3, 5 or 7 days. Top row of photos correspond to whole retina photodocumented 0.10 – 0.25 mm from either side of the optic disc (magnification of 20x; scale bar = 100μm). Bottom row of photos reveals higher magnification of the inner/outer segments of the photoreceptors and outer nuclear layer (magnification of 40X; scale bar = 50μm. RPE = Retinal pigment epithelium, POS = Photoreceptor outer segments, PIS = Photoreceptor inner segments, ONL = Outer nuclear layer, INL = Inner nuclear layer, IPL = Inner plexiform layer, GCL= Ganglion cell layer.

Three days (72hrs) of light exposure produced a slight reduction of the photoreceptor nuclei to approximately 6-7 rows with substantial damage to the composition of the outer and inner photoreceptor segments. When comparing to the photoreceptor segments of **Day 0 and Day 1**, it is difficult to distinguish the transition zone from outer to inner segments with **Day 3**. Additionally, there is no uniform structure or shape to the segments and a macrophage appears to be present in the subretinal space indicating possible apoptosis of the photoreceptor nuclei.

Five days (120hrs) of light exposure revealed a greater reduction in the photoreceptor nuclei compared to the control and previous days. Five days of exposure resulted in an ONL of 4-5 rows with continued degradation and loss of the inner and outer segments of the photoreceptors and the presence of a macrophage subretinal space. However, the greatest reduction in the photoreceptor nuclei occurred at the longest period of exposure of **7 days (168hrs)**, reducing the ONL to a mere 1-2 rows of nuclei. Additionally, the segments of the photoreceptors decreased to point where the ONL almost appears to be positioned directly next to the RPE.

Surprisingly, the RPE layer appears to be relatively intact as observed with light microscopy analysis, although perhaps a deeper, more detailed analysis may reveal other structural changes, such as loss of nuclei, loss of melanin granules or a breakdown of the blood retinal barrier (BRB) (Putting *et al.,* 1993). Since these animals were non-pigmented, loss of melanin granules could not be a measurable indicator. Additionally, vitreous fluorophotometry was not performed to assess the BRB.

When examining retinal histology in the albino mice exposed to continuous blue light, two trials were performed to analyze damage 10 days post the original designated damage. Therefore if a mouse was exposed for 1 day (24hrs), after its designated exposure, it was placed back into normal cyclic conditions (12hrs on/12 hrs off) and evaluated 10 days later. **Figure 4.4.7** reveals representative whole sections of retina as well as a magnified view of the outer and inner segments of the photoreceptors.

When referring to the whole retinal sections, **Day 0 (Control – No blue light exposure)** reveals a tight, compact outer nuclear layer consisting of 8-10 rows of photoreceptor nuclei, tight inner nuclear layer and a uniform composition of the inner and outer segments of the photoreceptors with a uniform and intact RPE layer. **Day 1 (24hrs)** appears to closely resemble **Day 0,** however there is a decreased amount of photoreceptor nuclei (approximately 6 rows) in the outer nuclear layer..

Day 3 (72hrs) exposure mouse reveals a greater reduction of photoreceptor nuclei to approximately 3 rows in the outer nuclear layer compared to **Day 0** and it appears as though the inner nuclear layer has increased in thickness or nuclei number compared to the control. This artificial increase in number or thickness is most likely due to intracellular swelling since all photos were taken at the same magnification. Nuclear swelling can be found as a degenerative change in the retina possibly indicating subsequent necrosis of affected retinal tissue (Sisk and Kuwabara, 1985).
When comparing immediate analysis versus 10 day recovery of **Day 3**, there is a greater reduction in the outer nuclear layer and inner nuclear layer swelling 10 days after continuous blue light exposure.

Day 5 (120hrs) also exhibited a decrease in photoreceptor nuclei (2-3 rows) of the outer nuclear layer with swelling of the inner nuclear layer. As with **Day 3,** when examining retinal histology immediate versus 10 day recovery, **Day 5** also exhibits a greater reduction in the outer nuclear layer with increased nuclear swelling after 10 days of recovery.

Seven days (168hrs) of exposure after a 10 day recovery period exhibited the greatest decrease in the outer nuclear layer with corresponding inner nuclear layer swelling. Both trials of BALB mice not only illustrated 1-2 rows of photoreceptor nuclei, but also cellular swelling of the remaining outer nuclear layer was noted, a finding not seen with other exposure days. When 10 days of recovery is compared to immediate analysis, there does not appear to be an increase in the outer nuclear layer reduction or inner nuclear layer swelling. The only notable difference is the cellular swelling present in the reduced outer nuclear layer.

On closer examination of the outer retina (including the RPE, inner/outer photoreceptor segments and outer nuclear layer), there is a definite decrease in the inner/outer segments of the photoreceptor layer as the exposure time increases.

Both trials of the control mice **Day 0 (0hrs),** exhibited a tight, uniform appearance to all visible layers. There is a distinct separation of the outer to inner segments of the photoreceptor segments and the ONL shows no observable signs of compromise. **Day 1 (24hrs)** reveals minor distortion to the inner/outer photoreceptor segments and the RPE appears to have lost nuclei with sporadic intracellular vesiculation. When comparing the 10 day recovery period analysis with immediate analysis, **Day 1**

(24hrs), exhibits a similar appearance in inner/outer photoreceptor segment thickness; however, the RPE layer after immediate exposure (**Figure 4.4.6)** does not exhibit nuclei loss or vesiculation.

In **Day 3 (72hrs)**, the inner/outer photoreceptor segments are barely visible. The thickness of the photoreceptor layer has decreased so dramatically that it appears as though the ONL is quite close to the RPE layer. When referring to the ONL, nuclei appear to have condensed chromatin centers with surrounding intracellular swelling. Although nuclei are present in the RPE, the actual RPE cells appear more columnar rather than cuboidal in appearance. Additionally, the distinction between individual RPE cells is difficult to observe. When **Day 3 (72hrs)** 10 days post recovery is compared to immediate analysis (see bottom row of **Figure 4.4.6**), immediate analysis reveals a decrease in thickness of the photoreceptor segments.

Day 5 (120hrs) reveals a dramatic decrease in thickness of the photoreceptor layer when compared to the **Control Day 0 mice**. It is virtually impossible to distinguish any visible separation of the outer to inner segments and the remaining layer appears to have a disrupted composition. The ONL thickness was decreased in both trials, with condensed chromatin centers and mild intracellular swelling of the remaining nuclei. Overlying RPE does appear to have some nuclei loss and adhesions between individual cells appear to be compromised in both trials.

Both trials of **Day 7 (168hrs)** exhibited the greatest decrease in thickness of the photoreceptor segment and outer nuclear layers. This extreme decrease in thickness of both layers is also seen when outer retinal layers are examined immediately after

exposure (see **Figure 4.4.6**). Additionally, there is notable swelling of the ONL nuclei when compared not only to **Day 0**, but also remaining **Days 1, 3, and 5** after a 10 day recovery period.

Another way to illustrate the differences in overall retinal thickness or individual layer thickness (outer nuclear, inner nuclear, or photoreceptor layers), both **Trials #1 and #2** can be seen graphically in **Figures 4.4.8, 4.4.9a, and 4.4.9b, 4.4.10** corresponding to whole retinal thickness, outer nuclear layer thickness, inner nuclear layer thickness, and photoreceptor segment thickness respectively after a 10 day recovery period.

As shown in **Figure 4.4.8**, there is a corresponding decline in the thickness of the overall retina as the period of exposure of the albino mice is increased. Both trials exhibit a decrease in thickness, with the greatest decrease in thickness occurring at **Day 7 (168hrs)**, the longest exposure time of the mice. **Figures 4.4.9a and 4.4.9b** also reveal a continual decline in the thickness of both the outer nuclear layer (**Figure 4.4.9a**) and inner nuclear layer (**Figure 4.4.9b**) respectively. When referring to **Figure 4.4.9a**, there is a dramatic decrease in the outer nuclear layer thickness from **Day 1 (24hrs)** to **Day 3 (72hrs)** in both trials and when referring to **Figure 4.4.6**, one can appreciate the notable decrease in the outer nuclear layer at **Day 3 (72hrs)**. The decrease in thickness of the inner nuclear layer (**Figure 4.4.9b)** appears to be less dramatic than that of the outer nuclear layer and this finding is not surprising since photochemical damage to the retina primarily affects the outer retina, in particular RPE, photoreceptor inner/outer segments and the outer nuclear layer (Noell *et. al.*, 1966; Kuwabara and Storn, 1968). **Figure 4.4.10** reveals the dramatic decrease in

thickness of the inner and outer photoreceptor segments, revealing the damage of the outer retina.

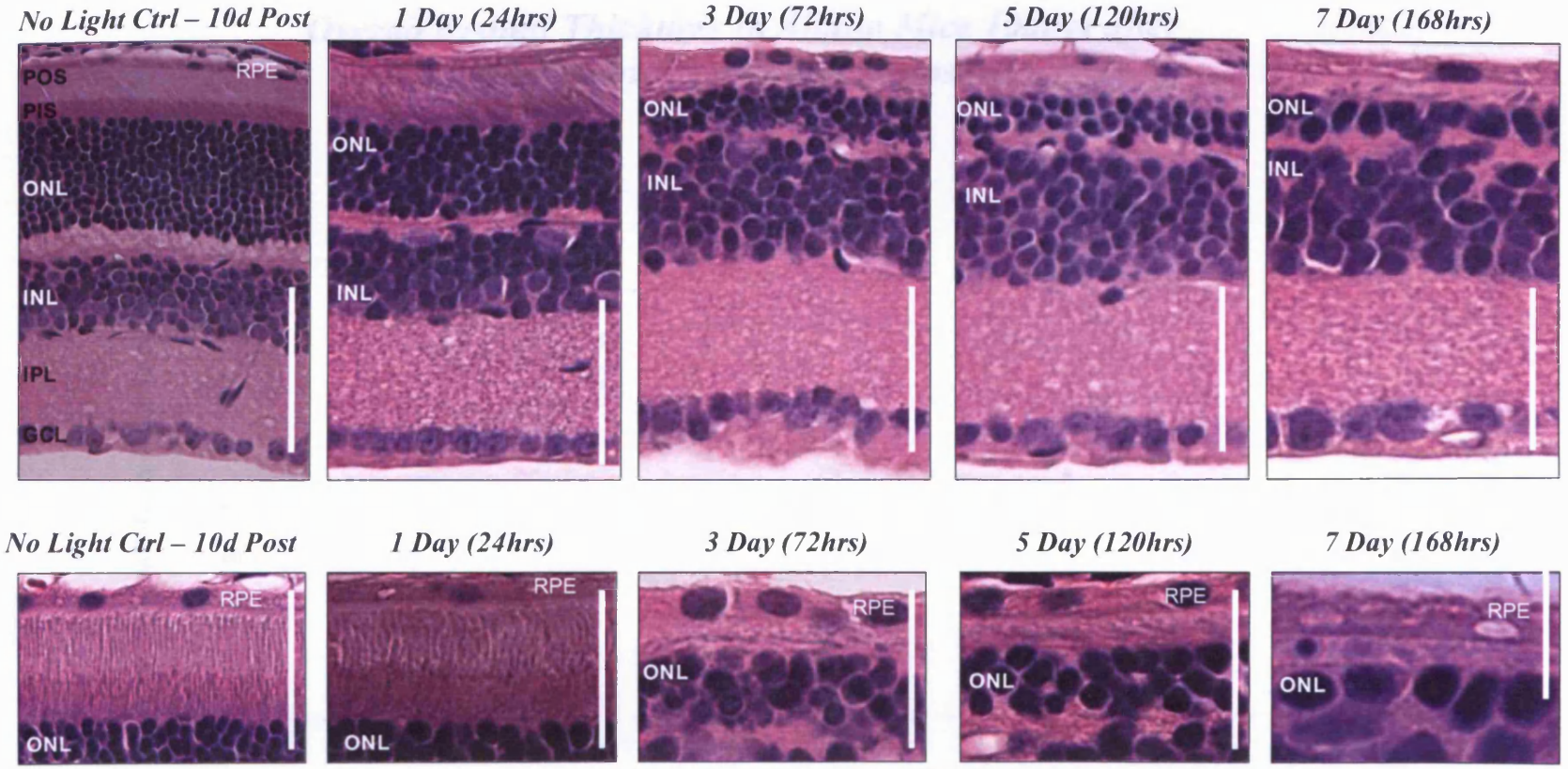

Figure 4.4.7 Histological Analysis of Whole retina and of Inner/outer Photoreceptor Segment Analysis of Albino mice Exposed to Continuous after a 10 day recovery period. Top row of photos correspond to whole retina photodocumented 0.10 – 0.25 mm from either side of the optic disc (magnification of 20x; scale bar = 100μm). Bottom row of photos reveals higher magnification of the inner/outer segments of the photoreceptors and outer nuclear layer (magnification of 40X; scale bar = 50μm. RPE = Retinal pigment epithelium, POS = Photoreceptor outer segments, PIS = Photoreceptor inner segments, ONL = Outer nuclear layer, INL = Inner nuclear layer, IPL = Inner plexiform layer, GCL= Ganglion cell layer.

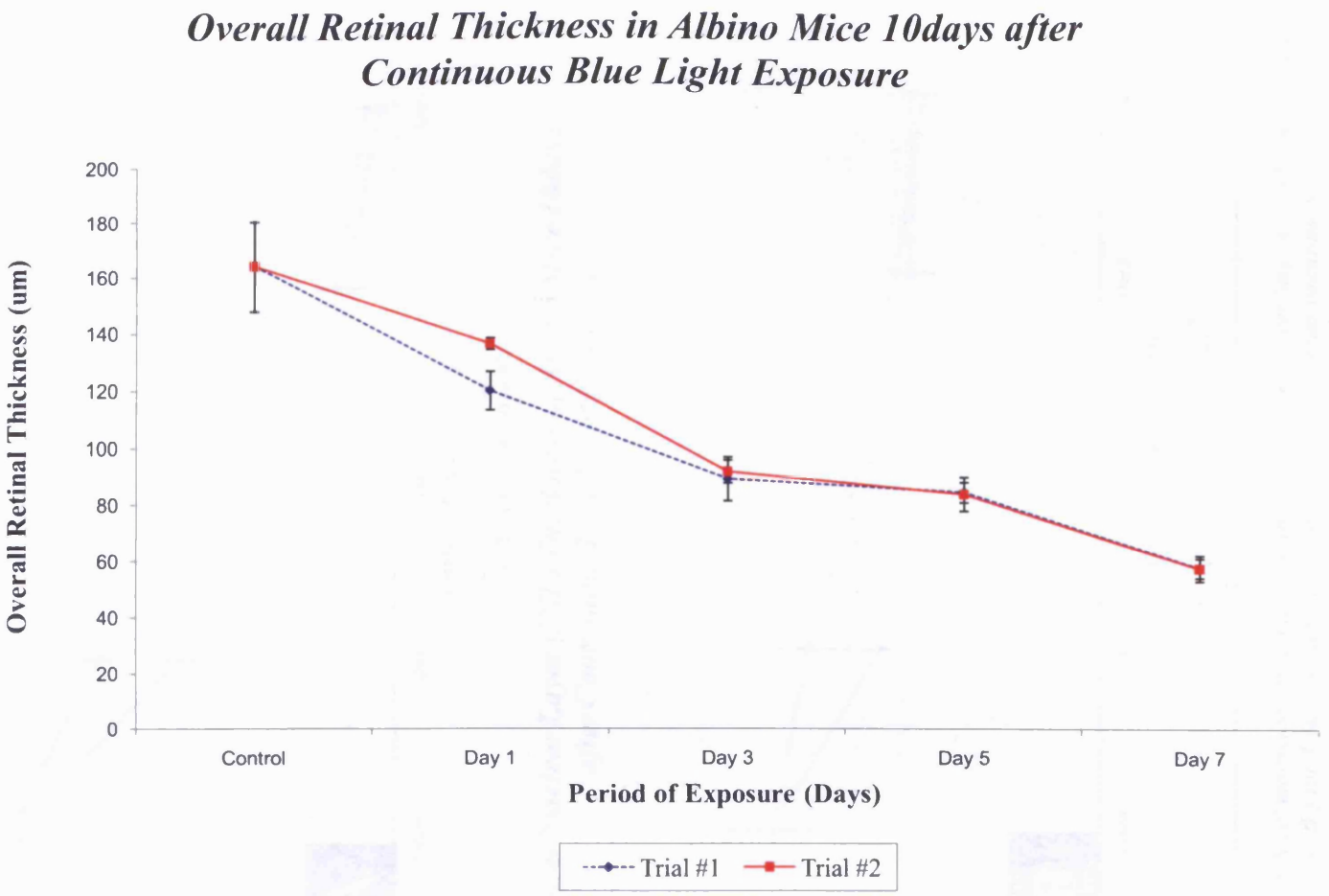

Figure 4.4.8 Graphical description of the morphometric analysis performed on whole retinal sections of Trial #1 and #2 histology. For each animal during each trial, there was a minimum of 4 sections taken. Three to four measurements were made per field, which were averaged to provide a single value for each retina. Trial 1 was from 1 animal, while Trial 2 was from 2 animals. Data are expressed as mean ±S.D.

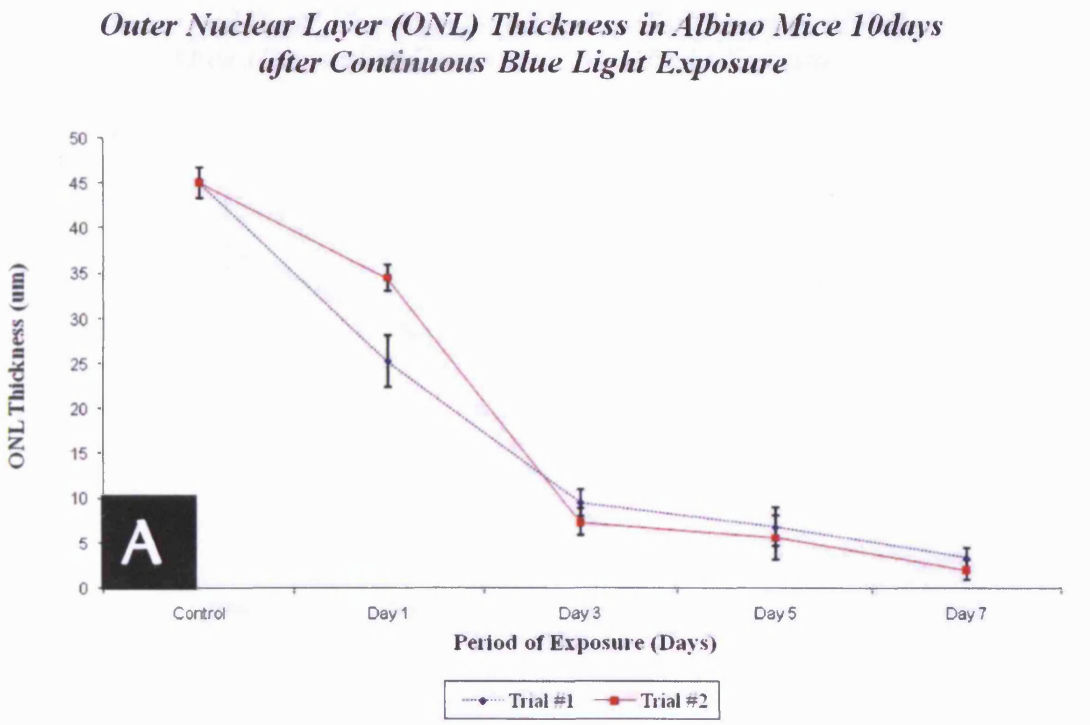

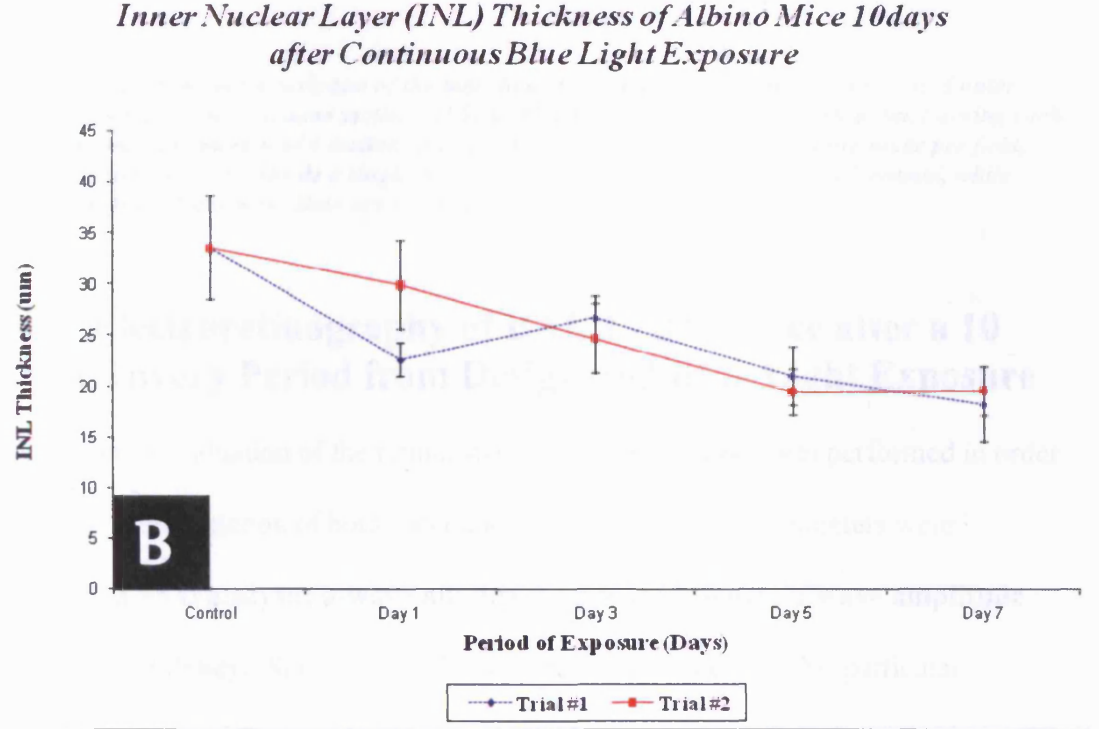

Figure 4.4.9 Graphical morphometric analysis of the outer nuclear layer (see 'A') and inner nuclear layer thickness (see 'B') for Trials #1 and 2 of albino mice 10 days after continuous blue light exposure. For each animal during each trial, there was a minimum of 4 sections taken. Three to four measurements were made per field, which were averaged to provide a single value for each retina. Trial 1 was from 1 animal, while Trial 2 was from 2 animals. Data are expressed as mean ±S.D.

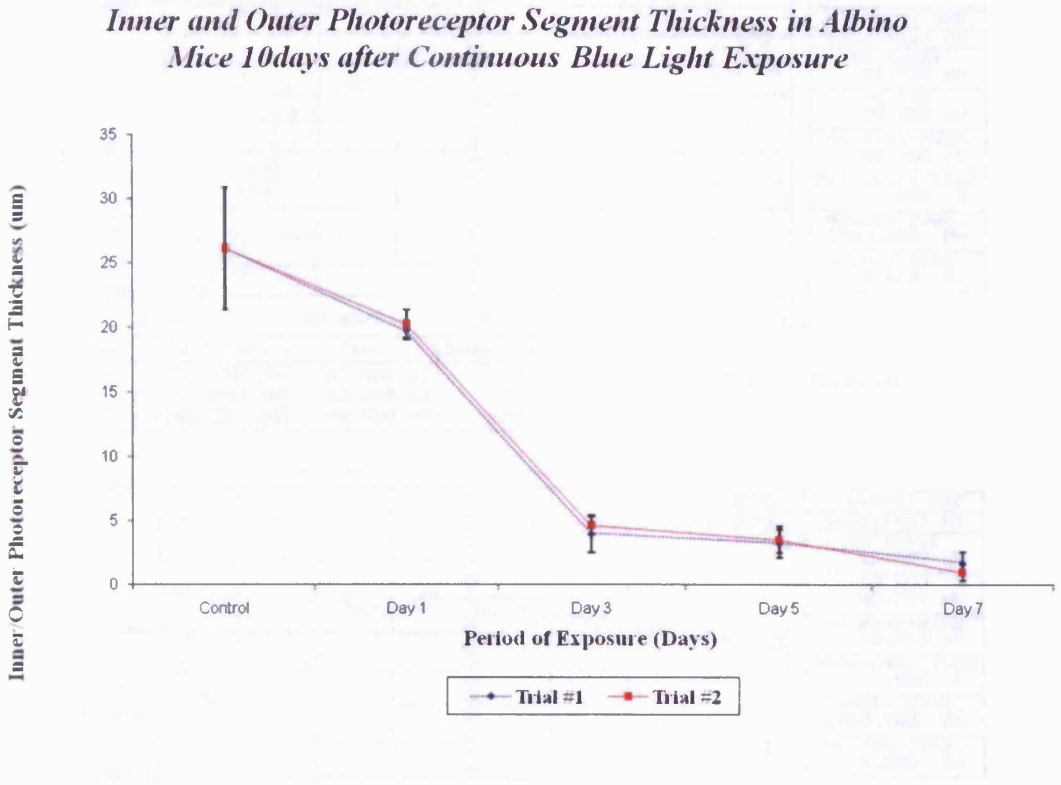

Figure 4.4.10 ***Graphical description of the morphometric analysis performed on inner and outer photoreceptor segment thickness sections of Trial #1 and #2 histology. For each animal during each trial, there was a minimum of 4 sections taken. Three to four measurements were made per field, which were averaged to provide a single value for each retina. Trial 1 was from 1 animal, while Trial 2 was from 2 animals. Data are expressed as mean ±S.D.***

4.4.5 Electroretinography of BALB/cBYJ mice after a 10 day Recovery Period from Designated Blue Light Exposure

In addition to evaluation of the retinal structure, ERG analysis was performed in order to assess visual function of both outer and inner retina. Four parameters were analyzed in ERG analysis; **a-wave amplitude, a-wave latency, b-wave amplitude and b-wave latency.** Since the number of mice was limited for this particular experiment, two mice were analyzed for each time point after their designated exposure. Shown in Figure **4.4.11** are examples of representative ERGs from a mouse exposed to blue light for 7 days pre, and after a 10 day recovery period.

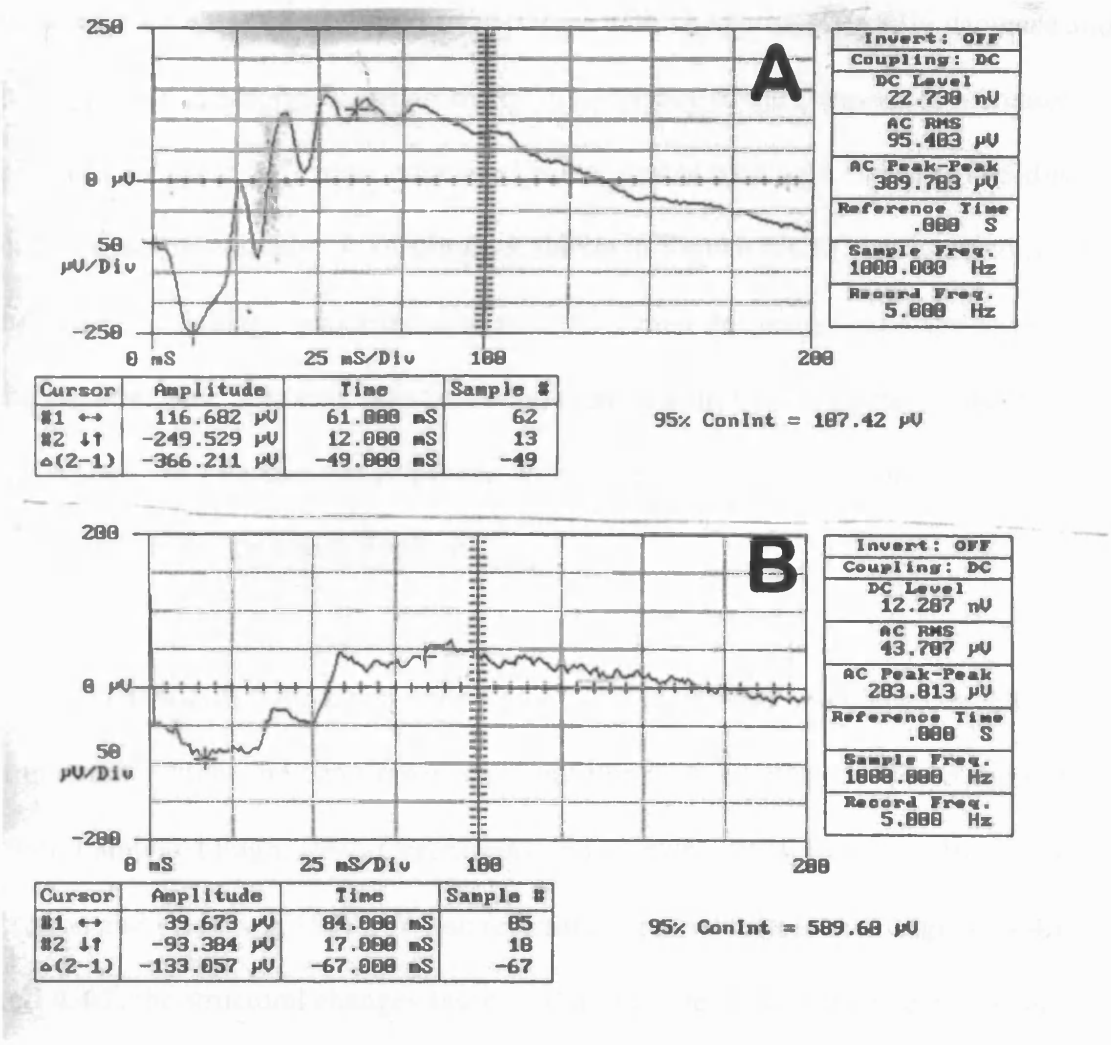

Figure 4.4.11 Representative ERGs from a mouse exposed to continuous blue light for 7 days. Shown in 'A' is a pre-ERG, and 'B' is an ERG after a 10 day recovery period.

Shown in **Figure 4.4.12a and 4.4.12b** are changes in the a-wave amplitude and latency from Trial #1 (blue line) and Trial #2 (red line) mice before blue light exposure and after a 10 day recovery period from their designated exposure. As shown in **Figure 4.4.12a**, as the period of exposure increases, there is a decrease in the amplitude of the a-wave, with corresponding increased a-wave latency (**Figure 4.4.12b**). This pattern of decreasing amplitude with increasing latency was found to be similar between both trials of mice. **Figure 4.4.13a and 4.4.13b** illustrates the percentage change of the a-wave amplitude and latency compared to the values before exposure. As shown in **Figure 4.4.13a,** the greatest decrease in the a-wave amplitude

occurred with **5 days and 7 days** of exposure with an approximate 83% decrease and 70% decrease in amplitude, respectively. The latency of the a-wave was increased an averaged 75% and 53% more compared values before blue light exposure at **5 days** and **7 days,** respectively. A scattergram shown in **Figure 4.4.14** clearly demonstrates the pattern of damage associated with mice after their designated exposure time. As shown, after blue light exposure (red dots) there is a shift in the scatterpoints of the graph showing a decrease in amplitude with increased latency time, indicating an irreversible effect on visual function.

As stated previously, the a-wave correlates to the number of photoreceptor cells stimulated by light and outer/inner photoreceptor segment integrity (Hood and Birch, 1990; Lamb and Pugh, 1992, Organisciak and Winkler, 1994; Hood and Birch, 1997;; Robson and Frishman, 1998). When referring to retinal histology in **Figures 4.4.6 and 4.4.7,** the structural changes associated in the outer retinal layers correspond to the functional changes indicated in the a-wave analysis.

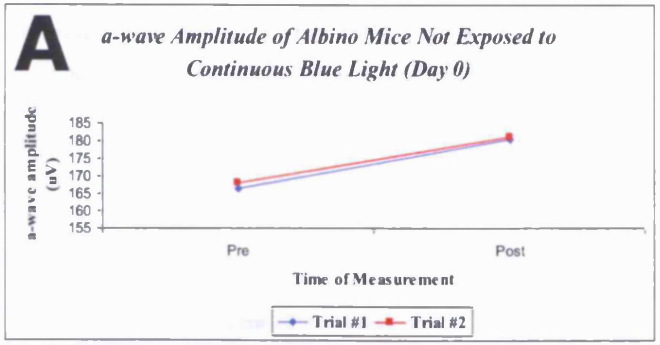

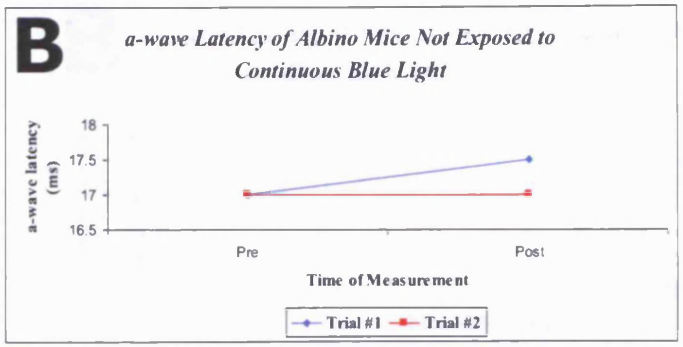

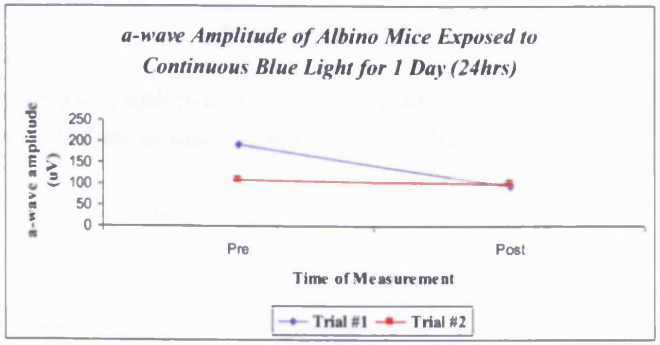

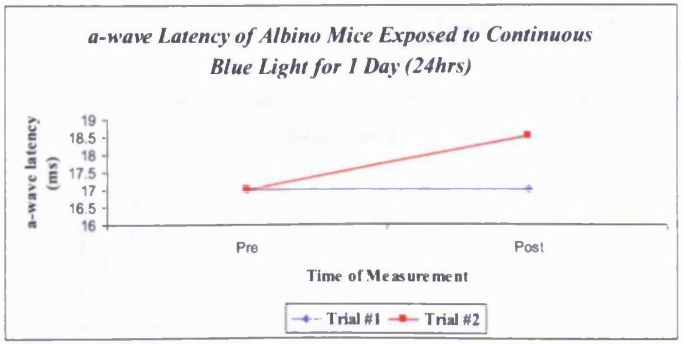

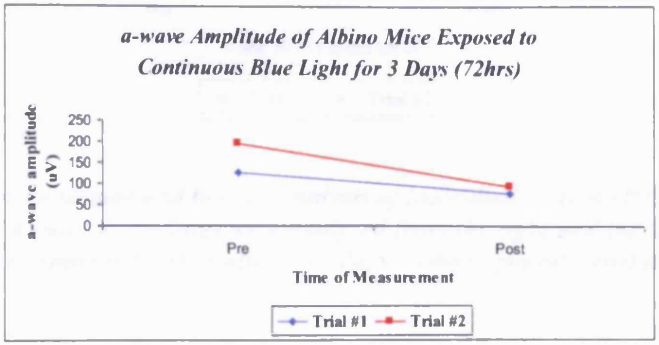

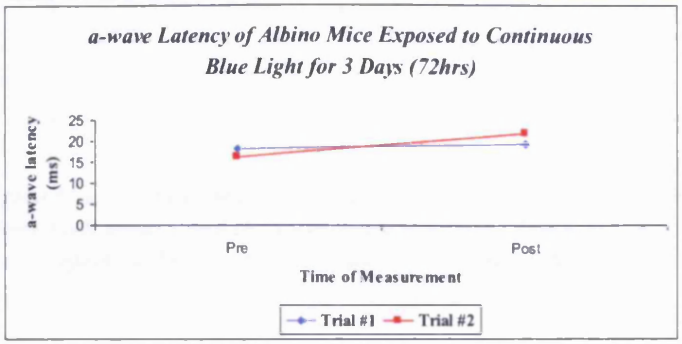

Figure 4.4.11a and b *continued overleaf*

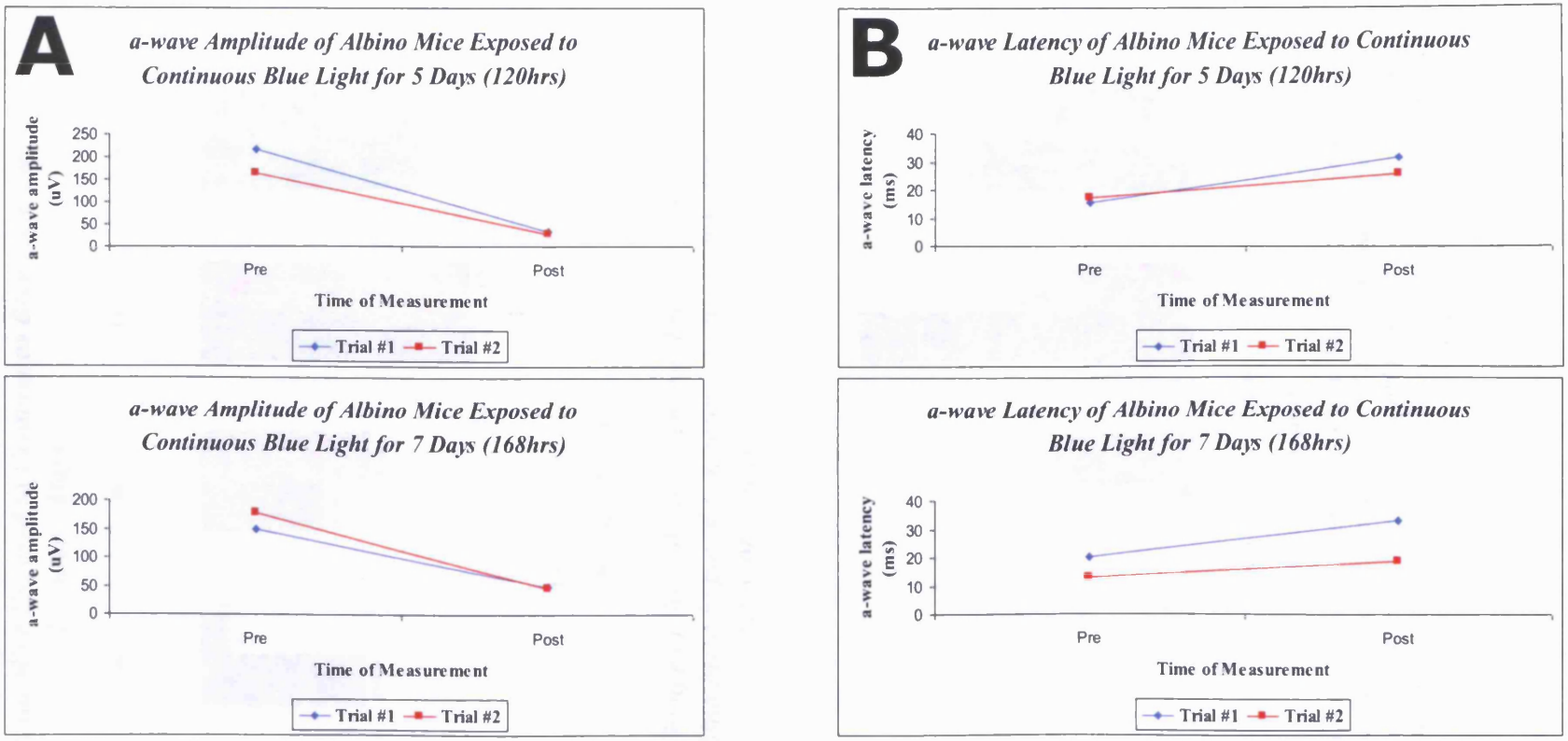

Figure 4.4.12 a-wave amplitude and latency analysis of individual BALB/cBYJ mice before blue light exposure and after a 10 day recovery period from designated exposure (1,3,5 or 7 days). Recordings were analyzed from the right and the left eyes from each mouse and then averaged together. The x-axis refers to the time of measurement (before exposure (pre) or after a 10 days recovery period (post) and the y-axis refers to the a-wave amplitude ('A') or the latency of the a-wave ('B').

A

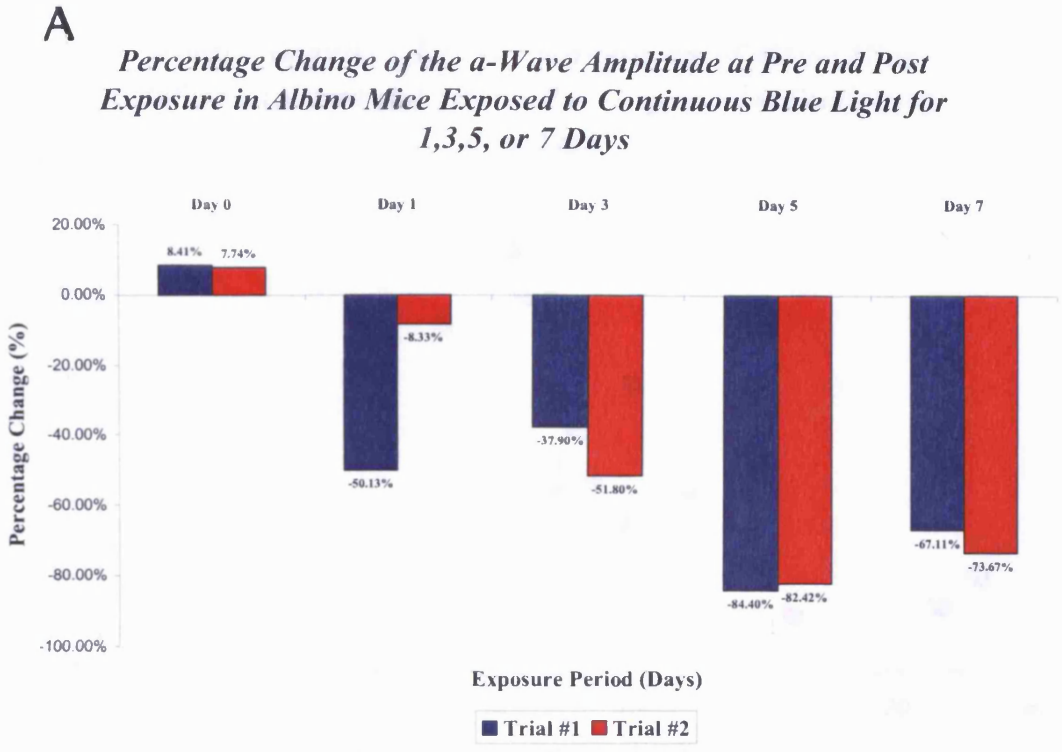

B

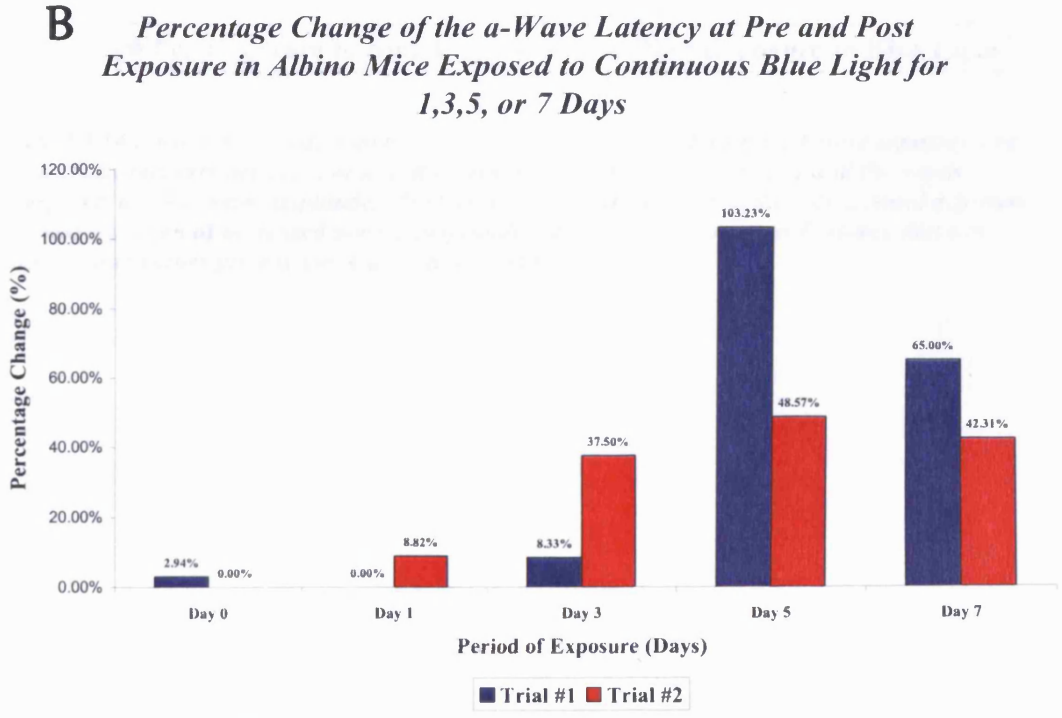

Figure 4.4.13 Percentage change of the a-wave amplitude ('A') and latency ('B') in BALB/cBYJ mice exposed to continuous blue light. The percentage change reflects the increase (+ values) or decrease (-values) of the amplitude or latency compared to original values prior to designated blue light exposure. The x-axis corresponds to the period of exposure (1, 3, 5, or 7 days) and the y-axis corresponds to the percentage change of the a-wave amplitude ('A') or latency ('B').

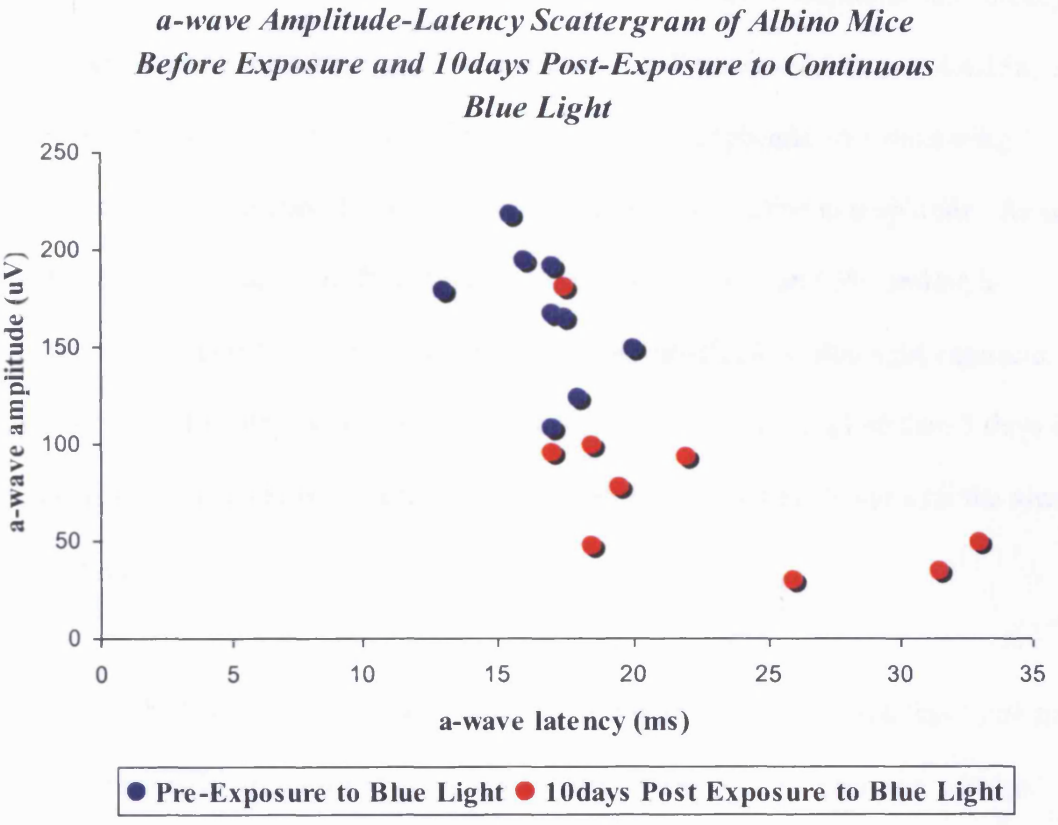

Figure 4.4.14 a-wave Amplitude-Latency Scattergram of BALB/cBYJ mice before exposure and after a 10day recovery period. The x-axis corresponds to the a-wave latency and the y-axis corresponds to the a-wave amplitude. As shown, after mice underwent their designated exposure, there was a pattern of decreased a-wave amplitude with associated increased latency times in comparison to values prior to any blue light exposure.

Additional analysis was performed on changes of the b-wave amplitude and latency. Changes in the amplitude of the b-wave are seen in **Figures 4.4.15a and 4.4.15a**. As seen in these figures, there is a decline in the b-wave amplitude with increasing exposure time, with **Days 5 and 7** showing the greatest decline in amplitude. As seen with the a-wave amplitude, **five days of exposure** results in an 85% decline in amplitude compared to its original amplitude measured before blue light exposure. Additionally, **five days of exposure** appears to have a greater decline than **7 days of exposure (67% decrease in amplitude),** a similar finding also found with the a-wave amplitude.

Although the b-wave latency appears to increase with longer blue light exposure time, the increase in latency after 10 days of recovery versus prior to exposure was less dramatic than the increased latency found with the a-wave. **Figures 4.4.16b and 4.4.16b** reveal that increased latency of the b-wave occurs at **3, 5, and 7 days** of exposure with an approximate increase in latency of 20% compared to latencies found before blue light exposure.

The scattergram of the b-wave amplitude-latency shown in **Figure 4.4.17**, reveals a similar pattern to the a-wave scattergram (**Figure 4.4.14**) demonstrating decreased amplitude associated with increased latency after continuous blue light exposure.

As stated previously, the b-wave reflects the efficiency of synaptic transmission between the photoreceptors and second order neurons in the outer plexiform layers (Organisciak and Winkler, 1994). Therefore, if there is degeneration or a break down of the outer retina, there would be less of a signal transmitted to the inner retina,

resulting in decreased b-wave amplitudes. Since there was significant damage to the outer nuclear layer and photoreceptor segments (see **Figures 4.4.6 and 4.4.7**), it is not surprising that the compromised outer retina results in corresponding delays of inner retina function. The loss of photoreceptors and their function drives the downstream losses since the initiating stimulus affects them ever if there is no morphological change downstream. Therefore, although the layers of the inner retina do not appear to show gross morphological changes, there is an irreversible affect on visual function.

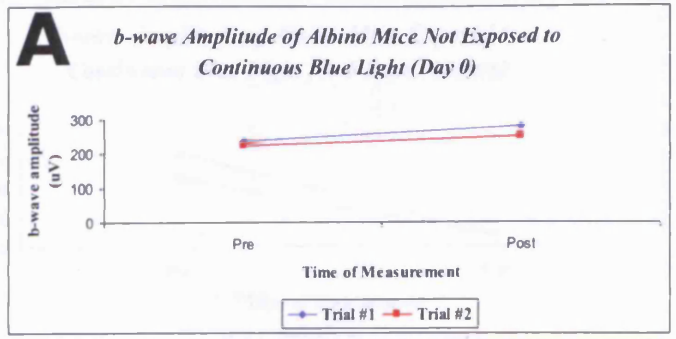

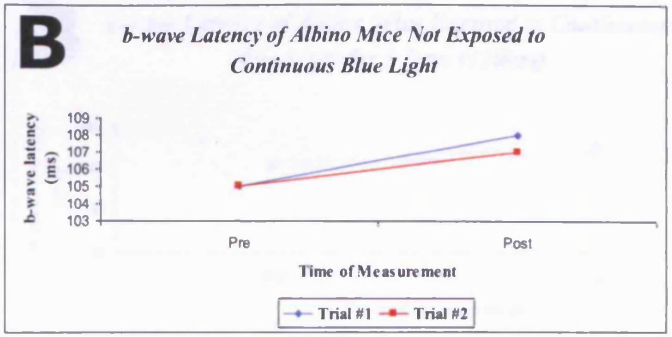

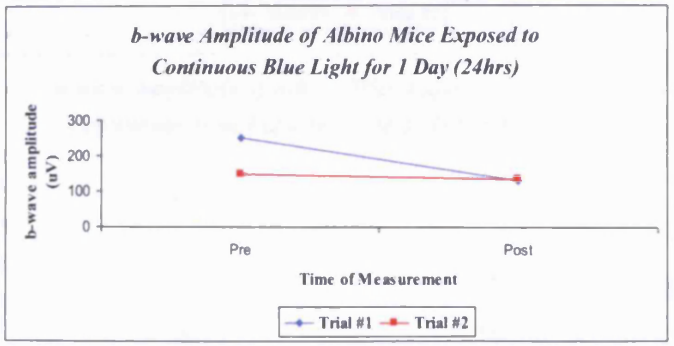

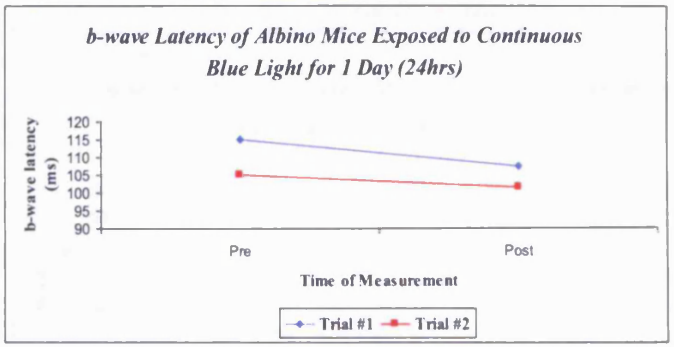

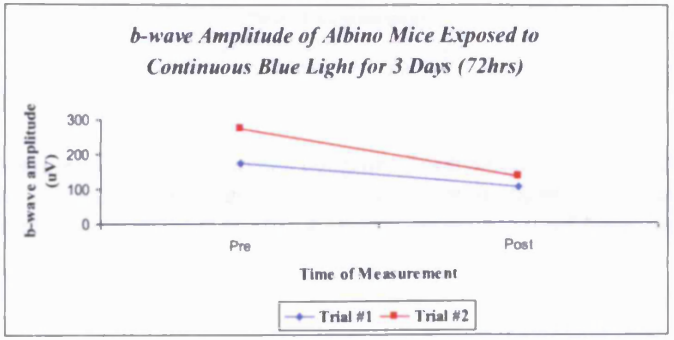

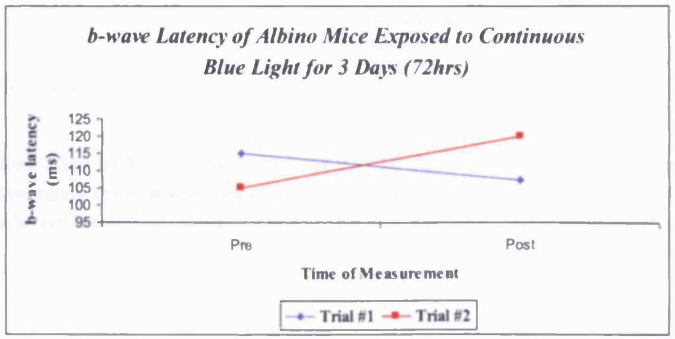

Figure 4.4.14a and b *continued overleaf*

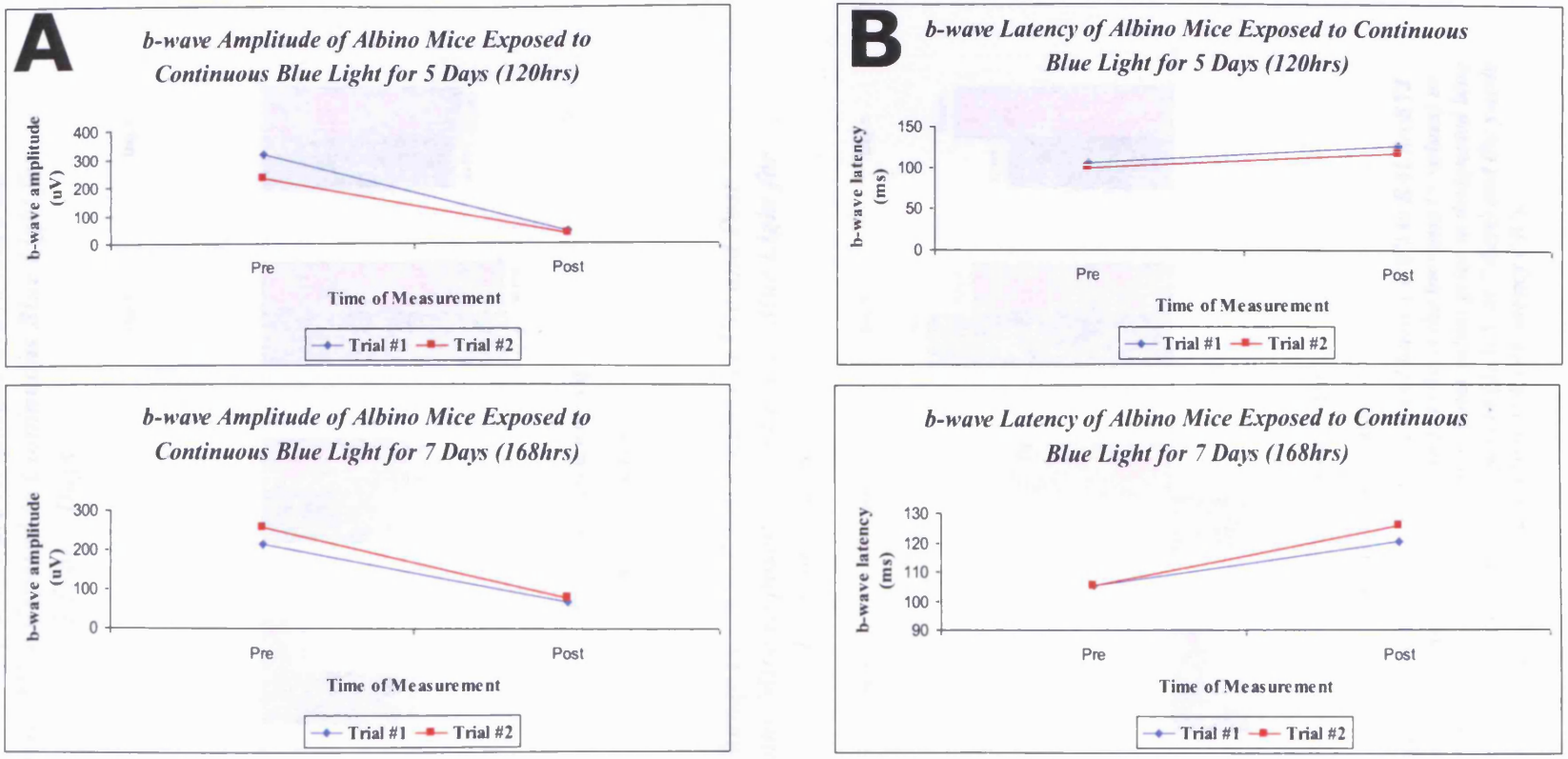

Figure 4.4.15 b-wave amplitude and latency analysis of individual BALB/cBYJ mice before blue light exposure and after a 10 day recovery period from designated exposure (1,3,5 or 7 days). Recordings were analyzed from the right and the left eyes from each mouse and then averaged together. The x-axis refers to the time of measurement (before exposure (pre) or after a 10 days recovery period (post) and the y-axis refers to the b-wave amplitude ('A') or the latency of the b-wave ('B').

A

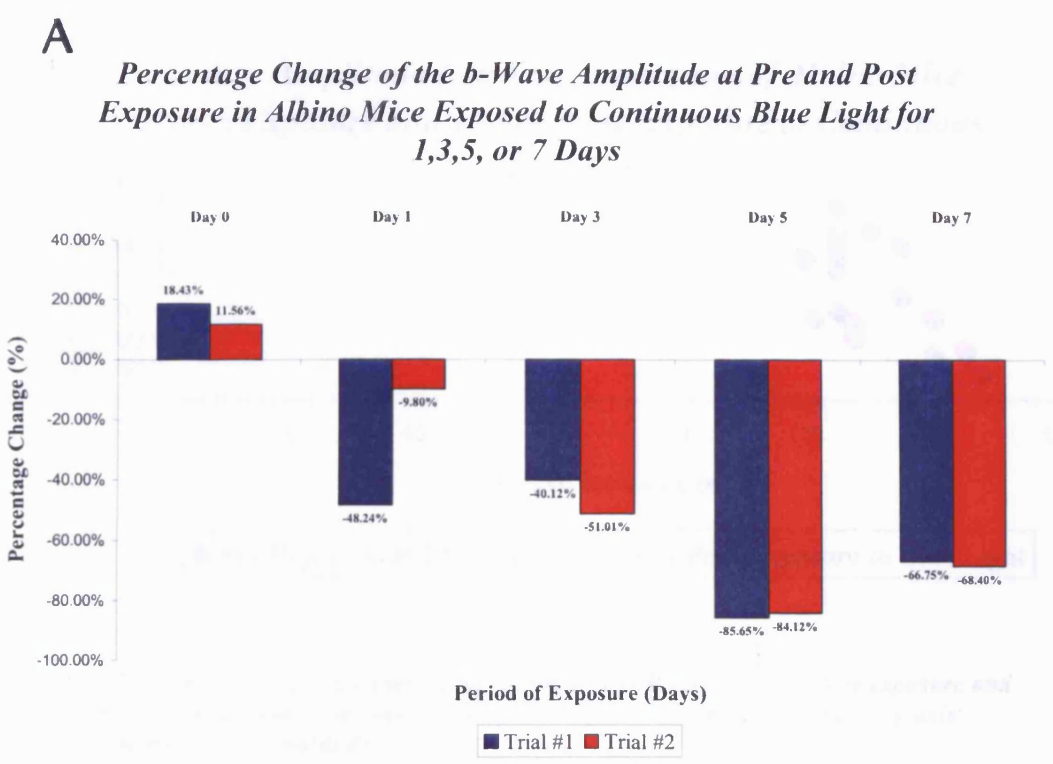

B

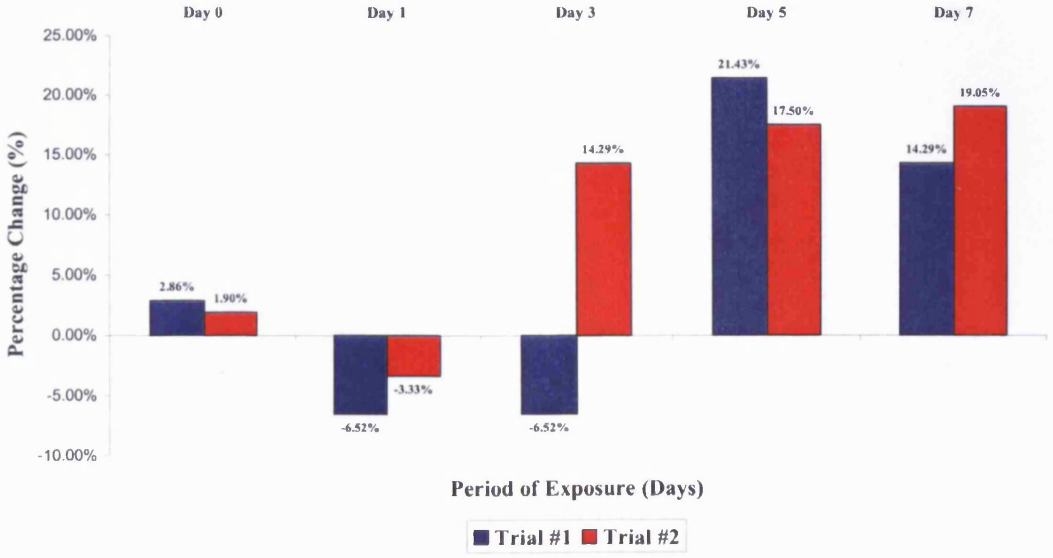

Figure 4.4.16 Percentage change of the b-wave amplitude ('A') and latency ('B') in BALB/cBYJ mice exposed to continuous blue light. The percentage change reflects the increase (+ values) or decrease (-values) of the amplitude or latency compared to original values prior to designated blue light exposure. The x-axis corresponds to the period of exposure (1, 3, 5, or 7 days) and the y-axis corresponds to the percentage change of the b-wave amplitude ('A') or latency ('B').

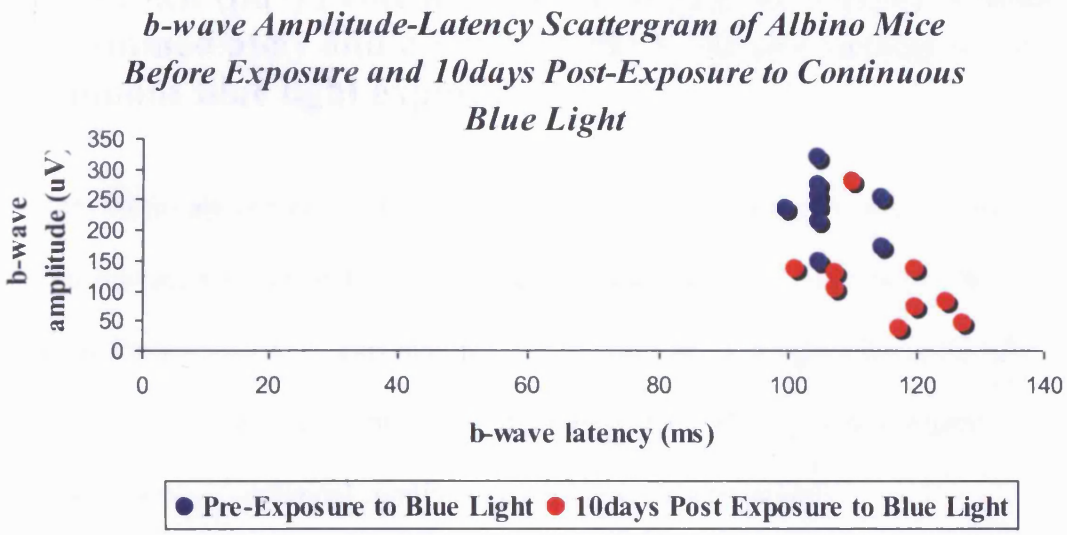

Figure 4.4.17 b-wave Amplitude-Latency Scattergram of BALB/cBYJ mice before exposure and after a 10day recovery period. The x-axis corresponds to the b-wave latency and the y-axis corresponds to the b-wave amplitude.

4.4.6 NF-κB (p65) Protein Expression in BALB/cBYJ Albino Mice Immediately and after a 10 day recovery period from continuous blue light exposure

Western blot analysis was performed in order to analyze the expression of NF-κB (p65) in albino mice exposed to continuous blue light over 1, 3, 5 or 7 days. As shown in **Figure 4.4.18,** all exposure periods resulted in an upregulation of NF-κB expression compared to the controls (no light exposure). Due to limited animal numbers and trials, statistical significance could not be determined.

A

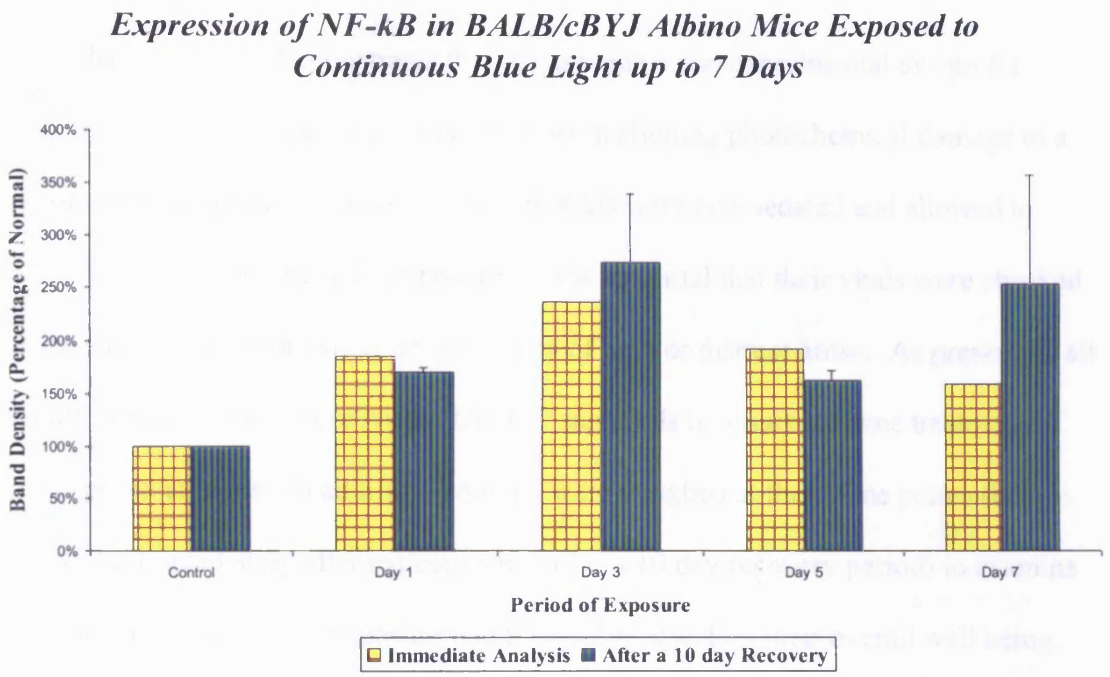

B

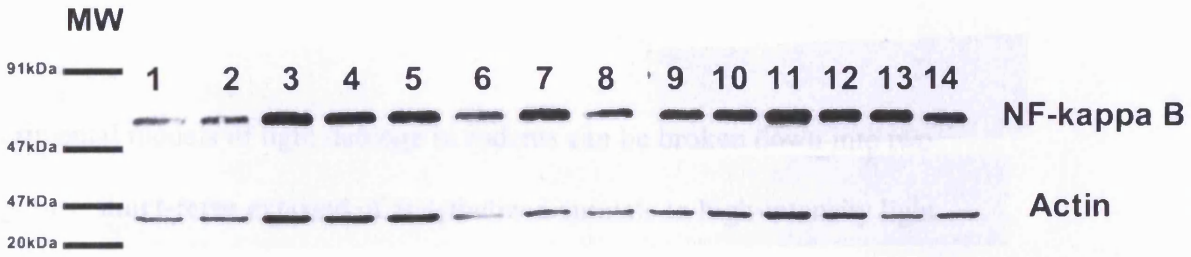

Lanes	Designated Exposure	Lanes	Designated Exposure
1	Control - Immediate	8	Day 1 – 10 days Post (Trial #2)
2	Control – 10 days Post	9	Day 5 – Immediate
3	Day 1 – Immediate	10	Day 5 – 10 days Post (Trial #1)
4	Day 1 – 10 days Post (Trial #1)	11	Day 5 – 10 days Post (Trial #2)
5	Day 1 – 10 days Post (Trial #2)	12	Day 7 – Immediate
6	Day 3 – Immediate	13	Day 7 – 10 days Post (Trial #1)
7	Day 3 – 10 days Post (Trial #1)	14	Day 7 – 10 days Post (Trial #2)

Figure 4.4.18 NF-κB protein expression in BALB/cBYJ mice exposed to continuous blue light for 1,3,5 or 7 days. 'A' represents a graphical description of NF-κB expression normalized to actin immediately and 10 days after designated exposure. As stated previously, only 1 trial was used for immediate analysis and two trials were used for examination after 10 days of recovery, therefore the numbers shown in ( ) indicate the Trial number. 'B' gives the actual blots for NF-κB(p65) and Actin for all trials of albino mice exposed to blue light. The key for lane numbers are shown in the table below the blots.

4.5 Chapter Discussion

This chapter clearly demonstrates that the apparatus and experimental design for continuous blue light exposure was effective in eliciting photochemical damage in a non-pigmented strain of rodents. Since animals were non-sedated and allowed to move freely during blue light exposure, it was essential that their vitals were checked twice a day to assure no signs or symptoms of pain or distress arose. As presented, all monitored parameters were within IACUC standards to assure humane treatment of the exposed animals. In addition, animals were weighed at three time points (before exposure, immediately after exposure and after a 10 day recovery period) to examine whether continuous light exposure had a negative effect on their overall well being. As shown, there was no permanent effect of light exposure on the animal's health or comfort.

Experimental models of light damage in rodents can be broken down into two categories: **short-term** exposed of anesthetized animals to high-intensity light requiring an optical system to focus light onto a particular area of the retina (Noell *et al.,* 1966, Ham *et al.,* 1982, Gorgels and van Norren 1995) or **long-term,** continuous exposure of freely moving animals to low intensity light (Noell *et al.,* 1966, Rapp and Williams 1979). Of those models mentioned, our experimental design mimics the long-term model, or Noell's category of Type II photochemical damage.

Common tools to evaluate photochemical damage of the retina include electroretinography (ERG), light microscopy and electron microscopy. For this particular study, we did not utilize the electron microscopy technique since gross

morphological changes were evident by light microscopy alone. However, it is important to note that electron microscopy is the most definitive and detailed due to the electron microscope providing the greatest resolution and detection of subtle changes (Lanum 1978). Therefore, for this work, photochemical damage to the retina of the BALB/cBYJ mice was assessed by the utilization of the following methods: 1.) observation of gross morphological changes in the retina using light microscopy and 2.) assessing visual function by the ERG.

Morphological changes were examined immediately after designated exposure (only 1 trial) and after a 10 day recovery period (2 trials). Of all the tools to examine retinal light damage, morphological analysis appears to be the most common (Organisciak and Winkler, 1994). Morphological descriptions of the photoreceptor cell damage can provide useful information about the sites of damage and the time course of the pathological process (Smith 2001).

Immediate gross morphology of the BALB/c retina revealed that the experimental blue light apparatus could elicit photochemical damage to the retina after **three days of exposure.** This was noted by the decrease in thickness of the ONL, with a greater decrease observed in the thickness and composition of the inner and outer segments of the photoreceptors. With continued exposure at **5 and 7 days**, there is a greater decline in ONL thickness and the apparent disappearance of the photoreceptor segments after 7 days of exposure. Therefore the longest duration of exposure to continuous blue light produced the greatest effects, both histologically and functionally (see ERG discussion below).

Analysis of retinal morphology after a 10 day recovery reveals continued progression of photochemical damage. A decrease in the thickness of the ONL is evident in **Day 1** after a 10 day recovery period, and the thickness continues to decline in **Days 3, 5, and 7** of exposure, with corresponding loss of the photoreceptor inner and outer segments.

These findings correlate with Noell's 1966 study on retinal light damage in albino rats. In their work, Noell *et al.,* describes histological changes such as nuclear pyknosis, cellular swelling, loss of photoreceptor nuclei and subsequent loss of function (through ERG analysis) (Noell *et al.,* 1966). Additionally he found that by examining histology over the course of many days, the photoreceptor segments, ONL, and RPE disappeared leaving behind relatively intact inner nuclear layers in contact with Bruch's membrane. In our particular study, there was no loss of the RPE layer, although it does appear to exhibit swelling changes, also consistent with Noell's findings in the albino rat. In the early stages of retinal morphological analysis in the albino rat, Noell found increased cellular swelling between the apical and basal portions of the RPE with an enlargement of nuclei (Noell *et al.,* 1966). Analysis of the RPE layer in the BALB/c mice immediately after their exposure reveals apparent RPE swelling with increased nuclei size at **Days 5 and 7**.

Additional light damage studies done by Kuwabara and Gorn (1968) found initial morphological changes in the photoreceptor outer segments with progressive involvement over the next 1-5 days of exposure with an intact RPE. These findings can also correlate to those found in the BALB/c immediate morphological analysis. As exposure period continues, there is an intact RPE with progression of

morphological changes and loss of nuclei, indicating photochemical damage. Although Kuwabara and Gorn (1968) utilized high intensity light at short exposure periods, O'Steen *et al.,* (1972) found similar findings with lower light intensity and longer exposure periods. O'Steen *et al.,* (1972) exposed rats to 200lux for 4-6 months and found progression of morphological changes in the outer retina with intact RPE. Additionally, Moriya *et al.,* (1986) examined the stress on rat photoreceptors under 80 lux of light exposure and found similar results with irreversible morphological changes if exposure exceeded 12-15hrs.

In addition to analysis of the morphological and histology changes, functional analysis was performed by electroretinography (ERG). Major components of the ERG consist of the *a-* and *b-waves.* The negative a-wave is due to photoreceptor hyperpolarization and is the most direct index of rod photoreceptor function (Reviews Audo *et al.,* 2008, and Weymouth and Vingrys, 2008) and inner and outer photoreceptor segment integrity (Hood and Birch, 1990, Lamb and Pugh, 1992, Organisciak and Winkler, 1994,; Robson and Frishman, 1998). The positive b-wave is known to occur as a result of post-phototransduction or post-receptoral function (Gurevich and Slaughter, 1993, Green and Kapousta-Bruneau 1999, Audo *et al.,* 2008, Weymouth and Vingrys, 2008). It is assumed that the generation of the b-wave reflects the efficiency of synaptic transmission between the photoreceptors and second order neurons in the outer plexiform layers (Organisciak and Winkler, 1994).

In this study, there was a visible correlation between morphological/ histological photochemical damage of the retina and the functional losses associate with those changes. As shown, as exposure time increased, amplitudes of the a- and b-waves

decreased with corresponding increased latencies. It is not surprising that although morphological changes were not as severe in the inner nuclear layer as in the outer nuclear layer; a corresponding decrease in visual function was noted in the inner nuclear layer due to the downstream effect from the damaged outer retina.

As shown, in the non-pigmented rodent system, there was evidence of photochemical damage of the retina via morphological and functional analysis. However, it is important to note that the extent of pigmented versus non-pigmented light damage yields a number of discrepancies. Noell *et al.* studied retinal damage in albino rats and pigmented rats under identical illuminance conditions and found that to reach the same loss of ERG waves, the exposure time had to be doubled, even with dilated pupils (Noell *et al.,* 1966). Other experimental studies found that light-induced photoreceptor cell damage was independent of pigmentation phenotype (Lawwill 1973, La Vail *et al.,* 1987). Rapp *et al.* provided controlled light exposure in fully dilated pupils of albino and pigmented rats to equally bleach the two strains and found that the extent of retinal degeneration was similar between the two strains (Rapp and Williams, 1980, Rapp and Williams, 1992).

In addition to photochemical damage analysis via morphology and ERG, we also investigated the activity of NF-κB in the light damage retinas of the albino mice. As shown, there is an increase in the activity of NF-κB expression during all exposure periods compared to the controls (no light exposure). It was difficult to determine any statistical significance due to limited animal numbers and limited trials. However, these initial findings correlate with Zeng *et al.,* (2008) who also found activation of NF-κB during retinal degeneration of *rd* mice. Nuclear translocation of NF-κB was

noted in microglial of the outer nuclear and outer plexiform layers (Zeng *et al.*, 2008). An earlier study conducted by the same research group also revealed that tumor necrosis factor-alpha (TNF-α), a target and inducer gene for NF-κB activation, was also primarily produced in the activated microglial cells in the outer retina of *rd* mice (Zeng *et al.*, 2005). Combined, these findings could indicate that the role of NF-κB in photoreceptor apoptosis may be associated with the regulation of proinflammatory molecules (Zeng *et al.*, 2008).

However, our findings are not consistent with Krishnamoorthy *et al.*, (1999), who found that in-vitro exposure of 661W cells (transformed mouse photoreceptor cell line (Baeuerle and Baltimore, 1988) to visible light creates conditions of photo-oxidative stress, causing the production of reactive oxygen intermediates leading to oxidative damage which results in the down-modulation of NF-kB and subsequent apoptosis of the cells.

In summary this chapter demonstrated that:

- The constructed blue light apparatus was efficient at eliciting photochemical retinal damage in a non-pigmented system of albino mice, BALB/cBYJ
- Photochemical damage in the albino system was evident both morphologically and functionally – both resulting in an irreversible effect on visual structure and function
- Exposure of BALB/cBYJ to continuous blue light results in an upregulation of NF-κB expression

Chapter 5.0:

In-vivo morphological and functional analysis of pigmented mice exposed to continuous blue light up to 7 days

5.1 Chapter Introduction

Photochemical damage of the retina is noted in short exposures to high intensity light, as well as in long exposures to low intensity light (Anderson *et al.,* 1972; Seiler *et al.,* 2000). Constant light illumination, even at low to moderate intensities, has been shown to damage both the sensory retina and the overlying RPE (Noell *et al.,* 1966; Ham *et al.,* 1978; Noell 1980; Williams and Howell 1983; Organisciak *et al.,* 1989; Perez and Perentes 1994). Photochemical damage due to constant illumination has been connected to dysfunction in the phototransduction cascase (Noell *et al.,* 1966; Williams and Howell 1983). The ability for photoreceptors to recover from light damage largely depends on the cellular damage occurring in the inner and outer segments of the photoreceptors, however once damage has reached the nuclear level, damage is irreversible (Wyse 1980; Moriya *et al.,* 1986). Additionally, studies have suggested that extent of damage has been associated with the number of melanosomes in the iris, RPE and choroid (Boulton *et al.,* 2001b; Heiduschka *et al.,* 2007; Guo *et al.,* 2008). As discussed previously (**Chapter 1**), 'pigmented' color of the RPE can be attributed to its melanin, which is abundant in both the apical and midportion regions of the cells of the RPE and plays a role decreasing light scatter, binding chemicals, acting as a free radical scavenger or generator, absorbing energy in the visible or UV range (Boulton 1998).

Some studies argue that melanin plays little to no role in retinal light damage pathogenesis (Lawwill 1973; La Vail *et al.,* 1987; Gorgels and van Norren 1998), however, this chapter will clearly demonstrate that the presence of melanin in the iris, choroid and RPE, do in fact play an important role in the degree of degeneration occurring with continuous light damage.

As shown in **Chapter 4,** in a non-pigmented rodent strain, the BALB/cBYJ, the continuous blue light exposure elicited visible morphological changes to the retina with an irreversible effect on visual function immediately and after a 10 day recovery on all exposure periods. This chapter will examine the effects of continuous blue light exposure on a pigmented strain of mice, 129Sv, immediate and after a 10 day recovery period. Additionally, since the 129Sv express the α-crystallins (of particular interest, αA-crystallin), these experiments can serve as a positive control to examine the morphological and functional changes associated with continuous light exposure in a pigmented strain of mice lacking the αA-crystallin protein (**Chapter 6**).

5.2 Chapter Aims

As stated above, Chapter 5 will investigate photochemical damage elicited from continuous blue light exposure in pigmented mice. Additionally it will evaluate the presence and expression of the α-crystallins. Since this strain of mice contain αA-crystallin, it will serve as a control to compare with results from αA-crystallin knock-out mice (see **Chapter 6**). In order to accomplish this, the following aims will be addressed:

5.2a.) Analysis of any retinal morphological changes associated with sub-threshold, continuous blue light exposure in a pigmented mouse strain with αA-crystallin

5.2b.) Assessment of visual function before exposure, immediately after and 10 days post-exposure

5.2c.) Changes in retinal protein expression of the α-crystallins and NF-κB at immediate exposure and after 10day recovery period

5.3 Experimental Design (*Detailed descriptions of the methods can be found in Chapter 2.0)*

Comparison of wild-type mice (**Chapter 5)** to the αA-crystallin knock-out mice (**Chapter 6)** required that mice were on similar genetic backgrounds. Therefore wild-type, pigmented 129Sv mice were chosen to examine morphological and functional changes to continuous blue light exposure for proper comparison to the knock-outs.

The experimental set-up and design for this chapter is similar to the description in **Chapter 4**, with a few minor changes. Due to limited numbers with the BALB/cBYJ strain, examination was done at 1, 3, 5 and 7 days. For wild-type and the knock-out mice (**Chapter 6),** exposures will occur daily up to 7 days, with analysis occurring immediately after the designated exposure and after a 10 day recovery period. It is important to note that during the 10 day recovery period, mice were placed back into normal lighting conditions in the animal facility with a 12hrs on/ 12hrs off cyclic pattern.

In brief, animals were originally purchased from Taconic Animal Facilities (Rockville, MD) and maintained in the Comparative Medical Center at Salus University (please refer to **Section 2.12 in Chapter 2** for animal colony maintenance and refer to **Appendix 1** for IACUC approved animal protocols). Animals (6-10wks) were exposed to continuous blue light up to 7 days. After exposure, morphological and functional analysis was performed immediately and 10 days after their designated exposure time, through histology and electroretinography, respectively.

An unfortunate event occurred with the first trial of wild-type mice due to a miscalculation error on the dilutions of the anesthetics, Ketamine and Xylazine. Due to this unfortunate event, the ERGs were post-poned and the animal care director and veterinarian were contacted to discuss and remedy the situation (Please refer to **Appendix 1** for the **Adverse Event** form). ERGs were not performed on the first trial, but mice were placed in the exposure apparatus for morphological analysis. ERG analysis was performed on the remaining three trials. Therefore, four trials were performed with wild-type mice, rather than three. An additional trial for wild-type mice was not an issue, since wild-type mice are efficient and large breeders.

Detailed descriptions of the experimental blue light apparatus (see **Section 2.3.4),** blue light experimental design (see **Section 2.3.5**), ERG testing (see **Section 2.4**), histology (see **Section 2.6**) and protein analysis (see **Section 2.5**) can be found in **Chapter 2**.

5.4 Chapter Results

5.4.1 Daily Humidity and Temperature Readings of Wild-Type Mice Exposed to Continuous Blue Light

During all trials of blue light exposure, parameters were monitored on a daily basis, twice a day. These parameters included maximum, minimum, and average temperature/humidity readings of the blue light apparatus. All temperature/humidity readings were taken with (Big Digit Hygro-Thermometer, Extech Instruments, USA).

Figures **5.4.1 and 5.4.2** illustrates the average values and standard error of the mean for temperature and humidity of all four trials of exposed wild-type mice. When referring to the overall average readings of both the temperature and humidity, at no point does the maximum limit of temperature or humidity result. As previously stated in **Chapter 4,** the NIH Guide for the Care and Use of Laboratory Animals, a maximum temperature of 80˚F is considered dangerous to the animal and the range of humidity percentage must fall between 30 – 70%.

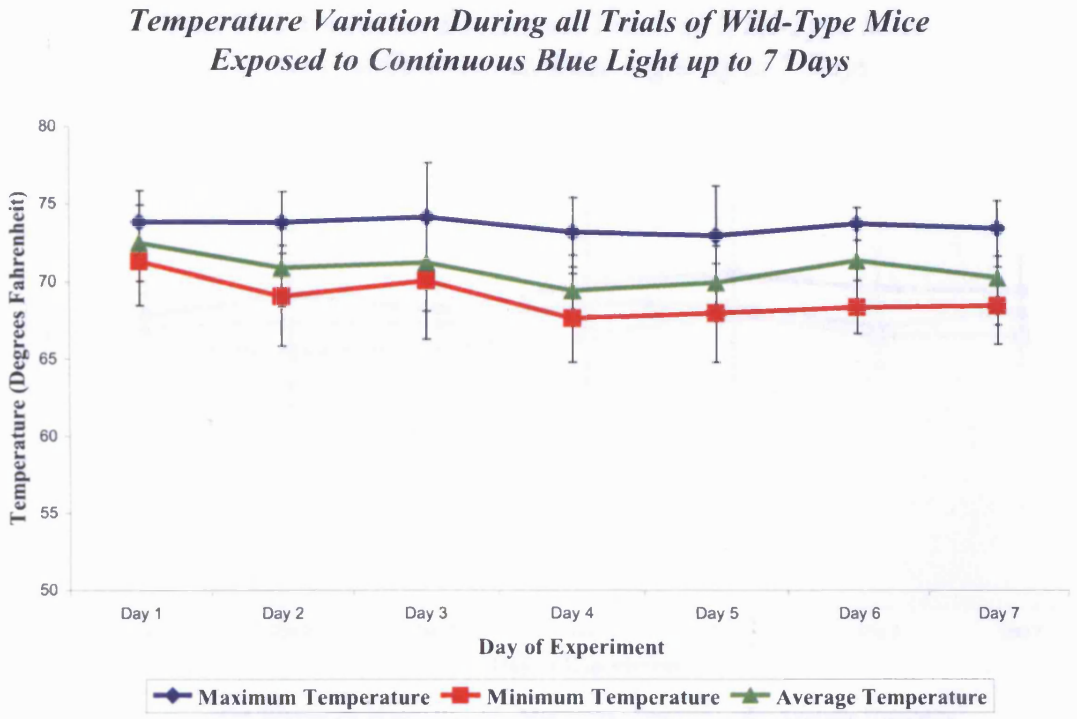

Figure 5.4.1: Shown above is the maximum, minimum and average temperature readings taken during all four trials of pigmented wild-type mice exposed to blue light up to 7 days. The x-axis corresponds to the day of the experiment and the y-axis refers to the temperature in degrees Fahrenheit. Individual readings at maximum, minimum and average were taken twice a day (every 12hrs) and recorded to assure that the overall temperature of the apparatus does not exceed 80˚F, which could cause extreme distress to the animals being exposed. Vertical bars indicate the standard error.

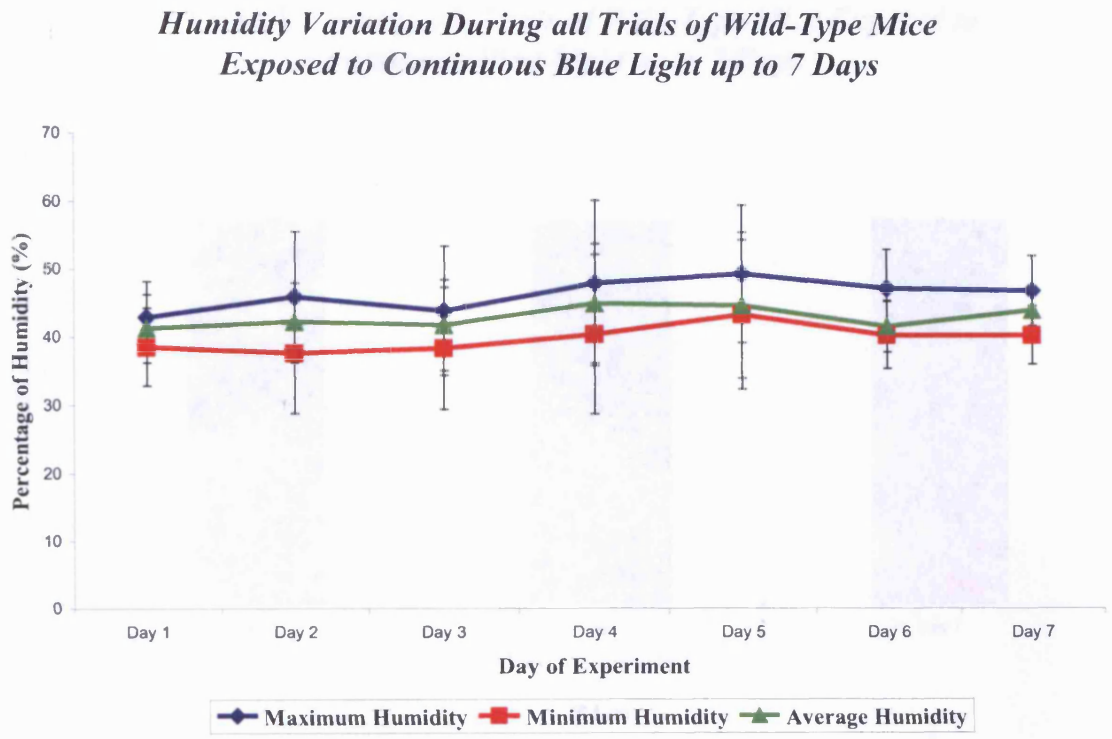

Figure 5.4.2: Shown above is the maximum, minimum and average humidity readings taken during all four trials of pigmented wild-type mice exposed to blue light up to 7 days. The x-axis corresponds to the day of the experiment and the y-axis refers to the temperature in degrees Fahrenheit. Individual readings at maximum, minimum and average were taken twice a day (every 12hrs). Vertical bars indicate the standard error.

5.4.2 Experimental Lux Readings

The monitoring of lux of the blue light apparatus was also a routine experimental parameter. Lux were measured at specified points (at the very start of the experiment (Day 1), in the middle of the experiment (Day 4) and at the end of the experiment (Day 7)) to assure that the amount of illuminance was constant throughout the experiment. As revealed in **Figure 5.4.3** there was very little, if any, deviation from the average illuminance of approximately 620 lux, indicating constant illuminance throughout the seven days of experimental exposure. Readings were taken with the Traceable NIST Calibrator (Fisher Scientific, USA) apparatus located at the level of mice being exposed.

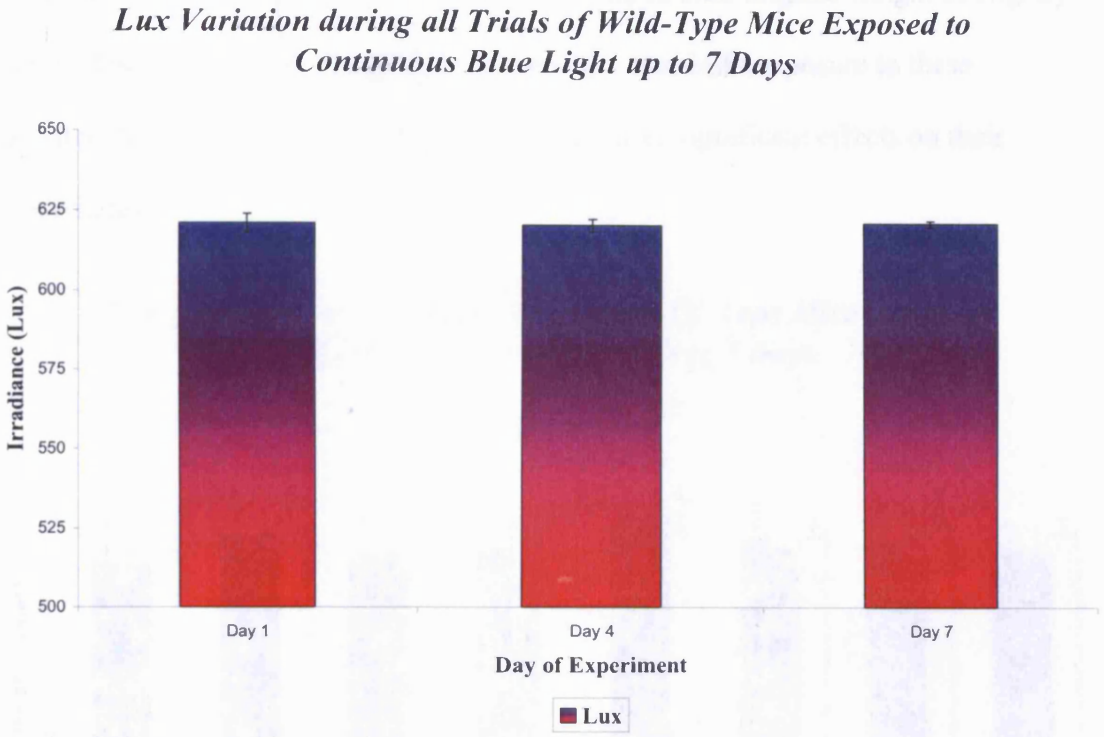

Figure 5.4.3: Shown above are the average lux measurements of the experimental blue light apparatus at Day 1, 4 and 7 of the experiment for all four trials of wild-type mice. The x-axis corresponds to the day of the experiment and the y-axis refers to the illuminance lux. Vertical bars indicate the standard error.

5.4.3 Behavioral Patterns of Exposed and Non-Exposed Wild-Type Mice

As stated in **Chapter 4,** based on approved animal protocols, animals were required to be checked every 12hrs to assure that there was no pain or distress while being exposed to the continuous blue light. During all four trials, there was no indication of any pain or distress noted in the exposed wild-type mice.

Additionally, there was a mild effect on the weights of the mice being exposed. As shown in **Figure 5.4.4,** there was no significant change in weight from pre exposure to immediately after exposure in control and day 1 animals. However, mice exposed to blue light for 2-7 days appeared to have a decrease in their weight from pre-exposure to immediately after exposure. All mice demonstrated an increase in their

weight during the 10 day recovery period, returning to their original weight or slightly greater. These findings indicates that, on average, blue light exposure in these unsedated, freely moving wild-type mice produced no significant effects on their dietary status.

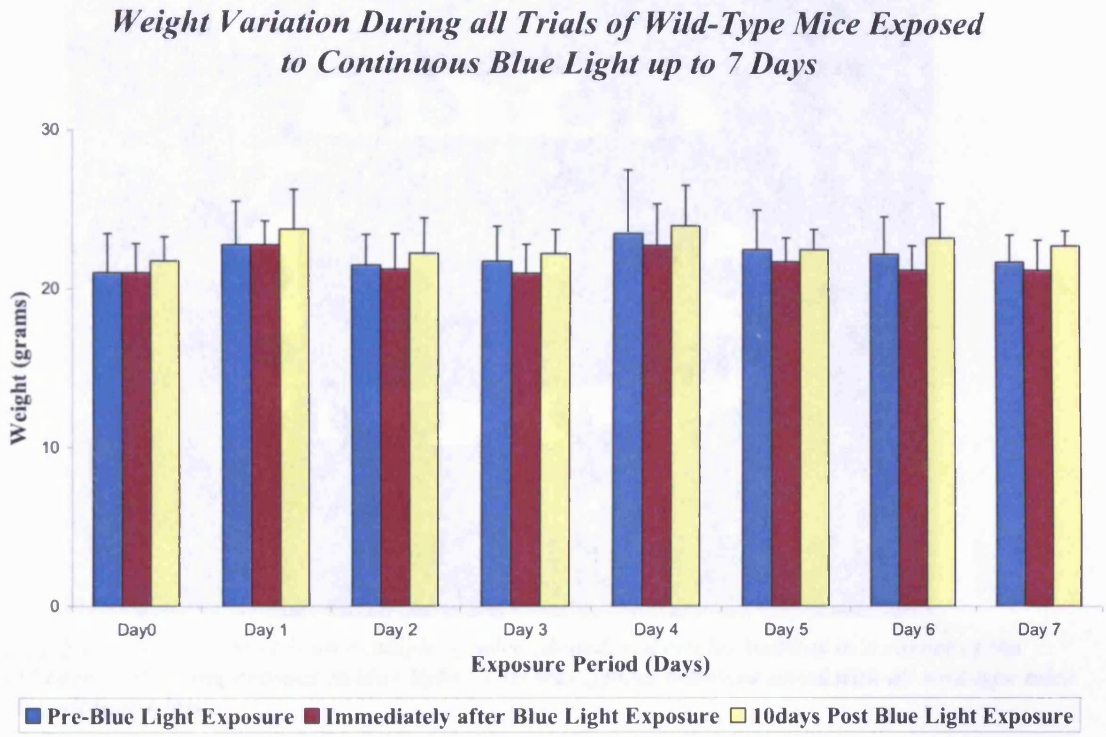

***Figure 5.4.4**: Shown above are the average weight measurements of all four trials of pigmented wild-type mice exposed to blue light up to 7 days. Day 0 refers to the control or no-blue light exposed mouse. Weights were taken before blue light exposure, immediately after blue light exposure or at the 10 day recovery period from blue light exposure. The x-axis corresponds to the number of days the mice were exposed and the y-axis refers to the weight of the mice. Vertical bars indicate the standard error.*

There were particular behaviors noted during all trials of wild-type mice that were not found with the albino mice (**Chapter 4**). Since it was vital to keep the exposure apparatus below 80°F, an air conditioner as well as a fan was placed at one end of the apparatus. Therefore, a constant amount of cool air would flow through the apparatus during experimental conditions, resulting in the mice huddling together in a corner of the wired cage (see **Figure 5.4.5***)* in attempts to shield their eyes from continuous airflow or possibly to keep warm. To combat this problem, at the 12hr daily checks,

mice were rotated to the right (see **Figure 5.4.6***)*, therefore exposed mice closest to the fan would only be there for twelve hrs versus 24 or more. Additionally, since a total of six cages could fit in the apparatus, mice were kept in single cages for as long as possible and then paired up as necessary to fit all mice for each trial.

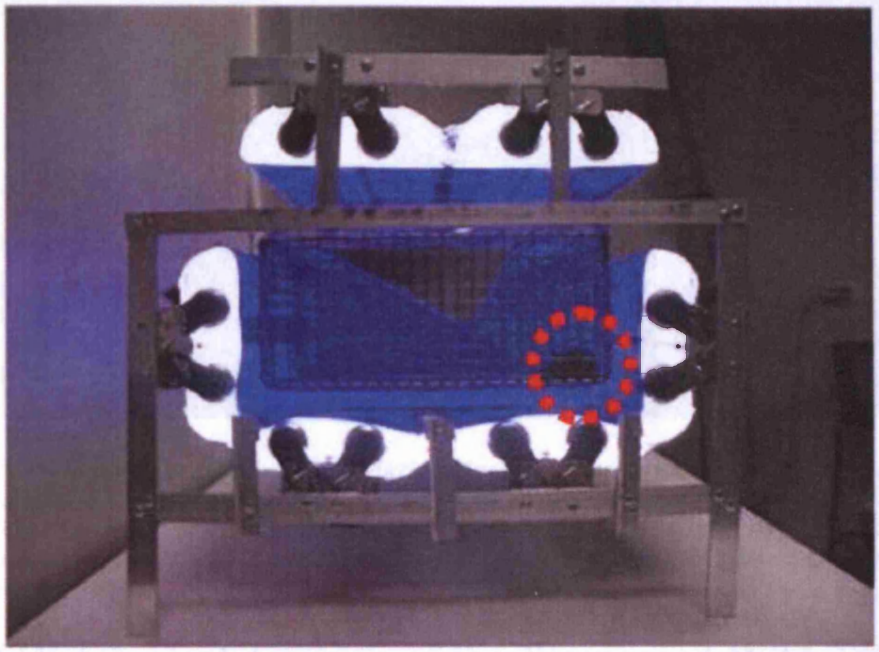

***Figure 5.4.5**: Shown above is an example of mice (dotted, red circle) huddled in a corner of the wired cage while being exposed to blue light. This was typical behavior noted with all wild-type mice during all four trials.*

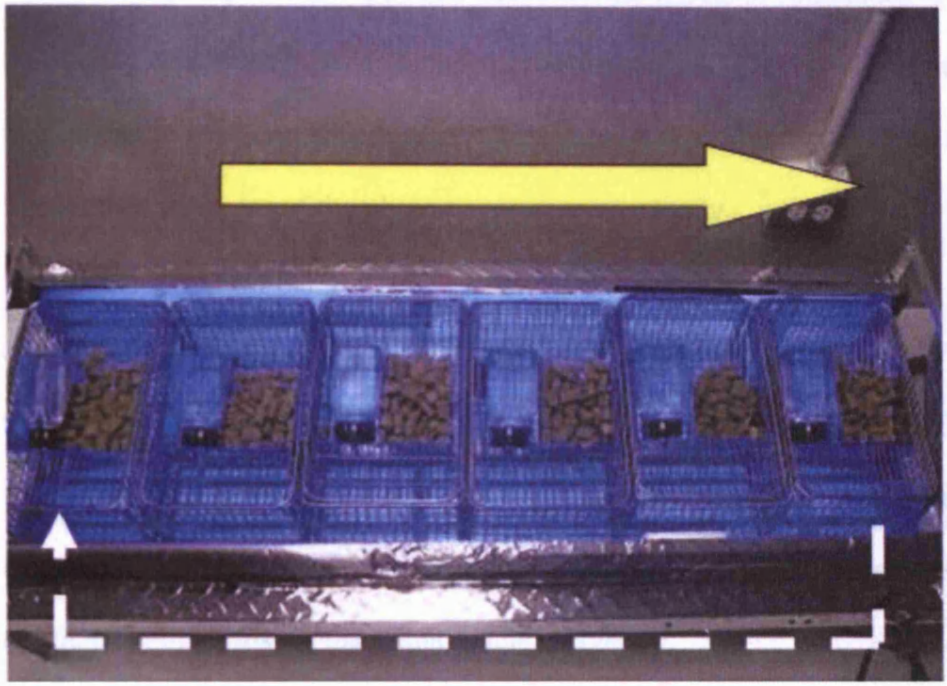

Figure 5.4.6 Illustration of cage rotation during blue light exposure. Shown are all six cages filling the apparatus. The solid yellow line shows the direction of rotation of the cages every 12 hours. The dotted white line refers to the movement of the cage closest to the fan; therefore after 12 hours, the cage farthest to the right will be rotated so its new position will now be farthest to the left for another 12 hours.

5.4.4 Histological Analysis of the Pigmented Wild-Type Retina after Exposure to Continuous Blue Light

Retinal histology of wild-type mice exposed to continuous blue light daily up to 7 days was examined immediately and after a 10 day recovery period from their designated exposure. The area of capture for analysis of retinal morphology can be seen in **Figure 4.4.5**. All eyes were sectioned at the level of the optic nerve and photodocumentation was performed 0.10 – 0.25mm from either side of the optic disc. Most of the damage noted occurred in this region; equatorial and peripheral retina remained unaffected.

In order to analyze any photochemical damage which may have occurred during exposure, histological sections of mouse retina were analyzed to determine any cellular loss.

Four trials of pigmented wild-type mice examined the effects of continuous blue light exposure immediately after the designated exposure period. **Figures 5.4.7 and 5.48** contain representative whole sections of retina as well as a magnified view of the outer and inner segments of the photoreceptors, respectively.

When referring to **Figure 5.4.7**, **Day 0 (no blue light control)** and **Days 1 – 7** of continuous blue light exposure contain normal rows of photoreceptor nuclei (8-10 rows) with a tight, uniform structure to the inner and outer photoreceptor segments. Additionally, there does not appear to be any compromise of overall retinal thickness or significant cellular loss in the retinal nuclear layers.

Upon closer examination of the RPE, photoreceptor segments and outer nuclear layer (see **Figure 5.48**), **Day 0 (no blue light control)** and **Days 1 -5** exhibit tight, uniform outer photoreceptor segment structure with clear delineation of outer to inner portions of the photoreceptors. The overlying RPE layer appears intact with no presence of any surrounding macrophages in the subretinal space. Additionally, there does not appear to be any significant loss of nuclei or melanin loss in the RPE.

Throughout all trials of exposure, **Day 6** consistently exhibited the presence of macrophages in the subretinal space, possibly indicating apoptosis of the photoreceptor nuclei. Although present, photoreceptor segments still remained uniform with an intact overlying RPE layer.

However, although gross retinal thickness appeared similar to the control mice (**Day 0**), on closer examination of the outer retina of **Day 7** there appears to be an onset of

early photochemical damage to the outer segments. It is difficult to determine the transition zone between the outer to inner segments of the photoreceptors and vesiculation of both the inner and outer segments of the photoreceptors is present, indicating possible photochemical damage. Additionally, pyknotic nuclear appear sporadically in the outer nuclear layer. The overlying RPE continue to appear intact with no apparent nuclei loss or melanin loss.

Therefore immediate histological analysis of whole retinal sections and detailed analysis of the outer retina reveal that there appears to be no significant photochemical damage occurring **Days 1 - 6** of exposure. The only indication of photochemical damage was present with the longest period of exposure, **7 days**. Although there was no cellular loss observed in the outer nuclear layer, there were pyknotic nuclei sporadically present and outer and inner segments of the photoreceptors revealed vesiculation.

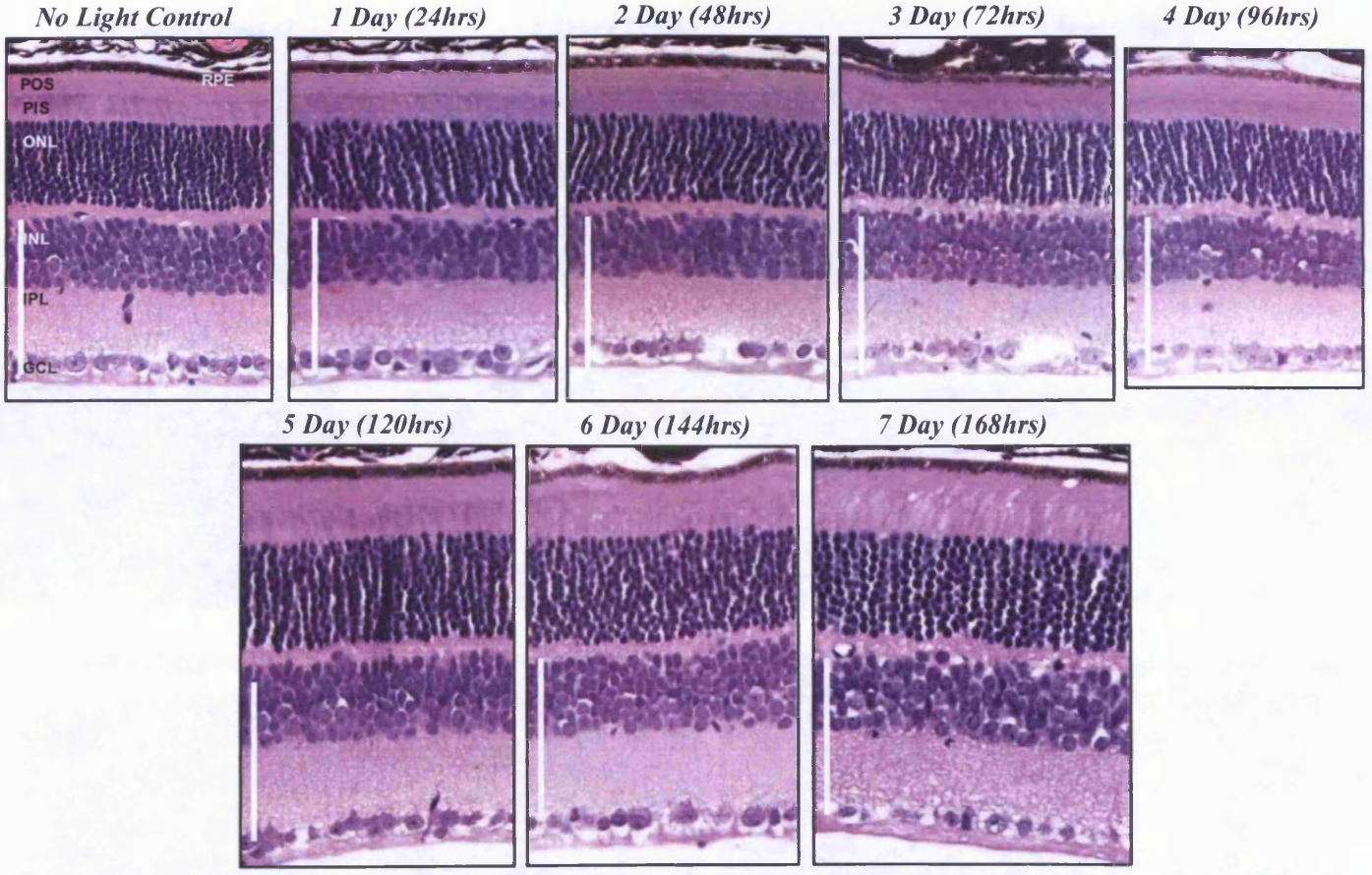

Figure 5.4.7 Immediate whole retinal histological analysis of pigmented wild-type mice exposed to continuous blue light for 1 - 7 days. All photos correspond to whole retina photodocumented 0.10 – 0.25 mm from either side of the optic disc (magnification of 20x; scale bar = 100μm). These sections are representative of all four trials of exposed mice. Experiment was repeated a minimum of four times. RPE = Retinal pigment epithelium, POS = Photoreceptor outer segments, PIS = Photoreceptor inner segments, ONL = Outer nuclear layer, INL = Inner nuclear layer, IPL = Inner plexiform layer, GCL= Ganglion cell layer.

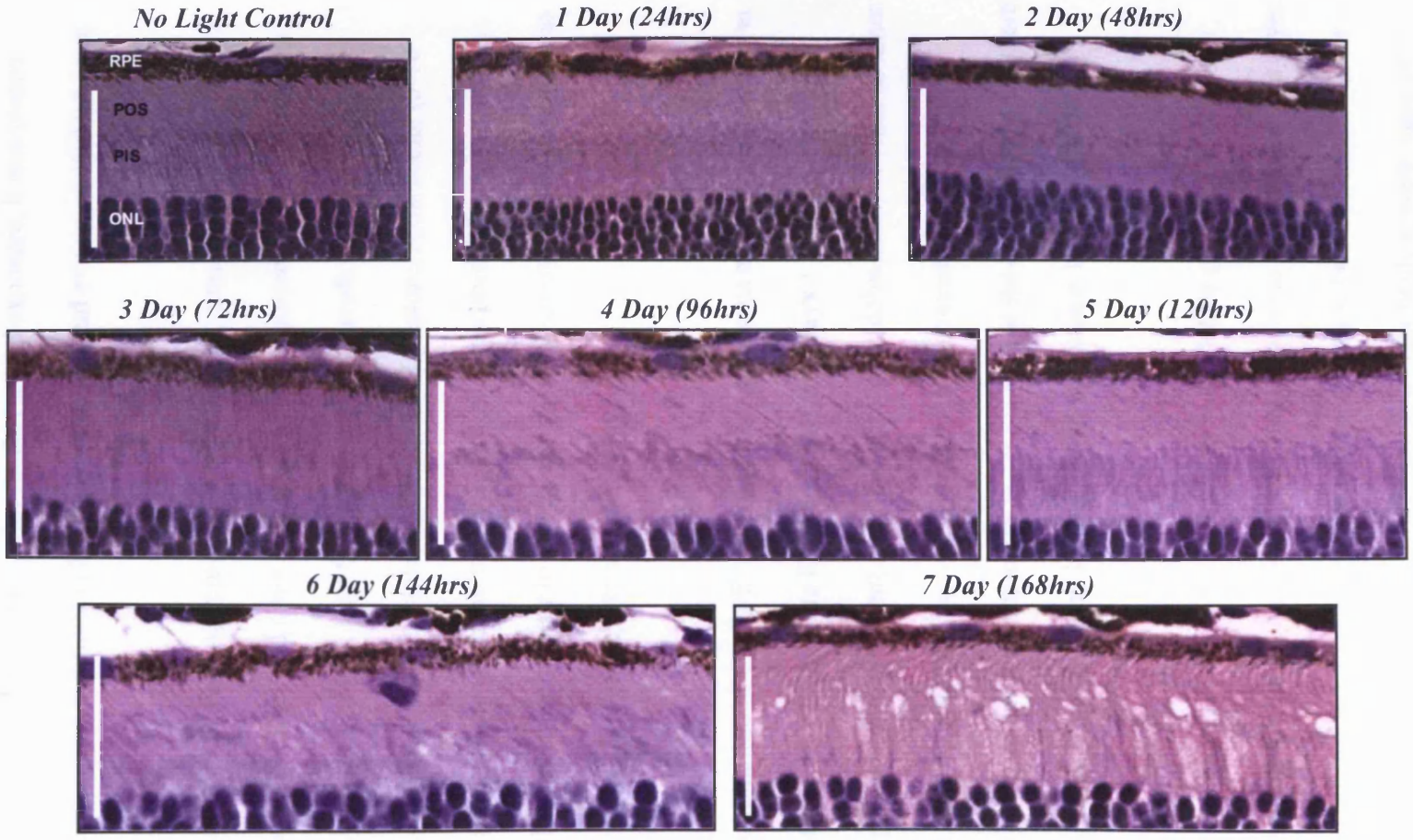

Figure 5.4.8 ***Representative, higher magnification (40x) view of the RPE, inner and outer segments of the photoreceptors (POS/PIS) and outer nuclear layer (ONL) of pigmented wild-type mice immediately after exposure to continuous blue light for 1-7 days. Scale bar = 50μm.***

Additionally, retinal histology of wild-type mice exposed to continuous blue light 1 - 7 days was examined 10 days post the original designated damage. Therefore if a mouse was exposed for 1 day (24hrs), after its designated exposure, it was placed back into normal cyclic conditions (12hrs on/12 hrs off) and evaluated 10 days later.

Figures 5.4.9 and 5.4.10 contain representative whole sections of retina as well as a magnified view of the outer and inner segments of the photoreceptors, respectively. When referring to **Figure 5.4.9**, **Day 0 (no blue light control)** and **Days 1 – 7** of continuous blue light exposure contain normal rows of photoreceptor nuclei (8-10 rows) with a tight, uniform structure to the inner and outer photoreceptor segments. Additionally, there does not appear to be any compromise of overall retinal thickness or significant cellular loss in the retinal nuclear layers.

Upon closer examination of the RPE, photoreceptor segments and outer nuclear layer (see **Figure 5.4.10**), **Day 0 (no blue light control)** and **Days 1 -4** exhibit tight, uniform outer photoreceptor segment structure with clear delineation of outer to inner portions of the photoreceptors. The overlying RPE layer appears intact with no presence of any surrounding macrophages in the subretinal space. Additionally, there does not appear to be any significant loss of nuclei or melanin loss in the RPE.

Outer retinal examination of **Days 5 -7** exhibited vesiculation of the outer and inner photoreceptor segments along with sporadic pyknotic nuclei in the outer nuclear layer. Additionally, it was difficult to determine the transition zone between outer to inner segments. Although the photoreceptor segments and outer nuclear show signs of

photochemical damage, the overlying RPE layer does not show any signs of compromise or damage; there is no nuclei loss or significant melanin loss.

Another way to illustrate the differences in overall retinal thickness or individual layer thickness (outer nuclear, inner nuclear, or photoreceptor layers) can be seen graphically in **Figures 5.4.11 and 5.4.12** immediately and after a 10 day recovery period from designated blue light exposure, respectively. As shown in **Figure 5.4.11**, there is no statistically significant difference between the overall retinal thickness and individual layer thickness of the exposed animals compared to the control (no light exposure) immediately after exposure. There is, however, a significant difference in **Days 6 and 7** of exposure, as shown in **Figure 5.4.12,** in the outer and inner nuclear layer thicknesses, after a 10 day recovery period.

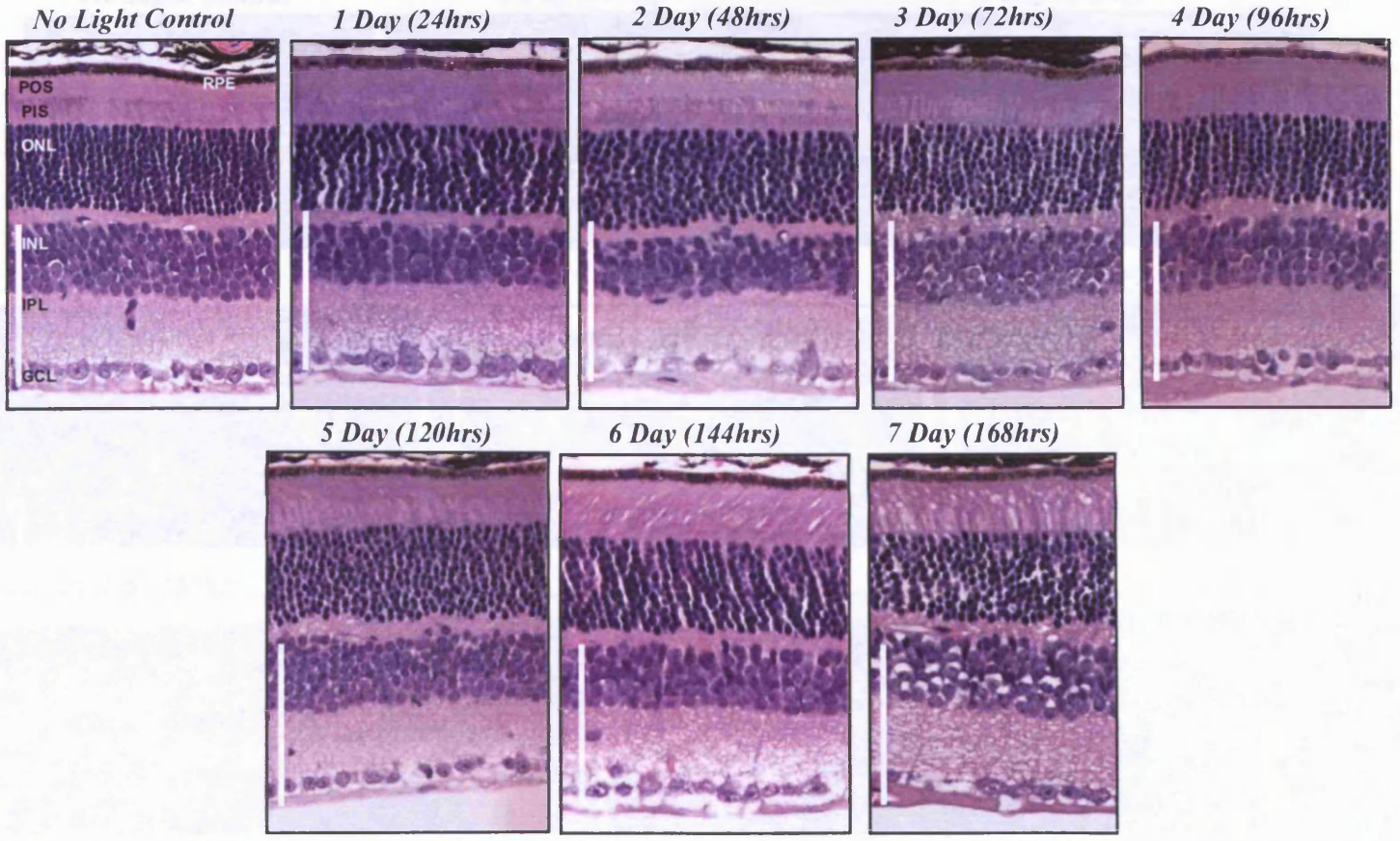

Figure 5.4.9 Whole retinal histological analysis of pigmented wild-type mice exposed to continuous blue light 1 - 7 days after 10 days of recovery. All photos correspond to whole retina photodocumented 0.10 – 0.25 mm from either side of the optic disc (magnification of 20x; scale bar = 100μm). These sections are representative of all four trials of exposed mice. Experiment was repeated a minimum of four times. RPE = Retinal pigment epithelium, POS = Photoreceptor outer segments, PIS = Photoreceptor inner segments, ONL = Outer nuclear layer, INL = Inner nuclear layer, IPL = Inner plexiform layer, GCL= Ganglion cell layer.

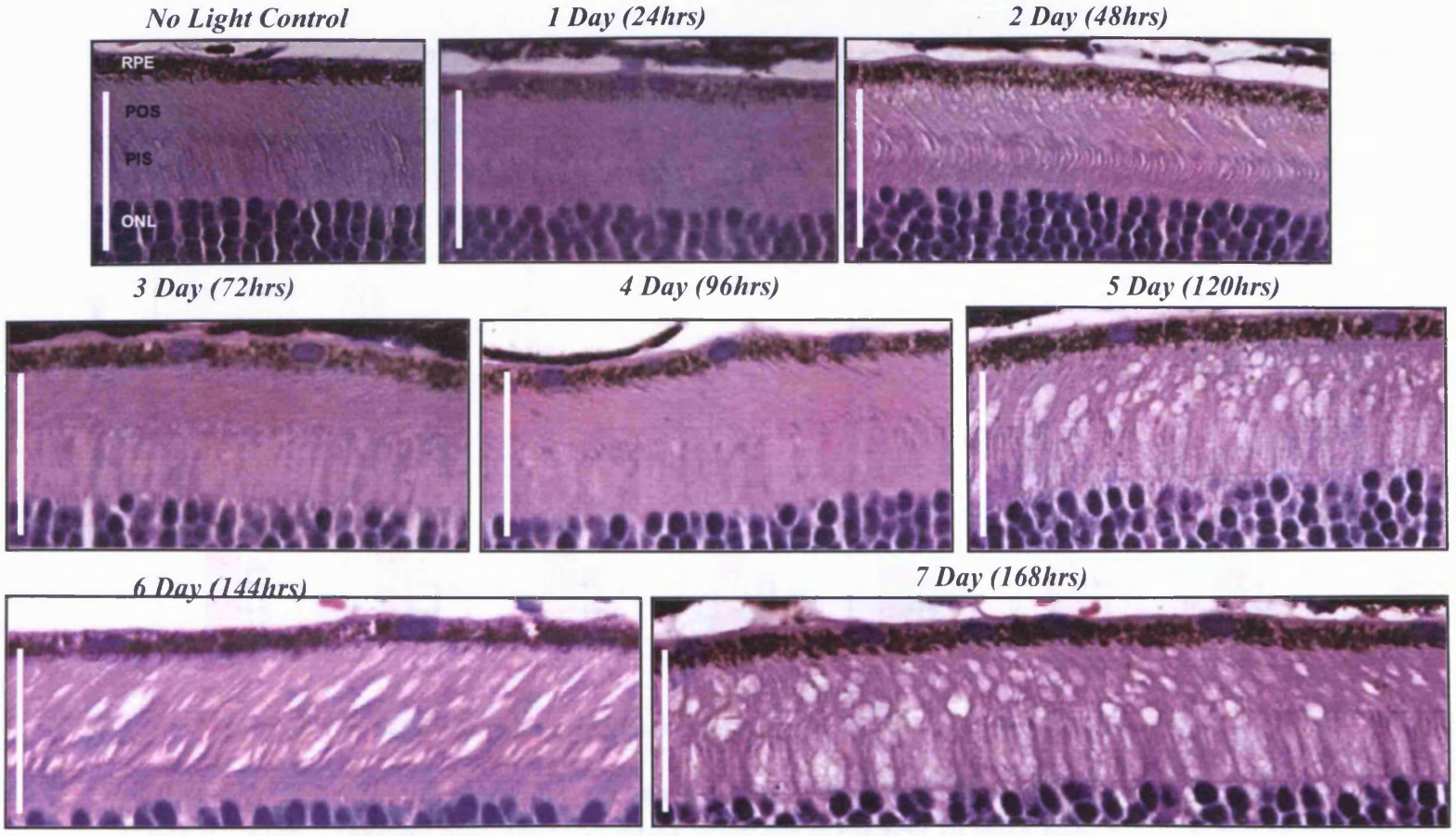

Figure 5.4.10 ***Representative, higher magnification (40x) view of the RPE, inner and outer segments of the photoreceptors (POS/PIS) and outer nuclear layer (ONL) of pigmented wild-type mice exposed to continuous blue light for 1-7 days after 10 days of recovery. Scale bar = 50μm.***

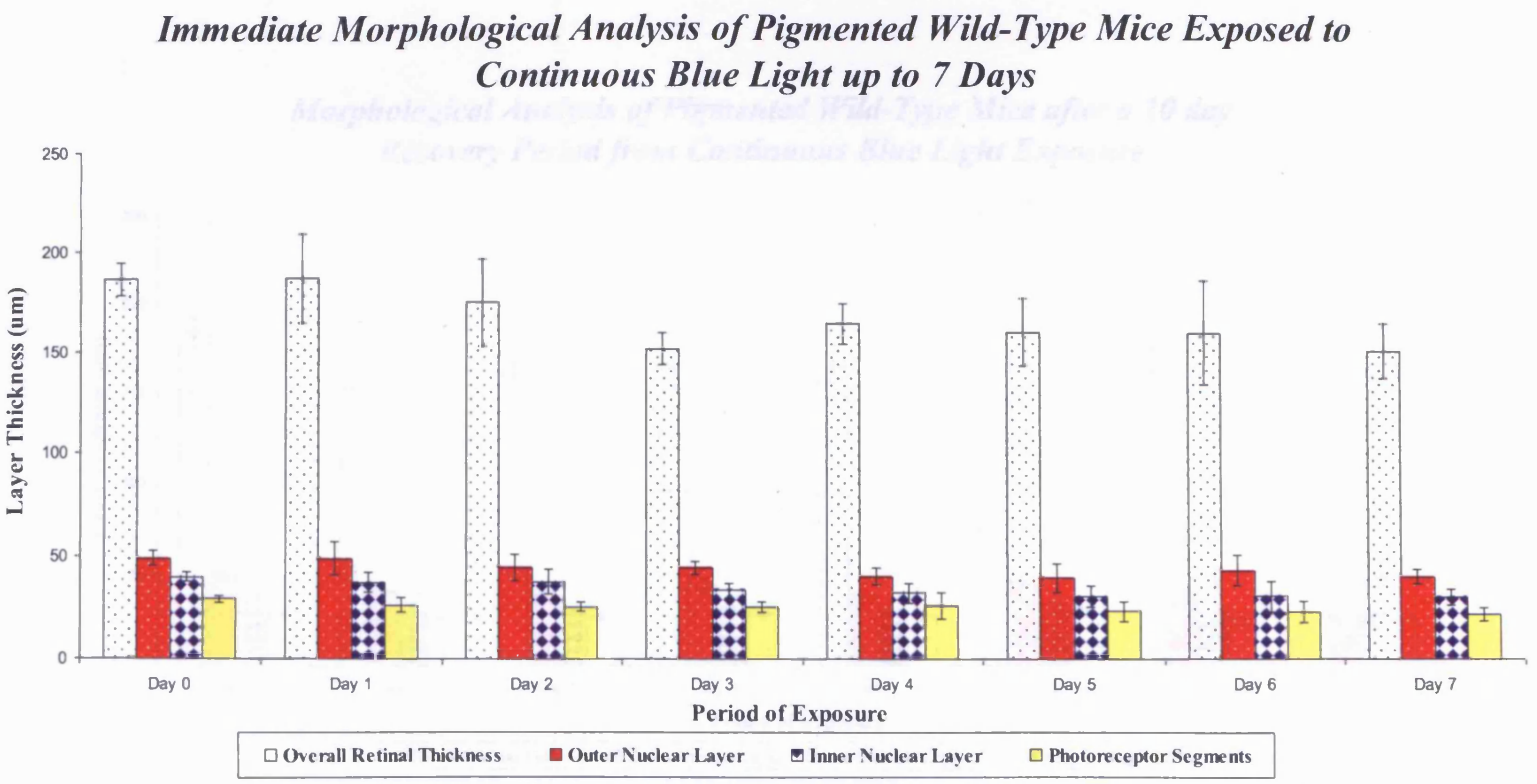

***Figure 5.4.11** Graphical morphometric analysis of overall retinal thickness, outer nuclear thickness, inner nuclear thickness and photoreceptor segment thickness in wild-type mice immediately after designated blue light exposure. For each animal during each trial, there was a minimum of 4 sections taken (four trials were performed). Three to four measurements were made per field, which were averaged to provide a single value for each retina. Data are expressed as mean ±S.D and statistical significance was assessed with a one-way ANOVA followed by Dunnett's multiple comparison test. A $p<0.05$ was considered statistically significant, n=4.*

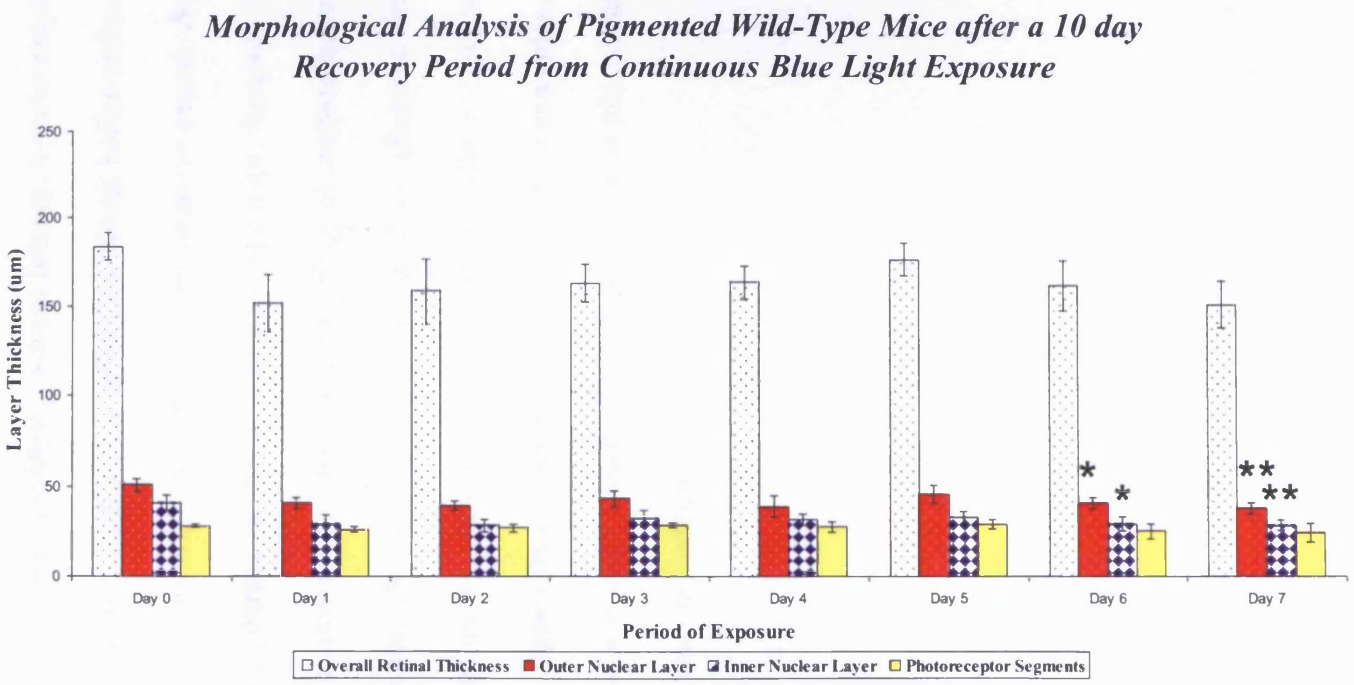

Figure 5.4.12 Graphical morphometric analysis of overall retinal thickness, outer nuclear thickness, inner nuclear thickness and photoreceptor segment thickness in wild-type mice 10 days after designated blue light exposure. For each animal during each trial, there was a minimum of 4 sections taken (four trials were performed). Three to four measurements were made per field, which were averaged to provide a single value for each retina. Data are expressed as mean ±S.D and statistical significance was assessed with a one-way ANOVA followed by Dunnett's multiple comparison test. A $p<0.05$ was considered statistically significant. ($p < 0.05$, **$p < 0.01$ compared to control retina, n=4).*

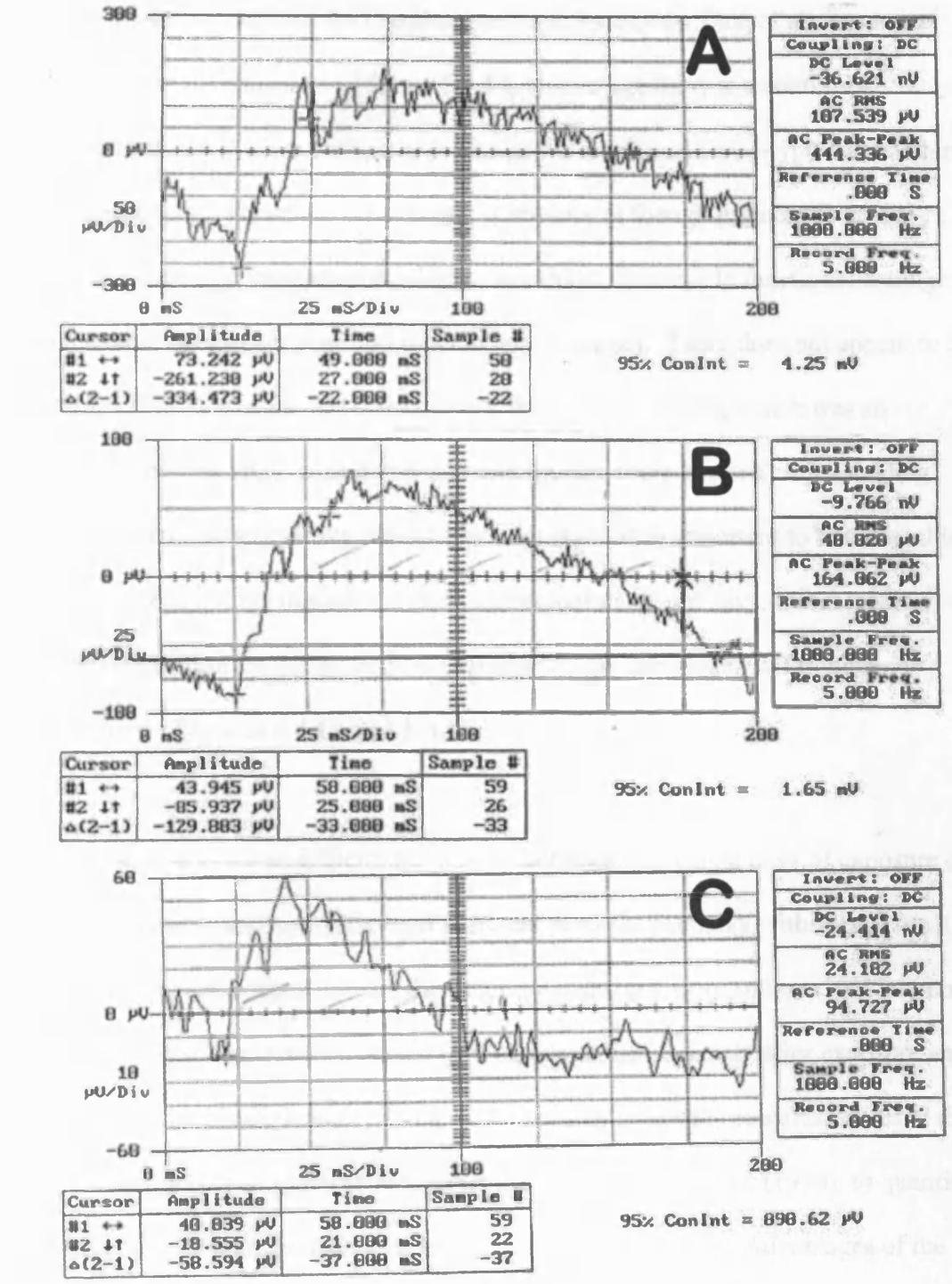

Figure 5.4.13 Representative ERGs from a mouse exposed to continuous blue light for 7 days. Shown in 'A' is a pre-ERG, 'B' is an immediate ERG, and 'C' is an ERG after a 10 day recovery period.

Figure **5.4.14** illustrates the ERG parameter trajectories over time of all pigmented wild-type mice. As shown in **Figure 5.4.14,** on average there is a continued degradation of the a-wave and b-wave amplitudes in exposed wild-type mice with no signs of recovery. Therefore on average, it appears as though pigmented wild-type that are exposed to continuous blue light, do exhibit irreversible functional damage of both the outer retina (a-wave) and inner retina (b-wave). There does not appear to be a notable difference in the latencies of both the a- and b-waves, which was an unexpected finding since with decreased amplitudes, there is often corresponding increased latencies, suggesting retinal layer damage. It is important to note that this illustration does not distinguish between individual exposure days. For a more detailed description on the changes in exposed versus unexposed wild-type mice, please refer to **Figures 5.4.15 and 5.4.16.**

For ERG analysis, it was difficult to contrast between individual days of exposure due to limited controls and limited animal numbers (n=3 for each day within each trial). Therefore, for each control mouse, the outcome measures were summarized into one quantity over the 3 assessment period (pre exposure, immediately after exposure and after a 10 day recovery period). Since we have three repeated measures, we used the Area Under the curve (AUC) as recommended by Matthews et al. (1990), to quantify each mouse ERG function over the duration and post exposure. Advantages of the AUC is its easy derivation, yet the disadvantages of the AUC include the loss of information about the time process; therefore, differences may be due to deviation between pre exposure and immediately after exposure or the immediately after and the 10 day recovery exposure periods.

As shown in **Figure 5.4.15,** the green dashed lines represent the 95% confidence bounds for the cases (all mice exposed, n=21), with individual trajectories mapped out for each control. No light exposure controls are designated as follows: blue line (Trial #1), red line (Trial #2), and purple line (Trial #3). For each control mouse, a one sample t-test was performed which examined whether the mean for the exposed mice is statistically different from the observed value of each of the control mice. This corresponds to a response feature analysis (Everitt, 1995) on the derived AUC variable. Therefore, this will answer for each individual control whether their observed values are statistically different from the average of the exposed mice. Test results are reported as a t-statistics, with p-value (Pr>|t|), as the level of significance, where a p-value < 0.05 corresponds to statistical significance (Degrees of freedom for the one sample t-tests are 20 for wild-type)**(please see Tables 5.1 - 5.3).**

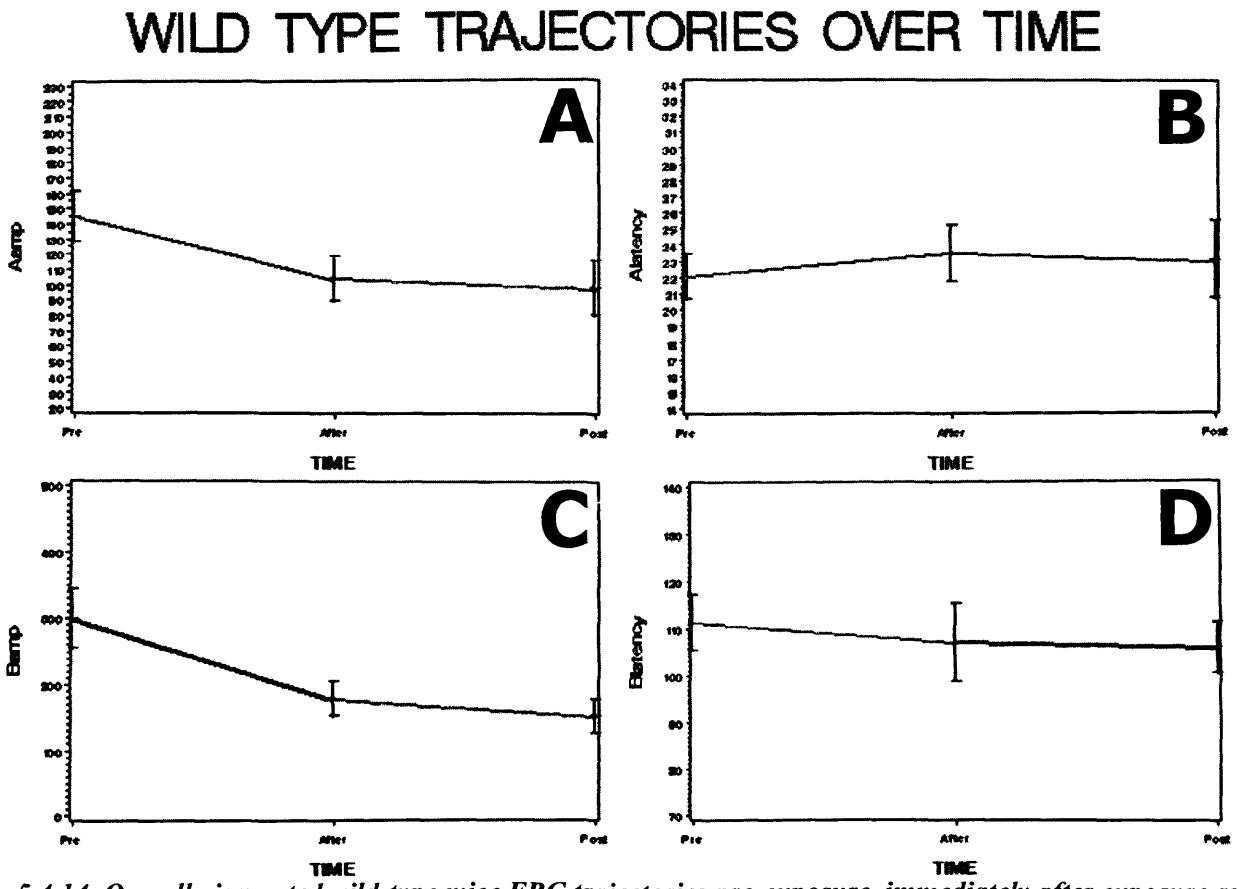

Figure 5.4.14 Overall pigmented wild-type mice ERG trajectories pre-exposure, immediately after exposure and after a 10 day recovery period. As shown above, on-average, for both the a-wave amplitude ('A') and b-wave amplitude ('C'), there is no recovery post exposure; in fact, continued degradation from the exposure to 10 days later is shown. For the a-wave ('B') and b-wave ('D') latencies, it appears on-average, there is minimal change over the three assessment periods. Data at measurement period represent the mean ± S.D. Data points represent ERG parameters from all wild-type mice without considering the time of exposure. (Please refer to Appendix for raw statistical values).

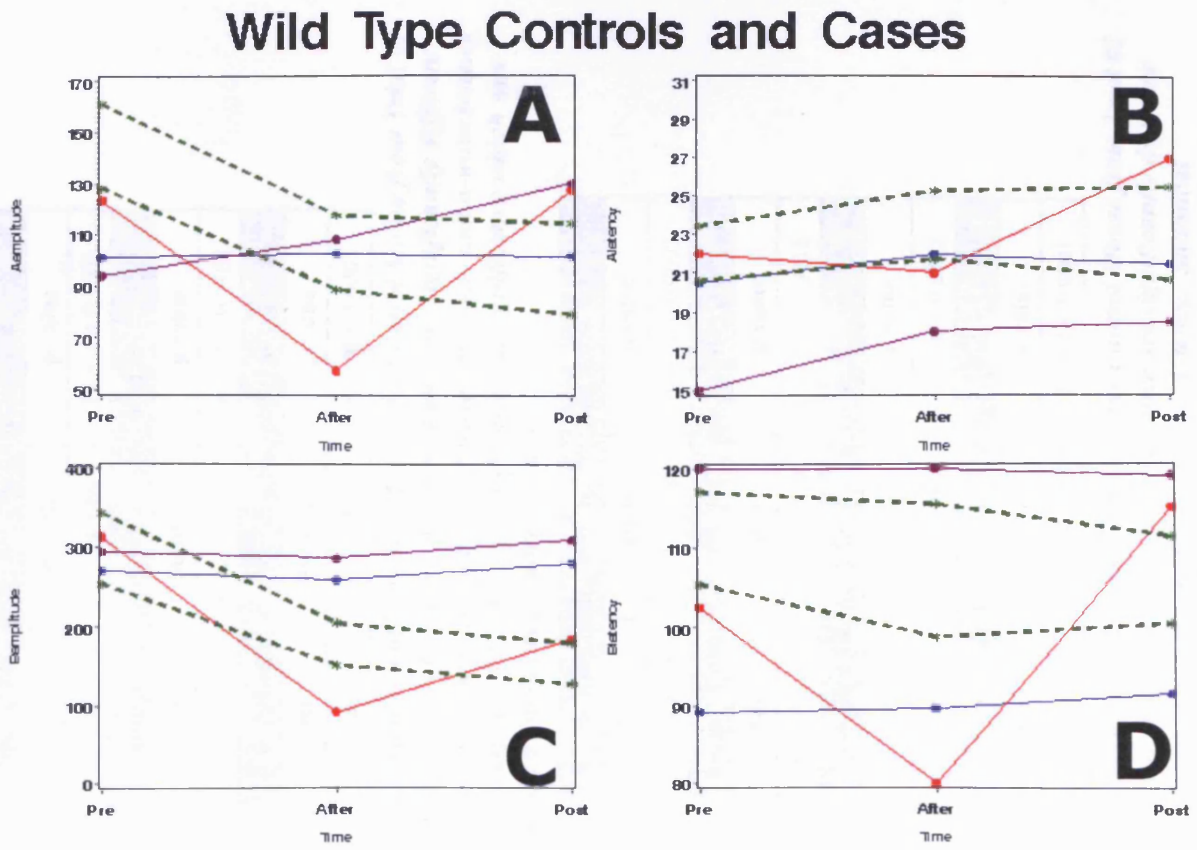

Figure 5.4.15 Comparison of control mice to exposed mice at pre-exposure, immediately after exposure and after a 10 day recovery period from blue light exposure. The blue line refers to Trial #1 control mouse, the red line refers to Trial #2 control mouse and the purple line refers to Trial #3 mouse (a-wave amplitude shown in 'A', b-wave amplitude shown in 'C', a-wave latency shown in 'B" and b-wave latency shown in 'D'). Data at measurement period represent the mean ± S.D. Data points represent ERG parameters from all wild-type mice without considering the time of exposure. (Please refer to Appendix for raw statistical values and Tables 5.1 – 5.3).

Shown in **Tables 5.1, 5.2,** and **5.3** are the summarized statistical contrasts of the exposed mice over the four measurements (a-wave, a-latency, b-wave and b-latency) compared to controls from each trial.

a-wave Amplitude: Tests for Location: Mu0 = 203.75		
Test	**Statistic**	**p value**
Student's t	t – 2.10116	Pr > |t| < 0.0485
b-wave Amplitude: Tests for Location: Mu0 = 535.38		
Test	**Statistic**	**p value**
Student's t	t – 7.44684	Pr > |t| < 0.0001
a-wave Latency: Tests for Location: Mu0 = 43		
Test	**Statistic**	**p value**
Student's t	t – 2.100713	Pr > |t| < 0.0485
b-wave Latency: Tests for Location: Mu0 = 180.13		
Test	**Statistic**	**p value**
Student's t	t - 6.645852	Pr > |t| < 0.0001

Table 5.1 Comparison of Exposed Mice to the Control Mouse from Trial #1 (Blue Line). On all four measure, exposed mice are significantly different from the control values, although the a-wave amplitude and a-wave latency are near the alpha = 0.05 threshold for statistical significance which was assessed with a one-paired student's t-test

a-wave Amplitude: Tests for Location: Mu0 = 182.75		
Test	**Statistic**	**p value**
Student's t	t – 4.324582	Pr > |t| < 0.0003
b-wave Amplitude: Tests for Location: Mu0 = 341.25		
Test	**Statistic**	**p value**
Student's t	t – 3.682978	Pr > |t| < 0.0015
a-wave Latency: Tests for Location: Mu0 = 45.5		
Test	**Statistic**	**p value**
Student's t	t – 0.403983	Pr > |t| < 0.6905
b-wave Latency: Tests for Location: Mu0 = 188.75		
Test	**Statistic**	**p value**
Student's t	t - 5.036318	Pr > |t| < 0.0001

Table 5.2 Comparison of Exposed Mice to the Control Mouse from Trial #2 (Red Line). On all four measure, exposed mice are significantly different from the control values except for the a-wave latency. Statistical significance was assessed with a one-paired student's t-test (A $p < 0.05$ was considered statistically significant.

a-wave Amplitude: Tests for Location: Mu0 = 219.75		
Test	**Statistic**	**p value**
Student's t	t – 0.407123	Pr > |t| < 0.6882
b-wave Amplitude: Tests for Location: Mu0 = 588.5		
Test	**Statistic**	**p value**
Student's t	t – 10.4927	Pr > |t| < 0.0001
a-wave Latency: Tests for Location: Mu0 = 34.75		
Test	**Statistic**	**p value**
Student's t	t – 7.69992	Pr > |t| < 0.0001
b-wave Latency: Tests for Location: Mu0 = 239.5		
Test	**Statistic**	**p value**
Student's t	t – 4.4342	Pr > |t| < 0.0003

***Table 5.3** Comparison of Exposed Mice to the Control Mouse from Trial #3 (Purple Line). On all four measure, exposed mice are significantly different from the control values except for the a-wave amplitude. Statistical significance was assessed with a one-paired student's t-test (A p< 0.05 was considered statistically significant.*

Figure 5.4.16 illustrates the ERG measurements of the mice during their exposure period. With the exception of **1 Day of exposure,** at no point do the mice recovery to their original a- or b-wave amplitudes after being exposed to continuous blue light. Some mice appear to exhibit some recovery in their a- and b-wave amplitudes (**Days 3 and 4**), yet amplitudes do not reach their original starting point. **Days 5 -7** illustrate a continual decline in the amplitudes, indicating that the longer the animal was exposed to continuous blue light, the less likely they were to recover.

a-wave Amplitude of Wild-Type Pigmented Mice Not Exposed to Continuous Blue Light (Day 0)

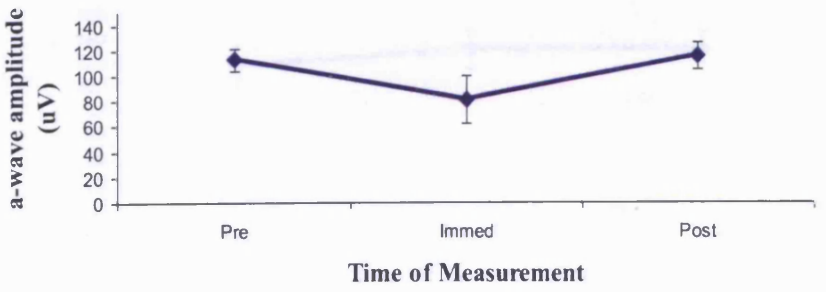

a-wave Latency of Wild-Type Pigmented Mice Not Exposed to Continuous Blue Light (Day 0)

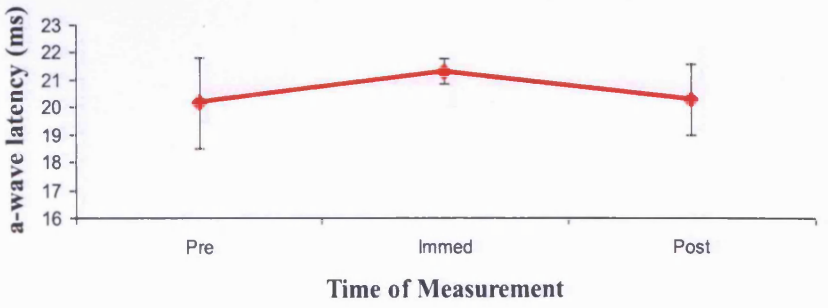

b-wave Amplitude of Wild-Type Pigmented Mice Not Exposed to Continuous Blue Light (Day 0)

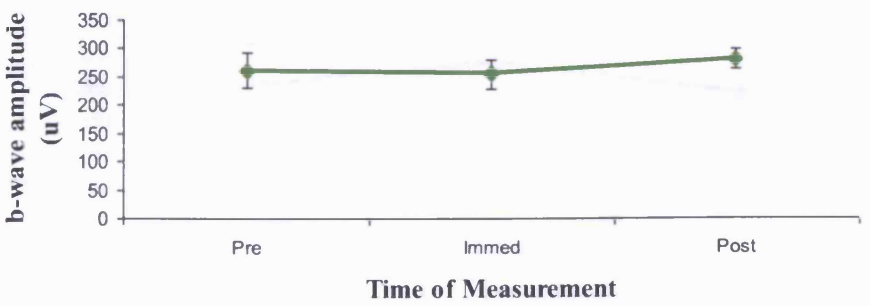

b-wave Latency of Wild-Type Pigmented Mice Not Exposed to Continuous Blue Light (Day 0)

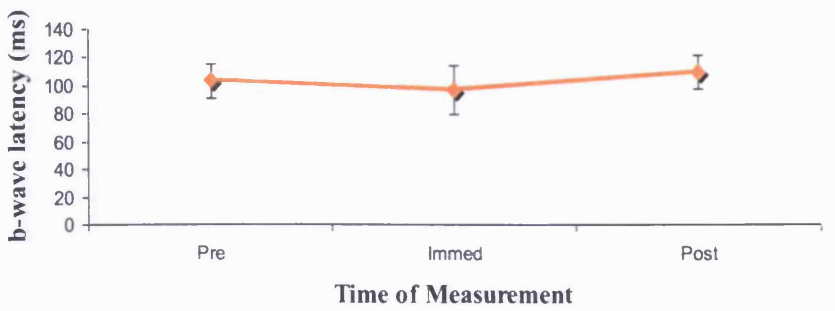

Figure 5.16 *continued overleaf*

a-wave Amplitude of Wild-Type Pigmented Mice Exposed to Continuous Blue Light for 1Day (24hrs)

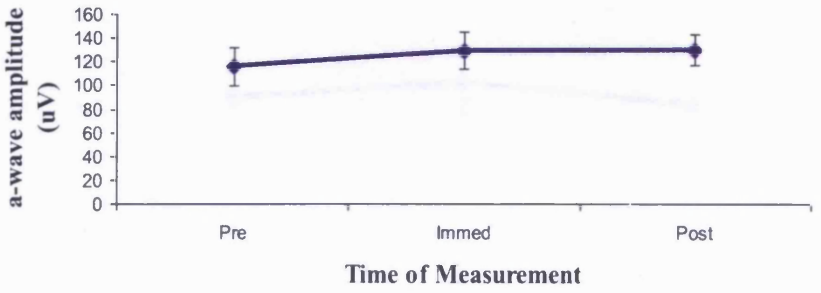

a-wave Latency of Wild-Type Pigmented Mice Exposed to Continuous Blue Light for 1 Day (24hrs)

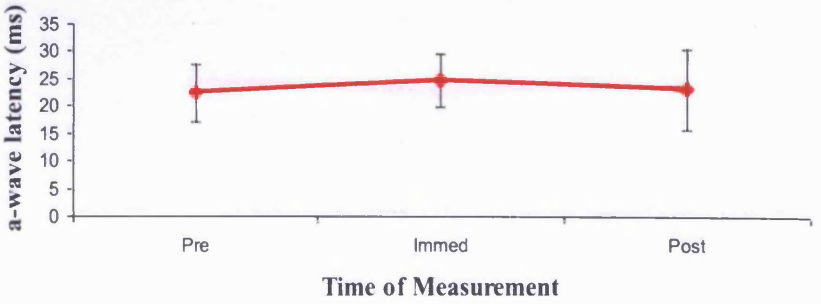

b-wave Amplitude of Wild-Type Pigmented Mice Exposed to Continuous Blue Light for 1Day (24hrs)

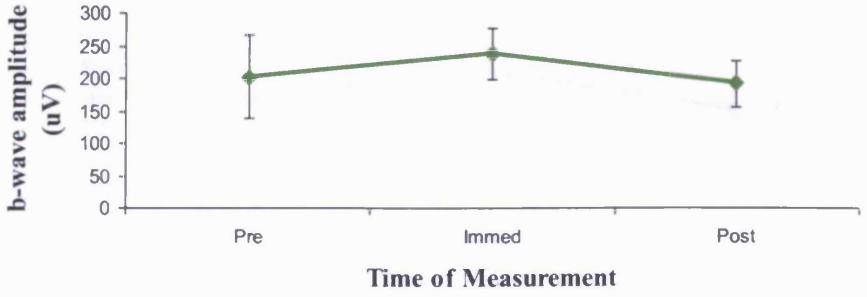

b-wave Latency of Wild-Type Pigmented Mice Exposed to Continuous Blue Light for 1 Day (24hrs)

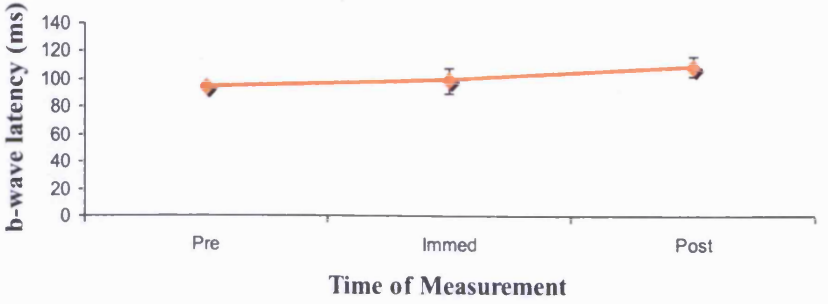

Figure 5.4.16 *continued overleaf*

a-wave Amplitude of Wild-Type Pigmented Mice Exposed to Continuous Blue Light for 2 Days (48hrs)

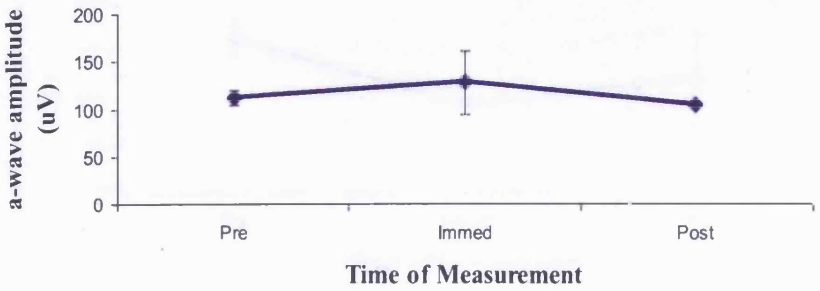

a-wave Latency of Wild-Type Pigmented Mice Exposed to Continuous Blue Light for 2 days (48hrs)

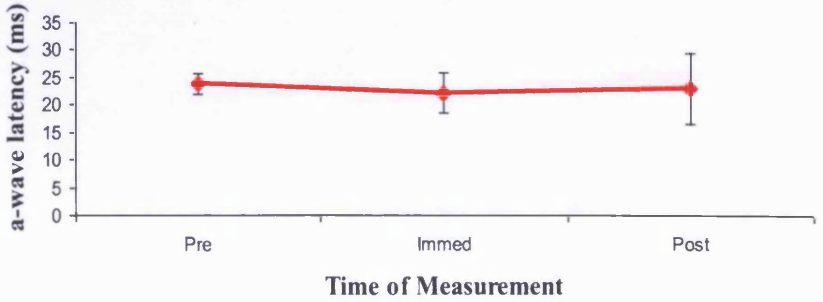

b-wave Amplitude of Wild-Type Pigmented Mice Exposed to Continuous Blue Light for 2 days (48hrs)

b-wave Latency of Wild-Type Pigmented Mice Exposed to Continuous Blue Light for 2 days (48hrs)

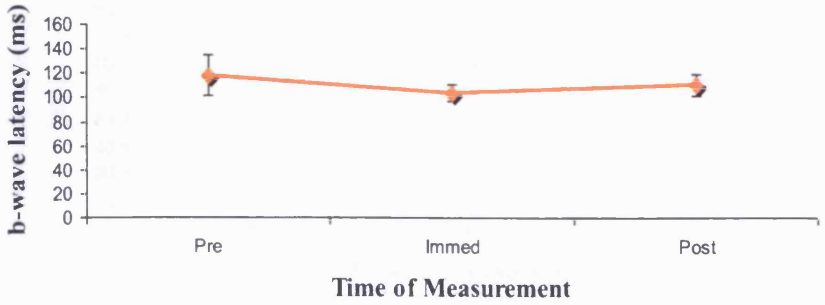

Figure 5.4.16 *continued overleaf*

a-wave Amplitude of Wild-Type Pigmented Mice Exposed to Continuous Blue Light for 3 Days (72hrs)

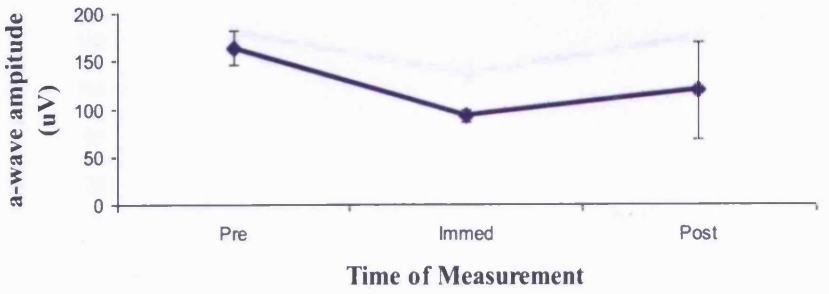

a-wave Latency of Wild-Type Pigmented Mice Exposed to Continuous Blue Light for 3 days (72hrs)

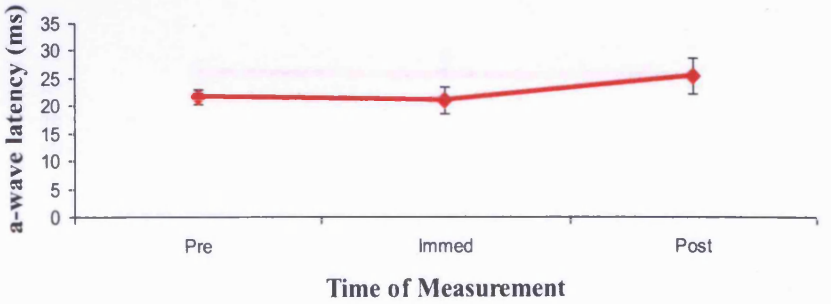

b-wave Amplitude of Wild-Type Pigmented Mice Exposed to Continuous Blue Light for 3 days (72hrs)

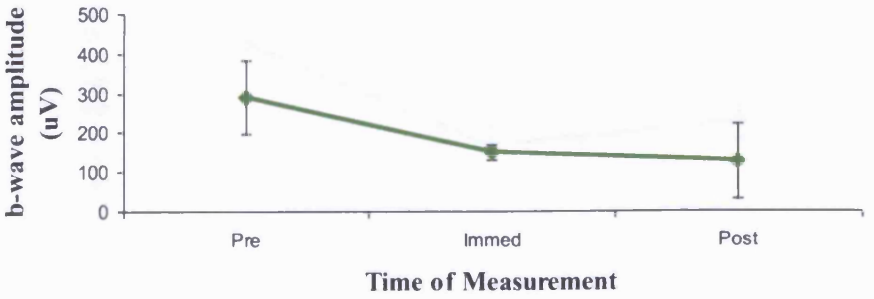

b-wave Latency of Wild-Type Pigmented Mice Exposed to Continuous Blue Light for 3 Days (72hrs)

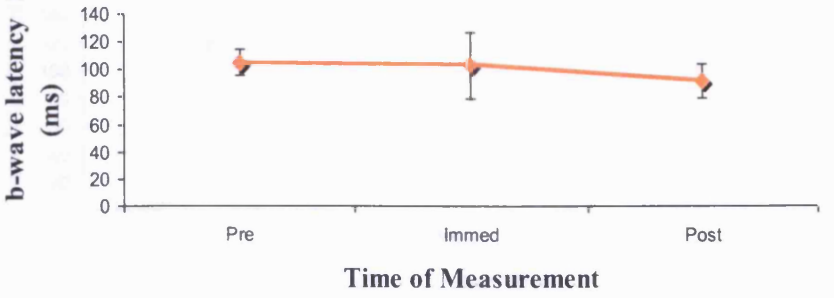

Figure 5.4.16 *continued overleaf*

a-wave Amplitude of Wild-Type Pigmented Mice Exposed to Continuous Blue Light for 4 Days (96hrs)

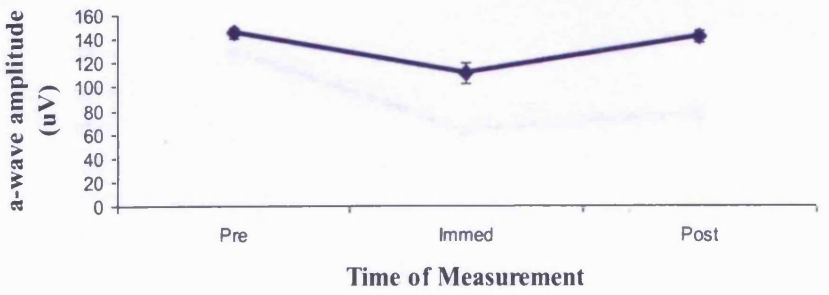

a-wave Latency of Wild-Type Pigmented Mice Exposed to Continuous Blue Light for 4 days (96hrs)

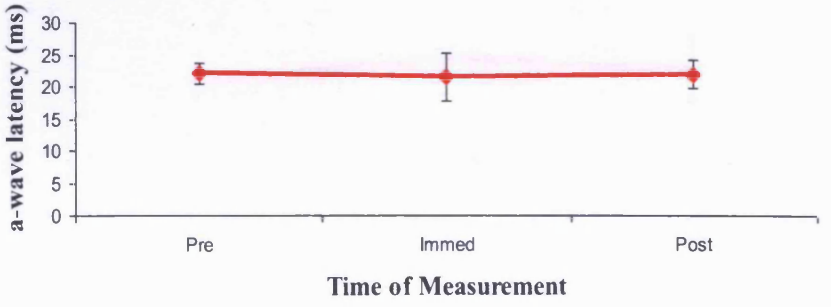

b-wave Amplitude of Wild-Type Pigmented Mice Exposed to Continuous Blue Light for 4 days (96hrs)

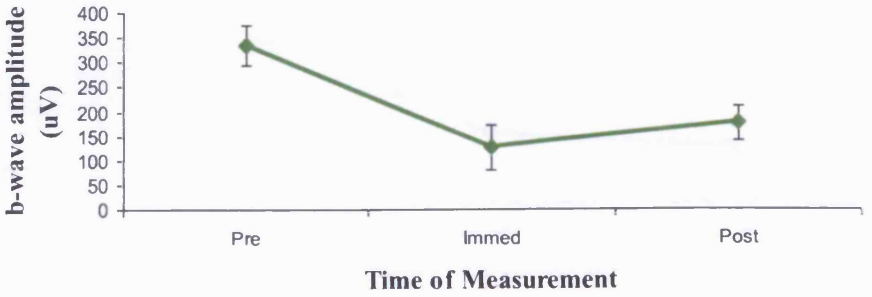

b-wave Latency of Wild-Type Pigmented Mice Exposed to Continuous Blue Light for 4 Days (96hrs)

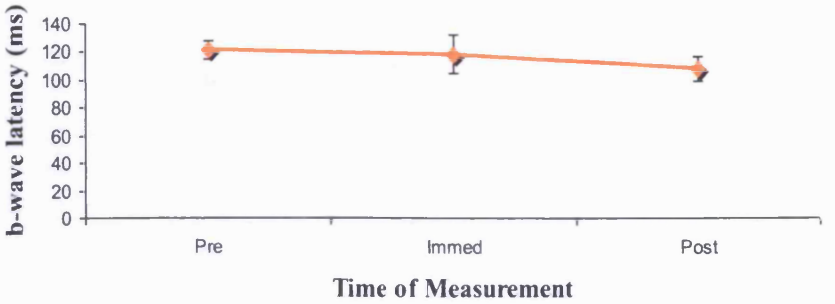

Figure 5.4.16 *continued overleaf*

a-wave Amplitude of Wild-Type Pigmented Mice Exposed to Continuous Blue Light for 5 days (120hrs)

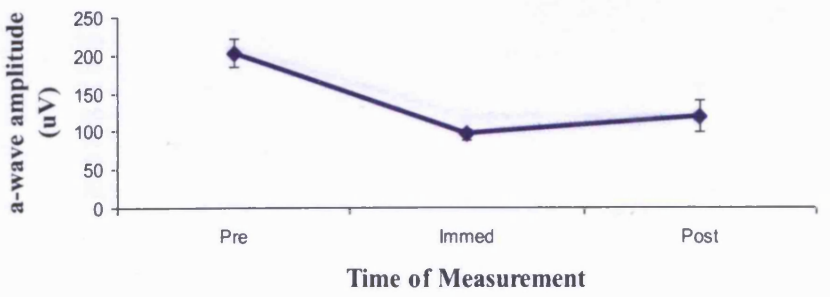

a-wave Latency of Wild-Type Pigmented Mice Exposed to Continuous Blue Light for 5 days (120hrs)

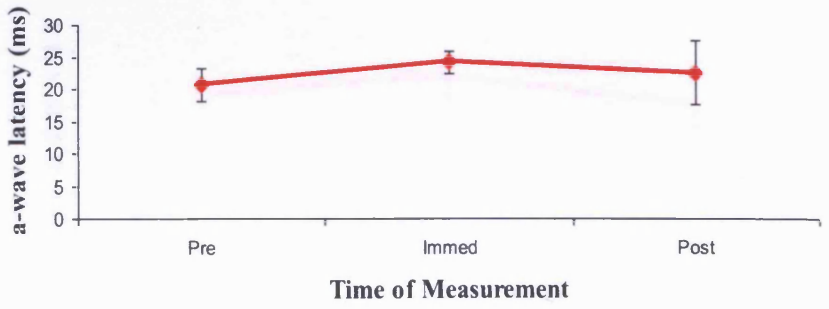

b-wave Amplitude of Wild-Type Pigmented Mice Exposed to Continuous Blue Light for 5 days (120hrs)

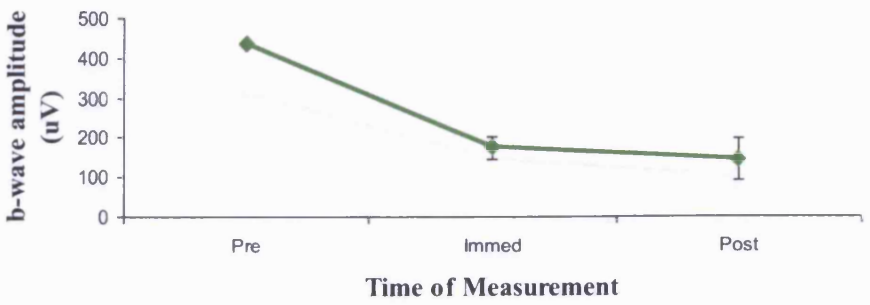

b-wave Latency of Wild-Type Pigmented Mice Exposed to Continuous Blue Light for 5 Days (120hrs)

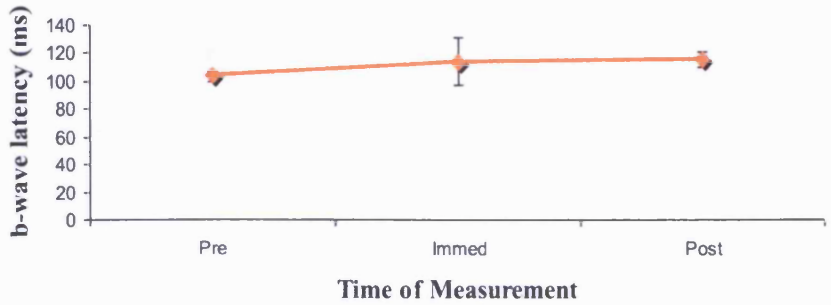

Figure 5.4.16 *continued overleaf*

a-wave Amplitude of Wild-Type Pigmented Mice Exposed to Continuous Blue Light for 6 days (144hrs)

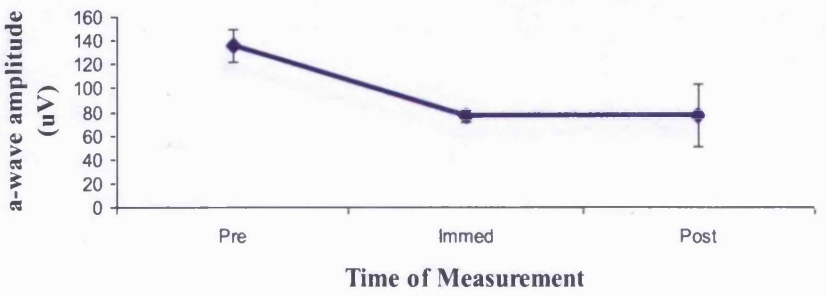

a-wave Latency of Wild-Type Pigmented Mice Exposed to Continuous Blue Light for 6 days (144hrs)

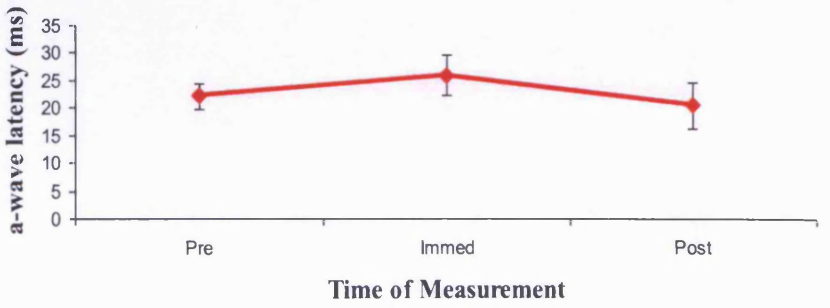

b-wave Amplitude of Wild-Type Pigmented Mice Exposed to Continuous Blue Light for 6 days (144hrs)

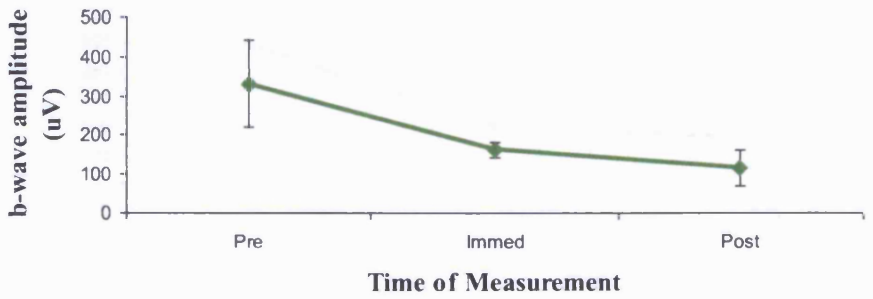

b-wave Latency of Wild-Type Pigmented Mice Exposed to Continuous Blue Light for 6 Days (144hrs)

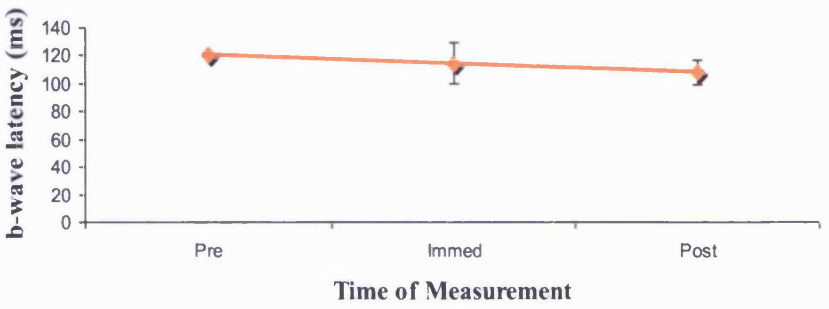

Figure 5.4.16 *continued overleaf*

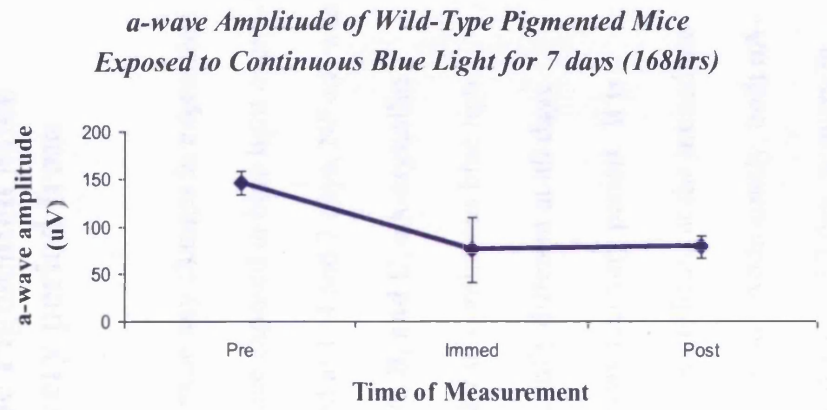

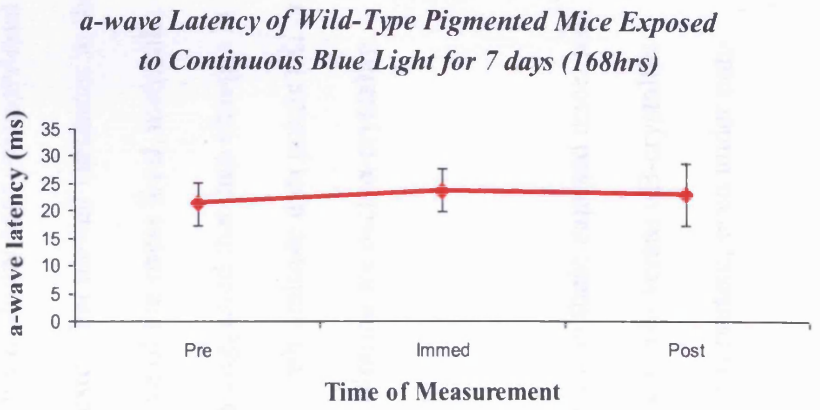

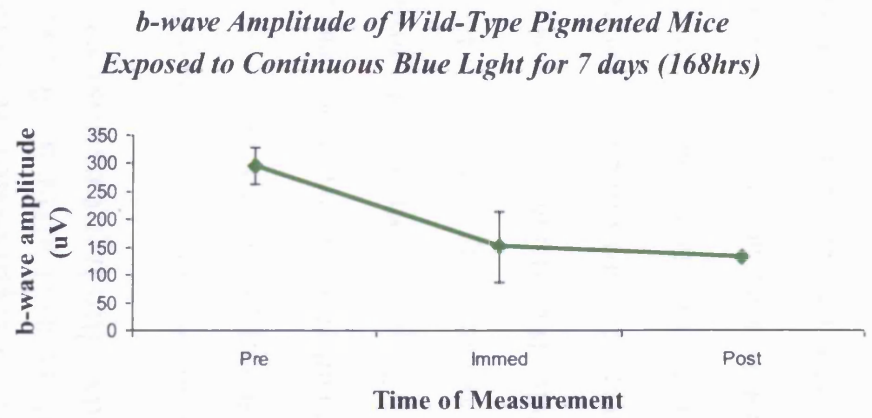

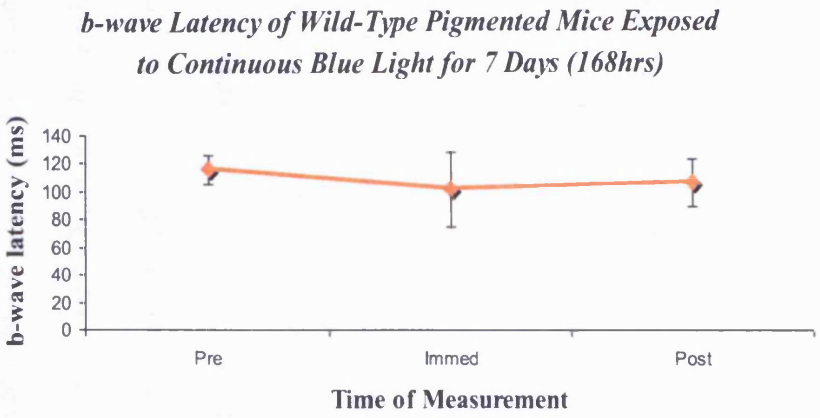

Figure 5.4.16 ERG measurements of pigmented wild-type mice exposed to continuous blue light over 1-7 days. Measurements included a- and b-wave amplitudes and a- and b-wave latencies. Measurements were performed at three time points for each trial (pre-exposure to blue light, immediately after exposure to blue light and after a 10day recovery). Data at each time point represents the mean ± S.D. (3 trials were performed; each exposure day, n=3).

5.4.6 Protein Expression in Wild-Type Pigmented Mice Immediately and after a 10 day recovery period from continuous blue light exposure

Western Blot analysis was performed in order to examine any changes in expression of αA- and αB-crystallin and NF-κB expression in mice exposed to blue light over 1-7 days (αA- and αB-crystallin expression was examined at 1, 4 and 7 days, NF-κB was examined at 1-7 days). As shown in **Figures 5.4.17A, B, and C**, αA-crystallin expression was statistically significant at **Days 4 and 7** of continuous blue light exposure, while αB-crystallin expression was significantly different at all days analyzed, but upregulation was greater during the 10 day recovery period. It is important to note that both αA- and αB-crystallin were significant at the immediate time point of **4 days,** but not after a 10 day recovery period. Additionally, both αA- and αB- showed a significant difference immediate and after a 10 day recovery in mice exposed for **7 days.** The protein expression of the α-crystallins was highly variable between individual mice. This finding of high variability between individual mice was also reported by Xi *et al.,* 2003a who suggested that normal variations in the expression of various crystallin genes may be reflective of the stress level, metabolic status, and/or age of these animals. Additionally they suggested that data changes in crystallin expression should be interpreted cautiously with multiple data points (Xi *et al.,* 2003a). The number of retinas used for Western Blotting for each α-crystallin was 3.

With regards to the retinal expression of the α-crystallins in these exposed mice, one can clearly distinguish between the visible differences in αA- versus αB-crystallin expression (**Figure 5.4.17C**). αB-crystallin expression is present, even under non-

stressed conditions and appears to parallel expression of the αA-crystallin in **Day 4 (Immediate) and Day 7 (after a 10 day recovery).**

A

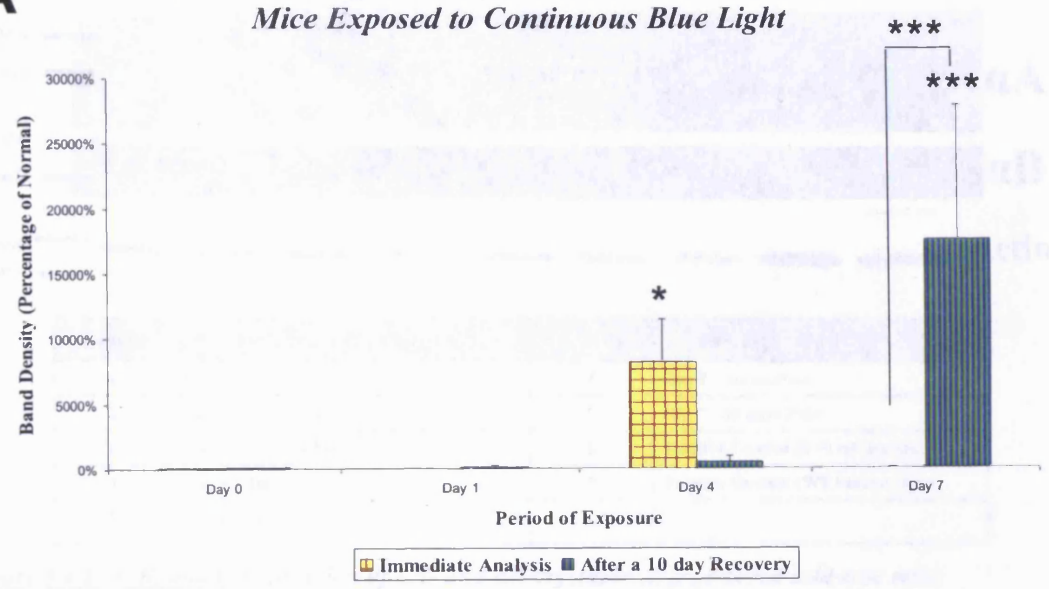

B

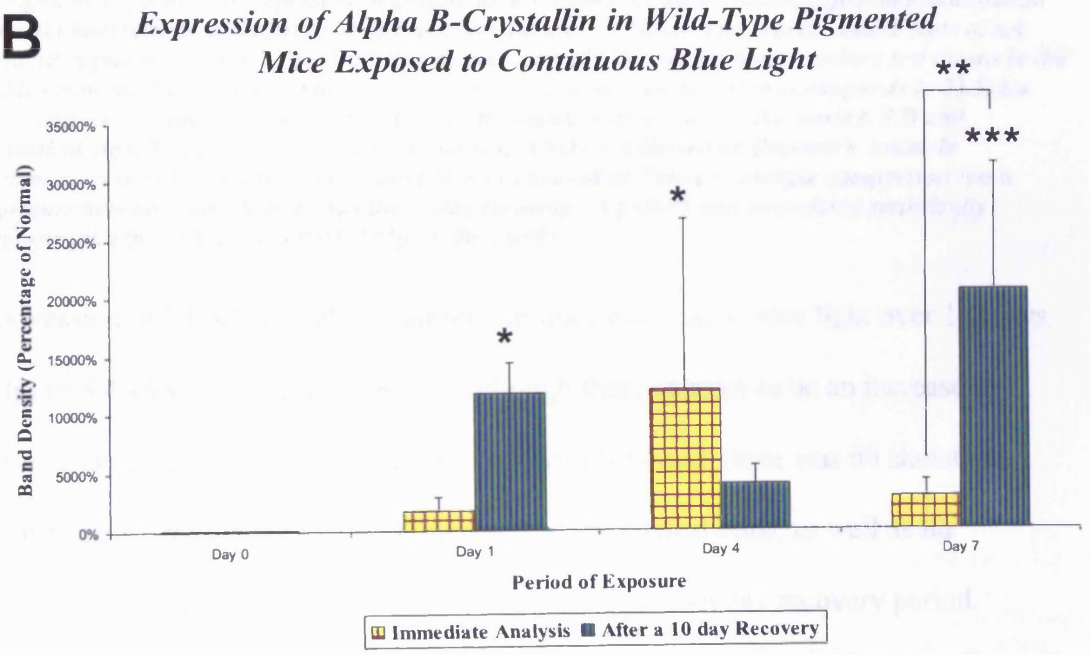

Figure 5.4.17A and B continued overleaf

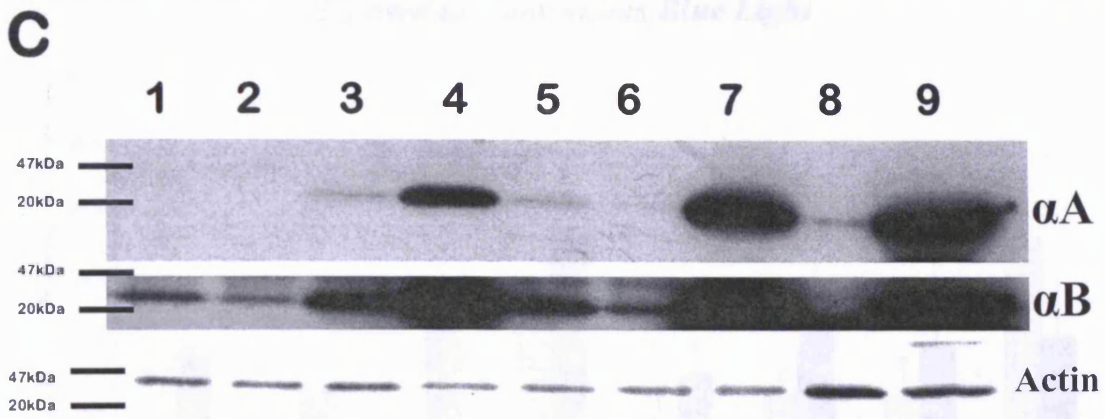

Lanes	Designated Exposure	Lanes	Designated Exposure
1	Control	6	Day 7 – Immediate
2	Day 1 - Immediate	7	Day 7 –10 days Post
3	Day 1 – 10 days Post	8	Positive Control (Y79 cell lysate)
4	Day 4 – Immediate	9	Positive Control (WT Mouse Lens)
5	Day 4 – 10 days Post		

***Figure 5.4.17A, B, and C** Expression of αA- and αB-crystallin in pigmented wild-type mice immediately and after a 10 day recovery period from 1, 4 or 7 days of exposure. . 'A' represents a graphical description of αA-crystallin expression normalized to actin immediately and 10 days after designated exposure. 'B' represents a graphical description of αB-crystallin expression normalized to actin immediately and after a 10 day recovery period. 'C' illustrates representative blots of αA- and αB-crystallin, as well as actin as an internal control (The key for lane numbers are shown in the table below the blots). αA-crystallin corresponds to 20kDa, αB-crystallin corresponds to 23.5kDa and actin corresponds to 43kDa. In 'A' and 'B', data are expressed as the mean ± S.D and statistical significance was assessed by a one-way ANOVA followed by Dunnett's multiple comparison test to compare exposed mice to non-exposed or Tukey's multiple comparison test to compare between immediate versus the 10day recovery. A $p<0.05$ was considered statistically significant. ($*p < 0.05$, $**p < 0.01$, $***p < 0.001$, n=3).*

Expression of NF-κB was also examined in mice exposed to blue light over 1-7 days. **Figure 5.4.18A and B** illustrates that although there appears to be an increase in expression from immediate to the 10 day recovery period, there was no statistical significance between the exposed mice versus the control mice, as well as no significant difference from the immediate period to the 10 day recovery period.

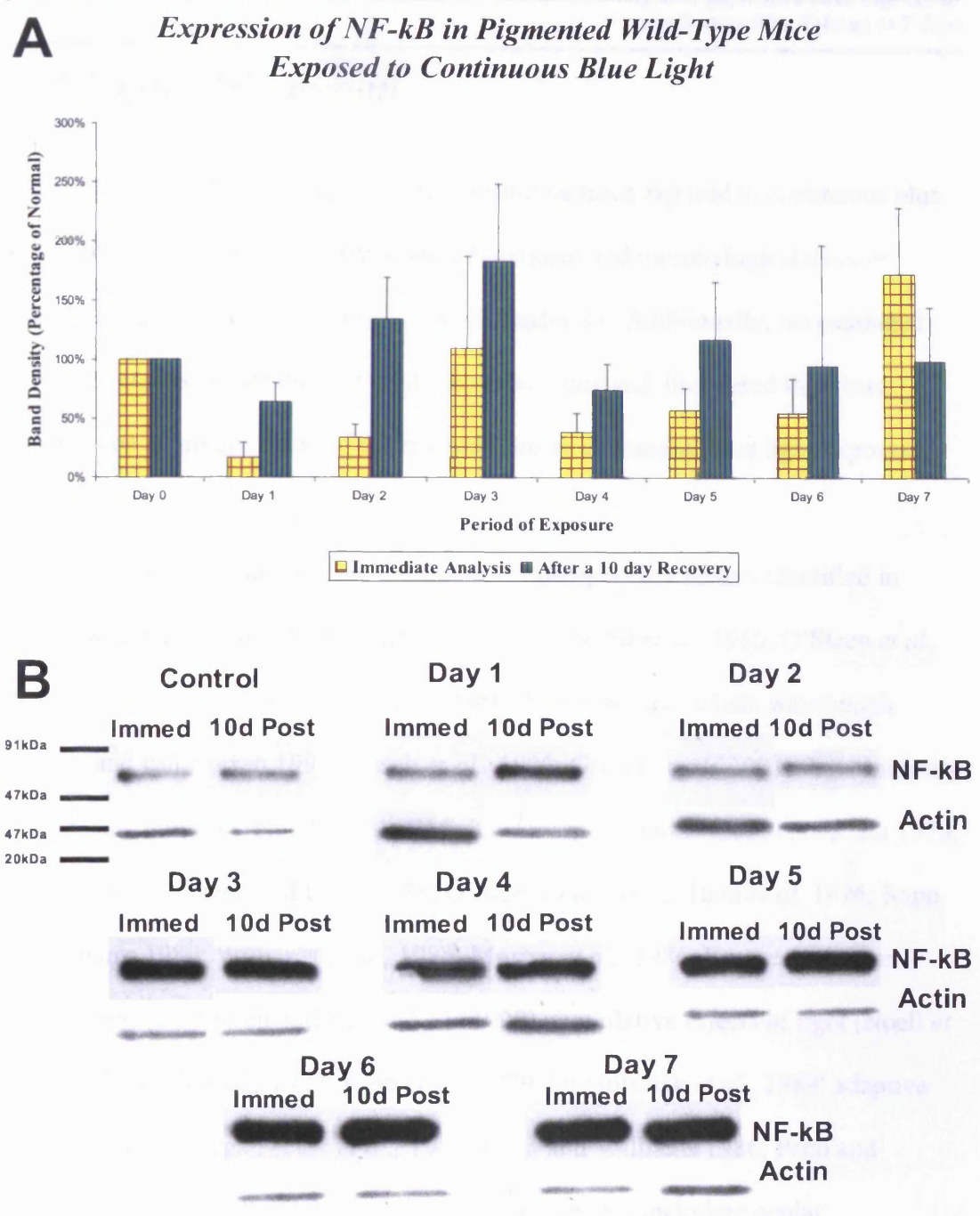

Figure 5.4.18 Expression of NF-κB pigmented wild-type mice immediately and after a 10 day recovery period over 1-7 days of exposure. . 'A' represents a graphical description of NF-κB expression normalized to actin immediately and 10 days after designated exposure. Shown in 'B'are representative blots of NF-κB, as well as actin as an internal control. NF-κB corresponds to 63kDa and actin corresponds to 43kDa. In 'A'data are expressed as the mean ± S.D and statistical significance was assessed by a one-way ANOVA followed by Dunnett's multiple comparison test to compare exposed mice to non-exposed or Tukey's multiple comparison test to compare between immediate versus the 10day recovery. A $p<0.05$ was considered statistically significant. ($p < 0.05$, **$p < 0.01$, ***$p <0.001$, n=3).*

5.5 Chapter Discussion

In this chapter, we found that pigmented, wild-type mice exposed to continuous blue light over 1-7 days do exhibit irreversible functional and morphological damage, however not as severe as albino mice (see **Chapter 4)**. Additionally, we examined the protein expression of the α-crystallins in the retina and discovered that there appears to be an upregulation of the α-crystallins in continuous blue light exposure.

Reports have shown that there are a number of susceptibility factors identified in animals with regards to light damage experiments (Noell *et al.,* 1966; O'Steen *et al.,* 1974; Danciger *et al.,* 2000; Wu *et al.,* 2006). These factors include wavelength (Gorgels and van Norren 1995; Busch *et al.,* 1999; Grimm *et al.,* 2001), light intensity and exposure duration (Noell *et al.,* 1966; Kuwabara and Gorn 1968; Kuwabara 1970; O'Steen 1970; O'Steen and Lytle 1971; O'Steen *et al.,* 1972; Ham *et al.* 1976; Rapp and Williams 1980; Williams *et al.,* 1985; Moriya *et al.,* 1986; Kremers and van Norren 1989; van Norren and Schellekens 1990), cumulative effects of light (Noell *et al.,* 1966; Lawwill *et al.,* 1977; Ham *et al.,* 1979; Organisciak *et al.,* 1989) adaptive state (Noell 1979; Organisciak *et al.,* 1985; Penn and Williams 1986; Penn and Anderson 1987a; Penn *et al.,* 1987b) and animal genetics including ocular pigmentation and specie type (Lawwill 1973; Rapp and Williams 1980; La Vail and Gorrin 1987; Rapp and Smith 1992; Gorgels and Van Norren 1998).

Of particular interest for this study was the presence of pigment in the wild-type mice exposed to continuous blue light. The purpose for examination of wild-type pigmented mice was two-fold; first it would allow a comparison between morphological and functional changes associated with blue light exposure over 1-7

days in a non-pigmented (**Chapter 4)** versus pigmented rodent strain (**Chapter 5)** and second, it would allow a comparison between pigmented animals that contain αA-crystallin (**Chapter 5)** and those that are pigmented but do not contain αA-crystallin **(Chapter 6).**

As stated previously, conflicting studies have reported that pigmentation plays little to no role in retinal light damage pathogenesis (Lawwill 1973; La Vail *et al.,* 1987; Gorgels and van Norren 1998). This study demonstrates that although morphological and functional damage was not as severe as in the albino strain, there was an irreversible effect on the retinal function and morphology. However, it is important to note that our study differed from others in various ways. For example, Gorgels and van Norren (1998) examined pigmented and non-pigmented rats under anesthetized conditions with short-term, intense irradiations to the eye and subsequent examination with fundoscopy and light microscopy. They concluded that melanin is not the main chromophore in causing photochemical damage to the retina in pigmented animals, nor does it play a role in the toxic process (Gorgels and van Norren, 1998). LaVail and Gorrin (1987) also found that light-induced photoreceptor damage was independent of pigmentation phenotype in experimental chimeras and translocation mice.

Additional broadband blue light studies performed on pigmented versus albino rabbits found that the RPE damage of both types of rabbits were equally sensitive to blue light (Van Best *et al.,* 1997) and if light levels are controlled to produce equal steady-state bleaching, the retinal degeneration is similar between pigmented and non-pigmented strains (Rapp *et al.,* 1980; Rapp *et al.,* 1992).

It was clearly shown in **Chapter 4** that the BALB/cBYJ mice not only exhibited visible proof of photochemical damage by the loss of the outer nuclear layer and subsequent visual function, but the longer the animal was exposed, the greater the retinal damage and the greater the loss of visual function. In pigmented mice, the morphological damage was not visibly evident until the longest duration of exposure, **Days 6 and 7**, with an irreversible effect on visual function from **Days 5-7.** These findings correlate with Noell's work in 1966 which examined retinal light damage in pigmented and albino rats under identical illuminance conditions. In his work he found that for pigmented rats to achieve the same reduction in a-wave amplitude as albino rats, exposure duration had to be more than doubled (even with the pupils dilated) (Noell *et al.*, 1966). Although exposure time was not doubled in our study, both strains of mice were exposed to the same illuminance, under the same conditions, with dilated pupils and while damage was noted almost immediately after 3 days of exposure in the albino mice, evidence of any retinal damage was not apparent until **6 or 7 days of exposure** in pigmented mice.

A similar study also examined the long-term effects of light damage in pigmented and albino rats after exposure to moderate (500 lux) but continuous illumination for 1 week (Wasowicz *et al.*, 2002). They concluded that albino rat retinas exhibited visible morphological changes, whereas the pigmented rats did not, but both strains did exhibit changes in retinal biochemical markers and amino acids (Wasowicz *et al.*, 2002). This work was similar to our study with regards to morphological changes, although instead of examining retinal biochemical markers and amino acid composition, we examined the expression of α-crystallins and NF-κB.

The role of α-crystallins in light damage has been previously studied in intense light exposure experiments (Miyagi *et al.*, 2002; Sakaguchi *et al.*, 2003; Tanito *et al.*, 2006), dim cyclic light (Organisciak *et al.*, 2003) and the rd1 mouse (Cavusoglu *et al*, 2003). In our study involving exposure at moderate levels of continuous visible light, protein expression of αA-crystallin was not evident until exposure duration increased. αB-crystallin expression was present at all exposure times, and appeared to be upregulated with increasing light exposure. The αB-crystallin upregulation was also noted in the rod outer segments and RPE after exposure to intense light (Sakaguchi *et al.*, 2003). Examination of the α-crystallins in the wild-type mice was necessary for future comparison to αA-crystallin knock-out studies (**see Chapter 6**).

Expression of NF-κB appeared to be up-regulated in mouse retinas during their 10 day recovery period compared to analysis at the immediate time point, however this upregulation was not significant. NF-κB has been linked to the α-crystallins in the area of inflammation (Masilamoni *et al.*, 2006, Ousman *et al.*, 2007). In particular, *in-vivo* and *in-vitro* studies found that αB-crystallin prevents cell death of astrocytes by inhibiting caspase-3 activation, and suppresses the inflammatory role of NF-kB (Ousman *et al.*, 2007). Additionally, it was shown that if cells were pre-treated with α-crystallins, NF-κB activity was suppressed, therefore downregulating the expression of proinflammatory cytokines (Masilamoni *et al.*, 2006). Expression of the α-crystallins was not examined in the albino mice, however, perhaps the expression of NF-κB is less in the pigmented due to the increasing expression of α-crystallins as light exposure duration increases.

Since there were functional and morphological changes noted in the pigmented mice, which were not as drastic as those noted in the albino mice, future studies should utilize the technique of transmission electron microscopy to examine changes not visible with light microscopy. Additionally, although we examined the protein expression of the α-crystallins, we were unable to localize the exact location of expression and or any changes associated with that expression. Therefore immunocytochemistry would be a useful technique for future studies. It is also important to add that the influence of genetic factors in explaining the protection against light cannot be excluded, because the degree of retinal susceptibility varies between pigmented versus non-pigmented strains exposed to the same light intensity (La Vail and Gorrin 1987, LaVail *et al.,* 1997).

In summary this study has shown that:

- Pigmented, wild-type mice do exhibit irreversible morphological and functional photochemical damage at longer exposure durations, however it is not as severe as the albino
- αA- and αB-crystallins appear to be upregulated in light damage as the duration increases, possibly exhibiting a protective role in photochemical light damage
- NF-κB is not significantly upregulated in pigmented, wild-type mice exposed to continuous blue light daily up to 7 days

Chapter 6.0:

In-vivo morphological and functional analysis of pigmented αA-crystallin knock-out mice exposed to continuous blue light up to 7 days

6.1 Chapter Introduction

α-crystallins (αA- and αB-crystallin) belong to the family of small heat shock proteins and can act as molecular chaperones (Horwitz 1992; Boyle and Takemoto, 1994; Wang *et al.*, 1995; Andley *et al.*, 1996; Derham and Harding, 1999; Horwitz 2000; Derham and Harding, 2002; Horwitz 2003; Thiagarajan *et al.*, 2004; Cheng *et al.*, 2008; Ecroyd and Carver, 2008; Ghosh *et al.*, 2008; Tanaka *et al.*, 2008). A majority of the α-crystallins functional and structural role has been examined in the lens, since these proteins were once thought to be exclusive to this tissue (Review in Andley 2007). However, due to their expression in multiple tissues and their effectiveness in possible protection in post-mitotic cells, their role has become more appealing with regards to the sensory retina and the RPE.

The αA-crystallin gene is found on chromosome 21, and encodes for a 173 amino acid protein, and has found to be expressed in the spleen, thymus, brain, and retina (Kato *et al.*, 1991; Bhat *et al.*, 1991; Horwitz 1992; Srinivasan *et al.*, 1992; Deretic *et al.*, 1994). The αB-crystallin gene is found on chromosome 11 and encodes for a 175 amino acid protein. Expression of αB-crystallin is universal in stressed biological systems and abundant in cells with minimal mitotic capacity (Groenen PTJA, *et al.*, 1994; Alge *et al.*, 2002). Ocular expression of α-B has also been found in rat retinal pigmented epithelium (RPE) (Nishikawa *et al.*, 1994), ciliary body and iris (Iwaki *et al.*, 1990) and retina (Iwaki *et al.*, 1990; Xi *et al.*, 2003a).

Although both αA- and αB-crystallin share similar amino acid sequences and structures, they vary in their tissue specificity and phosphorylation sites, appear to

protect different proteins, and are active under different conditions (Voorter *et al.*, 1986, Kantorow and Piatigorsky 1998, Andley *et al.*, 2000, Mao *et al.*, 2004, Rao *et al.*, 2008).

Of particular interest of these α-crystallins are their expressions in the sensory retina and RPE with an ability to provide possible protective mechanisms under stressed conditions. Xi *et al.* (2003a) localized expression of αA and αB-crystallins to distinct retinal layers in the mouse retina. αA was distributed in the ganglion cell layer nuclei, and the inner and outer photoreceptor nuclear layers, but was undetectable in the photoreceptor inner and outer segments. αB was detected in the same retinal layers as αA, but was additionally found in the inner segments of the photoreceptors (Xi *et al.*, 2003a).

Previous retinal analysis of the α-crystallins found low levels of α-crystallin have been detected in frog retinal photoreceptors (in post-Golgi membranes) suggesting a role in rhodopsin trafficking and renewal of the outer segments of the photoreceptors (Deretic *et al.*, 1994). In addition, crystallins were identified as components of retinal drusen in patients with age-related macular degeneration (AMD) (Crabb *et al.*, 2002) and it was later suggested that the accumulation of crystallins was a stress response and may be involved in trapping damaged proteins and preventing their aggregation in the presence of AMD (Nakata *et al.*, 2005). α-crystallins role in the retina appears to parallels their structural and functional role in the lens (Andley *et al.*, 1996; Bova *et al.*, 1997; Sun *et al.*, 1997; Horwitz *et al.*, 1998; Muchowski and Clark 1998; Derham

et al., 2001). Furthermore both αA- and αB-crystallin were shown to prevent apoptosis through the inhibition of caspases (Kamradt *et al.*, 2001; Alge *et al.*, 2002).

Increased expression of crystallins in light damaged photoreceptors and the decreased expression of αA-crystallin in the retinal dystrophic rat suggest a possible role for crystallins in protecting the photoreceptors from light damage (Crabb *et al.*, 2002; Sakaguchi *et al.*, 2003). A recent study done by Rao *et al* (2008) revealed that αA-crystallin protected photoreceptors in experimentally induced uveitis and was upregulated in the diabetic retina of rats (Wang *et al.*, 2007). These findings warrant further investigation into the role α-crystallins, in particular αA-crystallin, plays in the protection of photoreceptors against continuous blue light damage.

As previously show in **Chapter 5**, pigmented mice (containing αA-crystallin), demonstrated less morphological and functional damage compared to the albino mice (**Chapter 4**), however this chapter will demonstrate the effect continuous blue light damage has on a pigmented strain of mice lacking αA-crystallin. The information presented will provide a better understanding into the role of α-crystallins in low intensity, continuous light photochemical damage to the murine retina.

6.2 Chapter Aims

As stated above, Chapter 6 will investigate photochemical damage elicited from continuous blue light exposure in pigmented mice lacking αA-crystallin in comparison to pigmented mice that do express αA-crystallin (**Chapter 5**). In order to accomplish this, the following aims will be addressed:

6.2a.) Analysis of any retinal morphological changes associated with sub-threshold, continuous blue light exposure in pigmented mouse strain lacking αA-crystallin

6.2b.) Assessment of visual function before exposure, immediately after and 10 days post-exposure

6.2c.) Changes in retinal protein expression of the α-crystallins, and NF-κB at immediate exposure and a 10day recovery period

6.3 Experimental Design

The experimental set-up and design for this chapter is identical similar to the description in **Chapter 4**, with the exception of an additional control mouse. For the αA-crystallin knock-out mice, two control mice were used for each trial, one wild-type and one knock-out. Exposures occurred 1 – 7 days, with analysis occurring immediately after the designated exposure and after a 10 day recovery period. It is important to note that during the 10 day recovery period, mice were placed back into normal lighting conditions in the animal facility with a 12hrs on/ 12hrs off cyclic pattern.

In brief, animals were a generous gift from Eric Wawrousek, PhD at the Transgenics and Genome Manipulation Division of the National Eye Institute (NIH, Bethesda, MD). Animals were maintained in the Comparative Medical Center at Salus University (please refer to **Section 2.12 in Chapter 2** for animal colony maintenance and refer to **Appendix 1** for IACUC approved animal protocols). Animals (6-10wks) were exposed to continuous blue light up to 7 days. After exposure, morphological and functional analysis was performed immediately and 10 days after their designated exposure time, through histology and electroretinography, respectively. Three trials were performed for the αA-crystallin knock-out mice exposures.

Detailed descriptions of the experimental blue light apparatus (see **Section 2.3.4),** blue light experimental design (see **Section 2.3.5**), ERG testing (see **Section 2.4**), histology (see **Section 2.6**) and protein analysis (see **Section 2.5**) can be found in **Chapter 2**.

6.4 Chapter Results

6.4.1 Daily Humidity and Temperature Readings of αA-crystallin Knock-Out Mice Exposed to Continuous Blue Light

During all trials of blue light exposure, parameters were monitored on a daily basis, twice a day. These parameters included maximum, minimum, and average temperature/humidity, and lux readings of the blue light apparatus done at day 1, 4 and 7 of the experiment. All temperature/humidity readings were taken with (Big Digit Hygro-Thermometer, Extech Instruments, USA).

Figures **6.4.1 and 6.4.2** illustrates the average values and standard error of the mean for temperature and humidity of all three trials. When referring to the overall average readings of both the temperature and humidity, at no point does the maximum limit of temperature or humidity result. As previously stated in **Chapter 4,** the NIH Guide for the Care and Use of Laboratory Animals, a maximum temperature of 80°F is considered dangerous to the animal and the range of humidity percentage must fall between 30 – 70%. There is more variation with the humidity readings versus the temperature readings. This may be due to the time of year which the trials were run. The first trial of the αA-crystallin knock-out mice was done at the end of August 2007 and trial two and three were done in November of 2007 and December of 2007 respectively. The measured humidity values in August of 2007 were nearly double of those measured in November and December of 2007 which can be attributable to the time of year the experiment was being done.

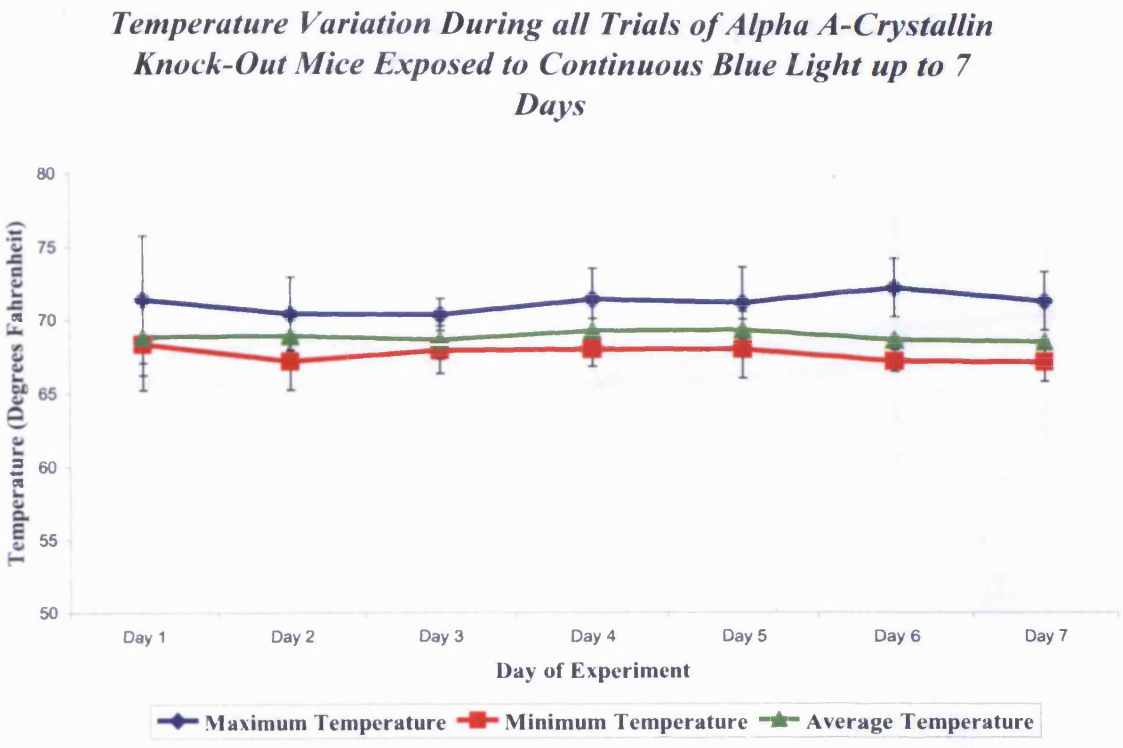

Figure 6.4.1: Shown above is the maximum, minimum and average temperature readings taken during all three trials of pigmented αA-crystallin knock-out mice exposed to blue light up to 7 days. The x-axis corresponds to the day of the experiment and the y-axis refers to the temperature in degrees Fahrenheit. Individual readings at maximum, minimum and average were taken twice a day (every 12hrs) and recorded to assure that the overall temperature of the apparatus does not exceed 80°F, which could cause extreme distress to the animals being exposed. Vertical bars indicate the standard error.

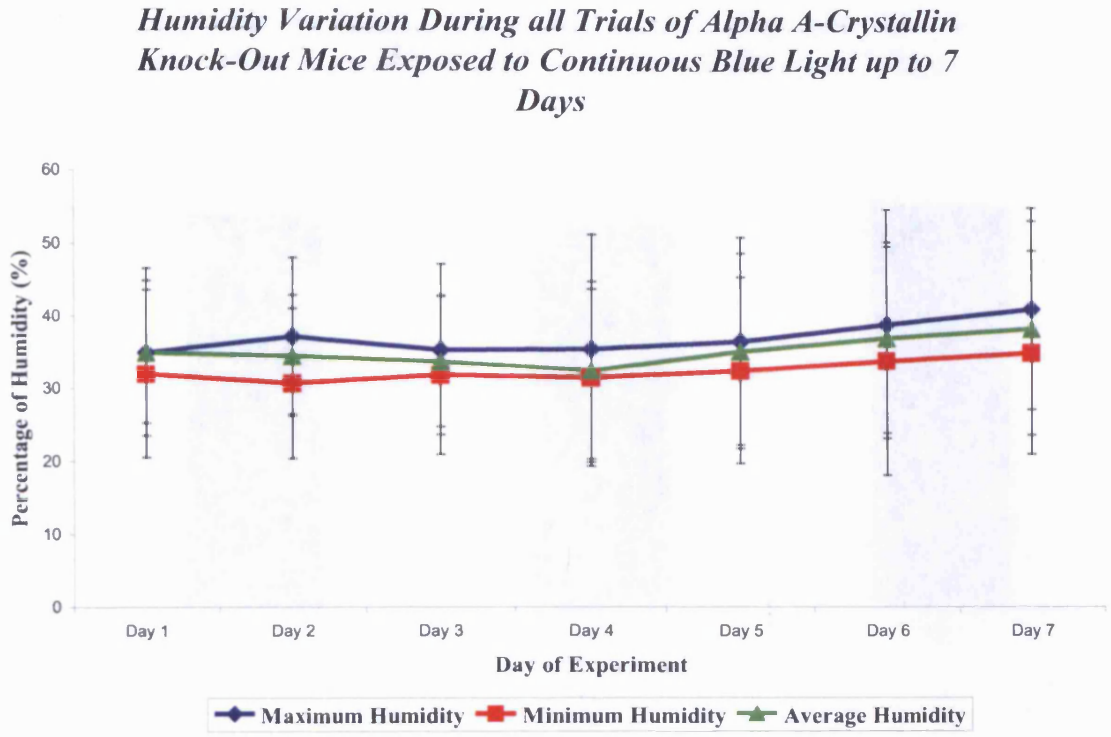

Figure 6.4.2: Shown above is the maximum, minimum and average humidity readings taken during all three trials of pigmented αA-crystallin knock-out mice exposed to blue light up to 7 days. The x-axis corresponds to the day of the experiment and the y-axis refers to the temperature in degrees Fahrenheit. Individual readings at maximum, minimum and average were taken twice a day (every 12hrs). Vertical bars indicate the standard error.

6.4.2 Experimental Lux Readings

The monitoring of lux of the blue light apparatus was also a routine experimental parameter. Lux were measured at specified points (at the very start of the experiment (Day 1), in the middle of the experiment (Day 4) and at the end of the experiment (Day 7)) to assure that the amount of illuminance was constant throughout the experiment. As revealed in **Figure 6.4.3** there was very little, if any, deviation from the average illuminance of approximately 620 lux, indicating constant illuminance throughout the seven days of experimental exposure. Readings were taken with the Traceable NIST Calibrator (Fisher Scientific, USA) apparatus located at the level of mice being exposed.

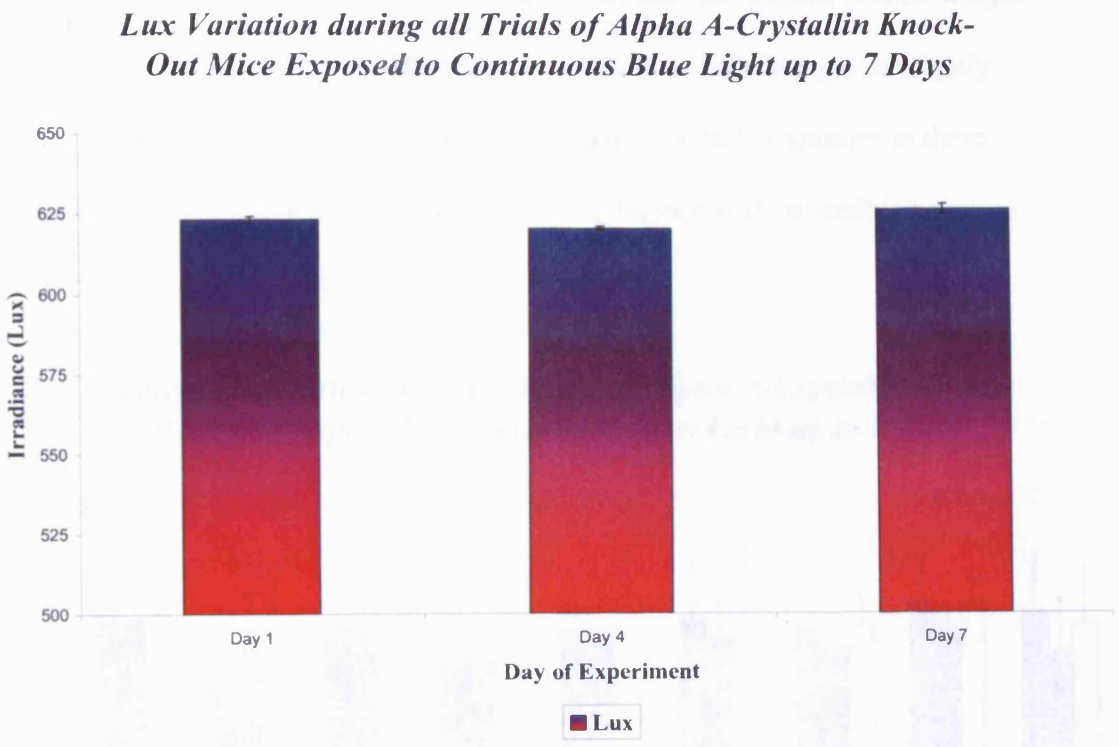

Figure 6.4.3: Shown above are the average lux measurements of the experimental blue light apparatus at Day 1, 4 and 7 of the experiment for all three trials of αA-crystallin knock-out mice. The x-axis corresponds to the day of the experiment and the y-axis refers to the illuminance lux. Vertical bars indicate the standard error.

6.4.3 Behavioral Patterns of Exposed and Non-Exposed αA-crystallin Knock-Out Mice

As stated in **Chapter 3,** based on my approved animal protocol, animals were required to be checked every 12hrs to assure that there was no pain or distress while being exposed to the continuous blue light. During all three trials, there was no indication of any pain or distress noted in the exposed αA K/O mice.

Additionally, there was a moderate effect on the weights of the mice being exposed. As shown in **Figure 6.4.4,** there was very little change in weight from pre exposure to immediately after exposure in control and day 1 animals. However, mice exposed to blue light for 2-7 days appeared to have a decrease in their weight from pre-exposure

to immediately after exposure. All mice demonstrated an increase in their weight during the 10 day recovery period, returning to their original weight or slightly greater. These findings indicates that, on average, blue light exposure in these unsedated, freely moving knock-out mice produced minimal, reversible negative effects on their dietary status.

Weight Variation During all Trials of Alpha A-Crystallin Knock-Out Mice Exposed to Continuous Blue Light up to 7 Days

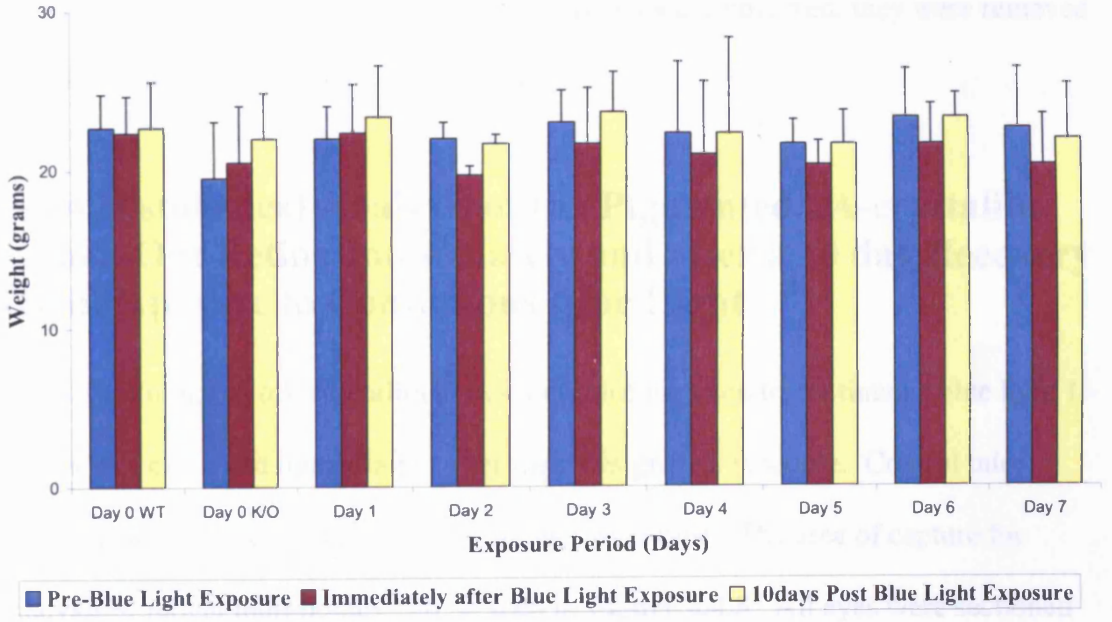

***Figure 6.4.4**: Shown above are the average weight measurements of all three trials of αA-crystallin knock-out mice exposed to blue light up to 7 days. Day 0 refers to the WT or K/O control (no-blue light exposed mice). Weights were taken before blue light exposure, immediately after blue light exposure or at the 10 day recovery period from blue light exposure. The x-axis corresponds to the number of days the mice were exposed and the y-axis refers to the weight of the mice. Vertical bars indicate the standard error.*

Similar behaviors found with wild-type mice (see **Chapter 5, Section 5.4.3**) were also noted with the knock-out mice. Examples of these behaviors include periodic seclusion in cage corners and huddling with other cage mates. As stated previously, to combat these problems, every 12 hrs mice were rotated to the right; therefore exposed mice closest to the fan would only be there for twelve hrs versus 24 or more.

Additionally, since a total of six cages could fit in the apparatus, mice were kept in single cages for as long as possible and then paired up as necessary to fit all mice for each trial.

However, another behavior was noted with the exposed knock-out mice; cage climbing. During observation, mice would occasionally climb the sides of the cage and try to hide between the side of the cage and the food holder. Therefore, mice were checked on every 6hrs and if these behaviors were observed, they were removed and placed back into the bottom of the cage.

6.4.4 Histological Analysis of the Pigmented αA-crystallin Knock-Out Retina Immediately and after a 10 day Recovery from Exposure to Continuous Blue Light

Retinal histology of αA-crystallin knock-out mice exposed to continuous blue light 1 - 7 days was examined immediately after their designated exposure. Control mice included both an αA-crystallin knock-out and wild-type. The area of capture for analysis of retinal morphology can be seen in **Figure 4.4.5**. All eyes were sectioned at the level of the optic nerve and photodocumentation was performed 0.10 – 0.25mm from either side of the optic disc. Most of the damage noted occurred in this region; equatorial and peripheral retina remained unaffected.

In order to analyze any photochemical damage which may have occurred during exposure, histological sections of mouse retina were analyzed to determine any cellular loss.

Three trials of pigmented αA-crystallin knock-out mice examined the effects of continuous blue light exposure immediately after the designated exposure period. **Figures 6.4.5 and 6.4.6** contain representative whole sections of retina as well as a magnified view of the outer and inner segments of the photoreceptors, respectively.

When referring to **Figure 6.4.5**, **Day 0 (WT and αA-crystallin K/O no blue light controls)** and **Days 1 – 7** of continuous blue light exposure contain normal rows of photoreceptor nuclei (8-10 rows) with a tight, uniform structure to the inner and outer photoreceptor segments. Additionally, there does not appear to be any compromise of overall retinal thickness or significant cellular loss in the retinal nuclear layers.

Immediate analysis of retinal morphology of αA-crystallin knock-out mice appears to share similar histological characteristics as the wild-type mice (see **Chapter 5, Figure 5.4.7**). In both strains there does not appear to be any cellular loss of the retinal nuclear layers or disorganization of the photoreceptor segments.

Upon closer examination of the RPE, photoreceptor segments and outer nuclear layer (see **Figure 6.4.6**), **Day 0 (WT and αA-crystallin K/O no blue light controls)** and **Days 1 -7** exhibit tight, uniform outer photoreceptor segment structure with clear delineation of outer to inner portions of the photoreceptors. The overlying RPE layer appears intact with no presence of any surrounding macrophages in the subretinal space. Additionally, there does not appear to be any significant loss of nuclei or melanin loss in the RPE.

When comparing **Figure 6.4.6** with wild-type outer retinal analysis (**Figure 5.4.8**), there also appears to similar findings. Although there is vesiculation of the photoreceptor outer segments with **wild-type Day 7**, αA-crystallin knock-out mice did not exhibit these outer segment changes.

Therefore immediate histological analysis of whole retinal sections and detailed analysis of the outer retina reveal that there appears to be no significant photochemical damage occurring **Days 1 - 7** of exposure. These findings correlate with immediate analysis of the wild-type mice exposed to continuous blue light for 1-7 days.

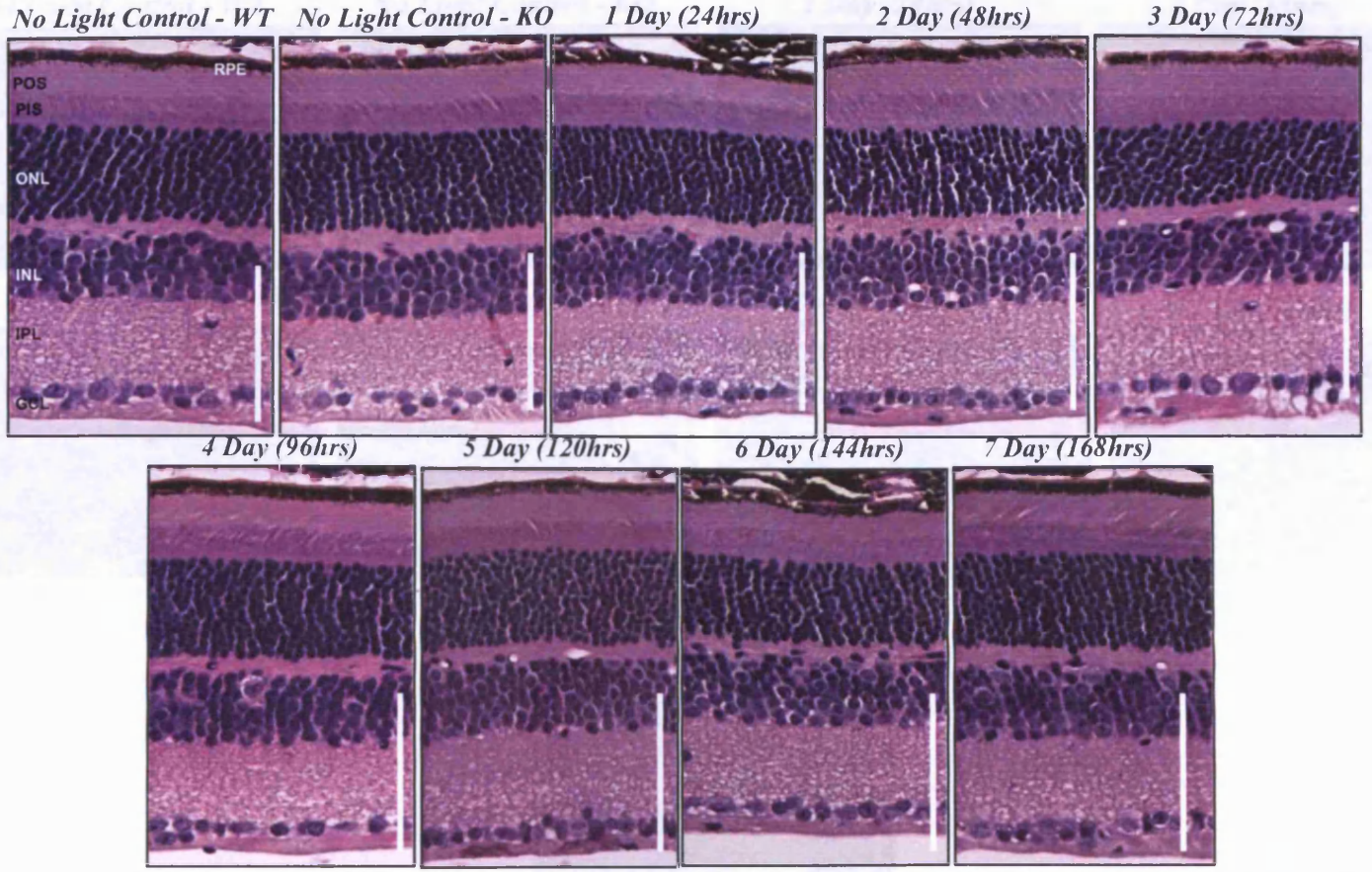

Figure 6.4.5 Immediate whole retinal histological analysis of pigmented alpha a-crystallin knock-out mice exposed to continuous blue light for 1 - 7 days. All photos correspond to whole retina photodocumented 0.10 – 0.25 mm from either side of the optic disc (magnification of 20x; scale bar = 100μm). These sections are representative of all three trials of exposed mice. Experiment was repeated a minimum of four times. RPE = Retinal pigment epithelium, POS = Photoreceptor outer segments, PIS = Photoreceptor inner segments, ONL = Outer nuclear layer, INL = Inner nuclear layer, IPL = Inner plexiform layer, GCL= Ganglion cell layer.

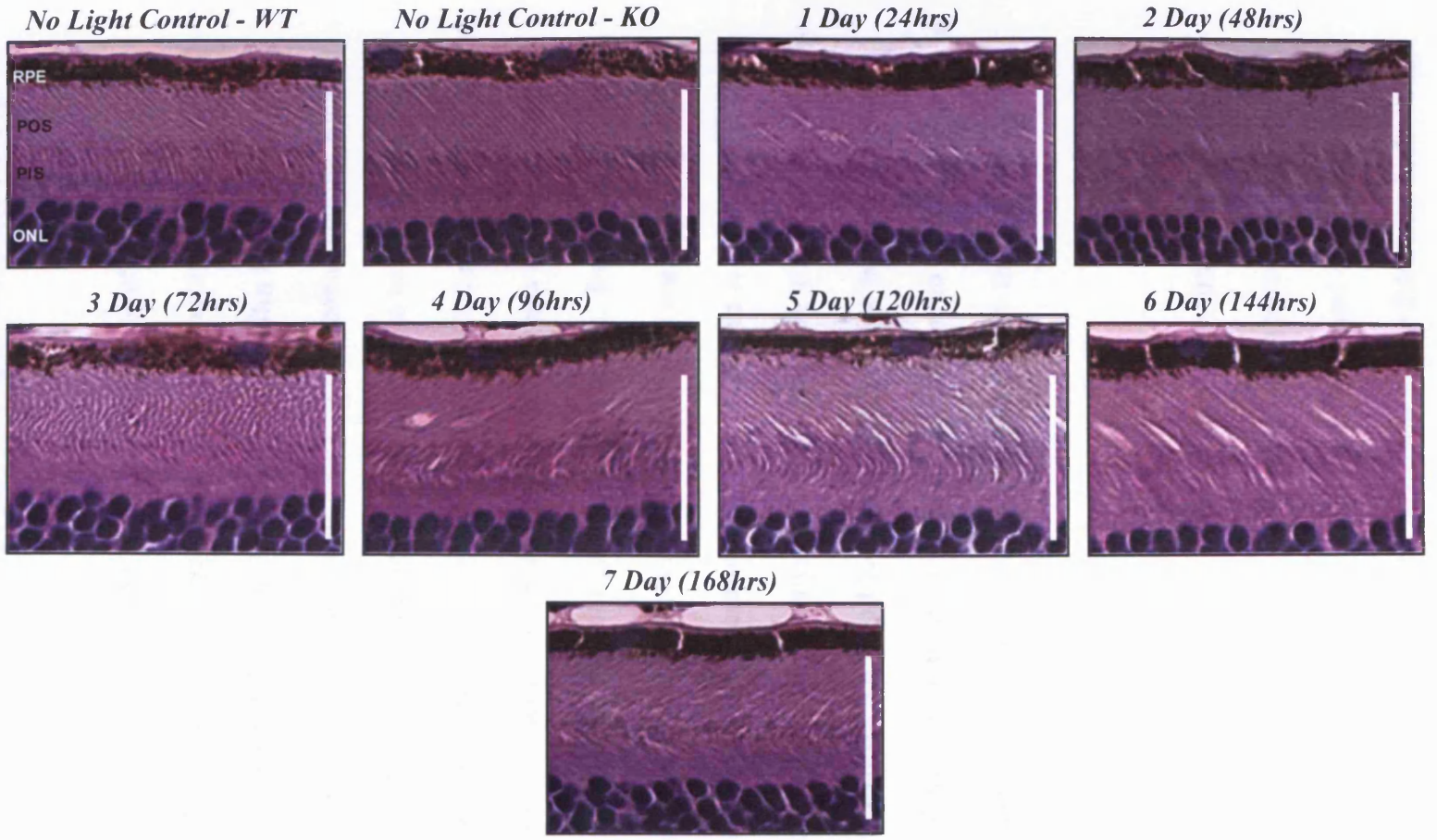

***Figure 6.4.6** Representative, higher magnification (40x) view of the RPE, inner and outer segments of the photoreceptors (POS/PIS) and outer nuclear layer (ONL) of pigmented alpha a-crystallin knock-out mice immediately after exposure to continuous blue light for 1-7 days. Scale bar = 50μm.*

Additionally, retinal histology of αA-crystallin knock-out mice exposed to continuous blue light 1 - 7 days was examined 10 days post the original designated damage.

Figures 6.4.7 and 6.4.8 contain representative whole sections of retina as well as a magnified view of the outer and inner segments of the photoreceptors, respectively. When referring to **Figure 6.4.7, Day 0 (WT and αA-crystallin K/O no blue light controls)** and **Days 1 – 7** of continuous blue light exposure contain normal rows of photoreceptor nuclei (8-10 rows) and there does not appear to be any compromise of overall retinal thickness or significant cellular loss in the retinal nuclear layers. Tight, uniform structure to the inner and outer photoreceptor segments is present in both controls, but **Days 1-7** do not exhibit tight, uniform structure. During all days of exposure, there appears to be spacing between photoreceptor segments with corresponding vesiculation (closer examination of outer retina is seen in **Figure 6.4.8**). These findings differ from analysis of wild-type retina after a 10 day recovery period (**Chapter 5, Figures 5.4.9 and 5.4.10**). Although there is not an apparent significant cellular loss of the retinal layers, there does appear to be disorganization in the outer retina of the αA-crystallin knock-out mice at an early time than in the wild-type.

Figures 6.4.9 and 6.4.10 illustrate the differences in overall retinal thickness or individual layer thickness (outer nuclear, inner nuclear, or photoreceptor layers) immediately and after a 10 day recovery period from designated blue light exposure respectively. Although there appears to be no notable visible difference in the retinal layer thicknesses immediately after exposure, morphometrical analysis revealed a

significant difference in the outer nuclear layer thickness throughout all exposure periods (**Figure 6.4.9**) compared to the control mouse. **Seven days** of exposure also lead to a significant decrease in photoreceptor segment thickness immediately after being exposed to continuous blue light.

Morphometrical analysis after a 10 day recovery from exposure reveals significant decreases in overall retinal thickness, and outer and inner nuclear layers. Changes are more statistically significant with increased exposure times. These findings of decreased thickness in the outer and inner nuclear layers were not found with wild-type mice. As stated previously, Xi *et al.,* 2003a localized distribution of murine αA-crystallin in the outer and inner nuclear layers, as well as the ganglion cell layer. Due to these animals lacking the αA-crystallin protein, perhaps these layers are more susceptible to apoptosis under photochemical conditions, even at moderate levels.

Figures 6.4.10 and 6.4.11 compared retinal layer thicknesses between wild-type and αA-crystallin knock-out mice immediately and after a 10 day recovery period, respectively. There were no statistically significant changes between both strains.

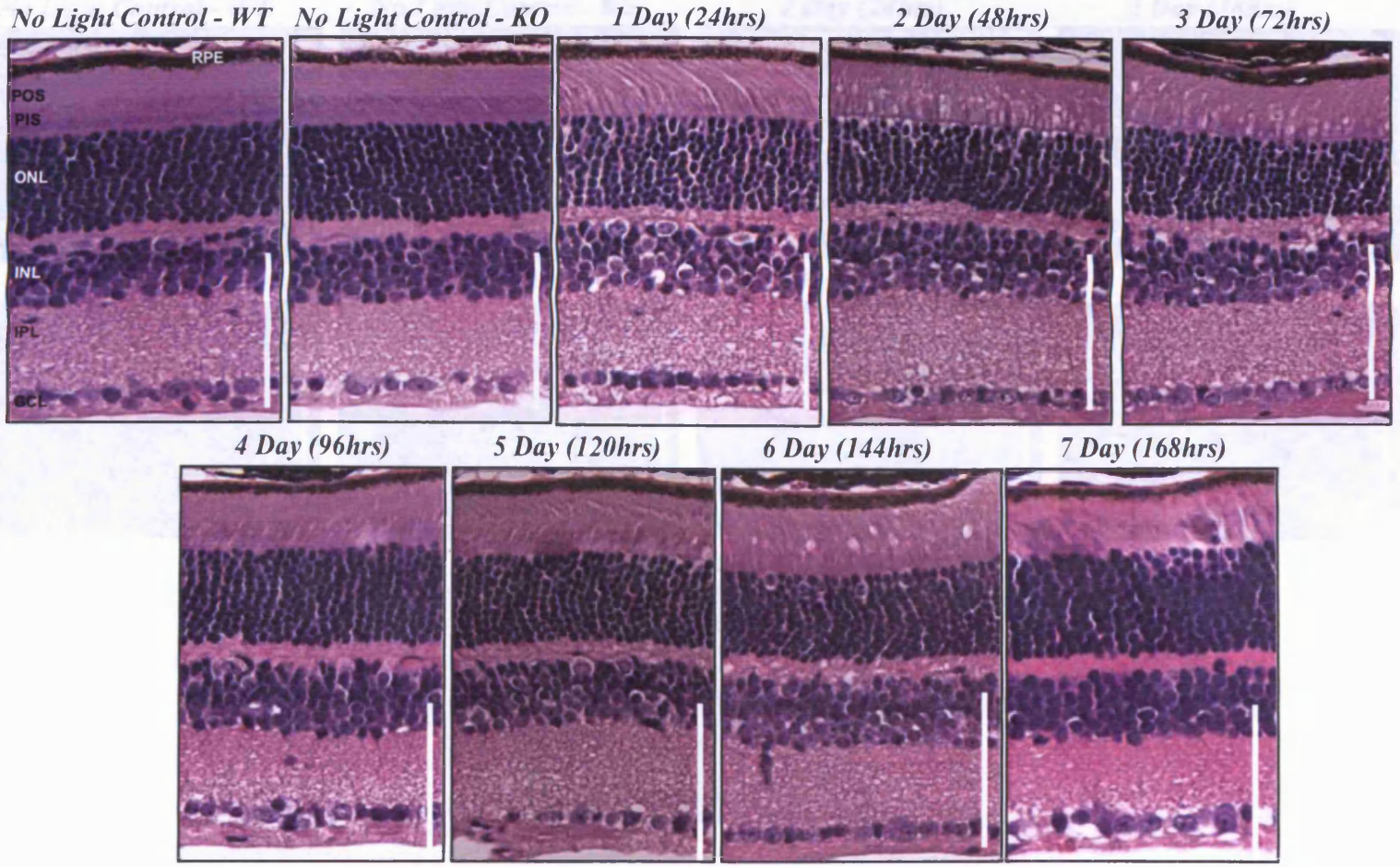

***Figure 6.4.7** Whole retinal histological analysis of pigmented alpha a-crystallin knock-out mice exposed to continuous blue light 1 - 7 days after 10 days of recovery. All photos correspond to whole retina photodocumented 0.10 – 0.25 mm from either side of the optic disc (magnification of 20x; scale bar = 100μm). These sections are representative of all three trials of exposed mice. RPE = Retinal pigment epithelium, POS = Photoreceptor outer segments, PIS = Photoreceptor inner segments, ONL = Outer nuclear layer, INL = Inner nuclear layer, IPL = Inner plexiform layer, GCL= Ganglion cell layer.*

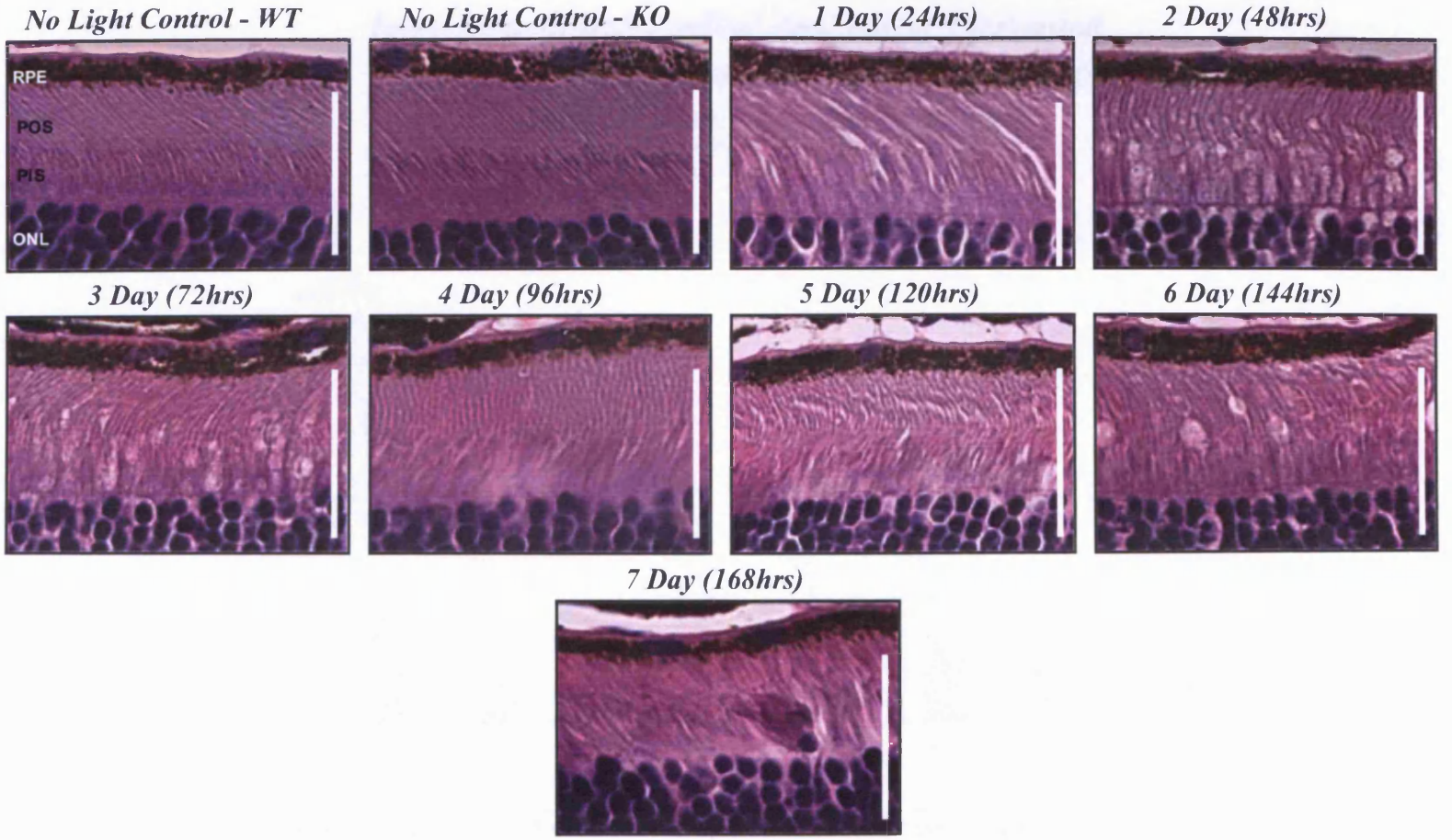

Figure 6.4.8 Representative, higher magnification (40x) view of the RPE, inner and outer segments of the photoreceptors (POS/PIS) and outer nuclear layer (ONL) of pigmented alpha a-crystallin mice exposed to continuous blue light for 1-7 days after 10 days of recovery. Scale bar = 50μm.

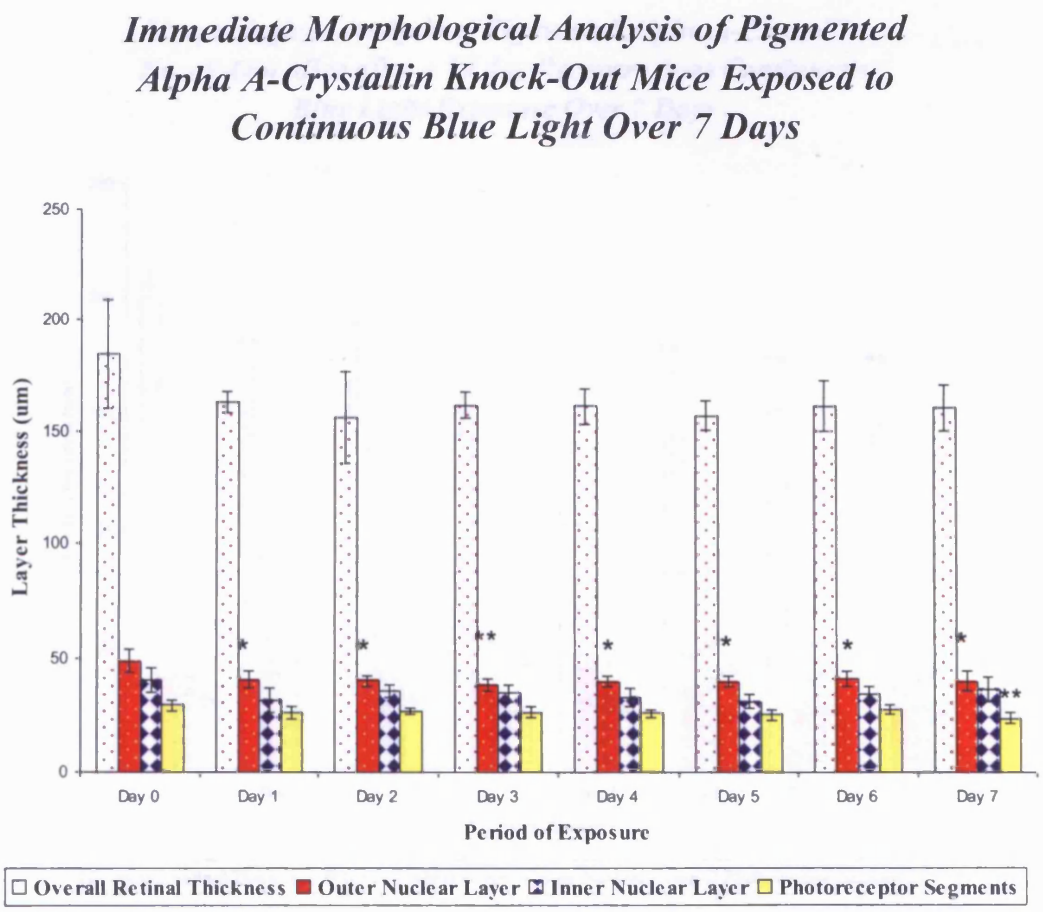

Figure 6.4.9 Graphical morphometric analysis of overall retinal thickness, outer nuclear thickness, inner nuclear thickness and photoreceptor segment thickness in αA-crystallin Knock-Out mice immediately after designated blue light exposure. For each animal during each trial, there was a minimum of 4 sections taken (four trials were performed). Three to four measurements were made per field, which were averaged to provide a single value for each retina. Data are expressed as mean ±S.D and statistical significance was assessed with a one-way ANOVA followed by Dunnett's multiple comparison test. A $p<0.05$ was considered statistically significant, n=3. ($p< 0.05$ and **$p < 0.01$).*

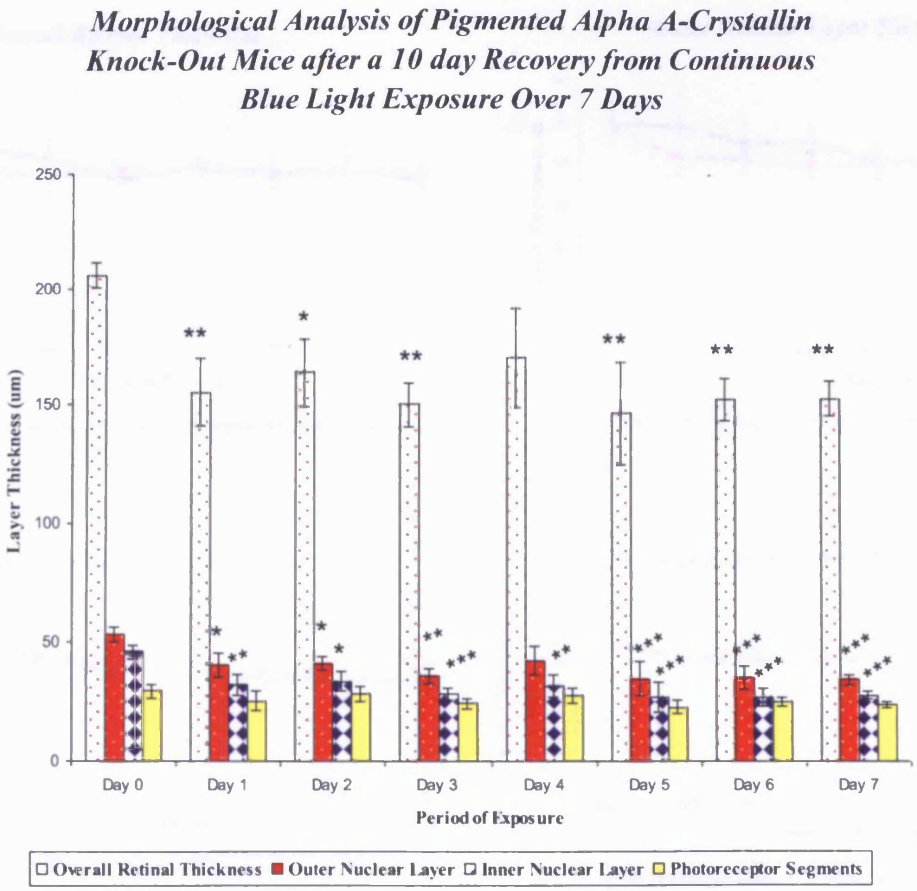

Figure 6.4.10 Graphical morphometric analysis of overall retinal thickness, outer nuclear thickness, inner nuclear thickness and photoreceptor segment thickness in αA-crystallin Knock-Out mice 10 days after designated blue light exposure. For each animal during each trial, there was a minimum of 4 sections taken (four trials were performed). Three to four measurements were made per field, which were averaged to provide a single value for each retina. Data are expressed as mean ±S.D and statistical significance was assessed with a one-way ANOVA followed by Dunnett's multiple comparison test. A $p<0.05$ was considered statistically significant. ($p < 0.05$, **$p < 0.01$, ***$p<0.001$ compared to control retina, n=3).*

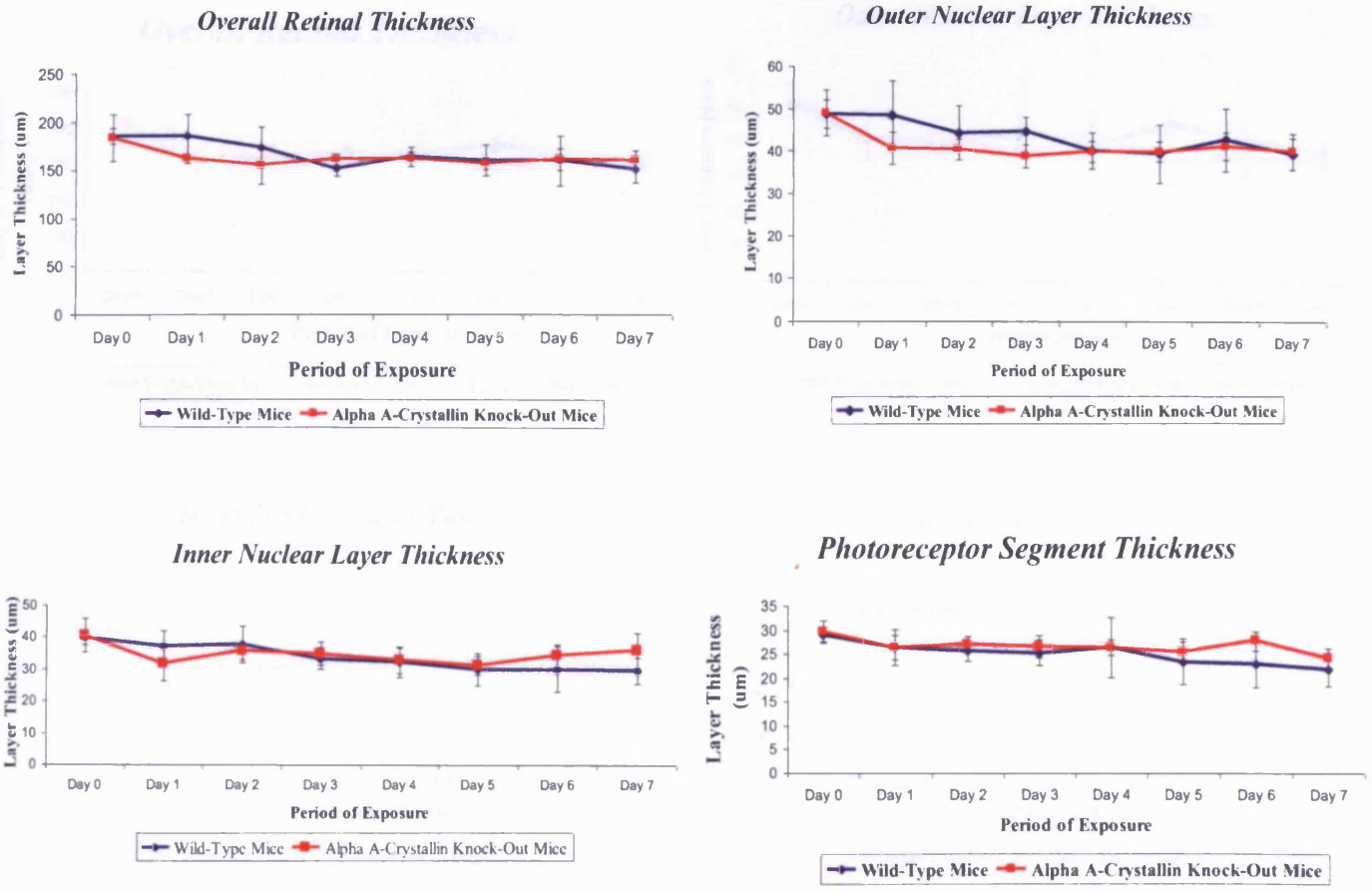

Figure 6.4.11 *Comparison of Morphometric Values of Layer Thickness of Wild-Type Mice and αA-crystallin Knock-out Mice Immediately after Continuous Blue Light Exposure over 7 Days. Values shown represent the mean ± S.D and statistical significance was assessed with a one-way ANOVA followed by Tukey's multiple comparison test. A $p<0.05$ was considered statistically significant, n=3.*

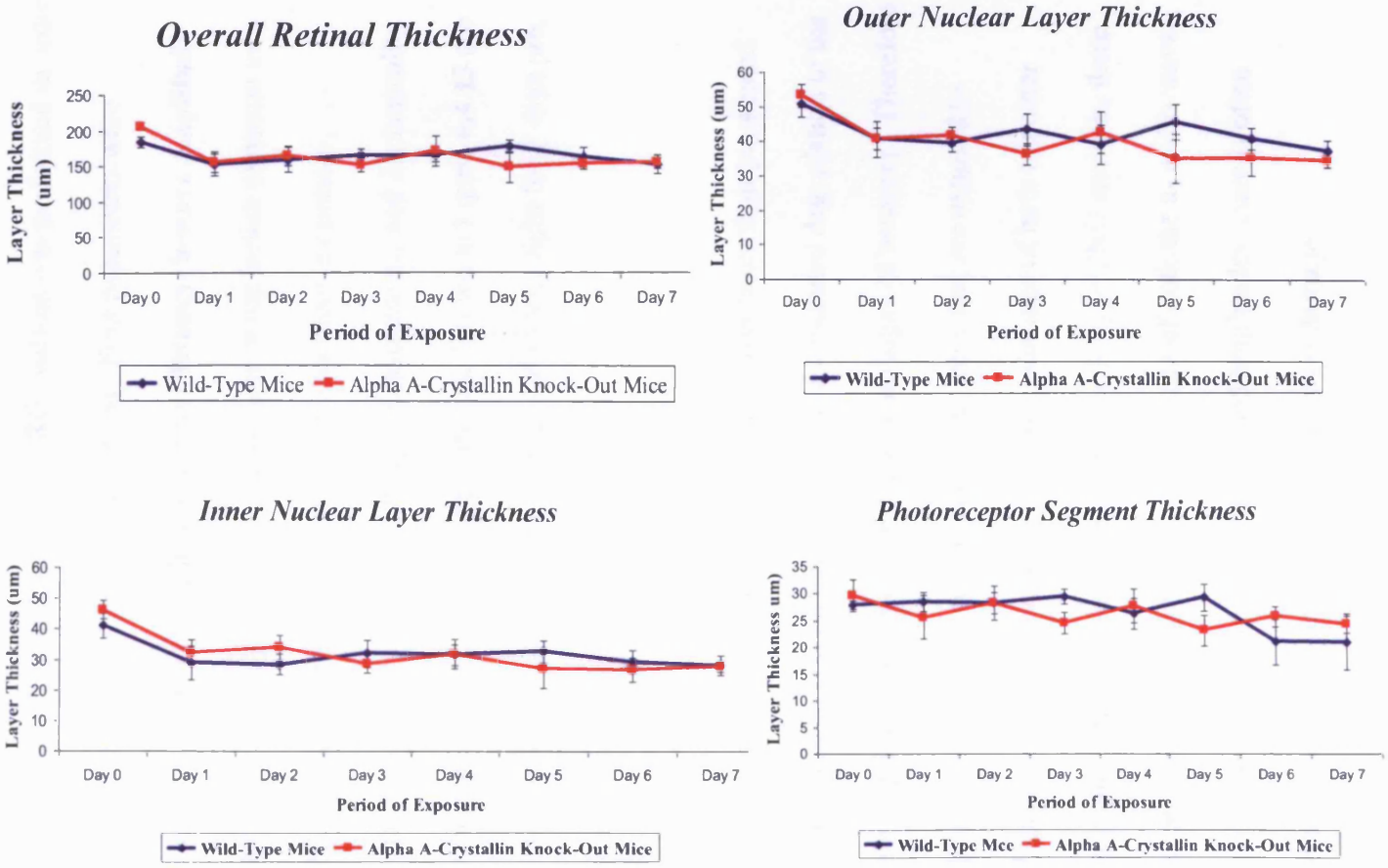

<u>Figure 6.4.12</u> Comparison of Morphometric Values of Layer Thickness of Wild-Type Mice and αA-crystallin Knock-out Mice after a 10 day Recovery Period of Continuous Blue Light Exposure over 7 Days. Values shown represent the mean ± S.D and statistical significance was assessed with a one-way ANOVA followed by Tukey's multiple comparison test. A $p<0.05$ was considered statistically significant, n=3.

6.4.5 Electroretinography of Pigmented αA-crystallin Knock-Out mice Immediately and after a 10 day Recovery Period from Designated Blue Light Exposure

In addition to evaluation of the retinal structure, ERG analysis was performed in order to assess visual function of both outer and inner retina. Four parameters were analyzed in ERG analysis; **a-wave amplitude, a-wave latency, b-wave amplitude and b-wave latency.** Mice were examined at three time point: before exposure to blue light, immediately after exposure, and after a 10 day recovery period. (Reproducibility statistics of both right and left eye measurements and the normality of ERG outcome measures can be seen in **Appendix 2).** Shown in Figure **6.4.13** are examples of representative ERGs from a mouse exposed to blue light for 7 days pre, immediately after, and after a 10 day recovery period.

Figure **6.4.14** illustrates the ERG parameter trajectories over time of all pigmented αA- crystallin knock-out mice and on average there is a continued degradation of the a-wave and b-wave amplitudes in exposed mice with no signs of recovery. Therefore on average, it appears as though pigmented knock-out mice that are exposed to continuous blue light, do exhibit irreversible functional damage of both the outer retina (a-wave) and inner retina (b-wave). Similar to wild-type ERG analysis, there does not appear to be a notable difference in the latencies of both the a- and b-waves, which was an unexpected finding since with decreased amplitudes, there is often corresponding increased latencies, suggesting retinal layer damage.

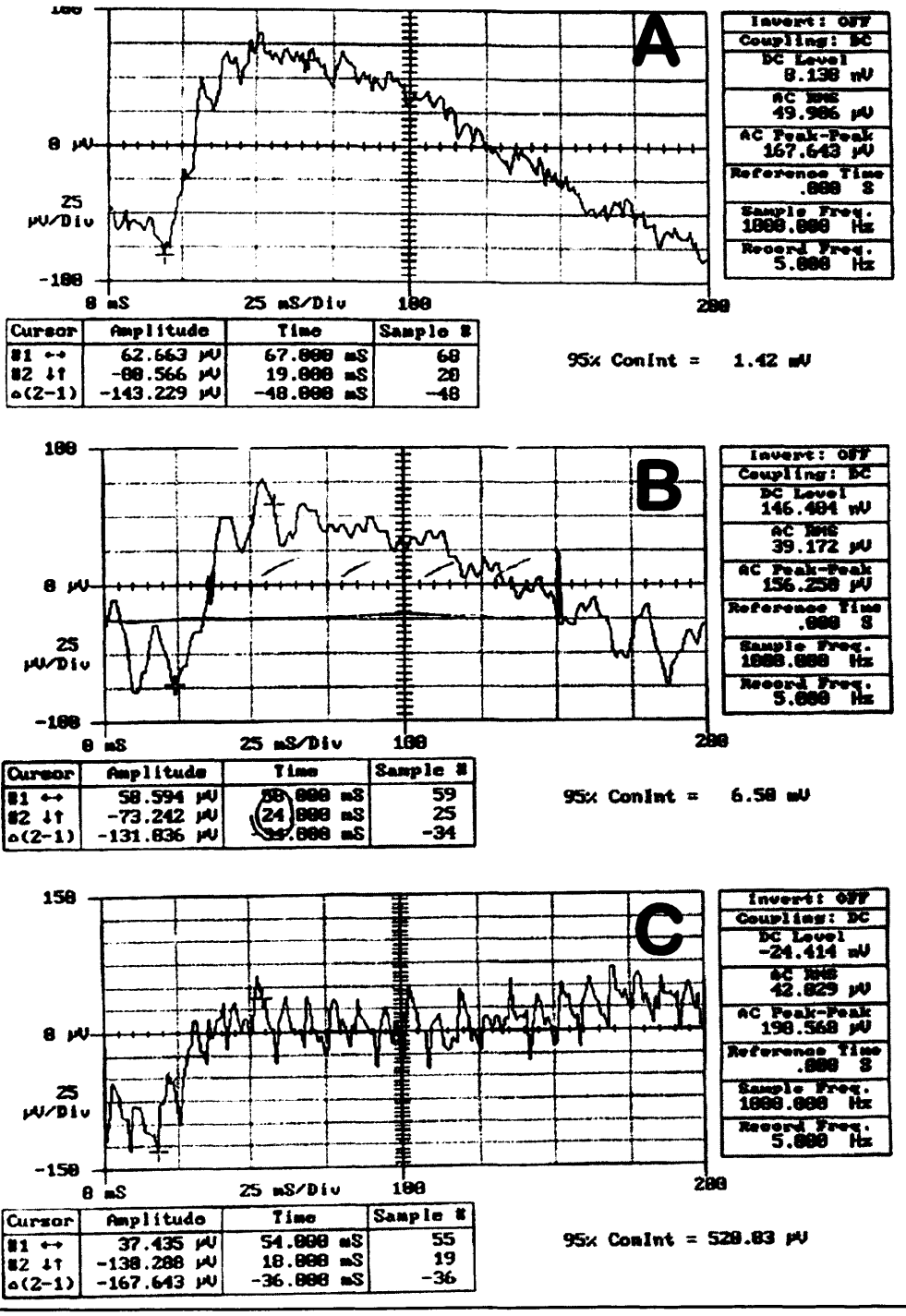

Figure 6.4.13 Representative ERGs from a mouse exposed to continuous blue light for 7 days. Shown in 'A' is a pre-ERG, 'B' is an immediate ERG, and 'C' is an ERG after a 10 day recovery period.

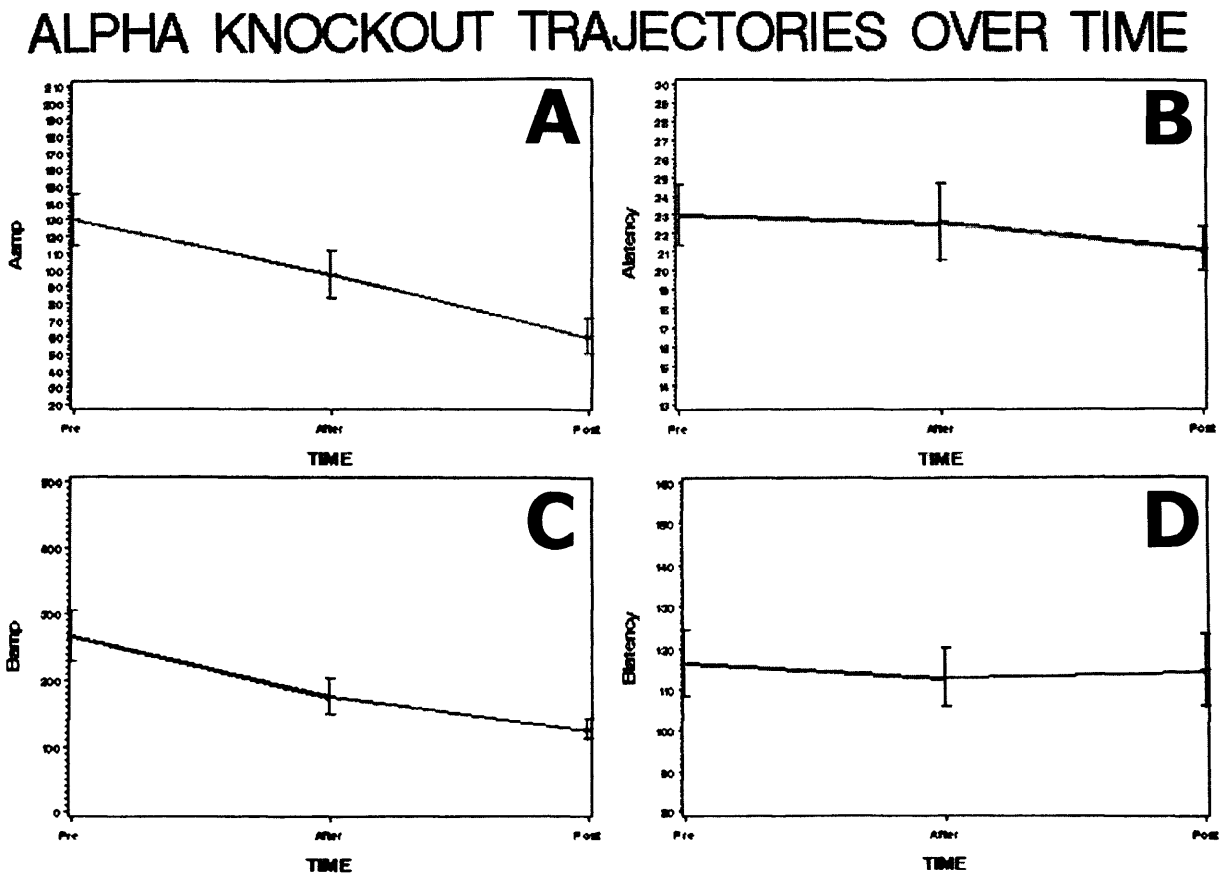

Figure 6.4.14 Overall pigmented αA-crystallin knock-out mice ERG trajectories pre-exposure, immediately after exposure and after a 10 day recovery period. As shown above, on-average, for both the a-wave amplitude ('A') and b-wave amplitude ('C'), there is no recovery post exposure; in fact, continued degradation from the exposure to 10 days later is shown. For the a-wave ('B') and b-wave ('D') latencies, it appears on-average, there is minimal change over the three assessment periods. Data at measurement period represent the mean ± S.D. Data points represent ERG parameters from all knock-out mice without considering the time of exposure. (Please refer to Appendix for raw statistical values).

Since, on average, both wild-type and αA-crystallin knock-out mice showed no signs of functional recovery after a 10 day period, both strains were compared to determine whether one degenerated faster or at a greater degree than the other. Since changes were noted in the a- and b-wave amplitudes, **Figure 6.4.15** compares the average visual function pre, immediately and after a 10 day recovery period to continuous blue light exposure in wild-type versus αA-crystallin knock-out. Both the a- and b-wave amplitudes degenerate faster and to a greater degree in the αA-crystallin knock-out mice, compared to the wild-type. Additionally, we took these comparisons a step further and used a special type of mixed-effects model: a linear piece-wise mixed-effects model that modeled separate rates of change from pre- to immediate and immediate through post. This enabled us to examine each change between time points for each type (wild-type or knock-out). Shown in **Tables 6.1 and 6.2** are estimates of the change per period for each type, as well as pairwise comparisons.

When referring to **Figure 6.4.15 and Tables 6.1 and 6.2,** the a-wave amplitude (corresponding to outer retinal function) in **wild-type mice** degenerates more significantly ($p < 0.0001$) in the time period from pre-exposure to immediately after exposure than the αA-crystallin knock-out mice. Although knock-out mice showed significant change from pre-exposure to immediately after, this was not as significant as the wild-type. No significant differences between both types of mice were noted in pre to immediately after their designated exposure period.

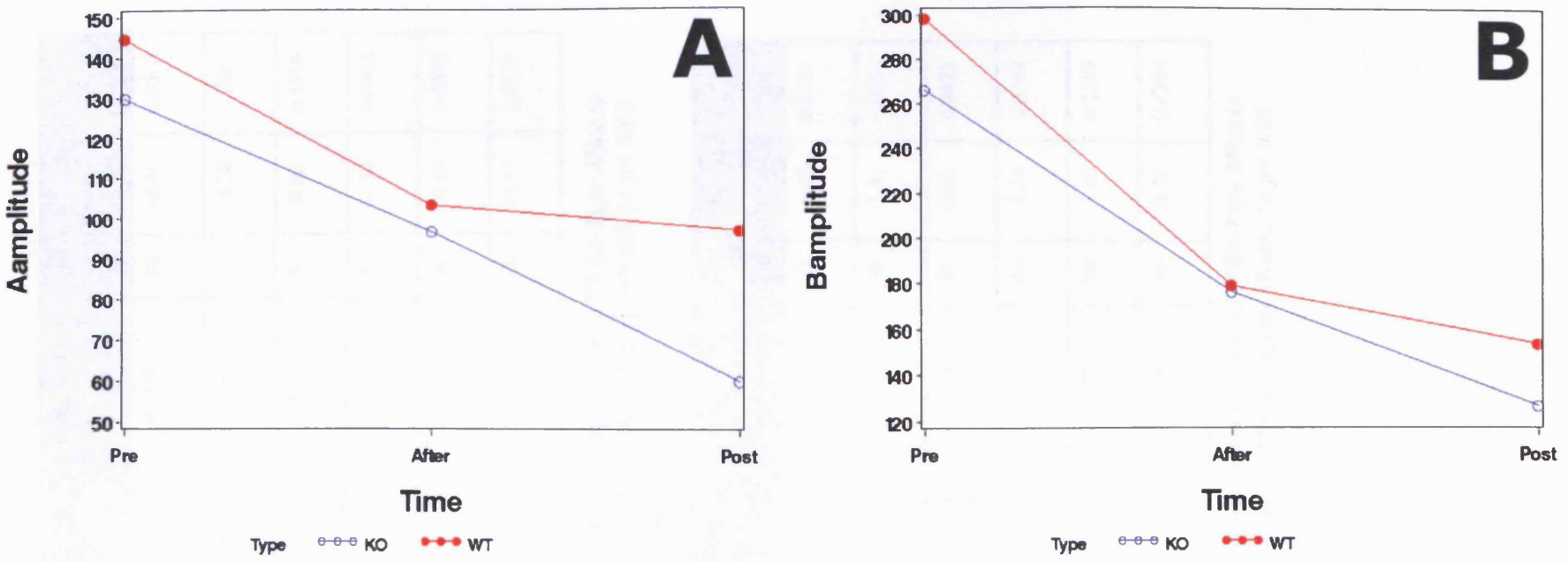

Figure 6.4.15 ***Comparison between wild-type and αA-crystallin knock-out mice pre, immediate, and after a 10 day recovery period to continuous blue light exposure over 1 – 7 days. As shown above, on-average, for both the a-wave amplitude ('A') and b-wave amplitude ('B'), visual function of the knock-out mice degenerate faster and to a greater extent than their wild-type counterparts. Data at measurement period represent the mean ± S.D. (Please refer to Appendix 2 for raw statistical values and Tables 6.1 and 6.2 for comparison values).***

Change Estimates and Pairwise Comparisons for the a-wave Amplitude					
Pair comparisons	Estimate	Standard Error	DF	t value	Pr > |t|
KO - change Pre to Exposure	-33.3333	9.7702	80	-3.41	0.0010
WT - change Pre to Exposure	-41.5952	9.7702	80	-4.26	<.0001
KO vs WT Pre to Exposure	8.2619	13.8171	80	0.60	0.5516
KO - change Exposure to Post	-36.5238	9.7702	80	-3.74	0.0003
WT - change Exposure to Post	-6.5000	9.7702	80	-0.67	0.5078
KO vs WT Exposure to Post	-30.0238	13.8171	80	-2.17	0.0327

***Table 6.1** a-wave Amplitude Pairwise Comparisons of Wild-Type Mice to αA-crystallin Knock-Out Mice Using a Mixed Effects Model. (A p< 0.05 was considered statistically significant)*

Change Estimates and Pairwise Comparisons for the b-wave Amplitude					
Pair comparisons	Estimate	Standard Error	DF	t value	Pr > |t|
KO - change Pre to Exposure	-89.5238	21.9931	80	-4.07	0.0001
WT - change Pre to Exposure	-118.93	21.9931	80	-5.41	<.0001
KO vs WT Pre to Exposure	29.4048	31.1029	80	0.95	0.3473
KO - change Exposure to Post	-49.7619	21.9931	80	-2.26	0.0264
WT - change Exposure to Post	-25.3810	21.9931	80	-1.15	0.2519
KO vs WT Exposure to Post	-24.3810	31.1029	80	-0.78	0.4354

***Table 6.2** b-wave Amplitude Pairwise Comparisons of Wild-Type Mice to αA-crystallin Knock-Out Mice Using a Mixed Effects Model. (A p< 0.05 was considered statistically significant)*

When comparisons were made in the change of a-wave amplitude from the immediate time point to after a 10 day recovery period, wild-type mice did not show significant change, but the knock-out revealed highly significant change ($p < 0.001$). Additionally, when both types of mice were compared, there was a significant change between the knock-out and wild-type during their 10 day recovery period.

b-wave amplitude comparison values can be seen in **Table 6.2**. Similar trends were noticed in the b-wave amplitude behavior compared to the a-wave. However this trend should not be surprising since photoreceptor function (a-wave amplitude) drives the downstream initiating stimulus generating the b-wave. Although there was no significant difference between the knock-out and wild-type mice from pre to immediate after exposure, there was a highly significant change in the wild-type from pre to immediately after exposure, similar to results with the a-wave. Knock-out mice also demonstrated significant change during pre to immediately after, yet not as drastic as the wild-type. Comparisons made immediately and after to their 10 day recovery period revealed that knock-out mice were significantly more effected than the wild-type mice. There was no significant change noted in wild-type mice behavior or when comparing wild-type to knock-out behavior.

Similar to previous mention in **Chapter 5**, **Figures 6.4.14 and 6.4.15** do not distinguish between individual exposure days. For a more detailed description on the changes in exposed versus unexposed knock-out mice or ERG functions of mice on specified days, please refer to **Figures 6.4.16 and 6.4.17** respectively. **Chapter 5** described that difficulty in ERG analysis due to limited controls. The situation for

knock-out mice was more difficult since a knock-out control mouse died unexpectedly in the middle of the experiment, therefore instead of three controls there were only two.

As shown in **Figure 6.4.16,** the green dashed lines represent the 95% confidence bounds for the cases (all mice exposed, n=21), with individual trajectories mapped out for each control. No light exposure controls are designated as follows: blue line (Trial #1), and red line (Trial #2). For each control mouse, a one sample t-test was performed which examined whether the mean for the exposed mice is statistically different from the observed value of each of the control mice. Test results are reported as a t-statistics, with p-value (Pr>|t|), as the level of significance, where a p-value < 0.05 corresponds to statistical significance (Degrees of freedom for the one sample t-tests are 20 for wild-type)(**please see Tables 6.3 - 6.4).**

Figure 6.4.17 illustrates the ERG measurements of the mice during their exposure period. At no point do the mice recovery to their original a- or b-wave amplitudes after being exposed to continuous blue light. A continual decline in the amplitudes is noted indicating that the longer the animal was exposed to continuous blue light, the less likely they were to recover. This pattern is similar to the pattern found in the wild-type exposed mice.

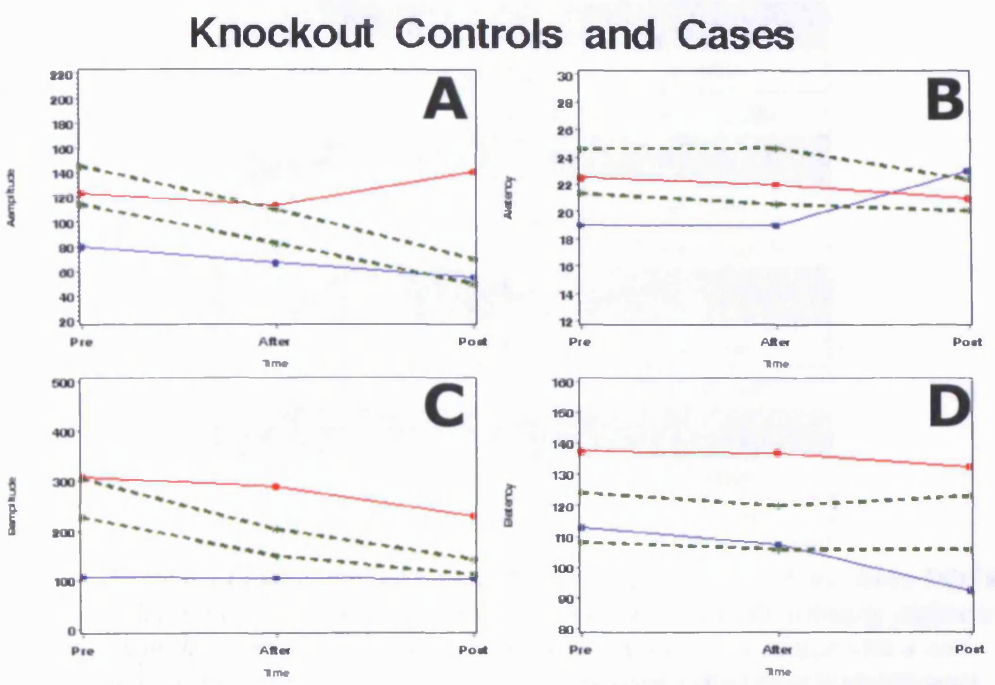

Figure 6.4.16 Comparison of control mice to exposed mice at pre-exposure, immediately after exposure and after a 10 day recovery period from blue light exposure. The blue line refers to Trial #1 control mouse and the red line refers to Trial #2 control mouse (a-wave amplitude shown in 'A', b-wave amplitude shown in 'C', a-wave latency shown in 'B" and b-wave latency shown in 'D'). Data at measurement period represent the mean ± S.D. Data points represent ERG parameters from all wild-type mice without considering the time of exposure. (Please refer to Appendix for raw statistical values and Tables 6.3 – 6.4).

a-wave Amplitude: Tests for Location: Mu0 = 133.75		
Test	**Statistic**	**p value**
Student's t	t – 5.495549	Pr > |t| < 0.0001
b-wave Amplitude: Tests for Location: Mu0 = 40		
Test	**Statistic**	**p value**
Student's t	t – 3.370403	Pr > |t| < 0.0030
a-wave Latency: Tests for Location: Mu0 = 210.25		
Test	**Statistic**	**p value**
Student's t	t – 9.203504	Pr > |t| < 0.0001
b-wave Latency: Tests for Location: Mu0 = 210.25		
Test	**Statistic**	**p value**
Student's t	t - 2.916385	Pr > |t| < 0.0085

Table 6.3 Comparison of Exposed Mice to the Control Mouse from Trial #1 (Blue Line). On all four measure, exposed mice are significantly different from the control values. Statistical significance was assessed with a one-paired student's t-test (A p< 0.05 was considered statistically significant).

a-wave Amplitude: Tests for Location: Mu0 = 245.75		
Test	**Statistic**	**p value**
Student's t	t – 5.22436	Pr > |t| < 0.0001
b-wave Amplitude: Tests for Location: Mu0 =43.75		
Test	**Statistic**	**p value**
Student's t	t – 0.696154	Pr > |t| < 0.4943
a-wave Latency: Tests for Location: Mu0 = 556		
Test	**Statistic**	**p value**
Student's t	t – 10.3859	Pr > |t| < 0.0001
b-wave Latency: Tests for Location: Mu0 = 272		
Test	**Statistic**	**p value**
Student's t	t – 7.06203	Pr > |t| < 0.0001

Table 6.4 Comparison of Exposed Mice to the Control Mouse from Trial #2 (Red Line). On all four measure, exposed mice are significantly different from the control values except for the b-wave amplitude. Statistical significance was assessed with a one-paired student's t-test (A p< 0.05 was considered statistically significant.

a-wave Amplitude of Wild-Type Pigmented Mice Not Exposed to Continuous Blue Light (Day 0)

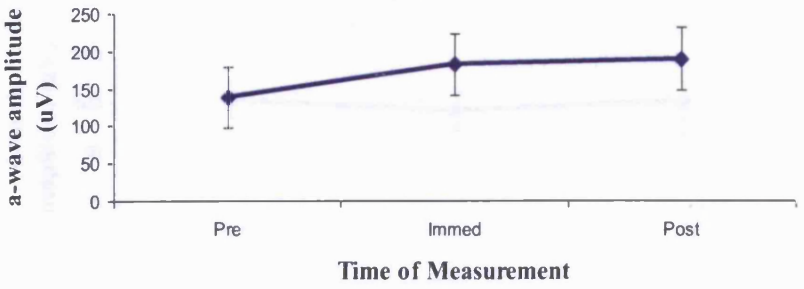

a-wave Latency of Wild-Type Pigmented Mice Not Exposed to Continuous Blue Light (Day 0)

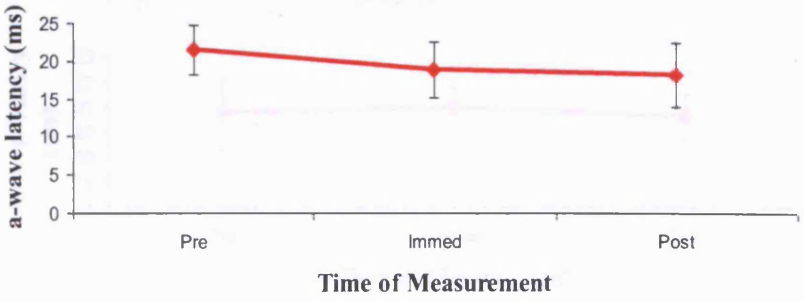

b-wave Amplitude of Wild-Type Pigmented Mice Not Exposed to Continuous Blue Light (Day 0)

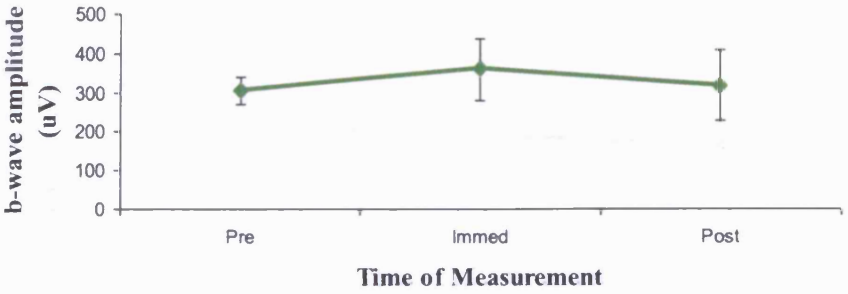

b-wave Latency of Wild-Type Pigmented Mice Not Exposed to Continuous Blue Light (Day 0)

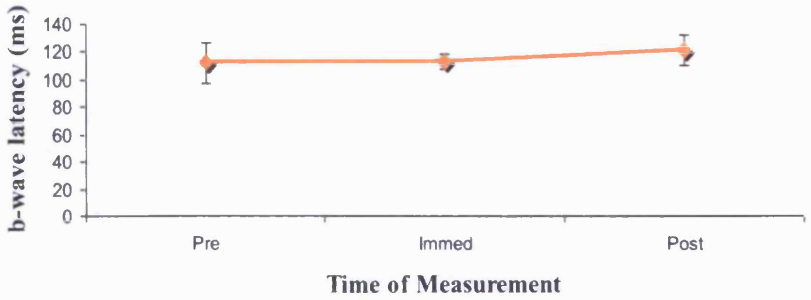

Figure 6.4.17 *continued overleaf*

a-wave Amplitude of Alpha A-crystallin Knock-Out Pigmented Mice Not Exposed to Continuous Blue Light (Day 0)

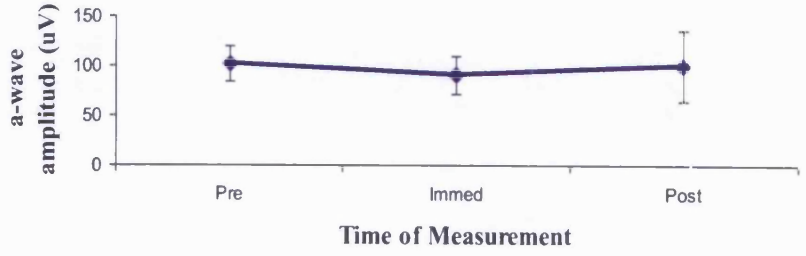

a-wave Latency of Alpha A-crystallin Knock-Out Pigmented Mice Not Exposed to Continuous Blue Light (Day 0)

b-wave Amplitude of Alpha A-crystallin Knock-Out Pigmented Mice Not Exposed to Continuous Blue Light (Day 0)

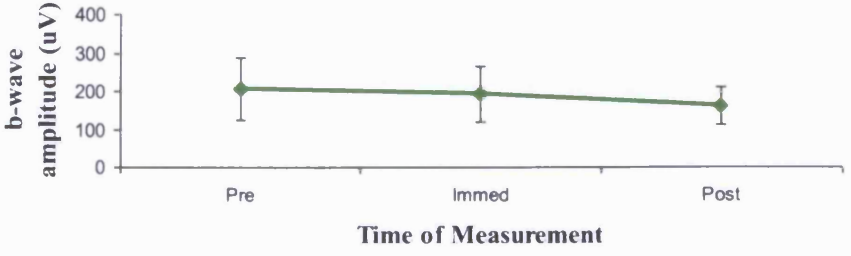

b-wave Latency of Alpha A-crystallin Knock-Out Pigmented Mice Not Exposed to Continuous Blue Light (Day 0)

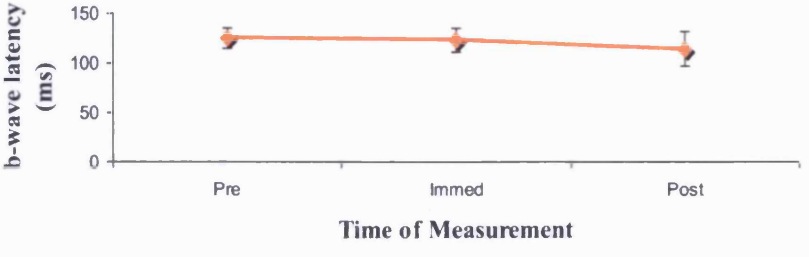

Figure 6.4.17 *continued overleaf*

a-wave Amplitude of Alpha A-crystallin Knock-Out Pigmented Mice Exposed to Continuous Blue Light for 1Day (24hrs)

a-wave Latency of Alpha A-crystallin Knock-Out Pigmented Mice Exposed to Continuous Blue Light for 1 Day (24hrs)

b-wave Amplitude of Alpha A-crystallin Knock-Out Pigmented Mice Exposed to Continuous Blue Light for 1Day (24hrs)

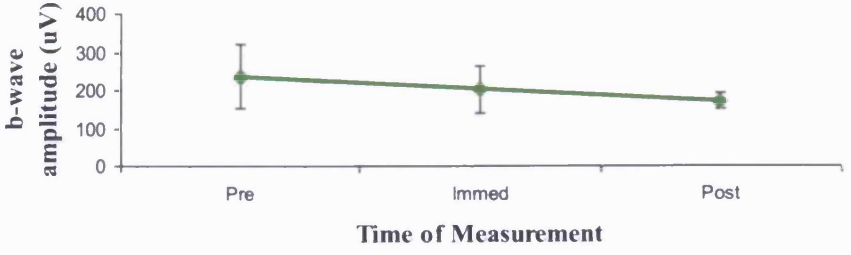

b-wave Latency of Alpha A-crystallin Knock-Out Pigmented Mice Exposed to Continuous Blue Light for 1 Day (24hrs)

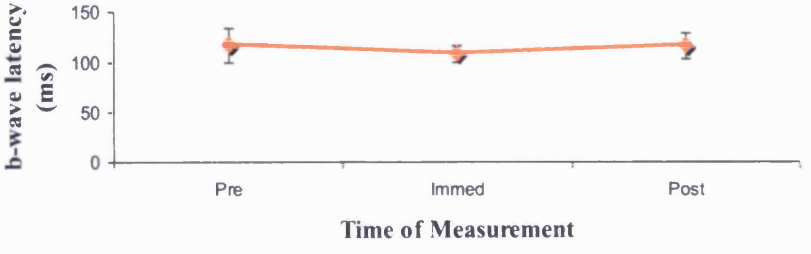

Figure 6.4.17 *continued overleaf*

a-wave Amplitude of Alpha A-crystallin Knock-Out Pigmented Mice Exposed to Continuous Blue Light for 2 Days (48hrs)

a-wave Latency of Alpha A-crystallin Knock-Out Pigmented Mice Exposed to Continuous Blue Light for 2 days (48hrs)

b-wave Amplitude of Alpha A-crystallin Knock-Out Pigmented Mice Exposed to Continuous Blue Light for 2 days (48hrs)

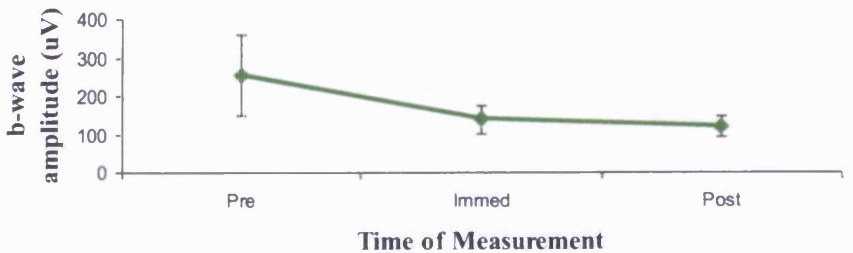

b-wave Latency of Alpha A-crystallin Knock-Out Pigmented Mice Exposed to Continuous Blue Light for 2 days (48hrs)

Figure 6.4.17 *continued overleaf*

a-wave Amplitude of Alpha A-crystallin Knock-Out Pigmented Mice Exposed to Continuous Blue Light for 3 Days (72hrs)

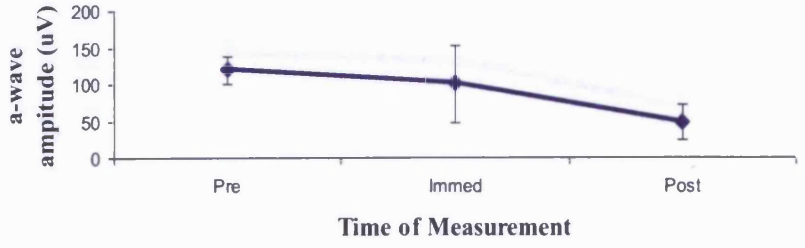

a-wave Latency of Alpha A-crystallin Knock-Out Pigmented Mice Exposed to Continuous Blue Light for 3 days (72hrs)

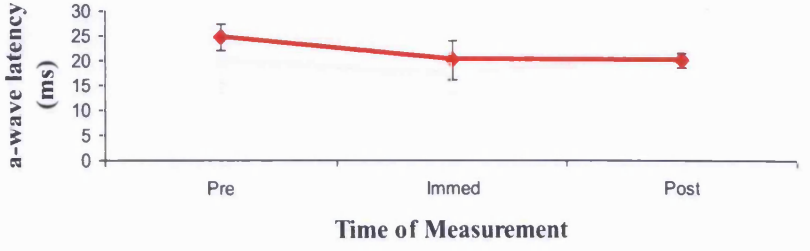

b-wave Amplitude of Alpha A-crystallin Knock-Out Pigmented Mice Exposed to Continuous Blue Light for 3 days (72hrs)

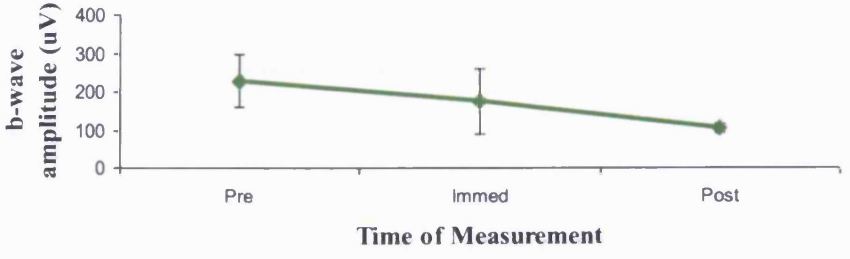

b-wave Latency of Alpha A-crystallin Knock-Out Pigmented Mice Exposed to Continuous Blue Light for 3 Days (72hrs)

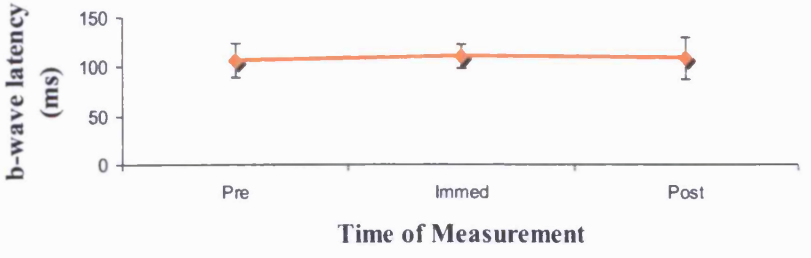

Figure 6.4.17 *continued overleaf*

a-wave Amplitude of Alpha A-crystallin Knock-Out Pigmented Mice Exposed to Continuous Blue Light for 4 Days (96hrs)

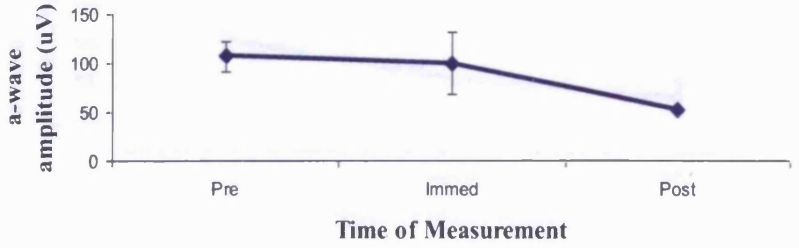

a-wave Latency of Alpha A-crystallin Knock-Out Pigmented Mice Exposed to Continuous Blue Light for 4 days (96hrs)

b-wave Amplitude of Alpha A-crystallin Knock-Out Pigmented Mice Exposed to Continuous Blue Light for 4 days (96hrs)

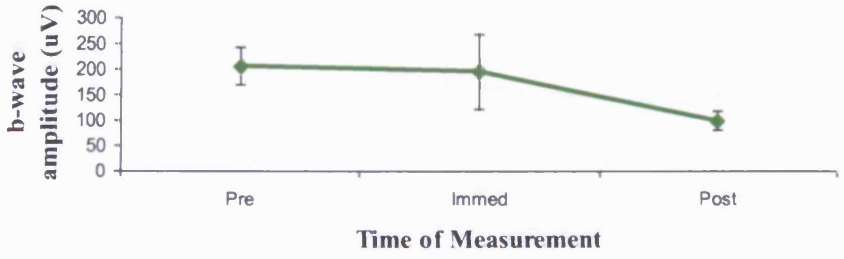

b-wave Latency of Alpha A-crystallin Knock-Out Pigmented Mice Exposed to Continuous Blue Light for 4 Days (96hrs)

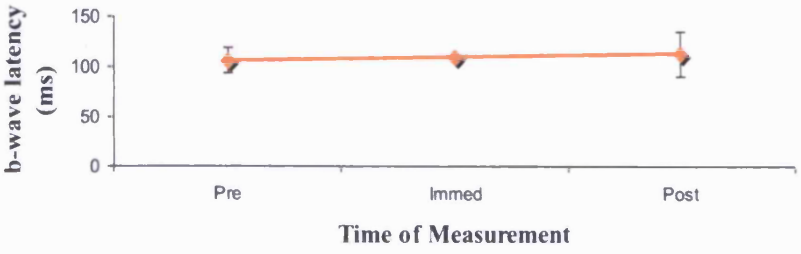

Figure 6.4.17 *continued overleaf*

a-wave Amplitude of Alpha A-crystallin Knock-Out Pigmented Mice Exposed to Continuous Blue Light for 5 days (120hrs)

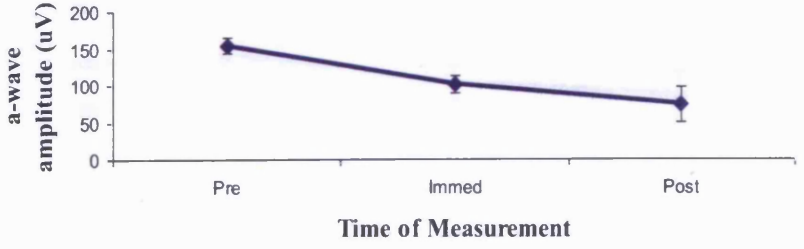

a-wave Latency of Alpha A-crystallin Knock-Out Pigmented Mice Exposed to Continuous Blue Light for 5 days (120hrs)

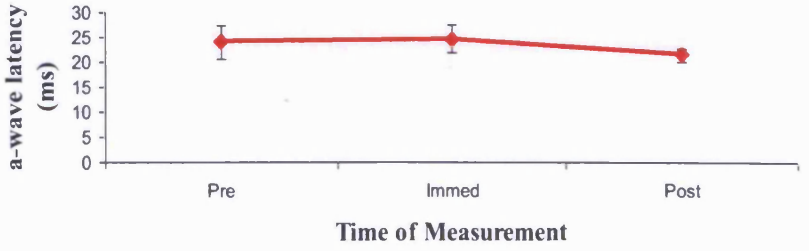

b-wave Amplitude of Alpha A-crystallin Knock-Out Pigmented Mice Exposed to Continuous Blue Light for 5 days (120hrs)

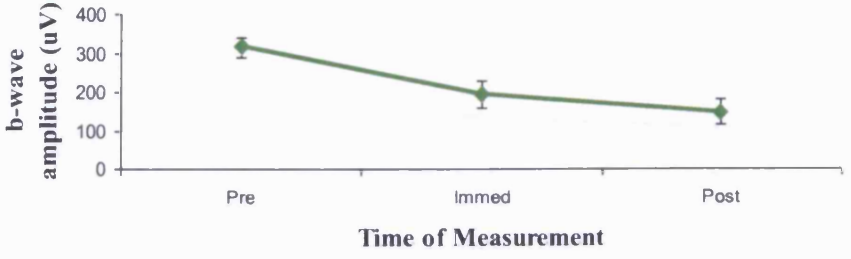

b-wave Latency of Alpha A-crystallin Knock-Out Pigmented Mice Exposed to Continuous Blue Light for 5 Days (120hrs)

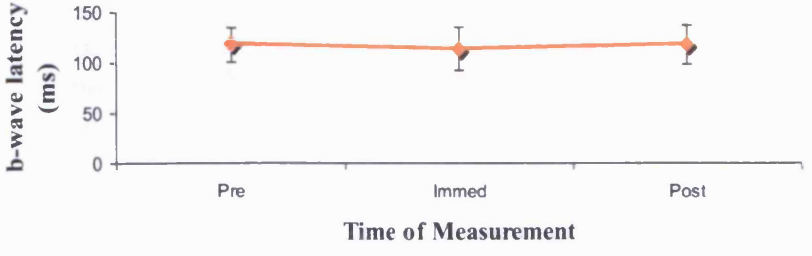

Figure 6.4.17 *continued overleaf*

a-wave Amplitude of Alpha A-crystallin Knock-Out Pigmented Mice Exposed to Continuous Blue Light for 6 days (144hrs)

a-wave Latency of Alpha A-crystallin Knock-Out Pigmented Mice Exposed to Continuous Blue Light for 6 days (144hrs)

b-wave Amplitude of Alpha A-crystallin Knock-Out Pigmented Mice Exposed to Continuous Blue Light for 6 days (144hrs)

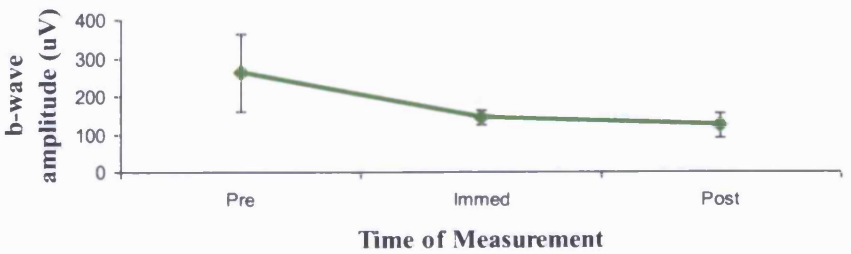

b-wave Latency of Alpha A-crystallin Knock-Out Pigmented Mice Exposed to Continuous Blue Light for 6 Days (144hrs)

Figure 6.4.17 *continued overleaf*

a-wave Amplitude of Alpha A-crystallin Knock-Out Pigmented Mice Exposed to Continuous Blue Light for 7 days (168hrs)

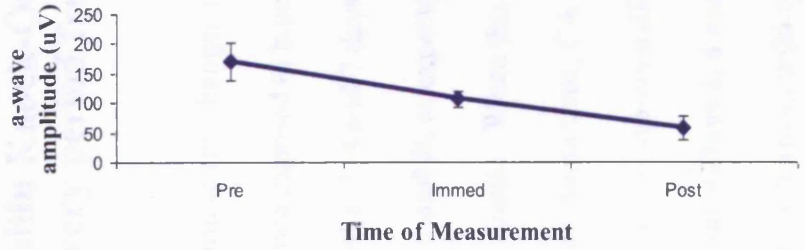

a-wave Latency of Alpha A-crystallin Knock-Out Pigmented Mice Exposed to Continuous Blue Light for 7 days (168hrs)

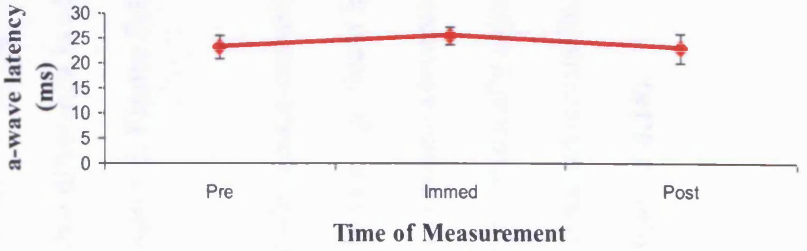

b-wave Amplitude of Alpha A-crystallin Knock-Out Pigmented Mice Exposed to Continuous Blue Light for 7 days (168hrs)

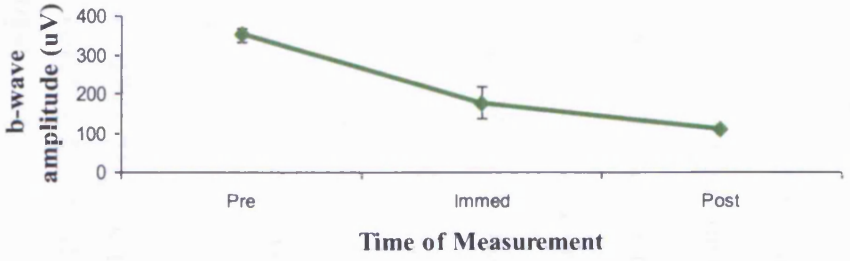

b-wave Latency of Alpha A-crystallin Knock-Out Pigmented Mice Exposed to Continuous Blue Light for 7 Days (168hrs)

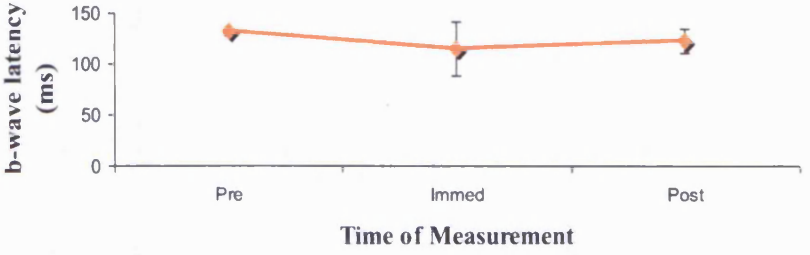

Figure 6.4.17 ERG measurements of pigmented αA-crystallin knock-out mice exposed to continuous blue light over 1-7 days. Measurements included a- and b-wave amplitudes and a- and b-wave latencies. Measurements were performed at three time points for each trial (pre-exposure to blue light, immediately after exposure to blue light and after a 10day recovery). Data at each time point represents the mean ± S.D. (3 trials were performed; each exposure day, n=3).

6.4.6 Protein Expression in αA-crystallin Knock-Out Mice Immediately and after a 10 day recovery period from continuous blue light exposure

Western Blot analysis was performed in order to examine any changes in expression of αA- and αB-crystallin and NF-κB expression in mice exposed to blue light up to 7 days (αA- and αB-crystallin expression was examined at 1, 4 and 7 days, NF-κB was examined at 1-7 days). As shown in **Figures 6.4.18A and B,** as expected αA-crystallin expression was not detected in knock-out animals. When this blot was performed, the Y79 cell lysate (Santa Cruz Antibodies, Santa Cruz, CA USA) was not available and wild-type lens was used as a positive control. αB-crystallin expression was detected however it was not statistically significant at **Days 1, 4 and 7** of continuous blue light exposure. Similar to expression patterns in wild-type mice, the expression of αB-crystallin was also highly variable between individual mice at the same time point. Although there was no significant difference in expression of αB-crystallin in the knock-out mice, there was considerable difference in αB- expression found in the wild-type versus the knock-out (**see Chapter 5, Figure 5.4.17**).

Expression of NF-κB was also examined in αA-crystallin knock-out mice exposed to blue light up to 7 days. **Figure 6.4.19A and B** illustrates a significant increase in NF-κB expression after a 10 day recovery from 7 days of exposure compared to the control. Remaining differences in expression were not statistically significant, however there was a greater upregulation of NF-κB in the αA-crystallin knock-out mice compared to wild-type mice (**see Chapter 5, Figure 5.4.18**).

A

Expression of Alpha B-Crystallin in Pigmented Alpha A-Crystallin Knock-Out Mice Exposed to Continuous Blue Light

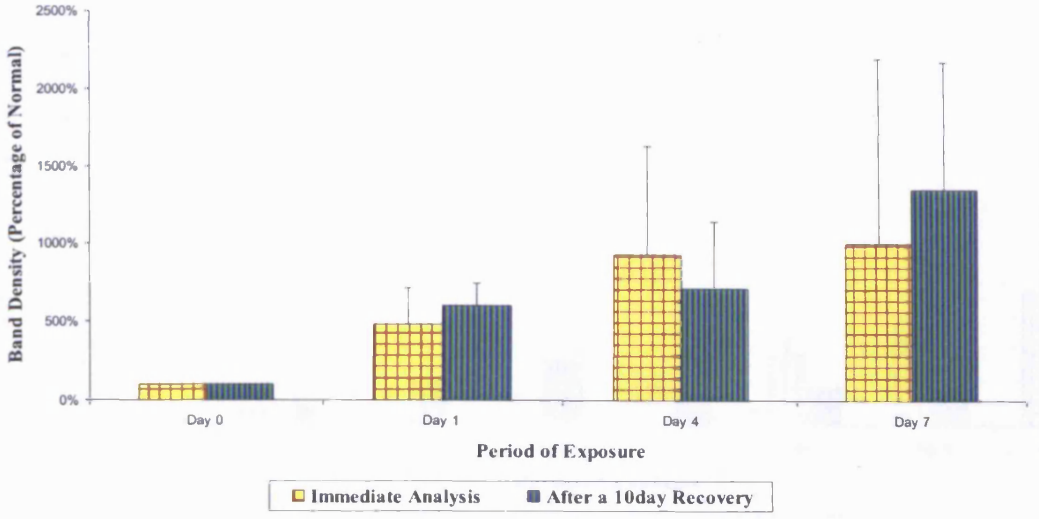

B

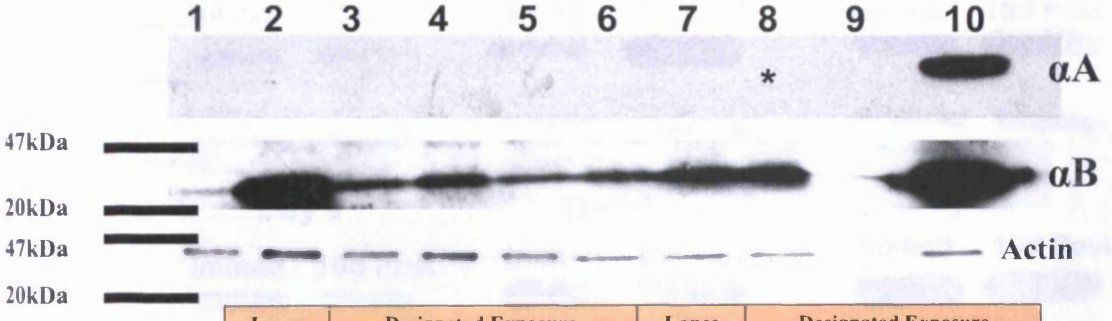

Lanes	Designated Exposure	Lanes	Designated Exposure
1	Control	6	Day 7 – Immediate
2	Day 1 - Immediate	7	Day 7 –10 days Post
3	Day 1 – 10 days Post	8	Positive Control (Y79 cell lysate)
4	Day 4 – Immediate	9	Empty
5	Day 4 – 10 days Post	10	Postive Control (WT Lens)

Figure 6.4.18A, and B *Expression of αA- and αB-crystallin in pigmented αA-crystallin knock-out mice immediately and after a 10 day recovery period from 1, 4 or 7 days of exposure. . 'A' represents a graphical description of αB-crystallin expression normalized to actin immediately and 10 days after designated exposure. 'B' illustrates representative blots of αA- and αB-crystallin, as well as actin as an internal control (The key for lane numbers are shown in the table below the blots). αA-crystallin corresponds to 20kDa, αB-crystallin corresponds to 23.5kDa and actin corresponds to 43kDa. In 'A' and 'B', data are expressed as the mean ± S.D and statistical significance was assessed by a one-way ANOVA followed by Dunnett's multiple comparison test to compare exposed mice to non-exposed or Tukey's multiple comparison test to compare between immediate versus the 10day recovery. A $p<0.05$ was considered statistically significant (n=3) (* corresponds to absence of Y79 cell lysate in αA-crystallin blot).*

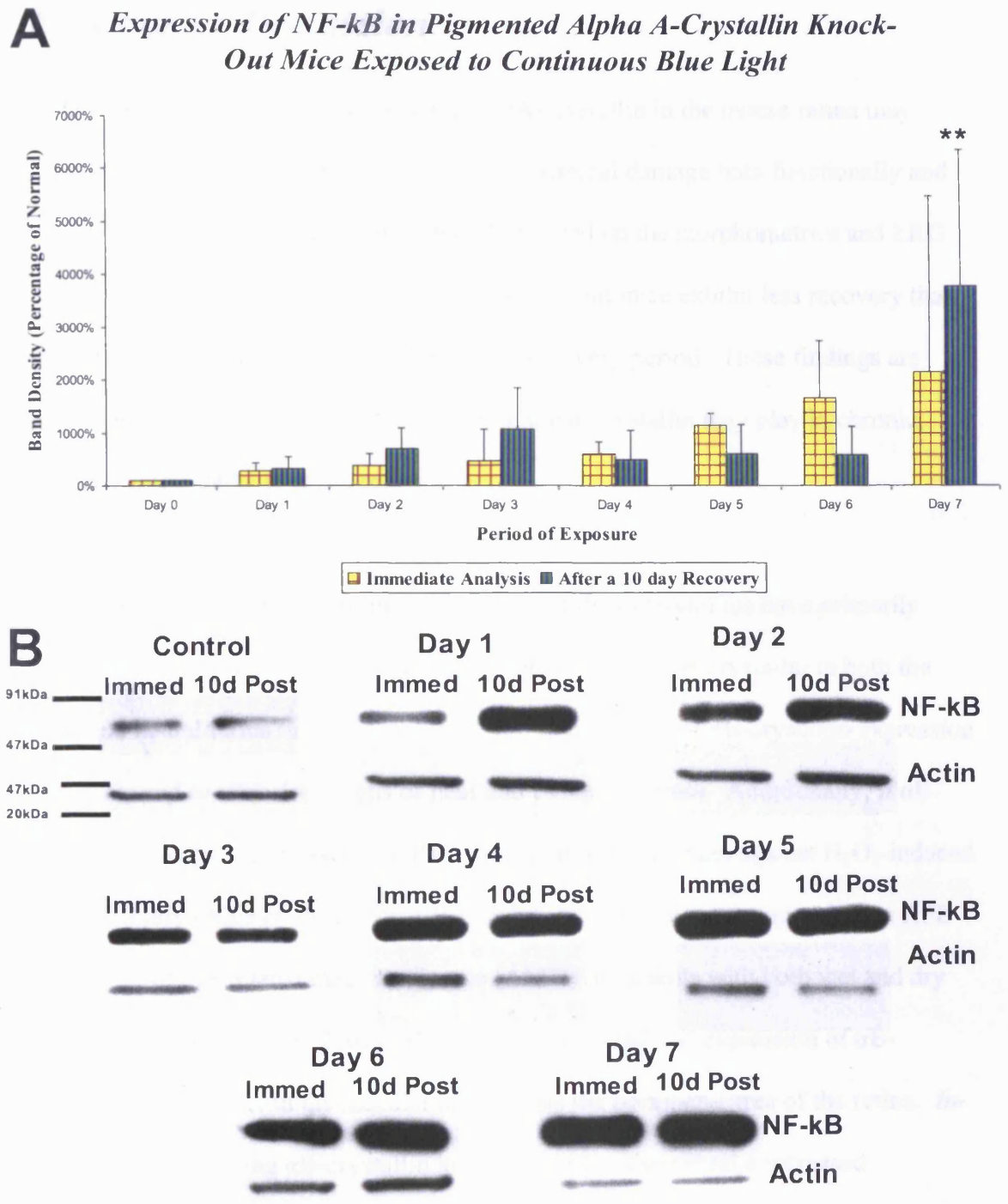

Figure 6.4.19A and B Expression of NF-κB in pigmented αA-crystallin knock-out mice immediately and after a 10 day recovery period over 1-7 days of exposure. . 'A' represents a graphical description of NF-κB expression normalized to actin immediately and 10 days after designated exposure. Shown in 'B'are representative blots of NF-κB, as well as actin as an internal control. NF-κB corresponds to 63kDa and actin corresponds to 43kDa. In 'A'data are expressed as the mean ± S.D and statistical significance was assessed by a one-way ANOVA followed by Dunnett's multiple comparison test to compare exposed mice to non-exposed or Tukey's multiple comparison test to compare between immediate versus the 10day recovery. A $p<0.05$ was considered statistically significant. ($p < 0.05$, **$p < 0.01$, n=3).*

6.5 Chapter Discussion

In this study we found that the absence of αA-crystallin in the mouse retina may increase its susceptibility to moderate photochemical damage both functionally and morphologically. It is important to note that based on the morphometrics and ERG results, it appears as though αA-crystallin knock-out mice exhibit less recovery than their wild-type counterparts after the 10 day recovery period. These findings are critical in determining the potential role that the α-crystallin may play in chronic, photochemical damage to the retina.

Previous studies examining retinal expression of the α-crystallins have primarily focused on the protective, possibly anti-apoptotic role of αB-crystallin in both the RPE and neural retina. Alge *et al.*, 2002, found induction of αB-crystallin expression in *in-vivo* and *in-vitro* conditions of heat and oxidative stress. Additionally, if αB-crystallin was over-expressed, the RPE appeared to be resistant against H_2O_2-induced cellular injury (Alge *et al.*, 2002). αB-crystallin has also been suggested as an RPE biomarker of age-related macular disease (AMD) in patients with both wet and dry forms of AMD (De *et al.*, 2007). Both studies revealed that expression of αB-crystallin was greater in the macular area versus the peripheral area of the retina. *In-vitro* studies involving αB-crystallin knock-out mice also reveal a increased susceptibility to oxidative damage in the RPE (Yaung *et al.*, 2007) and link αB-crystallin to caspase-3 activation and Bcl-2 (Kamradt *et al.*, 2001; Alge *et al.*, 2002; Liu *et al.*, 2004; Mao *et al.*, 2004; Yaung *et al.*, 2007).

Intense light exposure experiments have also been shown to increase the expression of αB-crystallin in the photoreceptors and RPE of the rat (Sakaguchi *et al.*, 2003) suggesting possible protection of cells from light damage. Lens epithelium-derived growth factor (LEDGF) was also shown to induce αB-crystallin and heat shock protein 27 promoting photoreceptor survival in light damage rats (Machida *et al.*, 2001, Singh *et al.*, 2001).

Although a number of studies have focused on αB-crystallin in the retina and RPE, recent works have investigated into the role αA-crystallin may play. Rao *et al.*, 2008, examined the protective role of αA-crystallin in the photoreceptors of experimental autoimmune uveitis in mice. An additional finding in this work was the presence of αA-crystallin localized to the inner segments of the photoreceptors. Localization of αA-crystallin has previously been found in the outer nuclear layer, inner nuclear layer and ganglion cell layer, but not in the inner or outer segments of the photoreceptors (Xi *et al.*, 2003a). Decreased expression of αA-crystallin in the retinal dystrophic rat suggested a possible role for αA-crystallins in protecting the photoreceptors from light damage (Crabb *et al.*, 2002; Sakaguchi *et al.*, 2003) and upregulation in the diabetic retina of rats (Wang *et al.*, 2007) may indicate a possible inflammatory response.

This study primarily focused on the morphological and functional changes associated with continuous blue light exposure up to 7 days in mice lacking αA-crystallin. Although both wild-type and knock-out mice exhibited mild morphological changes visualized with light microscopy, deeper morphometric analysis revealed that significant changes in layer thickness were noted in the outer and nuclear layers of the

retina after a 10 day recovery period of the αA-crystallin knock-out mice. Since αA-crystallin has been localized to these retinal layers (Xi *et al.,* 2003a), perhaps the absence of αA- makes these layers more susceptible to moderate photochemical damage.

As shown in **Chapter 3,** αA-crystallin K/O RPE were more susceptible to mitochondrial damage with increasing exposure of both H_2O_2 and *t*-BOOH. Similar to the *in-vitro* studies, αA-crystallin knock-out mice appear to more susceptible to photo-oxidative stress associated with moderate photochemical damage of the retina.

Morphological changes also correlated with the functional changes observed with ERG analysis. When the knock-out mice were compared to their wild-type counterparts, similar were their decline in irreversible visual function, however it was greater during the 10 day recovery period compared to the immediate analysis. Based on the combined morphological and functional analysis, perhaps αA-crystallin knock-out mice lack the ability to recover from environmental stressors compared to their wild-type counterparts.

Lenticular studies found that the anti-apoptotic function of αA-crystallin is greater than αB-crystallin (Andley *et al.,* 2000), while Mao *et al.,* 2004, found similar degrees of protection against apoptosis in both lens and non-lens tissues. Although αB-crystallin was upregulated in knock-out mice immediate and after a 10 day recovery, it was not significant and not as drastic as in wild-type mice. Perhaps the activity and efficiency of αB-crystallin is dependent on the presence and activity of αA-crystallin.

Knock-out studies involving αA-crystallin mice revealed that in the lens there are dense inclusion bodies containing αB-crystallin, suggesting that αA-crystallin may play a role in the solubility of other crystallins (Brady *et al.,* 1997). Andley 2007 has also suggested that the absence of αA- or αB-crystallin may trigger a stress response in the retina, leading to increased expression of γ-crystallins. Perhaps this inter-dependent role may also occur in the retina.

NF-κB expression was not significantly upregulated in the retina of αA-crystallin knock-out mice, although its degree of expression was much less in the exposed wild-type mice (**Chapter 5)** compared to the knock-out mice. As reviewed in **Chapter 5,** NF-κB has been linked to the α-crystallins in the area of inflammation (Masilamoni *et al.,* 2006, Ousman *et al.,* 2007). Studies found that the α-crystallins prevents cell death by inhibiting caspase-3 activation, and suppresses the inflammatory role of NF-kB (Ousman *et al.,* 2007). Therefore, if there is an absence of αA-crystallin with no significant upregulation of αB-crystallin, there may be corresponding upregulated levels of NF-kB, indicating possible inflammation. Further investigation into this connection should utilize immunocytochemistry and examination of IκBα expression. In the cell, NF-kB is stored in the cytoplasm in its inactive state by interaction with IκBα. On activation, IkBa undergoes degradation through an ubiquitin-dependent pathway (Beg *et al.,* 1993; Sun *et al.,* 1993), allowing translocation of NF-kB to nucleus (Beg and Baldwin, 1993, Zabel *et al.,* 1993) and subsequently binding to DNA regulatory elements within NF-kB target genes.

Since there were functional and morphological changes noted in the αA-crystallin knock-out mice, which were significantly different from the wild-type mice, future studies should utilize the technique of electron microscopy to examine changes not visible with light microscopy. Additionally, immunocytochemistry would be useful in localizing proteins (α-crystallins and NF-κB) and their changes associated with continuous blue light exposure up to 7 days.

In summary this study has shown that:

- αA-crystallin knock-out mice do exhibit irreversible morphological and functional photochemical damage at longer exposure durations with greater damage occurring during a 10 day recovery period
- αB-crystallin appears to be upregulated in light damage but it is not significant and may be dependent on the presence and function of αA-crystallin
- NF-κB may expression appears to be greater in the αA-crystallin knock-out mice compared to the wild-type indicating possible regulation from the α-crystallins

Chapter 7.0:
General Discussion and Conclusions

7.1 General Discussion

The premise of this work was to examine the potential protective role of α-crystallins in the retina. Results presented in these studies have demonstrated that the presence of α-crystallins, in particular, αA-, may play a protective role in oxidative stress to the RPE and photochemical damage of the retina at both a functional and morphological level. Additionally, the presence or absence of αA- may affect expression and potency of αB-crystallin in response to stress-related conditions.

The presence and function of α-crystallins in the retina appear to parallel their roles in the maintenance and transparency of the lens, by acting as molecular chaperones (Ellis and van der Vies, 1991; Horwitz 1992; Jakob *et al.*, 1993; Das and Surewicz, 1995; Derham and Harding, 1999; Barral *et al.*, 2004). Molecular chaperones prevent undesired protein aggregation by binding non-native intermediates that may arise in response to cellular stress or during protein translation *in vivo* (Horwitz 1992; Andley 2008). α-crystallin traps unfolded or denatured proteins and suppresses their non-specific irreversible aggregation without utilization of ATP (Derham and Harding, 1999) This efficient function of α-crystallin in suppressing protein aggregation is especially important in maintaining lens transparency where there is no blood supply and in which metabolism is localized only to the lens epithelium, since a majority of the fibre cells contain no nuclei or other cellular organelles (Bloemendal *et al.*, 2004).

Due to this pivotal role in the lens, a majority of the knowledge and work on the α-crystallins has been derived from various lenticular studies (elegant reviews in Piatigorsky 1989; Sax and Piatigorsky 1994; Derham and Harding 1999; Horwitz

2000; Horwitz 2003; Augusteyn 2004; Bloemendal *et al.*, 2004; Andley 2006; Andley 2007; Andley 2008).

This lenticular role closely parallels the potential protective presence of α-crystallins in both the RPE and the retina in suppressing protein denaturation and subsequent aggregation in the retina. As reviewed in **Chapter 1**, both the RPE and retina are post-mitotic and exposed to numerous environmental, metabolic, and oxidative stressors from several sources (Winkler *et al.*, 1996; Winkler *et al.*, 1999; Beatty *et al.*, 2000; Cai *et al.*, 2000; Strunnikova *et al.*, 2004).

As shown in **Figure 7.1**, '**1**' is a general graphical description of α-crystallins role in the lens. The lack of blood supply and minimal protein turnover in the lens makes proteins more susceptible to unfolding with age, constant light exposure and oxidative stress. α-crystallins bind to unfolded proteins, preventing irreversible aggregation and subsequent lens opacities, or cataracts. Shown in '**2**' is the potential pattern in the retina. Unlike the lens, the RPE and retina are exposed to a highly oxygenated environment, high amounts of cellular metabolism, potential for peroxidation of lipids (due to outer segment membrane concentrations of PUFAs), large amounts of mitochondria, and constant light exposure. Similar to the lenticular role, once proteins have become denatured or unfolded due to surrounding environmental stressors, α-crystallins bind and prevent irreversible aggregation. Unlike the lens, protein aggregation in the retina is not necessary for transparency, but rather it is important in maintaining the function of proteins necessary for routine cellular maintenance.

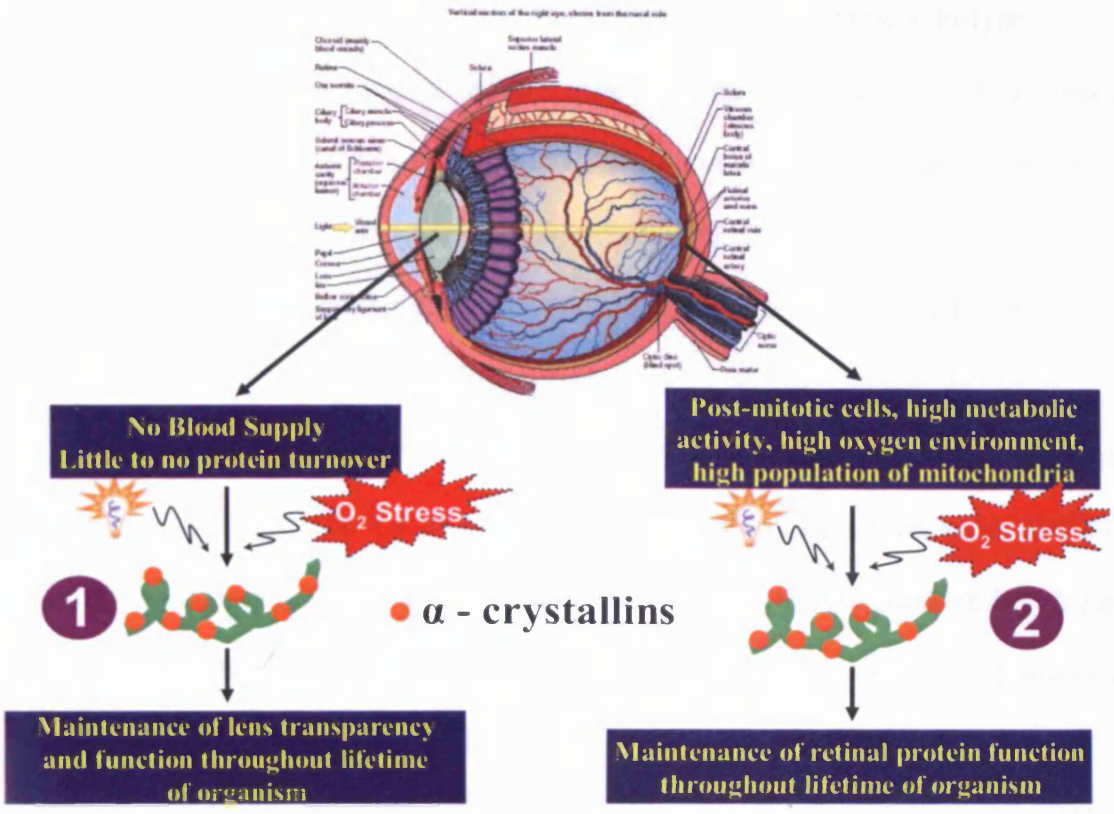

***Figure 7.1** Simple graphical description of α-crystallins function in the lens (1) and the retina and RPE (2). As shown the role of α-crystallin in the retina parallels that of the lens. However, in the lens, α-crystallins ultimately assist in preventing light scattering (cataract) due to protein aggregation. In the retina, α-crystallins assist in maintaining irreversible aggregation which could lead to loss of protein function and ultimate compromise of visual processing. Source of the eye cartoon: www.scienceclarified.com/.../uesc_05_img0242.jpg*

The presence and expression of α-crystallins in the RPE and retina become exceptionally important since their association as sHSPs enable the adaptation of cells to gradual, chronic changes in their surrounding environment, often being able to survive lethal conditions (Garriso *et al.,* 2001). Additionally, their stabilized presence in cells with minimal mitotic activity further supports their longevity throughout the lifetime of the organism (Piatigorsky 1989; Iwaki *et al.,* 1990; Sax and Piatigorsky 1994; Horwitz 2000). The ability of α-crystallins to act as molecular chaperones without the consumption of ATP makes them an efficient defense mechanism against the many cellular compromises associated with aging and environmental stressors in systems like the retina and RPE (Wong and Lin 1989; Horwitz 1992; Sax and Piatigorsky 1994).

As shown in **Chapter 3,** primary RPE were cultured from humans, wild-type mice RPE and αA-crystallin knock-out RPE. Although both the WT and K/O RPE shared similar growth characteristics between each other and their human counterparts, when oxidative stressors (H_2O_2 and *t*-BOOH) were added for 24hrs, the αA- K/O RPE were significantly more susceptible to mitochondrial damage than the WT-RPE or primary human or the ARPE-19. This finding correlates with previous studies that have examined viability of K/O RPE to oxidative stressors (Yaung *et al.,* 2007) and found that cell death was predominantly by apoptosis. Additionally, αA-crystallin K/O RPE had increased caspase-3 activation and mitochondrial membrane permeability (Yaung *et al.,* 2007). These findings are important since the RPE and retina are exposed to a number of stressors, which can ultimately lead to apoptosis of retinal cells with resultant visual loss. Damage to the mitochondria, in particular mitochondrial DNA (mtDNA), has been well documented as a possible cause for apoptosis of the RPE in retinal degeneration conditions such as age-related macular degeneration (ARMD) (Ballinger *et al.*, 1999; Jin *et al.*, 2001a; Bonnel *et al.*,2003). Perhaps αA-crystallin plays a role in protection of the mitochondria from surrounding reactive oxygen species generated during routine, physiological cellular metabolism or age-related overload.

Previous *in-vitro* studies on the lens epithelium found that cells transfected with αA-crystallin promote cell survival by inhibiting apoptosis (Andley *et al.,* 1998). Follow-up studies with αA-crystallin K/O animals found promotion of apoptosis through reduction of cell proliferation (Xi *et al.,* 2003a). It appears as though αA-crystallin is associated to enhance cell survival through its association with anti-apoptotic factors Bax and Bcl-X_s (Liu *et al.,* 2004). The Bcl-2 family contributes to the regulation of

the swelling of the mitochondria and opening of permeability pores (Gross *et al.*, 1999; Yaung *et al.*, 2007). Although it appears as though the absence of αA-crystallin makes the RPE more susceptible to cell death via oxidative stress, further investigation is necessary to determine the exact mechanism of mitochondrial pathways of apoptosis in RPE and retina under oxidative or photooxidative stress.

In-vitro studies (**Chapter 3)** provided baseline mitochondrial viability studies in WT versus K/O RPE, however the role of α-crystallins in photochemical damage of the retina was investigated further. Photochemical damage of the retina has been well documented and is incredibly multifactorial depending on exposure duration, temperature and wavelength of the inducing light, chromophore concentrations, environmental conditions and absorption of other ocular tissues (Organisciak and Winkler, 1994). Photochemical damage due to constant illumination has been connected to dysfunction in the phototransduction cascade (Noell *et al.*, 1966, Williams and Howell 1983).

Chapters 4, 5 and 6 examined morphological and functional changes associated with continuous blue light exposure up to 7 days in albino BALB/cBYJ mice, wild-type mice, and αA-crystallin knock-out mice, respectively. Continuous light illumination, even at low to moderate intensities, has been shown to damage both the sensory retina and the overlying RPE (Noell *et al.*, 1966; Ham *et al.*, 1978; Noell 1980; Williams and Howell 1983; Organisciak *et al.*, 1989; Perez and Perentes 1994). True comparisons between mice could technically only be made with WT and K/O mice, since both were pigmented and the only differentiation between the two was the absence of αA-crystallin.

As presented, there were greater morphological and functional changes in retinas of mice in which αA-crystallin was absent compared to their WT counterparts. In particular the damage appeared to be most significant in αA- K/O mice that were examined after the 10 day recovery period. This finding further supports the idea that the role of α-crystallins in the lens parallels the retina (see **Figure 7.1**). Perhaps αA-crystallin is more vital in long-term protection of retina. Parallel to findings of increased damage after the 10 day recovery period is the statistically significant upregulation of both αA- and αB-crystallin in wild-type mice during their 10 day recovery period. When αB-crystallin expression was examined in K/O mice, there was upregulation, but it was not significant compared to animals which were not exposed to continuous blue light. Additionally, it was not as drastic as the expression found in WT mice exposed to blue light.

As stated in **Chapter 6,** αA-crystallin appears to have greater anti-apoptotic abilities than αB-crystallin the lens (Andley *et al.*, 2000), however, reports have also shown that αA- and αB- display similar degrees of protection against apoptosis in lens and non-lens tissues (Mao *et al.*, 2004). Based on the findings from the *in-vivo* studies presented here involving the αA-crystallin knock-out, it appears as though αA- does play a role in protection of the retina from photochemical damage and may also assist in the function and capabilities of αB-crystallin in this regard also, although extensive studies are necessary for direct correlations.

It is also important to note that the photochemical damage in the studies described here was elicited by blue light. Many studies support blue light damage as a possible inducer in the degeneration of the RPE and photoreceptors in age related disease

(King *et al.*, 2004; Margrain *et al.*, 2004; Godley *et al.*, 2005; Algvere *et al.*, 2006; Chu *et al.*, 2006; Wu *et al.*, 2006; Thomas *et al.*, 2007; Siu *et al.*, 2008). Blue light induced lesions appear to be mediated by rhodopsin (Grimm *et al.*, 2000; Grimm *et al.*, 2001; Algvere *et al.*, 2006; Wu *et al.*, 2006; Tanito *et al.*, 2007; Thomas *et al.*, 2007). It is important to note that previous reports connect α-crystallins with photoreceptor segment renewal through its association with transportation of newly synthesized rhodopsin (Deretic *et al.*, 1994). Although there was continued retinal degeneration on a functional and morphological level with the K/O mice, perhaps retinal damage was also mediated through rhodopsin association. This possible connection to rhodopsin levels in the K/O mice requires further investigation.

To date, this is the only study that has examined the role of α-crystallins under moderate, continuous levels of blue light to the retina. Previous reports have examined the expression of α-crystallins under intense light exposures and in retinal dystrophic rats (Crabb *et al.*, 2002; Sakaguchi *et al.*, 2003). Both studies concluded that increased expression of crystallins in light damaged photoreceptors suggest a possible role for crystallins in protecting the photoreceptors from light damage.

As presented, clearly the absence of αA-crystallin affects the morphological and functional capacity of the retina after exposure to oxidative stressors or photochemical damage. Contrary to previous reports that claimed αA-crystallin was the 'lens-specific' α-crystallin (Bloemendal *et al.*, 2004) and that it is minimally expressed in non-lenticular tissues (Srinivasan *et al.*, 1992), αA-crystallin has been shown to be 30,000 more abundant than αB-crystallin by quantitative PCR methods in mouse retina (Xi *et al.*, 2003a) and appears to protect photoreceptors against mitochondrial

oxidative stressed mediated apoptosis (Rao *et al.*, 2008). This work accompanies corresponding studies showing that αA-crystallin does play a pivotal role, not only in the capabilities of the lens, but elsewhere, especially RPE and retina.

7.2 Conclusions

- *In-vitro* culturing of human RPE is similar to both wild-type and αA-crystallin knock-out RPE
- Human *in-vitro* expression of the α-crystallins were found in the RPE and neural retina
- The lack of αA-crystallin may make the RPE more susceptible to oxidative stress
- αA- and αB-crystallins in wild-type mice appear to be upregulated in light damage as the duration increases, possibly exhibiting a protective role in photochemical light damage
- αA-crystallin knock-out mice exhibit irreversible morphological and functional photochemical damage at longer exposure durations with greater damage occurring during a 10 day recovery period
- αB-crystallin expression in αA- K/O mice appears to be upregulated in light damage but this is not statistically significant and may be dependent on the presence and function of αA-crystallin

7.3 Future Work

This work has demonstrated the susceptibility αA-crystallin knock-out RPE and retina to oxidative stress and photochemical damage.

Additional *in-in-vitro* investigations into the role of α-crystallins may include:

- exposure of both WT and αA-crystallin K/O RPE to blue light exposure with subsequent protein examination of the α-crystallins (αA-, αB-) in comparison with human counterparts
- expose retinal explants from WT and αA K/O animals to blue light exposure and correlate *in-vitro* to *in-vivo* results
- obtain αB-crystallin knock-out mice or αA-/αB- double knock-out mice to further examine the role α-crystallins in oxidative and photochemical damage to the retina and RPE.

The above mentioned *in-vitro* work would highlight any difference between *in-vitro* versus *in-vivo* expression of the α-crystallins, as well as correlate the absence of αA- with αB-crystallin or both αA- and αB-crystallin in *in-vitro* oxidative environments in both the RPE and retinal explants. It would be interesting to also examine the affect blue light has on the RPE and the expression of α-crystallins in retinal explants.

Future *in-vivo* work would include repetition of current experiments to increase the number of animals available and utilization of transmission electron microscopy to examine detailed changes which may be occurring in the mitochondria of both the RPE and neural retina. Additionally, it would be useful to perform immunocytochemistry on the retina of both αA- K/O and WT to examine the differences in expression with continued blue light exposure.

Previous work by Organsiciak *et al.*, 2006 reports that expression of the α-crystallins varies according to the age of the animal or the onset of genetically induced stressed. All animals exposed in the current studies were between the ages of 6-10 weeks. Therefore, it was undetermined if any effect age may have had on the function and expression of the α-crystallins. Future work would utilize the exposure of both WT and αA- K/O animals to continuous blue light and determine whether or not aging plays a role in the expression of α-crystallins with moderate photochemical damage of the retina.

It would be also useful to obtain the αB- and αA-/αB-crystallin knock-out mice to further examine the role αB and both αA-/αB- may play in photochemical damage of the retina.

Chapter 8.0:
References

Adamis A.P., Shima D.T., Yeo K.T., Yeo T.K., Brown L.F., Berse B., D'Amore P.A., and Folkman J. (1993) Synthesis and secretion of vascular permeability factor/ vascular endothelial growth factor by human retinal pigment epithelial cells. *Biochem Biophys Res Commun,* 193:631-638.

Alexeyev M.F., Ledoux S.P., and Wilson G.L. (2004) Mitochondrial DNA and ageing. *Clin Sci (Lond),* **107**:355-364.

Alge C.S., Suppmann S., Priglinger S.G., Neubauer A.S., May C.A., Hauck S., Welge-Lussen U., Ueffing M., and Kampik A. (2003) Comparative proteome analysis of native differentiated and cultured dedifferentiated human RPE cells. *Invest Ophthalmol Vis Sci,* **44**:3629-3641.

Alge C.S., Priglinger S.G., Neubauer A.S., Kampik A., Zillig M., Bloemendal H., and Welge-Lussen U. (2002) Retinal Pigmented Epithelium is Protected Against Apoptosis by αB-crystallin. *Invest Ophthalmol Vis Sci,* **43**:3575-3582.

Algvere P.V., Marshall J., Seregard S. (2006) Age-related maculopathy and the impact of the blue light hazard. *Acta Ophthalmol Scand,* **84**:4-15.

Alizadeh M., Wada M., Gelfman C.M., Handa J.T., and Hjelmeland L.M. (2001) Downregulation of differentiation specific gene expression by oxidative stress in ARPE-19 cells. *Invest Ophthalmol Vis Sci,* **42**:2706-2713.

Ambati J., Ambati B.K., Yoo S.H., Ianchulev S., and Adamis A.P. (2003) Age-Related Macular Degeneration: Etiology, Pathogenesis and Therapeutic Strategies. *Surv Ophthalmol,* **48**:257-293.

Ames B.N., Shigenaga M.K., and Hagen T.M. (1995) Mitochondrial decay in aging. *Biochim Biophys Acta,* **24**:165-170.

Ames B.N., Shingenaga M.K., and Hagen T.M. (1993) Oxidants, antioxidants and the degenerative diseases of aging. *Proc Natl Acad Sci USA,* **90**:7915-7922.

Andersen J.K. (2004) Oxidative stress in neurodegeneration: cause or consequence? *Nat Med,* **5**:S18-S25.

Anderson D.H., Fisher S.K., and Steinberg R.H. (1978) Mammalian cones: disc shedding, phagocytosis, and renewal. *Invest Ophthalmol Vis Sci,* **17**:117.

Anderson K.V., Coyle F.P., O'Steen W.K. (1972) Retinal degeneration produced by low-intensity colored light. *Exp Neurol,* **35**:233-238.

Andley U.P. (2008) The lens epithelium: focus on the expression and function of the alpha-crystallin chaperones. *Int J Biochem Cell Biol,* **40**:317.323.

Andley U.P. (2007) Crystallins in the eye: Function and Pathology. *Prog Retin Eye Res,* **26**:78-98.

Andley U.P., Song Z., Wawrousek E.F., Fleming T.P., Bassnett S. (2000) Differential protective activity of alphaA and alphaB-crystallin in lens epithelial cells. *J Biol Chem*, **47**:36823-36831.

Andley U.P., Mathur S., Griest T.A., and Petrash J.M. (1996) Cloning, expression and chaperone-like activity of human αA-crystallin. *J Biol Chem*, **271**:31973-80.

Andreoli C.M., and Miller J.W. (2007) Anti-vascular endothelial growth factor therapy for ocular neovascular disease. *Curr Opin Ophthalmol*, **18**:502-508.

Antolin I., Rodriguez C., Sainz R.M., Mayo J.C., Uria H., Kotler M.L., Rodriguez-Colunga M.J., Tolivia D., and Menendez-Pelaez A., (1996) Neurohormone melatonin prevents cell damage: effect on gene expression for antioxidant enzymes. *FASEB J*, **10**:882-890.

Arikawa K., Molday L.L., Molday R.S., *et al.* (1992) Localization of peripherin/rds in the disk membranes of cone and rod photoreceptors: relationship to disk membrane morphogenesis and retinal degeneration. *J Cell Biol*, **116**:659.

Aswad D.W., Paranandi M.V., and Schurter B.T. (2000) Isoaspartate in peptides and proteins: formation, significance, and analysis. *J Pharm Biomed Anal*, **21**:1129-1136.

Audo I., Robson A.G., Holder G.E., and Moore A.T. (2008) The negative ERG: clinical phenotypes and disease mechanisms of inner retinal dysfunction. *Surv Ophthalmol*, **53**:16-40.

Augusteyn R.C. (2004) Alpha-crystallin: a review of its structure and function. *Clin Exp Optom*, **87**:356-366.

Augusteyn R.C., and Koretz J.F. (1987) A possible structure for alpha-crystallin. *FEBS Lett*, **222**:1-5.

Ayoub G.S., and Matthews G. (1992) Substance P modulates calcium current in retinal bipolar neurons. *Vis Neurosci*, **8**:539.

Baeuerle P.A., and Baltimore D. (1988) Activation of DNA-binding activity in an apparently cytoplasmic precursor of the NF-kappa B transcription factor. *Cell*, **53**:211-217.

Bailey T.A., Kanuga N., Romero I.A., Greenwood J., Luthert P.J., and Cheetham M.E. (2004) Oxidative Stress Affects the Junctional Integrity of Retinal Pigment Epithelial Cells. *Invest Ophthalmol Vis Sci*, **45**:675-684.

Ballinger S.W., Van Houten B., Jin G.F., Conklin C.A., and Godley B.F. (1999) Hydrogen peroxide causes significant mitochondrial DNA damage in human RPE cells. *Exp Eye Res*, **68**:765-772.

Barron M.J., Johnson M.A., Andrews R.M., Clarke M.P., Griffiths P.G., Bristow E., He L.P., Durham S., and Turnbull D.M. (2001) Mitochondrial abnormalities in ageing macular photoreceptors. *Invest Ophthalmol Vis Sci*, **42**:3016-3022.

Barsh G.S. (1996) The genetics of pigmentation: from fancy genes to complex traits. *Trends Genet,* **12**:299-305.

Bazan N.G., Rodriguez de Turco E.B., and Gordon W.C. (1994) Docosahexaenoic acid supply to the retina and its conservation in photoreceptor cells by active retinal pigment epithelium-mediated recycling. *World Rev Nutr Diet,* **75**:120-123.

Beatty S., Koh H., Phil M., Henson D., and Boulton M. (2000) The role of oxidative stress in the pathogenesis of age-related macular degeneration. *Surv Ophthalmol,* **45**:115-134.

Beckman K.B., and Ames B.N. (1997) Oxidants, Antioxidants and Ageing. Oxidative Stress and the Molecular Biology of Antioxidant Defenses. Cold Spring Harbor Laboratory Press, Pgs. 201-248.

Beg A.A., Finco T.S., Nantermet P.V., Baldwin A.S. (1993) Tumor necrosis factor and interleukin-1 lead to phosphorylation and loss of I kappa B alpha: a mechanism for NF-kappa B activation. *Mol Cell Biol,* **13**:3301-3310.

Beg A.A., and Baldwin A.S. (1993) The I kappa B proteins: multifunctional regulators of Rel/NF-kappa B transcription factors. *Genes Dev,* **7**:2064-2070.

Bergamini C.M., Gambetti S., Dondi A., and Cervellati C. (2004) Oxygen, reactive oxygen species and tissue damage. *Curr Pharm Des*, **10**:1611-1626.

Berman E.R. (1991a) The Lens: The Crystallins. Biochemistry of the Eye. Plenum Press, Pgs. 204-211.

Berman E.R. (1991b) The Retina: The Retinal Pigmented Epithelium. Biochemistry of the Eye. Plenum Press, Pgs. 380-406.

Besharse J.C., and Defoe D.M. (1998) Role of the retinal pigment epithelium in photoreceptor turnover. The Retinal Pigment Epithelium, Oxford University Press, Pgs. 152-172.

Bhat S.P., Horwitz J., Srinivasan A., and Ding L. (1991) αB-Crystallin exists as an independent protein in the heart and in the lens. *Eur J Biochem*, **102**:775-781.

Bhat S.P., and Nagineni C.N. (1989) Alpha B subunit of lens specific protein alpha-crystallin is present in other ocular and non-ocular tissues. *Biochem Biophys Res Commun*, **158**:319-325.

Biesemeier A., Kokkinou D., Julien S., Heiduschka P., Berneburg M., Bartz-Schmidt K.U., and Schraermeyer U. (2008) UV-A induced oxidative stress is more prominent in naturally pigmented aged human RPE cells compared to non-pigmented human RPE cells independent of zinc treatment. *J Photochem Photobiol,* **90**:113-120.

Bindels J.G., Siezen R.J., and Hoenders H.J. (1979) A model for the architechture of alpha-crystallin. *Ophthalmic Res*, **11**:441-452.

Bloemendal H., de Jong W., Jaenicke R., Lubsen N.H., Slingsby C. and Tardieu A. (2004) Ageing and vision: stucture, stability and function of lens crystallins. *Prog Biophys Mol Biol,* **86:**407-485.

Bloomfield S.A., and Dacheux R.F. (2001) Rod vision: pathways and processing in the mammalian retina. *Prog Ret Eye Res,* **20:**384.

Bok D. (1993) Retinal transplantation and gene therapy. Present realities and future possibilities. *Invest Ophthalmol Vis Sci,* **34:**473-476.

Bok D., and Hall M.O. (1971) The role of the pigment epithelium in the etiology of inherited retinal dystrophy in the rat. *J Cell Biol,* **49:**664-682.

Bonnel S., Mohand-Said S., and Sahel J.A. (2003) The aging of the retina. *Exp Gerontol*, **38:**825-831.

Borkman R.F., Knight G., and Obi B. (1996) The molecular chaperone alpha-crystallin inhibits UV-induced protein aggregation. *Exp Eye Res*, **62:**141-148.

Bost L.M., Aotaki-Keen A.E., Hjelmeland L.M. (1992) Coexpression of FGF-5 and bFGF by the retinal pigment epithelium in vitro. *Exp Eye Res,* **55:**727-734.

Bost L.M., Aotaki-Keen A.E., Hjelmeland L.M. (1994) Cellular adhesion regulates bFGF gene expression in human retinal pigment epithelial cells. *Exp Eye Res,* **58:**545-552.

Boulton M., and Saxby L.A. (2004a) The Lens: Evolution and Molecular Biology. Ophthalmology. Mosby, Pgs. 257-260.

Boulton M., Dayhaw-Barker P. (2001a) The role of the retinal pigment epithelium: topographical variation and ageing changes. *Eye*, **15:**384-389.

Boulton M., Rozanowska M., and Rozanowski B. (2001b) Retinal Photodamage. *J Photochem Photobiol,* **64:**144-161.

Boulton M. (1998) Melanin and the retinal pigment epithelium. The Retinal Pigment Epithelium. Oxford University Press, Pgs. 68-85.

Boulton M., Dontsov A., Jarvis-Evans J., Ostrovsky M., and Svistunenko D. (1993) Lipofuscin is a photoinducible free radical generator. *J Photochem Photobiol,* **19:**201-204.

Boulton M. (1990) Cell Culture. *Eye*, **4**:622-31.

Boulton M.E., McLeod D., and Garner A. (1989) Vasoproliferative retinopathies: clinical, morphogenetic and modulatory aspects. *Eye,* **Supplement:**S124-S139.

Boulton M., and Marshall J. (1985) Repigmentation of human retinal pigment epithelial cells in vitro. *Exp Eye Res,* **41:**209-218.

Boulton M., Marshall J., and Mellerio J. (1984) Retinitis pigmentosa: a quantitative study of the apical membrane of normal and dystrophic human retinal pigment epithelial cells in tissue culture in relation to phagocytosis. *Graefes Arch Clin Exp Ophthalmol*, **221**:214-29

Boulton M., Marshall J., and Mellerio J. (1983) Retinitis Pigmentosa: A Preliminary Report on Tissue Culture Studies of Retinal Pigment Epithelial Cells from Eight Affected Human Eyes. *Exp Eye Res*, **37**:307-313.

Bova M.P., Ding L.L., Horwitz J., and Fung B.K. (1997) Subunit exchange of alpha A-crystallin. *J Biol Chem*, **272**:29511-29517.

Boyle D., and Takemoto L. (1994) Characterization of the α-γ and α-β Complex: Evidence for an In Vivo Functional Role of α-Crystallin as a Molecular Chaperone. *Exp Eye Res*, **58**:9-16.

Brady J.P., Garland D., Green D.E., Tamm E.R., Giblin F.J., and Wawrousek E.F. (2001) AlphaB-crystallin in lens development and muscle integrity: a gene knockout approach. *Invest Ophthalmol Vis Sci*, **42**:2924-2934.

Brady J.P., Garland D., Douglas-Tabor Y., Robinson G., Groome A., and Wawrousek E.F. (1997) Target disruption of the mouse AlphaA-crystallin gene induces cataract and cytoplasmic inclusion bodies containing the small heat shock protein AlphaB-crystallin. *Proc Natl Acad Sci USA*, **94**:884-889.

Bryan J.A., and Campochiaro P.A. (1986) A retinal pigment epithelial cell derived growth factor(s). *Arch Ophthalmol*, **104**:422-425.

Burnette, W.N. (1981). "Western blotting": electrophoretic transfer of proteins from sodium dodecyl sulfate--polyacrylamide gels to unmodified nitrocellulose and radiographic detection with antibody and radioiodinated protein A. *Anal Biochem*, **112**:195-203.

Busch E.M., Gorgels T.G., Roberts J.E., and van Norren D. (1999) The effects of two stereoisomers of N-acetylcysteine on photochemical damage by UVA and blue light in rat retina. *Photochem Photobiol*, **70**:353-358.

Cai H., and Del Priore L.V. (2006) Gene expression profile of cultured adult compared to immortalized human RPE. *Mol Vis*, **12**:1-14.

Cai J., Nelson K.C., Wu M., Sternberg Jr., P., and Jones D.P. (2000) Oxidative damage and protection of the RPE. *Prog Retin Eye Res*, **19**:205-221.

Cai J., Wu M., Nelson K.C., Sternberg Jr., P., and Jones D.P. (1999) Oxidant induced apoptosis in cultured human retinal pigment epithelial cells. *Invest Ophthalmol Vis Sci*, **40**:959-965.

Campbell, D.B., Hess, E.J. Rapid genotyping of mutant mice using dried blood spots for polymerase chain reaction (PCR) analysis. *Brain Research Protocols*, **1**:117-123, 1997.

Campochiaro P.A. (1998) Growth factors in the retinal pigment epithelium and retina. The Retinal Pigment Epithelium, Oxford University Press, Pgs. 459-477.

Campochiaro P.A., Jerdon J.A., and Glaser BM. (1986) The extracellular matrix of human retinal pigment epithelial cells in vivo and its synthesis in vitro. *Invest Ophthalmol Vis Sci,* **11**:1615-21.

Cao W., Tombran-Tink J., Elias R., Sezate S., Mrazek D., McGinnis J.F. (2001) In vivo protection of photoreceptors from light damage by pigment epithelium-derived factor. *Invest Ophthalmol Vis Sci,* **42:**1646-1652.

Carter-Dawson L., Shen F., Harwerth R.S., Smith E.L. 3rd, Crawford M.L., and Chuang A. (1998) Glutamine immunoreactivity in Müller cells of monkey eyes with experimental glaucoma. *Exp Eye Res,* **66:**537-545.

Carter-Dawson L.D., and LaVail M.M. (1979) Rods and cones in the mouse retina. I: Structural analysis using light and electron microscopy. *J Comp Neurol,* **188(2):**245-262.

Cavusoglu N., Thierse D., Mohand-Saïd S., Chalmel F., Poch O., Van-Dorsselaer A., Sahel J.A., and Léveillard T. (2003) Differential proteomic analysis of the mouse retina: the induction of crystallin proteins by retinal degeneration in the rd1 mouse. *Mol Cell Proteomics,* **2:**494-505.

Çelet B., en Akman-Demir G., Serdarog¢lu P., Yentür S.P, Tas cý B., van Noort J.M., Eraksoy M., and Saruhan-Direskeneli G. (2000) Anti-αB-crystallin immunoreactivity in inflammatory nervous system diseases. *J Neurol,* **247:**935-939.

Chader G.J., Pepperberg D.R., Crouch R., and Wiggert B. (1998) Retinoids and the retinal pigment epithelium. The Retinal Pigment Epithelium, Oxford University Press, Pgs. 135-151.

Chan E.L., and Murphy J.T. (2003) Reactive oxygen species mediate endotoxin-induced human dermal endothelial NF-kappaB activation. *J Surg Res,* **111:**120-126.

Chance B., Sies H., Boveris A. (1979) Hydroperoxide metabolism in mammalian organs. *Physiol Rev*, **59:**527-605.

Cheng G., Basha E., Wysocki V.H., and Vierling E. (2008) Insights into Small Heat Shock Protein and Substrate Structure during Chaperone Action Derived from Hydrogen/Deuterium Exchange and Mass Spectrometry *J Biol Chem,* **283:**26634-26642.

Chiesa R., Gawinowicz-Kolks M.A., Kleiman N.J., and Spector A. (1988) Definition and comparison of the phosphorylation sites of the A and B chains of bovine alpha-crystallin. *Exp Eye Res,* **46:**199-208.

Chu R., Zheng X., Chen D., and Hu D.N. (2006) Blue light irradiation inhibits the production of HGF by human retinal pigment epithelium cells in vitro. *Photochem Photobiol,* **82:**1247-1250.

Cicerone C.M (1976) Cones survive rods in the light-damaged eye of the albino rat. *Science,* **194:**1183-1185.

Cohen A.I.: The retina. In Hart MJ Jr, editor: *Adler's Physiology of the Eye*, ed 9, St. Louis, 1992, Mosby, pg. 579.

Crabb J.W., Miyagi M., Gu X., Shadrach K., West K.A., Sakaguchi H., Kamei M., Hasan A., Yan L., Rayborn M.E., Salomon R.G., and Hollyfield J.G. (2002) Drusen Proteome analysis: An approach to the etiology of age-related macular degeneration. *Proc Natl Acad Sci USA,* **99:**14682-14687.

Crabb JW, Carlson A, Chen Y, Goldflam S, Intres R, West KA, Hulmes JD, Kapron JT, Luck LA, Horwitz J and Bok D (1998). Structural and functional characterization of recombinant human cellular retinaldehyde-binding protein. *Protein Science,* **7:**746-757.

Craig E.A., Ingolia T.D., and Manseau L.J. (1983) Expression of Drosophila heat-shock cognate genes during heat shock and development. *Dev Biol*, **99:**418-426.

Curcio C.A., and Drucker D.N. (1993a) Retinal ganglion cells in Alzheimer's disease and aging. *Ann Neurol,* **33:**248-257.

Curcio C.A., Millican C.L., Allen K.A., and Kalina R.E. (1993b) Aging of the human photoreceptor mosaic: evidence for selective vulnerability of rods in the central retina. *Invest Ophthalmol Vis Sci,* **34:**3278-3296.

da Cruz L., Robertson T., Hall M.O., Constable I.J., and Rakoczy P.E. (1998) Cell polarity, phagocytosis and viral gene transfer in cultured human retinal pigment epithelial cells. *Curr Eye Res*, **17**:668-72.

Danciger M., Yang H., Handschumacher L., LaVail M.M. (2005) Constant light-induced retinal damage and the RPE65-MET450 variant: assessment of the NZW/LacJ mouse. *Mol Vis,* **11:**374-379.

Danciger M., Lyon J., Worrill D., Hoffman S., Lem J., Reme C.E., Wenzel A., and Grimm C. (2004) New retinal light damage QTL in mice with the light-sensitive RPE65 LEU variant. *Mamm Genome*, **15:**277-283.

Danciger M., Matthes M.T., Yasamura D., Akhmedov N.B., Rickabaugh T., Gentleman S., Redmond T.M., La Vail M.M., and Farber DB. (2000) A QTL on distal chromosome 3 that influences the severity of light-induced damage to mouse photoreceptors. *Mamm Genome,* **11:**422-427.

Dasgupta S., Hohman T.C., and Carper D. (1992) Hypertonic stress induces alphaB-crystallin expression. *Exp Eye Res*, **54:**461-470.

Das K.P., and Surewicz W.K. (1995) On the substrate specificity of alpha-crystallin as a molecular chaperone. *Biochem J*, **311**:367-370.

Dawson D.W., Volpert O.V., Gillis P., Crawford S.E., Xu H., Benedict W., Bouck N.P. (1999) Pigment epithelium-derived factor: a potent inhibitor of angiogenesis. *Science*, **285**:245-248.

Davies M.J. (2004a) Reactive species formed on proteins exposed to singlet oxygen. *Photochem Photobiol Sci*, **3**:17-25.

Davies N.P., Morland A.B. (2004b) Macular pigments: their characteristics and putative role. *Prog Ret Eye Res*, **23**:533-559.

Davies S., Elliott M.H., Floor E., Truscott T.G., Zareba M., Sarna T., Shamsi F.A., Boulton M.E. (2001) Photocytotoxicity of lipofuscin in human retinal pigment epithelial cells. *Free Radic Biol Med*, **31**:256-265,

De S., Rabin D.M., Salero E., Lederman P.L., Temple S., and Stern J.H. (2007) Human retinal pigment epithelium cell changes and expression of alpha B-crystallin: a biomarker for retinal pigment epithelium cell change in age-related macular degeneration. *Arch Ophthalmol*, **125**:641-645.

Delori F.C., Goger D.G. and Dorey C.K. (2001) Age-related accumulation and spatial distribution of lipofuscin in RPE of normal subjects. *Invest Ophthalmol Vis Sci*, **42**:1855-1866.

Delyfer MN, Léveillard T, Mohand-Saïd S, Hicks D, Picaud S, Sahel JA. (2004) Inherited retinal degenerations: therapeutic prospects. *Biol Cell*, **86**:261-269.

Deretic D., Aebersold R.H., Morrison H.D. and Papermaster D.S. (1994) αA- and αB-crystallin in the retina. Association with the post-Golgi compartment of frog retinal photoreceptors. *J Biol Chem*, **269**:16853-16861.

Derham B.K., van Boekel M.A., Muchowski P.J., Clark J.I., Horwitz J., Hepburne-Scott H.W., de Jong W.W., Crabbe M.J., and Harding J.J. (2001) Chaperone function of mutant versions of alpha A- and alpha B-crystallin prepared to pinpoint chaperone binding sites. *Eur J Biochem*, **268**:713-721.

Derham B.K., and Harding J.J. (2002) Effects of modification of alpha-crystallin on its chaperone and other properties. *Biochem J*, **364**:711-7.

Derham B.K., and Harding J.J. (1999) α-Crystallin as a Molecular Chaperone. *Prog Retin Eye Res*, **18**:463-509.

Deutscher MP (ed.) (1990). Guide to protein purification. Methods Enzymol. Vol 182. Academic Press Inc. San Diego, CA.

Dowling J.E., and Boycott B.B. (1965) Neural connections of the retina: fine structure of the inner plexiform layer. *Cold Spring Harb Symp Quant Biol*, **30**:383.

Dunaief J.L., Dentchev T., Ying G.S., and Milam A.H. (2002) The role of apoptosis in age-related macular degeneration. *Arch Ophthalmol*, **120**:1435-42.

Dunn K.C., Marmorstein A.D., Bonilha V.L., Rodriguez-Boulan E., Giordano F., and Hjelmeland L.M. (1998) Use of the ARPE-19 cell line as a model of RPE polarity: basolateral secretion of FGF5. *Invest Ophthalmol Vis Sci*, **39**:2744-2749.

Dunn, KC, Aotaki-Keen, AE, Putkey, FR, Hjelmeland, LM. (1996) ARPE-19, a human retinal pigment epithelial cell line with differentiated properties. *Exp Eye Res*, **62**:155-169.

Ecroyd H., and Carver J.A. (2008) The effect of small molecules in modulating the chaperone activity of alphaB-crystallin against ordered and disordered protein aggregation. *FEBS J*, **275**:935-947.

Edwards, R.B. (1983) Glycosaminoglycan secretion by primary cultures and subcultures of human retinal pigment epithelium. *Birth Defects Orig Artic Ser*, **18**:95-100.

Edwards, R.B. (1981) The isolation and culturing of the retinal pigment epithelium of the rat. *Vision Res*, **21**:147-50.

Eichler W., Reiche A., Yafai Y., Lange J., and Wiedemann P. (2008) Growth-related effects of oxidant-induced stress on cultured RPE and choroidal endothelial cells. *Exp Eye Res*, **87**:342-348.

Eldred G.E., Lasky M.R. (1993) Retinal age pigments generated by self-assembling lysosomotropic detergents. *Nature*, **361**:724-726.

Ellis R.J., and van der Vies S.M. (1991). Molecular Chaperones. *Annu Rev Biochem*, **60**:321-347.

Ellozy A.R., Ceger P., Wang R.H., and Dillon J. (1996) Effect of the UV modification of alpha-crystallin on its ability to suppress nonspecific aggregation. *Photochem Photobiol*, **64**:344-348.

Everitt, B.S. (1995). The Analysis of Repeated Measures – A Practical Review with Examples, *Statistician*, 44, 113-135.

Farrer D.N., Graham E.S., Ham W.T. Jr, Geeraets W.J., Williams R.C., Mueller H.A., Cleary S.F., and Clarke AM. (1970) The effect of threshold macular lesions and subthreshold macular exposures on visual acuity in the Rhesus monkey. *Am Ind Hyg Assoc J*, **31**:198-205.

Feeney-Burns L., Hilderbrand E.S., and Eldridge S. (1984) Aging RPE: morphometric analysis of macular, equatorial and peripheral cells. *Invest Ophthalmol Vis Sci*, **25**:195-200.

Feeney L. (1978) Lipofuscin and melanin of human retinal pigment epithelium. Fluorescence, enzyme cytochemical, and ultrastructural studies. *Invest Ophthalmol Vis Sci,* **17**:583-600.

Feeney L. (1973) The phagolysosomal system of the pigment epithelium. A key to retinal disease. *Invest Ophthalmol Vis Sci*, **12**:635-638.

Fitzgerald P.G. and Graham D. (1991) Ultrastructural localization of alpha A-crystallin to the bovine lens fiber cell cytoskeleton. *Curr Eye Res,* **10**:417-436.

Foote C.S. (1968) Mechanisms of photosensitized oxidation. There are several different types of photosensitized oxidation which may be important in biological systems. *Science,* **162**:963-970.

Friedrichson T., Kalbach H.L., Buck P., and van Kuijk FJ. (1995) Vitamin E in macular peripheral tissues of the human eye. *Curr Eye Res,* **14**:693-701.

Fu Y., and Yau K.W. (2007) Phototransduction in mouse rods and cones. *Pflugers Arch*, **454 (5)**:805-819.

Gaillard E.R., Avalle L.B., Keller L.M., Wang Z., Reszka K.J., and Dillon J.P. (2004) A mechanistic study of the photooxidation of A2E, a component of human retinal lipofuscin. *Exp Eye Res*, **79**:313-319.

Gao H., and Hollyfield J.G. (1992) Aging of the human retina. Differential loss of neurons and retinal pigment epithelial cells. *Invest Ophthalmol Vis Sci*, **33**:1-17.

Gass J.D. (1972) Drusen and disciform macular detachment and degeneration. *Trans Am Ophthalmol Soc,* **70**:409-436.

Ghosh J.G., Houck S.A., Clark J.I. (2008) Interactive sequences in the molecular chaperone, human alphaB crystallin modulate the fibrillation of amyloidogenic proteins. *Int J Biochem Cell Biol,* **40**:954-967.

Ghosh S., May M.J., and Kopp E.B. (1998) NF-kappa B and Rel proteins: evolutionarily conserved mediators of immune responses. *Annu Rev Immunol,* **16**:225-260.

Gibbs D., and Williams D.S. (2003) Isolation and culture of primary mouse retinal pigment epithelial cells. *Adv Exp Med Biol,* **533**:347-352.

Ginsberg HM, LaVail MM. Light-induced retinal degeneration in the mouse: analysis of pigmentation mutants. In: LaVail MM, Hollyfield JG, Anderson RE, eds. *Retinal Degeneration: Experimental and Clinical Studies*. New York: Alan R. Liss; 1985:449–469.

Glenn J.V., Mahaffy H., Wu K., Smith G., Nagai R., Simpson D.A., Boulton M.E., Stitt A.W. (2008) AGE-modified substrate induces global gene expression changes in ARPE-19 monolayers: relevance to lysosomal dysfunction and lipofuscin accumulation. *Invest Ophthalmol Vis Sci,* **Aug 1 Epub.**

Godley B.F., Shamsi F.A., Liang F.Q., Jarrett S.G., Davies S., and Boulton M. (2005) Blue light induces mitochondrial DNA damage and free radical production in epithelial cells. *J Biol Chem*, **280**:21061-21066.

Gollapalli DR, Maiti P, Rando RR. (2003) RPE65 operates in the vertebrate visual cycle by stereospecifically binding all-trans-retinyl esters. *Biochemistry*, **42**:11824-30.

Gordon W.C., Casey D.M., Lukiw W.J., and Bazan N.G. (2002) DNA damage and repair in light-induced photoreceptor degeneration. *Invest Ophthalmol Vis Sci*, **43**:3511-3521.

Gordon W.C., and Bazan N.G. (1993) Visualization of [3H]docosahexaenoic acid trafficking through photoreceptors and retinal pigment epithelium by electron microscopic autoradiography. *Invest Ophthalmol Vis Sci*, **34**:2402-2411.

Gorgels T.G., and Van Norren D. (1998) Two spectral types of retinal light damage occur in albino as well as in pigmented rat: no essential role for melanin. *Exp Eye Res*, **66**:155-162.

Gorgels T.G., and van Norren D. (1995) Ultraviolet and green light cause different types of damage in rat retina. *Invest Ophthalmol Vis Sci*, **36**:861-863.

Gorn R.A., and Kuwabara T. (1967) Retinal damage by visible light. *Arch Ophthalmol*, **77**:115-118.

Green D.G., and Kapousta-Bruneau N.V. (1999) Electrophysiological properties of a new isolated rat retina preparation. *Vision Res*, **39**:2165-2177.

Grignolo A., Orzalesi N., Castellazzo R., and Vittone P. (1969) Retinal damage by visible light in albino rats. An electron microscope study. *Ophthalmologica*, **157**:43-59.

Grimm C., Wenzel A., Williams T., Rol P., Hafezi F., and Reme C. (2001) Rhodopsin-mediated blue-light damage to the retina: effect of photoreversal of bleaching. *Invest Ophthalmol Vis Sci*, **42**:497-505.

Grimm C., Remé C.E., Rol P.O., and Williams TP. (2000) Blue light's effects on rhodopsin: photoreversal of bleaching in living rat eyes. *Invest Ophthalmol Vis Sci*, **41**:3984-3990.

Grisanti S., and Tatar O. (2008) The role of vascular endothelial growth factor and other endogenous interplayers in age-related macular degeneration. *Prog Retin Eye Res*, **27**:372-390.

Groenen P.J.T.A., Merck K.B., de Jong W.W., and Bloemendal H. (1994) Structure and modifications of the junior-chaperone alpha-crystallin: from lens transparency to molecular pathology. *Eur J Biochem*, **225**:1-19.

Gundersen D., Orlowski J., and Rodriguez-Boulan E. (1991) Apical polarity of Na,K-ATPase in retinal pigment epithelium is linked to a reversal of the ankyrin-fodrin submembrane cytoskeleton. *J Cell Biol,* **112:**863-872.

Guo Y., Yao G., Lei B., and Tan J. (2008) Monte Carlo model for studying the effects of melanin concentrations on retina light absorption. *J Opt Soc Am A Opt Image Sci Vis,* **25:**304-311.

Gurevich L., and Slaughter M.M. (1993) Comparison of the waveforms of the ON bipolar neuron and the b-wave of the electroretinogram. *Vision Res,* **33:**2431-2435.

Hall M.O., Bok D., and Bacharach A.D. (1969) Biosynthesis and assembly of the rod outer segment membrane system. Formation and fate of visual pigment in the frog retina. *J Mol Biol,* **45:**397-406.

Halliwell B., Clement M.V., Ramalingam J., and Long L.H. (2000) Hydrogen peroxide. Ubiquitous in cell culture and in vivo? *IUBMB Life,* **50:**251-257.

Halliwell B., and Cross C.E. (1994) Oxygen-derived species: their relation to human disease and environmental stress. *Environ Health Perspect,* **Suppl 10:**5-12.

Halliwell B. (1991) Reactive oxygen species in living systems: source, biochemistry, and role in human disease. *Am J Med,* **91:**14S-22S.

Ham W.T. Jr., Mueller H.A., Ruffolo J.J. Jr., Guerry D. 3rd , Guerry R.K. (1982) Action spectrum for retinal injury from near-ultraviolet radiation in the aphakic monkey. *Am J Ophthalmol,* **93:**299-306.

Ham W.T. Jr, Ruffolo J.J. Jr, Mueller H.A., and Guerry D 3rd. (1980) The nature of retinal radiation damage: dependence on wavelength, power level and exposure time. *Vision Res,* **20:**1105-1111.

Ham W.T. Jr., Mueller H.A., Ruffolo J.J. Jr., and Clarke A.M. (1979) Sensitivity of the retina to radiation damage as a function of wavelength. *Photochem Photobiol,* **29:**735-743.

Ham W.T., Ruffolo J.J., Mueller H.A., Clarke A.M. and Moon M.E. (1978) Histologic analysis of photochemical lesions produced rhesus retina by short-wavelength light. *Invest Ophthalmol Vis Sci,* **17:**1029-1035.

Ham W.T. Jr., Mueller H.A., Sliney D.H. (1976) Retinal sensitivity to damage from short wavelength light. *Nature,* **260:**153-155.

Ham W.T. Jr., Mueller H.A., Goldman A.I., Newnam B.E., Holland L.M., and Kuwabara T. (1974) Ocular hazard from picosecond pulses of Nd: YAG laser radiation. *Science,* **185:**362-363.

Hargrave P.A. (2001) Rhodopsin structure, function and topography: The Friedenwald Lecture. *Invest Ophthalmol Vis Sci,* **42:**3-9.

Harman D. (1981) The Aging Process. *Proc Natl Acad Sci USA*, **78:**7124-7128.

Hart M.: (1992) Visual Adaptation. In Hart W.M. Jr., editor: *Adler's physiology of the eye*, ed 9, St. Louis, Mosby, pg. 523.

Haruta M., Sasai Y., Kawasaki H., Amemiya K., Ooto S., Kitada M., Suemori H., Nakatsuji N., Ide C., Honda Y., and Takahashi M. (2004) In vitro and in vivo characterization of pigment epithelial cells differentiated from primate embryonic stem cells. *Invest Ophthalmol Vis Sci*, **45**:1020-5.

Hauptmann H., and Cadenas E. (1997) The oxygen paradox: Biochemistry of active oxygen. Oxidative Stress and the Molecular Biology of Antioxidant Defenses. Cold Spring Harbor Laboratory Press. Pgs. 1-48.

Hawse J.R., Cumming J.R., Oppermann B., Sheets N.L., Reddy V.N., and Kantorow M. (2003) Activation of metallothioneins and alpha-crystallin/sHSPs in human lens epithelial cells by specific metals and the metal content of aging clear human lenses. *Invest Ophthalmol Vis Sci*, **44:**672-679.

Heiduschka P., Blitgen-Heinecke P., Tura A., Kokkinou D., Julien S., Hofmeister S., Bartz-Schmidt K.U., and Schraermeyer U. (2007) Melanin precursor 5,6-dihydroxyindol: protective effects and cytotoxicity on retinal cells in vitro and in vivo. *Toxicol Pathol*, **35:**1030-1038.

Hogan B., Beddington R., Costantini F., Lacy E. (1994) *Manipulating the Mouse Embryo. A Laboratory Manual*, 2nd edn. New York: Cold Spring Harbor Laboratory Press, p. 296

Hogan M.J., Alvarado J.A.: Retina. In Hogan M.J., Alvarado J.A., Weddell J.E., editors: *Histology of the human eye*, Philadelphia, 1971, Saunders, pg. 393.

Honda, S., Sugita, I., Miki, K., and Saito, I. (2004) The semi-quantitative comparison of oxidative stress mediated DNA single and double strand breaks using terminal deoxynucleotidyl transferase mediated end labeling combined with a slot blot technique. *Free Radic Res*, **38**:481-5.

Hood D.C., and Birch D.G. (1990) The A-wave of the human electroretinogram and rod receptor function. *Invest Ophthalmol Vis Sci*, **31:**2070-2081.

Hooks J.J., Nagineni C.N., Hooper L.C., Hayashi K., Detrick B. (2008) IFN-beta provides immuno-protection in the retina by inhibiting ICAM-1 and CXCL9 in retinal pigment epithelial cells. *J Immunol*, **180:**3789-3796.

Horwitz, J. (2003) Alpha-crystallin. *Exp Eye Res*, **76:**145-153.

Horwitz J. (2000) The function of alpha-crystallin in vision. *Semin Cell Dev Biol*, **11:**53-60.

Horwitz, J., Bova M.P., Ding L., Haley D.A., and Stewart P.L. (1999) Lens α-crystallin: Function and Structure. *Eye*, **13:**403-408.

Horwitz J., Bova M., Huang Q.L., Ding L., Yaron O., and Lowman S. (1998) Mutation of alpha B-crystallin: effects of chaperone-like activity. *Int J Biol Macromol,* **22:**263.269.

Horwitz J. (1993) The function of alpha-crystallin. *Invest Ophthalmol Vis Sci,* **34:**10-22.

Horwitz J. (1992) α-Crystallin can function as a molecular chaperone. *Proc Natl Acad Sci USA,* **89:**10449-10453.

Howes K.A., Liu Y., Dunaief J.L., Milam A., Frederick J.M., Marks A., and Baehr W. (2004) Receptor for Advanced Glycation End Products and Age-Related Macular Degeneration. *Invest Ophthalmol Vis Sci,* **45:**3713-3720.

Hu J., and Bok D. (2001) A cell culture medium that supports the differentiation of human retinal pigment epithelium into functionally polarized monolayers. *Mol Vis,* 7:14-9.

Hunot S., Brugg B., Ricard D., Michel P.P., Muriel M.P., Ruberg M., Faucheux B.A., Agid Y., and Hirsch E.C. (1997) Nuclear translocation of NF-kappaB is increased in dopaminergic neurons of patients with parkinson disease. *Proc Natl Acad Sci USA,* **94:**7531-7536.

Hurley J.B., and Chen J. (2001) Evaluation of the contributions of recoverin and GCAPs to rod photoreceptor light adaptation and recovery to the dark state. *Prog Brain Res,* **131:**395-405.

Ibaraki N., Chen S.C., Lin L.R., Okamoto H., Pipas J.M., and Reddy V.N. (2001) Human lens epithelial cell line. *Exp Eye Res,* **67**:577-85.

Ibaraki N., Chen S.C., Lin L.R., Okamoto H., Pipas J.M., Reddy V.N. (1998) Human lens epithelial cell line. *Exp Eye Res,* **67:**577-585.

Imai H., Kefalov V., Sakurai K., Chisaka O., Ueda Y., Onishi A., Morizumi T., Fu Y., Ichikawa K., Nakatani K., Honda Y., Chen J., Yau K.W., and Shichida Y. (2007) Molecular properties of rhodopsin and rod function. *J Biol Chem,* **282:**6677-6684.

Iriyama A., Fujiki R., Inoue Y., Takahashi H., Tamaki Y., Takezawa S., Takeyama K., Jang W.D., Kato S., and Yanagi Y. (2008) A2E, a pigment of the lipofuscin of retinal pigment epithelial cells, is an endogenous ligand for retinoic acid receptor. *J Biol Chem,* **283:**11947-11953.

Ishigooka H., Kitaoka T., Boutilier S.B., Bost L.M., Aotaki-Keen A.E., Tablin F., Hjelmeland L.M. (1993) Developmental expression of bFGF in the bovine retina. *Invest Ophthalmol Vis Sci,* **34:**2813-2823.

Iwaki T., Wisniewski T., Akiki I., Corbin E., Tomokane N., Tateishi J., and Goldman J.E. (1992) Accumulation of alphaB-crystallin in central nervouse system glia and neurons in pathologic conditions. *Am J Pathol,* **140:**345-356

Iwaki T., Kume-Iwaki A., Goldman J.E. (1990) Cellular distribution of alphaB-crystallin in non-lenticular tissues. *J Histochem Cytochem*, **38:**31-39.

Iwaki T., Kume-Iwaki A., Liem R.K., and Goldman J.E. (1989) AlphaB-crystallin is expressed in non-lenticular tissues and accumulates in Alexander's disease brain. *Cell*, **57:**71-78.

Jakob U., Gaestel M., Engel K., and Buchner J. (1993) Small heat shock proteins are molecular chaperones. *J Biol Chem*, **268:**1517-1520.

Jarrett S.G. and Boulton M.E. (2005) Antioxidant up-regulation and increased nuclear DNA protection play key roles in adaptation to oxidative stress in epithelial cells. *Free Radic Biol Med.* **15**:1382-91

Jiang S., Moriarty-Craige S.E., Orr M., Cai J., Sternberg P. Jr., and Jones D.P. (2005) Oxidant-induced apoptosis in human retinal pigment epithelial cells: dependence on extracellular redox state. *Invest Ophthalmol Vis Sci*, **46**:1054-61.

Jin G.F., Hurst J.S. and Godley B.F. (2001) Rod outer segments mediate mitochondrial DNA damage and apoptosis in human retinal pigmented epithelium. *Curr Eye Res*, **23:**11-19.

Jones S.E., Jomary C., Grist J., Makawana J., and Neal M.J. (1999) Retinal expression of gamma-crystallins in the mouse. *Invest Ophthalmol Vis Sci*, **40:**3017-3020.

Junqueira V.B.C., Barros S.B.M., Chan S.S., Rodrigues L., Giavarotti L., Abud R.L., and Deucher G.P. (2004) Aging and Oxidative Stress. *Mol. Aspects Med*, **25:**5-16.

Kaltschmidt B., Uherek M., Volk B., Baeuerle P.A., and Kaltschmidt C. (1997) Transcription factor NF-kappaB is activated in primary neurons by amyloid beta peptides and in neurons surrounding early plaques from patients with Alzheimer disease. *Proc Natl Acad Sci USA*, **94:**2642-2647.

Kamradt M.C., Chen F., and Cryns V.L. (2001) The small heat shock protein alphaB-crystallin negatively regulates cytochrome c- and caspase-8-dependent activation of caspase-3 by inhibiting its autoproteolytic maturation. *J Biol Chem*, **276:**16059-16063.

Kantorow M., and Piatigorsky J. (1998) Phosphorylations of alpha A- and alpha B-crystallin. *Int J Biol Macromol*, **22:**307-314.

Kapphahn R.J., Ethen C.M., Peters E.A., Higgins L., and Ferrington D.A. (2003) Modified αA-Crystallin in the Retina: Altered Expression and Truncation with Ageing. *Biochemistry*, **42:**15310-15325.

Kato K., Shinohara H., Kurobe N., Goto I., Inaguma Y., and Ohshima K. (1991) Immunoreactive αA-crystallin in rat non-lenticular tissues detected with a sensitive immunoassay method. *Biochim Biophys Acta*, **1080:**173-180.

Kerendian J., Enomoto H., and Wong C.G. (1992) Induction of stress proteins in SV-40 transformed human RPE-derived cells by organic oxidants. *Curr Eye Res,* **11**:385-96.

Khaliq A., Patel B., Jarvis-Evans J., Moriarty P., McLeod D., and Boulton M. (1995) Oxygen modulates production of bFGF and TGF-beta by retinal cells in vitro. *Exp Eye Res,* **60**:415-423.

Kim S.R., Jockusch S., Itagaki Y., Turro N.J., and Sparrow J.R. (2008)Mechanisms involved in A2E oxidation. *Exp Eye Res,* **86:**975-982.

Kim R., Lai L., Lee H.H., Cheong G.W., Kim K.K., Wu Z., Yokota H., Marqusee S., and Kim S.H. (2003) On the mechanism of chaperone activity of the small heat-shock protein of Methanococcus jannaschii. *Proc Natl Acad Sci USA*, **100**:8151-5.

King A., Gottlieb E., Brooks D.G., Murphy M.P., and Dunaief J.L. (2004) Mitochondria-derived reactive oxygen species mediate blue light-induced death of retinal pigment epithelial cells. *Photochem Photobiol*, **79:**470-475.

King G.L., and Suzuma K. (2000) Pigment-epithelium-derived factor--a key coordinator of retinal neuronal and vascular functions. *N Engl J Med,* **342:**349-351.

Kita M., and Marmor M.F. (1992) Effects on retinal adhesive force in vivo of metabolically active agents in the subretinal space. *Invest Ophthalmol Vis Sci,* **33:**1883-1887.

Klemenz R., Fröhli E., Steiger R.H., Schäfer R., Aoyama A. (1991) AlphaB-crystallin is a small heat shock protein. *Proc Natl Acad Sci USA,* **88:**3652-3656.

Kolb H., Fernandez E., and Nelson R. (2003) The organization of the vertebrate retina, July 2008, Webvision.med.utah.edu/

Kolb H. (1997) Amacrine cells of the mammalian retina: neurocircuitry and functional roles. *Eye.,* **11**:904-923.

Kolb H., Linberg K.A., and Fisher S.K. (1992) Neurons of the human retina: a golgi study. *J Comp Neurol,* **318:**147.

Kolb H., and Famiglietti E.V.(1976) Rod and cone pathways in retina of cat. *Invest Ophthalmol Vis Sci,* **15:**935.

Kraff M.C., Sanders D.R., Jampol L.M., and Lieberman H.L. (1985) Effect of an ultraviolet filtering intraocular lens on cystoid macular edema. *Ophthalmology,* **92:**366-369.

Kremers J.J., and van Norren D. (1989) Retinal damage in macaque after white light exposures lasting ten minutes to twelve hours. *Invest Ophthalmol Vis Sci,* **30:**1032-1040.

Krishnamoorthy R.R., Crawford M.J., Chaturvedi M.M., *et al.* (1999) Photooxidative stress down-modulates the activity of nuclear factor-kappaB via involvement of caspase-1, leading to apoptosis of photoreceptor cells. *J Biol Chem*, **274**:3734–3743.

Krishnan J., Lee G., Han S.U., and Choi S. (2008) Characterization of phototransduction gene knockouts revealed important signaling networks in the light-induced retinal degeneration. *J Biomed Biotechnol*, **2008**:327468.

Kuroki M., Voest E.E., Amano S., Beerepoot L.V., Takashima S., Tolentino M., Kim R.Y., Rohan R.M., Colby K.A., Yeo K.T., and Adamis A.P. (1996) Reactive oxygen intermediates increase vascular endothelial growth factor expression in vitro and in vivo. *J Clin Invest*, **98**:1667-1675.

Kuwabara T. (1970) Retinal recovery from exposure to light. *Am J Ophthalmol*, **70**:187-198.

Kuwabara T., and Gorn R.A. (1968) Retinal damage by visible light. An electron microscopic study. *Arch Ophthalmol*, **79**:69-78.

Kvanta A. (1994) Expression and secretion of transforming growth factor-beta in transformed and nontransformed retinal pigment epithelial cells. *Ophthalmic Res*, **26**:361-367.

Lamb L.E., and Simon J.D. (2004) A2E: A component of ocular lipofuscin. *Photochem Photobiol*, **79**:127-136.

Lamb T.D., and Pugh E.N. Jr. (1992) A quantitative account of the activation steps involved in phototransduction in amphibian photoreceptors. *J Physiol*, **449**:719-758.

Lanum J. (1978) The damaging effects of light on the retina: Empirical findings, theoretical and practical implications. *Surv Ophthalmol*, **22**:221-249.

LaVail M.M., Matthes M.T., Yasumura D., and Steinberg R.H. (1997) Variability in rate of cone degeneration in the retinal degeneration (rd/rd) mouse. *Exp Eye Res*, **65**:45-50.

LaVail M.M., and Gorrin G.M. (1987) Protection from light damage by ocular pigmentation: analysis using experimental chimeras and translocation mice. *Exp Eye Res*, **44**:877-879.

Lawwill T., Crockett S., and Currier G. (1977) Retinal damage secondary to chronic light exposure, thresholds and mechanisms. *Doc Ophthalmol*, **44**:379-402.

Lawwill T. (1973) Effects of prolonged exposure of rabbit retina to low intensity light. *Invest Ophthalmol Vis Sci*, **12**:45-51.

Lee E.S., and Flannery J.G. (2007) Transport of truncated rhodopsin and its effects on rod function and degeneration. *Invest Ophthalmol Vis Sci*, **48**:2868-2876.

Lem J., and Makino C.L. (1996) Phototransduction in transgenic mice. *Curr Opin Neurobiol,* **6:**453-458.

Li D., Sun F., and Wang K. (2004) Protein profile of aging and its retardation by caloric restriction in neural retina. *Biochem Biophys Res Commun,* **318:**253-258.

Li F., Cao W., and Anderson R.E. (2002) Protection of photoreceptor cells in adult rats from light-induced degeneration by adaptation to bright cyclic light. *Exp Eye Res,* **73:**569-577.

Liang F.Q., Green L., Wang C., Alssadi R., and Godley B.F. (2004) Melatonin protects human retinal pigment epithelial (RPE) cells against oxidative stress. *Exp Eye Res,* **78:**1069-1075.

Liang F.Q., and Godley B.F. (2003) Oxidative stress-induced mitochondrial DNA damage in human retinal pigment epithelial cells: a possible mechanism for RPE aging and age-related macular degeneration. *Exp Eye Res,* **76:**397-403.

Liles M.R., Newsome D.A., and Oliver P.D. (1991) Antioxidant enzymes in the aging human retinal pigment epithelium. *Arch Ophthalmol,* **109:**1285-1288.

Lin L.R., Carper D., Yokoyama T., and Reddy V.N. (1993) The effect of hypertonicity on aldose reductase, alpha B-crystallin, and organic osmolytes in the retinal pigment epithelium. *Invest Ophthalmol Vis Sci,* **34**:2352-9.

Lindquist S. (1986) The heat shock response. *Annu Rev Biochem,* **55:**1151-1191.

Liu J.P., Schlosser R., Ma W.Y., Dong Z., Feng H., Lui L., Huang X.Q., Liu Y., and Li D.W. (2004) Human alpha A- and alpha B-crystallins prevent UVA-induced apoptosis through regulation of PKCalpha, RAF/MEK/ERK and AKT signaling pathways. *Exp Eye Res,* **79:**393-403.

Lotery A., and Trump D. (2007) Progress in defining the molecular biology of age related macular degeneration. *Hum Genet,* **122:**219-236.

Lowe J., McDermott H., Pike I., Speudlove I., Landon M., and Mayer R. (1992) AlphaB-crystallin expresion in non-lenticular tissues and selective presence in ubiquinated inclusion bodies in human disease. *J Pathol,* **166:**61-68.

Lu L., Hackett S.F., Mincey A., Lai H., and Campochiaro P.A. (2006) Effects of different types of oxidative stress in RPE cells. *J Cell Physiol,* **206:**119-125.

Lund D.J. and Beatrice E.S. (1979) Ocular hazard of short pulse argon laser irradiation. *Health Phys,* **36:**7-11.

Lutsch G., Vetter R., Offhauss U., Wieske M., Grone H.J., Klemenz R., Schimke I., Stah J., and Benndorf R. (1997) Abundance and location of the small heat shock proteins HSP25 and alpha-B crystalline in rat and human heart. *Circulation,* **96:**3466-3476.

Ma Z.X., Hanson S.R.A., Lampi K.J., David L.L., Smith D.L., and Smith J.B. (1998) Age-related changes in human lens crystallins identified by HPLC and mass spectrometry. *Exp Eye Res*, **67**:21-30.

Machida S., Chaudhry P., Shinohara T., Singh D.P., Reddy V.N., Chylack L.T., Sieving P.A., and Bush R.A. (2001) Lens epithelium derived growth factor promotes photoreceptor survival in light-damaged and RCS rats. *Invest Ophthalmol Vis Sci,* **42**:1087-1095.

Mainster M.A., Ham W.T., and DeLori F.C. (1983) Potential Retinal Hazards. Instruments and Environmental Light Sources. *Ophthalmology,* **90**:927-932.

Mao Y.W, Liu J.P., Xiang H., and Li D.W. (2004) Human alphaA- and alphaB-crystallins bind to Bax and Bcl-X(S) to sequester their translocation during staurosporine-induced apoptosis. *Cell Death Differ,* **11**:512-26.

Margrain T.H., Boulton M., Marshall J., and Sliney D.H. (2004) Do blue light filters confer protection against age-related macular degeneration? *Prog Ret Eye Res,* **23**:523-531.

Marmor M.F. (1998) Structure, function and disease of the retinal pigment epithelium. The Retinal Pigment Epithelium, Oxford University Press, Pgs. 1-9.

Marmorstein A.D. (2001) The polarity of the retinal pigment epithelium. *Traffic,* **2**:867-872.

Marmorstein A.D., Finnemann S.C., Bonilha V.L., and Rodriguez-Boulan E. (1998) Morphogenesis of the retinal pigment epithelium: toward understanding retinal degenerative diseases. *Ann N Y Acad Sci,* **857**:1-12.

Marshall M.J., Nisbet N.W., Menage J., and Loutit J.F. (1972) Tissue repopulation during cure of osteopetrotic (mi/mi) mice using normal and defective (We/Wv) bone marrow. *Exp Hematol,* **10**:600-608.

Marshall J. (1970) Thermal and mechanical mechanisms in laser damage to the retina. *Invest Ophthalmol Vis Sci,* **9**:97-115.

Martin M., Macias M., Escames G., Reiter R.J., Agapito M.T., Ortiz G.G., and Acuna-Castroviejo, D. (2000) Melatonin-induced increased activity of the respiratory chain complexes I and IV can prevent mitochondrial damage induced by ruthenium red in vivo. *J Pineal Res,* **28**:242-248.

Masilamoni J.G., Jesudason J.P., Baben B., Jebaraj C.E., Dhandayuthapani S., and Jayakumar R. (2006) Molecular chaperone α-crystallin prevents detrimental effects of neuroinflammation. *Biochim Biophys Acta,* **1762**:283-294.

Mata NL, Moghrabi WN, Lee JS, Bui TV, Radu RA, Horwitz J, Travis GH. (2004) RPE65 is a retinyl ester binding protein that presents insoluble substrate to the isomerase in retinal pigment epithelial cells. *J Biol Chem,* **279**:635-43.

Matthews, J.N.S., Altman, D.G., Campbell, M.J., and Royston, P. (1990). Analysis of Serial Measurements in Medical-Research, *British Medical Journal,* 300, 230-235.

McLennan H.R., Degli Esposti M. (2004) The contribution of mitochondrial respiratory complexes to the production of reactive oxygen species. *J Bioenerg Biomembr*, **32:**153-162.

Melov S. (2004) Modeling mitochondrial function in aging neurons. *Trends. Neurosci*, **27:**601-606.

Miceli M.V., and Jazwinski S.M. (2005) Nuclear gene expression changes due to mitochondrial dysfunction in ARPE-19 cells: implications for age-related macular degeneration. *Invest Ophthalmol Vis Sci,* **46**:1765-73.

Migdale K., Herr S., Klug K., *et al.* (2003) Two ribbon synaptic units in rod photoreceptors of macque, human, and cat. *J Comp Neurol,* **455:**100.

Miller D. and Burns SK. (2004a) Visible Light. Ophthalmology. Mosby, Pgs. 31-32.

Miller D. and Scott C.A. (2004b) Light Damage to the Eye. Ophthalmology. Mosby, Pgs. 42-47.

Miyagi M., Sakaguchi H., Darrow R.M., Yan L., West K.A., Aulak K.S., Stuehr D.J., Hollyfield J.G., Organisciak D.T., and Crabb J.W. (2002) Evidence that light modulates protein nitration in rat retina. *Mol Cell Proteomics,* **4:**293-303.

Moriya M., Baker B.N., and Williams T.P. (1986) Progression and reversibility of early light induced alterations in rat retinal rods. *Cell Tissue Res,* **246:**607-621.

Moseley H., Foulds W.S., Allan D., and Kyle P.M. (1984) Routes of clearance of radioactive water from the rabbit vitreous. *Br J Ophthalmol,* **68:**145-151.

Mosmann T. (1983) Rapid colorimetric assay for cellular growth and survival: application to proliferation and cytotoxicity assays. *J Immunol Methods,* **65:**55-63.

Muchowski P.J., and Clark J.I. (1998) ATP-enhanced molecular chaperone functions of the small heat shock protein human alphaB crystallin. *Proc Natl Acad Sci USA*, **3:**1004-1009.

NIH Guidelines for the Genotyping of Rodents; http://oacu.od.nih.gov/ARAC/FinalGenotyping0602.pdf

Nagelhus E.A., Horio Y., Inanobe A., Fujita A., Haug F.M., Nielsen S., Kurachi Y., and Ottersen O.P. (1999) Immunogold evidence suggests that coupling of K+ siphoning and water transport in rat retinal Müller cells is mediated by a coenrichment of Kir4.1 and AQP4 in specific membrane domains. *Glia,* **26:**47-54.

Nagineni C.N., Samuel W., Nagineni S., Pardhasaradhi K., Wiggert B., Detrick B., and Hooks J.J. (2003) Transforming growth factor-beta induces expression of vascular endothelial growth factor in human retinal pigment epithelial cells: involvement of mitogen-activated protein kinases. *J Cell Physio,* **197**:453-462.

Nakata K., Crabb J.W., and Hollyfield J.G. (2005) Crystallin distribution in Bruch's membrane-choroid complex from AMD and age-matched donor eyes. *Exp Eye Res,* **80**:821-826.

Navarro A. (2004) Mitochondrial enzyme activities as biochemical markers of aging. *Mol Aspects Med,* **25**:37-48.

Newsome D.A., Dobard E.P., Liles M.R., and Oliver P.D. (1990) Human retinal pigment epithelial cells contain two distinct species of superoxide dismutase. *Invest Ophthalmol Vis Sci,* **31**:2508-2513.

Ng K.P., Gugiu B., Renganathan K., Davies M.W., Gu X., Crabb J.S., Kim S.R., Rózanowska M.B., Bonilha V.L., Rayborn M.E., Salomon R.G., Sparrow J.R., Boulton M.E., Hollyfield J.G., and Crabb J.W.(2008) Retinal pigment epithelium lipofuscin proteomics. *Mol Cell Proteomics,,* **7**:1397-1405.

Nishikawa S., Ishiguro S., Kato K., and Tamai M. (1994) A transient expression of alphaB-crystallin in the developing rat retinal pigmented epithelium. *Invest Ophthalmol Vis Sci,* **35**:4159-4164.

Noell W.K. (1980) Possible mechanisms of photoreceptor damage by light in mammalian eyes. *Vision Res,* **20**:1163-1171.

Noell W.K. (1979) Effects of environmental lighting and dietary vitamin A on the vulnerability of the retina to light damage. *Photochem Photobiol,* **29**:717-723.

Noell, W.K., Walker V., Kang B., and Berman S. (1966) Retinal damage by light in rats. *Invest Ophthalmol Vis Sci,* **5**:450-473.

Noell W.K. (1958) Differentiation, metabolic organization, and viability of the visual cell. *Arch Ophthalmol,* **60**:702-733.

Oertel M.F., May C.A., Bloemendal H., and Lutjen-Drecoll E. (2000) Alpha-B-crystallin expression in tissues derived from different species in different age groups. *Ophthalmologica.,* **214**:13-23.

Ogata N., Wang L., Jo N., Tombran-Tink J., Takahashi K., Mrazek D., Matsumura M. (2001) Pigment epithelium derived factor as a neuroprotective agent against ischemic retinal injury. *Curr Eye Res,* **22**:245-252.

Okatani Y., Wakatsuki A., and Reiter R.J. (2002) Melatonin protects hepatic mitochondrial respiratory chain activity in sensescence-accelerated mice. *Exp Eye Res,* **32**:143-148.

Oraedu A.C., Voaden M.J., and Marshall J. (1980) Photochemical damage in the albino rat retina: morphological changes and endogenous amino acids. *J Neurochem,* **35:**1361-1369.

Organisciak D.T., Darrow R., Gu X., Barsalou L., Crabb J.W. (2006) Genetic, age and light mediated effects on crystallin protein expression in the retina. *Photochem Photobiol,* **82:**1088-1096.

Organisciak D.T., Darrow R.M., Barsalou L., Kutty R.K., and Wiggert B. (2003) Susceptibility to retinal light damage in transgenic rats with rhodopsin mutations. *Invest Ophthalmol Vis Sci,* **44:**486-92.

Organisciak, D.T., and Winkler B.S. (1994) Retinal light damage: practical and theoretical considerations. *Prog Ret Eye Res,* **13:**1-29.

Organisciak D.T., Jiang Y.L., Wang H.M., Pickford M., and Blanks J.C. (1989) Retinal light damage in rats exposed to intermittent light. Comparison with continuous light exposure. *Invest Ophthalmol Vis Sci,* **30:**795-805.

Organisciak D.T., Wang H.M., Li Z.Y., and Tso M.O. (1985) The protective effect of ascorbate in retinal light damage of rats. *Invest Ophthalmol Vis Sci,* **26:**1580-1588.

Ortwerth B.J., Slight S.H., Prabhakaram M., Sun Y., and Smith J.B. (1992) Site-specific glycation of lens crystallins by ascorbic acid. *Biochem Biophys Acta,* **1117:**207-215.

O'Steen W.K., Anderson K.V., and Shear CR. (1974) Photoreceptor degeneration in albino rats: dependency on age. *Invest Ophthalmol Vis Sci,* **13:**334-339.

O'Steen W.K., Shear C.R., and Anderson K.V. (1972) Retinal damage after prolonged exposure to visible light. A light and electron microscopic study. *Am J Anat,* **134:**5-21.

O'Steen W.K., and Lytle R.B. (1971) Early cellular disruption and phagocytosis in photically-induced retinal degeneration. *Am J Anat,* **130:**227-233.

O'Steen W. K. (1970) Retinal and optic nerve serotonin and retinal degeneration as influenced by photoperiod. *Exp Neurol,* **27:**194-205.

Ostwald T.J., and Steinberg R.H. (1980). Localization of frog retinal pigment epithelium Na+-K+ ATPase. *Exp Eye Res,* **3:**351-360.

Ousman SS, Tomooka BH, van Noort JM, Wawrousek EF, O'Connor KC, Hafler DA, Sobel RA, Robinson WH, Steinman L. (2007) Protective and therapeutic role for alphaB-crystallin in autoimmune demyelination. *Nature,* **448:**474-479.

Parrish A.R., Catania J.M., Orozco J., Gandolfi A.J. (1999) Chemically induced oxidative stress disrupts the E-cadherin/catenin cell adhesion complex. *Toxicol Sci,* **51:**80-86

Pawar A.S., Qtaishat N.M., Little D.M., and Pepperberg D.R. (2008) Recovery of rod photoresponses in ABCR-deficient mice. *Invest Ophthalmol Vis Sci,* **49:**2743-2755.

Pawate S., Shen Q., Fan F., and Bhat N.R. (2004) Redox regulation of glial inflammatory response to lipopolysaccharide and interferongamma. *J Neurosci Res,* **77:**540-551.

Penn J.S., Anderson R.E. (1987a) Effect of light history on rod outer-segment membrane composition in the rat. *Exp Eye Res,* **44:**767-778.

Penn J.S., Naash M.I., and Anderson R.E. (1987b) Effect of light history on retinal antioxidants and light damage susceptibility in the rat. *Exp Eye Res,* **44:**779-788.

Penn J.S., Williams T.P. (1986) Photostasis: regulation of daily photon-catch by rat retinas in response to various cyclic illuminances. *Exp Eye Res,* **43:**915-928.

Pepe I.M. (1999) Rhodopsin and phototransduction. *J Photochem Photobiol,* **48:**1-10.

Perez, J, Perentes, E. (1994) Light-induced retinopathy in the albino rat in long-term studies: an immunohistochemical and quantitative approach. *Exp Toxicol Pathol,* **46:**229-235

Perlman I., and Normann R.A. (1998) Light adaptation and sensitivity controlling mechanisms in vertebrate photoreceptors. *Prog Retin Eye Res,* **17:**523-563

Pfeffer S.R. (1991) Targeting of proteins to the lysosome. *Curr Top Microbiol Immunol,* **170:**43-65.

Piatigorsky J. (1989) Lens crystallins and their genes: diversity and tissue-specific expression. *FASEB J,* **3**:1933-40.

Priebe L.A., Cain C.P., and Welch A.J. (1975) Temperature rise required for the production of minial lesions in the macaca mulatta retina. *Am J Ophthalmology,* **79**:405-443

Pryor W.A., Stanley J.P., and Blair E. (1976) Autoxidation of polyunsaturated fatty acids: II. A suggested mechanism for the formation of TBA-reactive materials from prostaglandin-like endoperoxides. *Lipids,* **11:**370-379.

Ramirez J.M., Ramirez A.I., Salazar J.J., de Hoz R., and Trivino A. (2001) Changes of astrocytes in retinal ageing and age-related macular degeneration. *Exp Eye Res,* **73:**601-615.

Ramirez J.M., Trivino A., Ramirez A.I., *et al.* (1996) Structural specializations of human retinal glial cells. *Vis Res,* **36:**2029.

Rao N.A., Saraswathy S., Wu G.S., Katselis G.S., Wawrousek E.F., and Bhat S. (2008) Elevated retina-specific expression of the small heat shock protein, alphaA-crystallin, is associated with photoreceptor protection in experimental uveitis. *Invest Ophthalmol Vis Sci,* **49:**1161-1171.

Rapp L.M., and Smith S.C. (1992) Morphologic comparisons between rhodopsin-mediated and short-wavelength classes of retinal light damage. *Invest Ophthalmol Vis Sci,* **33:**3367-3377.

Rapp L.M., and Williams TP. (1980) The role of ocular pigmentation in protecting against retinal light damage. *Vision Res,* **20:**1127-1131.

Rapp L.M, and Williams T.P. (1979) Damage to the albino rat retina produced by low intensity light. *Photochem Photobiol,* **29:**731-733.

Raviola E., and Gilula N.B. (1975) Intramembrane organization of specialized contacts in the outer plexiform layer of the retina: a freeze-fracture study in monkey ad rabbits. *J Cell Biol,* **65:**192.

Reiter R.J., Tan D.X., Osuna C., Gitto E., (2000) Actions of melatonin in the reduction of oxidative stress. A review. *J Biomed Sci,* **7:**444-458.

Remé C.R., Hafezi F., Marti A., Munz K., and Reinboth J.J. (1998) Light damage to retina and retinal pigment epithelium. The Retinal Pigment Epithelium. Oxford University Press, Pgs. 563-586.

Remington, L.A. (2005) Retina in Clinical Anatomy of the Visual System, 2nd edition, Elsevier, Butterworth, Heinemann, St. Louis, MI, Pgs. 55-85.

Ren S, *et al.* A Simplified Method to Prepare PCR Template DNA for Screening of Transgenic and Knockout Mice. *Contemporary Topics in Laboratory Animal Medicine*, **40(2)**: 27- 30, March 2001.

Renkawek K., de Jong W.W., Merk K.B., Frenken C.W., van Workum F.P., Bosman G.J. (1992) AlphaB-crystallin is present in reactive glial Creutzfeldt-Jakob disease. *Acta Neuropathol (Berl),* **83:**324-327.

Rizzolo L.J. (1991) Basement membrane stimulates the polarized distribution of integrins but not the Na,K-ATPase in the retinal pigment epithelium. *Cell Regul,* **11:**939-949.

Robinson M.L. and Overbeek P.A. (1996) Differential expression of αA- and αB-crystallin during murine ocular development. *Invest Ophthalmol Vis Sci,* **37:**2276-2284.

Robson J.G. and Frishman L.J. (1998) Dissecting the dark-adapted electroretinogram. *Doc Ophthalmol,* **95:**187-215.

Rodriguez de Turco E.B., Parkins N., Ershov A.V., and Bazan N.G. (1999) Selective retinal pigment epithelial cell lipid metabolism and remodeling conserves photoreceptor docosahexaenoic acid following phagocytosis. *J Neurosci Res,* **57:**479-486.

Roth F., Bindewald A., and Holz F.G. (2004) Keypathophysiologic pathways in age-related macular disease. *Graefes Arch Clin Exp Ophthalmol,* **242:**710-716.

Rozanowska M., Jarvis-Evans J., Korytowski W., Boulton M., Burke J.M., and Sarna T. (1995) Blue light induced reactivity of retinal age pigment. *J Biol Chem,* **270:**18825-18830.

Sakaguchi H., Miyagi M., Darrow R.M., Crabb J.S., Hollyfield J.G., Organisciak D.T., and Crabb J.W. (2003) Intense light exposure changes the crystallin content in retina. *Exp Eye Res,* **76:**131-133.

Sarks S.H., Arnold J.J., Killingsworth M.C., and Sarks J.P. (1999) Early drusen formation in the normal and aging eye and their relation to age related maculopathy: a clinicopathological study. *Br J Ophthalmol,* **83:**358-368.

Sarna T., Burke J.M., Korytowski W., Rozanowska M., Skumatz C.M.B., Zareba A., and Zareba M. (2003) Loss of melanin from human RPE with aging: possible role of melanin photooxidation. *Exp Eye Res,* **76:**89-98.

Sax C.M., and Piatigorsky J. (1994) Expression of the alpha-crystallin/small heat-shock protein/molecular chaperone genes in the lens and other tissues. *Adv Enzymol Relat Areas Mol Biol,* **69**:155-201.

Schägger H, von Jagow G (1987). Tricine-sodium dodecyl sulfate-polyacrylamide gel electrophoresis for the separation of proteins in the range from 1 to 100 kDa. *Anal Biochem,* **166:** 368-379.

Schauerte J.A., and Gafni A. (1995) Photodegradation of tryptophan residues and attenuation of molecular chaperone activity in alpha-crystallin are correlated. *Biochem Biophys Res Commun,* **212:**900-905.

Schutt F., Davies S., Kopitz J., Holz F.G., and Boulton M.E. (2000) Photodamage to human RPE cells by A2-E, a retinoid component of lipofuscin. *Invest Ophthalmol Vis Sci,* **41:**2303-2308.

Seigel G.M. (1999) The golden age of retinal cell culture. *Mol Vis,* **19**:4.

Seiler M.J., Liu O.L., Cooper N.G., Callahan T.L., Petry H.M., and Aramant R.B. (2000) Selective photoreceptor damage in albino rats using continuous blue light. A protocol useful for retinal degeneration and transplantation research. *Graefes Arch Clin Exp Ophthalmol,* **238:**599-607.

Sharma R.K., and Ehinger B.E.J. (2003) Development and structure of the retina. In Kaufman P.L., Alm A., editors: *Adler's physiology of the eye,* ed 10, St. Louis, Mosby, Pg. 319.

Sies H. (1991) Oxidants and Antioxidants. Oxidative Stress. Academic Press. Pgs. 1-7.

Singh K., Zewge D., Groth-Vasselli B., and Farnsworth P.N. (1996) A comparison of structural relationships among alpha-crystallin, human Hsp27, gamma-crystallins and beta B2-crystallin. *Int J Biol Macromol,* **19:**227-233.

Siu T.L., Morley J.W., Coroneo M.T. (2008) Toxicology of the retina: advances in understanding the defence mechanisms and pathogenesis of drug- and light-induced retinopathy. *Clin Experiment Ophthalmol,* **36:**176-185.

Smith R.S. (2001) Posterior Segment and Orbit. In *Systemic Evaluation of the Mouse Eye.*, CRC Press, Pgs. 25-44.

Smulders R.H.P.H., van Boekel M.A.M., and de Jong W.W. (1988) Mutations and modifications support a 'pitted-flexiball' model for alpha-crystallin. *Int J Biol Macromol*, **22:**187-196.

Sørensen BK, Højrup P, Østergård E, Jørgensen CS, Enghild J, Ryder LR, Houen G (2002). Silver staining of proteins on electroblotting membranes and intensification of silver staining of proteins separated by polyacrylamide gel electrophoresis. *Anal Biochem,* **304**: 33-41.

Spaide R. (2008) Autofluorescence from the outer retina and subretinal space: hypothesis and review. *Retina,* **28:**5-35.

Sparrow J.R., Kim S.R., Cuervo A.M., and Bandhyopadhyayand U. (2008) A2E, a pigment of RPE lipofuscin, is generated from the precursor, A2PE by a lysosomal enzyme activity. *Adv Exp Med Biol,* **613:**393-398.

Sparrow J.R., Nakanishi K., and Parish C.A. (2000) The lipofuscin fluorophore A2E mediates blue-light induced damage to retinal pigmented epithelial cells. *Invest Ophthalmol Vis Sci,* **41:**1981-1989.

Spector A., Chiesa R., Sredy J., and Garner W. (1985) cAMP-dependent phosphorylation of bovine lens alpha-crystallin. *Proc Natl Acad Sci USA*, **82:**4712-4716.

Spikes J.D., and Macknight M.L. (1972) Photodynamic effects on molecules of biological importance: amino acids, peptides and proteins. *Res Prog Org Biol Med Chem,* **1:**124-136.

Srinivasan A.N., Nagineni C.N., and Bhat S.P. (1992) Alpha A-Crystallin is Expressed in Non-Ocular tissues. *J Biol Chem*, **267:**23337-23341.

Strauss O. (2005) The retinal pigmented epithelium in visual function. *Physiol Rev,* **85:**845-881.

Steinberg R.H. (1985) Interactions between the retinal pigment epithelium and the neural retina. *Doc Ophthalmol*, **60:**327-346.

Strunnikova N., Zhang C., Teichberg D., Cousins S.W., Baffi J., Becker K.G., and Csaky K.G. (2004) Survival of Retinal Pigment Epithelium after Exposure to

Prolonged Oxidative Injury: A Detailed Gene Expression and Cellular Analysis. *Invest Ophthalmol Vis Sci*, **45**:3767-3777.

Strunnikova N., Baffi J., Gonzalez A., Silk W., Cousins S.W., and Csaky K.G. (2001) Regulated heat shock protein 27 expression in human retinal pigment epithelium. *Invest Ophthalmol Vis Sci*, **42**:2130-8.

Sun T.X., Das B.K., and Liang J.J. (1997) Conformation and functional differences between recombinant human lens alpha A- and alpha B-crystallin. *J Biol Chem*, **272**:6220-6225.

Sun S.C., Ganchi P.A., Ballard D.W., and Greene W.C. (1993) NF-kappa B controls expression of inhibitor I kappa B alpha: evidence for an inducible autoregulatory pathway. *Science*, **259**:1912-1915.

Szél A., Röhlich P., Caffé A.R., Juliusson B., Aquirre G., and Van Veen T. (1992) Unique topographic separation of two spectral classes of cones in the mouse retina. *J Comp Neurol*, **325(3)**:327-342.

Tanaka N., Tanaka R., Tokuhara M., Kunugi S., Lee Y.F., and Hamada D. (2008) Amyloid fibril formation and chaperone-like activity of peptides from alphaA-crystallin. *Biochemistry*, **47**:2961-2967.

Tanito M., Kaidzu S., Ohira A., and Anderson R.E. (2008) Topography of retinal damage in light-exposed albino rats. *Exp Eye Res*, **87**:292-295.

Tanito M,. Kaidzu S., Anderson R.E. (2007a) Delayed loss of cone and remaining rod photoreceptor cells due to impairment of choroidal circulation after acute light exposure in rats. *Invest Ophthalmol Vis Sci*, **48**:1864-1872.

Tanito M., Li F., Elliott M.H., Dittmar M., and Anderson R.E. (2007b) Protective effect of TEMPOL derivatives against light-induced retinal damage in rats. *Invest Ophthalmol Vis Sci*, **48**:1900-1905.

Tanito M, Haniu H, Elliott MH, Singh AK, Matsumoto H, Anderson RE (2006) Identification of 4-hydroxynonenal-modified retinal proteins induced by photooxidative stress prior to retinal degeneration. *Free Radic Biol Med*, **41**:1847-1859.

Tardieu A., Laporte D., Licinio P., Krop B., and Delaye M. (1986) Calf lens alpha-crystallin quaternary structure: a three layer tetrahedral model. *J Mol Biol*, **192**:711-724.

Taylor H.R., West S., Munoz B., Rosenthal F.S., Bressler S.B., and Bressler N.M. (1992) The long-term effect of visible light on the eye. *Arch Ophthalmol*, **110**:99-104.

Terai K., Matsuo A., and McGeer P.L. (1996) Enhancement of immunoreactivity for NF-kappa B in the hippocampal formation and cerebral cortex of Alzheimer's disease. *Brain Res*, **735**:159-168.

Terman A., Gustafsson B., Brunk U.T. (2006) Mitochondrial damage and intralysosomal degradation in cellular aging. *Mol Aspects Med,* **27:**471-482.

Thiagarajan G., Lakshmanan J., Chalasani M., and Balasubramanian D. (2004) Peroxynitrite Reaction with Eye Lens Proteins: α-Crystallin Retains Its Activity Despite Modification. *Invest Ophthalmol Vis Sci,* **45:**2115-2121.

Thomas B.B., Seiler M.J., Aramant R.B., Samant D., Qiu G., Vyas N., Arai S., Chen Z., Sadda S.R. (2007) Visual functional effects of constant blue light in a retinal degenerate rat model. *Photochem Photobiol,* **83:**759-765.

Thompson D.A., and Gal A. (2003) Vitamin A metabolism in the retinal pigment epithelium: genes mutations and diseases. *Prog Retin Eye Res,* **22:**683-703.

Toler S.M. (2004) Oxidative Stress Plays an Important Role in the Pathogenesis of Drug-Induced Retinopathy. *Exp Biol Med (Maywood),* **229:**607-615.

Tomany S.C., Cruickshanks K.J., Klein R., Klein B.E.K., and Knudtson M.D. (2004) Sunlight and the 10-year Incidence of Age-Related Maculopathy. *Arch Ophthalmol,* **122:**750-757.

Ueda T., Ueda T., Armstrong D. (1996) Preventive effect of natural and synthetic antioxidants on lipid peroxidation in the mammalian eye. *Ophthalmic Res,* **28:**184-192.

Urata Y., Honma S., Goto S., Todoroki S., Iida T., Cho S., Honma K., and Kondo T. (1999) Melatonin induces gamma-glutamylcysteine synthetase mediated by activator protein-1 in human vascular endothelial cells. *Free Radic Biol Med,* **27:**838-847.

van Antwerp D.J., Martin S.J., Kafri T., Green D.R., and Verma I.M. (1996) Suppression of TNF-alpha-induced apoptosis by NF-kappaB. *Science,* **274:**787-789.

van Best J.A., Putting B.J., Oosterhuis J.A., Zweypfenning R.C., and Vrensen G.F. (1997) Function and morphology of the retinal pigment epithelium after light-induced damage. *Microsc Res Tech,* **36:**77-88.

van Boekel M.A., Hoogakker S.E., Harding J.J., and de Jong W.W. (1996) The influence of some post-translational modifications on the chaperone-like activity of alpha-crystallin. *Ophthalmic Res,* **28:**32-38.

van den Heuvel R., Hendricks W., Quax W., and Bloemendal H. (1985) Complete structure of the hamster αA-crystallin gene. Reflection of an evolutionary history by means of exon shuffling. *J Mol Biol,* **185:**273-284.

van Norren D., and Schellekens P. (1990) Blue light hazard in rat. *Vision Res,* **30:**1517-1520.

Viatour P., Merville M.P., Bours V., and Chariot A. (2005) Phosphorylation of NF-kappaB and IkappaB proteins: implications in cancer and inflammation. *Trends Biochem Sci,* **30:**43-52.

Vives-Bauza C., Anand M., Shirazi A.K., Magrane J., Gao J., Vollmer-Snarr H.R., Manfredi G., Finnemann S.C. (2008) The age lipid A2E and mitochondrial dysfunction synergistically impair phagocytosis by retinal pigment epithelial cells. *J Biol Chem,* **283:**24770-24780.

Voorter C.E., and Mulders J.W., Bloemendal H., and de Jong W.W. (1986) Some aspects of the phosphorylation of alpha-crystallin A. *Eur J Biochem,* **160:**203-210.

Wakakura M., and Foulds W.S. (1993) Heat shock response and thermal resistance in cultured human retinal pigment epithelium. *Exp Eye Res.*, **56**:17-24.

Wang Y.D., Wu J.D., Jiang Z.L., Wang Y.B., Wang X.H., Liu C., and Tong M.Q. (2007) Comparative proteome analysis of neural retinas from type 2 diabetic rats by two-dimensional electrophoresis. *Curr Eye Res,* **32:**891-901.

Wang K., Wanchao M.A., Spector A. (1995) Phosphorylation of α-Crystallin in Rat Lenses in Stimulated by H_2O_2 But Phosphorylation Has No Effect on Chaperone Activity. *Exp Eye Res.* **61:**115-124.

Wasowicz M., Morice C., Ferrari P., Callebert J., and Versaux-Botteri C. (2002) Long-term effects of light damage on the retina of albino and pigmented rats. *Invest Ophthalmol Vis Sci,* **43:**813-820.

Werner J.S., Steele V.G., and Pfoff D.S. (1989) Loss of human photoreceptor sensitivity associated with chronic exposure to ultraviolet radiation. *Ophthalmology* **96:**1552-1558.

Wenzel A., Oberhauser V., Pugh E.N., Lamb T.D., Grimm C., Samardzija M., Fahl E., Seeliger M.W., Remé C.E., and von Lintig J. (2005) The retinal G protein-coupled receptor (RGR) enhances isomerohydrolase activity independent of light. *J Biol Chem,* **280:**29874-29884.

Weymouth A.E., and Vingrys A.J. (2008) Rodent electroretinography: methods for extraction and interpretation of rod and cone responses. *Prog Retin Eye Res,* **27:**1-44.

White T.J., Mainster M.A., Wilson P.W., and Tips J.H. (1971) Chorioretinal temperature increases from solar observation. *Bull Math Biophys*, **33**:1-17

Williams R.A., Howard A.G., Williams T.P. (1985) Retinal damage in pigmented and albino rats exposed to low levels of cyclic light following a single mydriatic treatment. *Curr Eye Res,* **4:**97-102.

Williams T.P., and Howell W.L. (1983) Action spectrum of retinal light-damage in albino rats. *Invest Ophthalmol Vis Sci,* **24:**285-287.

Winkler B.S., Boulton M.E., Gottsch J.D., and Sternberg P. (1999) Oxidative damage and age-related macular degeneration. *Mol Vis*, **5:**32-43.

Winkler B.S., Boulton M.E., Gottsch J.D., and Sternberg P. (1996) Oxidative damage and age-related macular degeneration. *Ophthalmic Res*, **28:**184-192.
Wistow G. (1993) Possible tetramer-based quarternary structure for the alpha-crystallin and small heat shock proteins. *Exp Eye Res*, **56:**729-732.

Wistow G., Piatigorsky J. (1988) Lens crystallins: the evolution and expression of proteins for a highly specialized tissue. *Annu Rev Biochem*, **57:**479-504.

Witkorsky P.:Functional anatomy of the retina. In Tasman W., Jaeger E.A., editors: *Duane's foundations of clinical ophthalmology*, Vol 1, Philadelphia, 1994, Lippincott.

Witmer A.N., Vrensen G.F., Van Noorden C.J., Schlingemann R.O. (2003) Vascular endothelial growth factors and angiogenesis in eye disease. *Prog Retin Eye Res*, **22:**1-29.

Wolf G. (2003) Lipofuscin and Macular Degeneration. *Nutr Rev*, **61:**342-346.

Wolff E. (1955) The Eyeball. In *The Anatomy of the Eye and Orbit*, McGraw-Hill Book Company, Pgs.88-121.

Wong C.G., and Lin N.G. (1989) Induction of stress proteins in culutred human RPE-derived cells. *Curr Eye Res*, **8:**537-545.

Wolter J.R. (1959) Glia of the human retina. *Am J Ophthalmol*, **49:**370-393.

Wu J., Seregard S., and Algvere P.V. (2006) Photochemical Damage of the Retina. *Surv Ophthalmol.*, **51:**461-481.

Wyse, J.P. (1980) Renewal of rod outer segments following light-induced damage of the retina. *Can J Ophthalmol*, **15**:15-19.

Xi J., Farjo R., Yoshida S., Kern T.S., Swaroop A., and Andley U.P. (2003a) A comprehensive analysis of the expression of crystallins in the mouse retina. *Mol Vis*, **9:**410-419.

Xi, J.H., Bai F., Andley U.P. (2003b) Reduced survival of lens epithelial cells in the alphaA-crystallin knockout mouse. *J Cell Sci*, **116:**1073-1085.

Yang L., Zhu X., and Tso M.O.M. (2007) Role of NF-κB and MAPKS in light-induced photoreceptor apoptosis. *Invest Ophthalmol Vis Sci*, **48:**4766-4776.

Yau K.W. (1994) Phototransduction mechanism in retinal rods and cones: The Friedenwald Lecture. *Invest Ophthalmol Vis Sci*, **35:**9-32.

Young R.W. (1974) Proceedings: Biogenesis and renewal of visual cell outer segment membranes. *Exp Eye Res*, **18:**215-223.

Young R.W. (1976) Visual cells and the concept of renewal. *Invest Ophthalmol Vis Sci*, **15:**700-725.

Young R.W., and Bok D. (1969) Participation in the retinal pigment epithelium in the rod outer segment renewal process. *J Cell Biol,* **42:**392-403.
Young R.W., and Droz B. (1968) The renewal of protein in retinal rods and cones. *J Cell Biol,* **39:**169-184.

Young R.W. (1967) The renewal of the photoreceptor cell outer segments. *J Cell Biol,* **33:**61.

Zabel U., Henkel T., Silva M.S., and Baeuerle P.A. (1993) Nuclear uptake control of NF-kappa B by MAD-3, an I kappa B protein present in the nucleus. *EMBO J,* **12:**201-211.

Zangar R.C., Davydov D.R., and Verma S. (2004) Mechanisms that regulate production of reactive oxygen species by cytochrome P450. *Toxicol Appl Pharmacol,* **199**:316-331.

Zarbin M.A. (2004) Current concepts in the Pathogenesis of Age-Related Macular Degeneration. *Arch Ophthalmol,* **122:**598-614.

Zareba M., Szewczyk G., Sarna T., Hong L., Simon J.D., Henry M.M., Burke JM. (2006) Effects of photodegradation on the physical and antioxidant properties of melanosomes isolated from retinal pigment epithelium. *Photochem Photobiol,* **82:**1024-1029.

Zeng H.Y., Tso M.O., Lai S., and Lai H. (2008) Activation of nuclear factor-kappaB during retinal degeneration in rd mice. *Mol Vis,* **14:**1075-1080.

Zeng C., Lee J.T., Chen H., Chen S., Hsu C.Y., and Xu J. (2005) Amyloid-beta peptide enhances tumor necrosis factor-alpha-induced iNOS through neutral sphingomyelinase/ceramide pathway in oligodendrocytes. *J Neurochem,* **94:**703-712.

Zinn K.M., and Mockel-Pohl S. (1973) Fine structure and function of ocular tissues: lens and zonules. *Int Ophthalmol Clin,* **13:**143-155.

Appendix 1

TYPE OR PRINT CLEARLY **PLEASE FILL IN EVERY BLANK OR MARK "NA"**

PENNSYLVANIA COLLEGE OF OPTOMETRY
INSTITUTIONAL ANIMAL CARE AND USE COMMITTEE (IACUC)
APPLICATION FOR IACUC APPROVAL

PROTOCOL # A-MT0505-00

Principal Investigator*:MELISSA E. TREGO Degree: OD

Address: PCO 8360 OLD YORK ROAD, ELKINS PARK Dept: RESEARCH Phone: 215-780-1427

Emergency Contact: MELISSA TREGO, ALEXANDER DIZHOOR Phone: 267-735-9657 (MET)

Project Title: ALPHA CRYSTALLINS AND RETINAL PROTECTION AGAINST LIGHT DAMAGE & OXIDATIVE STRESS

Co-Investigators*:

Name	Dept	Phone
Alexander Dizhoor	Research	1468
Pierrette Dayhaw-Barker	BasicSci	1257

Technicians*:

Name	Dept	Phone

*** Please supply C.V.'s and/or proof of experience and qualifications with aspects in protocol.**

I. RESEARCH CATEGORIES

Major Categories of Research Use: Please check as applicable. Please attach a narrative describing the detailed purpose of the animal use, the risks to the animals and handlers, the experimental design, and the benefits occurred by the research. If an application for funding exists that includes the above, it may be substituted for the narrative attachment.

A. X Euthanize and harvest tissue (detail method euthanasia)
B. ____ Immunization/Antibody Production (include antigen, adjutant use, route of immunization, method of obtaining blood as well as volume & frequency)
C. ____ Physiologic Measurements (provide detailed descriptions)
D. ____ Dietary Manipulations (food or water restriction, special diets, provide details on parameters, monitoring and justify)
E. ____ Pharmacology/Toxicology (materials used. dose, route of administration, frequency, duration, endpoint)
F. ____ Behavioral Studies (provide detailed description)
G. ____ Trauma (provide a detailed description)
H. ____ Oncology/Tumor Transplantation (provide information on origin, passage, adventitious pathogen testing [MAP], biohazard potential, endpoint)
I. ____ Sampling (tissue/substances amount, frequency, method, etc.)
J. ____ Dosing (agent, dose, route of administration, frequency, duration)
K. X Breeding Colony (justify need)
L. ____ Biohazardous /Infectious Agents (Describe the nature of hazard and personnel safety precautions)
M. ____ Chronic or Prolonged Restraint (provide justification for restraint, a description of the device and duration of the restraint)
N. ____ Surgery
  ____ Survival Surgery
  ____ Non-Survival Surgery
  ____ Multiple Major Survival Surgery: species____ (Same animal surviving two or more surgeries) Provide adequate justification for need.
O. ____ Specialized Housing/Husbandry (contact Veterinary Resources, and describe arrangements)

II. FUNDING SOURCE*

CURRENT OR ANTICIPATED
_____X___ NIH - K08 RESEARCH TRAINING GRANT
_____PHS
_____NSF
_____State Funds
_____Departmental/Internal Funds
_____Other External Funds (specify): _____

* Should match project budgetary information

III. ANIMAL USAGE

Species/Strain	SOURCE	Weight	Age	Sex	(# PER YEAR) YR1	YR2	YR3	Census
MICE:129Sv:CryA1	NIH	15-35 g	0-12 months	M and F	max. 200	200	200	~50
MICE:129Sv	Alexander Dizhoor, PhD Charles River or Teconic, Inc.	15-35 g	0-12 months	M and F	max. 200	200	200	~50

If additional species/strains are being requested, include on an additional page

Are animals to be housed individually or in groups? Individually and in groups (Male mice and lactating females will be housed individually)

Justify species and number of animals to be used: At the present time, the 129Sv:CryA1 line is not available by commercial vendor (only available through the NIH). Additionally, it is the only animal species available with the alpha-crystallin gene knockout. Establishing and maintaining the line will require regular routine breeding to provide age specific groups for forthcoming projects/protocols and the culling of older/less productive animals and introduction of new breeders. Approximately 200 animals per year should be sufficient for the statistical analysis of the morphological and physiological changes which occur in the retinal cells of the knockout mice. It is estimated that of those 200 animals, approximately 50 will be utilized for breeding, while the remaining 150 will be used for experimentation and harvesting of tissue. Additionally, approximately 200 animals per year should be sufficient for the use as controls in comparison with the knockout α-crystallin mice. It is estimated that of those 200 animals, approximately 50 will be utilized for breeding, while the remaining 150 will be used for experimentation and harvesting of tissue and used as controls. It is estimated at this time that no more than ~50 animals will be housed for breeding at any given time.

Does the procedure have the potential to involve momentary pain, distress, or discomfort without the use of anesthetics, analgesics, or tranquilizers? __X__Yes ___No

If yes, what anesthesia will be used: Ketamine (IP), Xylazine (IP)

Justify: For histological analysis of mice retinas, mice will be euthanized by IP injection of 210 mg/kg ketamine/21 mg/kg xylazine followed by cervical dislocation and perfused through the heart first with buffer saline and then 4% formaline solution, after which eyes will be enucleated for subsequent histological procedures. Isofluran can be used for anesthesia during mouse tail clipping (3-5mm long), although this procedure is required only for older animals, this does not cause pain/distress in younger mice (3 weeks of age). 3 week old pups will be used for the tail clipping. For blue light effects in the retinal damage, a standard anesthesia of IP or IM injection of 20 mg/kg Ketamine/8 mg/kg Xylazine will be used.

RESTRAINT METHODS, INCLUDING GENERAL ANESTHESIA FOR PROCEDURES:

SPECIES & #	PHYSICAL	CHEMICAL	DESCRIPTION (drug name, dose, route; for physical restraint--duration and frequency)
Mice (Euthanasia)		X	CO_2 (administered through anesthesia chamber, confirmation through exsanguinations)
Mice		X	210mg/kg ketamine (IP, IM) and 21 mg/kg xylazine (IP,IM)

nce

IV. SURGERY

Survival Surgery*

A. Procedure _____ Species_____
B. Anesthesia _____
C. Building & Room Number where surgery will take place _____
D. Person performing survival surgery _____
E. Describe Post-Operative Care (e.g., supportive fluids, analgesics, antibiotics, other drugs & frequency of observation) _____
_____
F. Person(s) providing & recording post-operative care _____

*Describe in detail the surgery, aseptic procedures & post-operative care in the NARRATIVE section.

Non-Survival Surgery

A. Procedure _____ Species_____
B. Anesthesia _____
C. Method of Euthanasia _____
D. Building & Room Number where surgery will take place _____
E. Person(s) performing non-survival surgery _____

V. LOCATIONS OF ANIMAL USAGE*

Please list all locations where Animal Procedures will be performed & check the appropriate blank. It is preferred, when possible, procedures should be performed in the CMC Procedure Rooms. These areas will be inspected, randomly, on a semiannual basis.

	Building	Floor/Room #	LABORATORY	ANIMAL FACILITIES PROCEDURE ROOM	TYPE OF PROCEDURE
	PCO, South Wing	4/S418-423	S418-S423	X	Euthanasia, Harvesting
	PCO, South Wing	4/S424	--------	X	Breeding, tail clipping, disposal

Animals may not be housed in an investigator's laboratory for more than 24 hours unless specifically approved by the IACUC. Submit documentation for this approval with this application.*

VI. BIOHAZARD INFORMATION

Infectious agents, radioactive substances, toxic chemicals/chemical carcinogens, recombinant DNA and ionizing and non-ionizing radiation to be used in animal protocols MUST BE reviewed and approved by the PCO Biosafety and/or Nuclear Radiation Committee(s) PRIOR TO submission to the IACUC.

Please indicate the general biohazard being used **in-vivo**:

Infectious Agents_____ Radioactive Substances_____ Toxic Chemicals/ Chemical Carcinogens_____ Recombinant DNA_____

onizing and Non-ionizing radiation _____

ame of Agent _____

lease provide:
A) BSL level (1, 2 or 3) for infectious agents _____
B) Concentration _____
C) Route of administration _____
D) Duration of exposure _____
E) Room location where agent is administered _____
F) Location of animal housing post exposure _____
G) Length of time animals will be kept following exposure _____
H) Method of animal disposal _____

re there risks from biohazardous materials or their metabolic products to: (Circle Y/N)

Yes (No) Investigators using agents
Yes (No) Animal Care Personnel
Yes (No) Other Personnel (Maintenance, employees, or visitors to animal care center)

If hazardous agents are to be used, approval from the appropriate committees is required.

II. TRAINING OF RESEARCH PERSONNEL

escribe your experience and training in the care and use of laboratory animals. Be specific about training courses.

ithin the past year, have you and/or your personnel (scientists, students, and technicians) attended continuing education rograms concerning the care and utilization of laboratory animals in biomedical research? Yes _X_ No ___
escribe the nature of the education programs/courses that were attended within the past year.

- Traveled to the laboratory of Dan Gibbs, PhD and David Williams, PhD at the UCSD School of Medicine in La Jolla, CA to observe and participate in the proper isolation of mouse RPE.
- Course: Occupational Health and Safety in the Laboratory Workshop; January 4, 2006 by Dr. Jean Marie Pagani

training CD titled, "Training in Basic Biomethodology for Laboratory Mice" has been viewed (see attachement)

ave taken the following on-line training provided by LATA:

1.) The Humane Care & Use of Laboratory Animals
2.) The Humane Care & Use of the Laboratory Mouse
3.) Anesthesia & Analgesia of Rodents
4.) Occupational Health and Safety with Laboratory Animals

ttended a hands-on training session with the CCMC (Animal facility orientation)

ill attend a hands-on training session with the CCMC (Mouse handling procedures)

no, when do you and/or your personnel plan on attending such a course?

III. AREA OF RESPONSIBILITY

he Animal Care Coordinator is responsible for maintaining programs of laboratory animal care, including animal procurement, usbandry, disease control and prevention, humane treatment and adequate veterinary care under the supervision of a doctor of eterinary medicine.

he Principal Investigator is responsible for all aspects of the research protocol including post-operative monitoring and care, esearch-related complications, and humane treatment by investigative personnel.

e Principal Investigator is responsible for making daily checks of their animals and for euthanizing animals in distress. In the ent that euthanasia or other intervention is necessary for humane reasons, the investigator will be consulted whenever possible. owever, if the investigator is unavailable, it is the responsibility of the Institution or it agent(s), including the attending

veterinarian, animal care staff, or IACUC members, to use whatever means is required to relieve the animal's pain or distress. This may range from mild tranquilization to relieve anxiety to euthanasia for insufferable pain. Death as an endpoint of convenience is not acceptable.

ASSURANCE OF COMPLIANCE WITH PUBLIC HEALTH SERVICE POLICY ON HUMANE CARE AND USE OF LABORATORY ANIMALS

The Pennsylvania College of Optometry assures that professionally acceptable standards governing the care, treatment, and use of animals, including appropriate use of anesthetic, analgesic, tranquilizing drugs, prior to, during, and following actual research, teaching, testing, surgery, or experimentation were followed.

The institution adheres to the standards and regulations under the Animal Welfare Act. There are no exceptions.

I have considered alternatives to animal use in these procedures and could find none.

LIST METHODS AND SOURCES USED TO CONSIDER ALTERNATIVES:

_____ Animal Welfare Information Center

X __ Literature Search

_____ Biological Abstracts

_____ Current Research Information Center

_____ Index Medicus

X __ Other (Please specify) Database Search _____

DATABASE LITERATURE SEARCH

Identify the services (computer databases, literature searches, etc.) that were used to obtain information on alternatives to painful procedures, use of live animals and prevention of unnecessary duplication of research.

A MINIMUM OF TWO DATABASES MUST BE USED.

Please check below the databases and your search strategy or key words. (Refer to instructions for examples.)

DATE OF SEARCH: March 27, 2006 _____

DATABASES: MEDLINE__X__; AGRICOLA____; EMBASE____; PSYCHINFO____; OTHER__X (Google Scholar)__

STRATEGY OR KEY WORDS: mouse breeding + knock out mice + colony management (for breeding purposes) retinal explants + light damage + protein isolation + RNA isolation (for use of *in vivo* studies)

Please include the literature reference used to consider alternatives to animal use:

DO NOT EXIST

PRINCIPAL INVESTIGATOR'S ACKNOWLEDGMENT OR RESPONSIBILITY

I certify that the activities described in this form do not unnecessarily duplicate previous experiments.

I certify the above protocol will be conducted in compliance with the Federal, State, and local policies and regulations. I also acknowledge full responsibility for knowledge of and compliance with all applicable standards governing radioactive or biohazardous materials involved in my project. I understand that compliance with these policies is a prerequisite for purchasing and housing animals, and for the use of animals in research and teaching at professional schools and colleges.

THE INFORMATION GIVEN ABOVE IS A COMPLETE AND ACCURATE SUMMARY OF PROCEDURES PERTAINING TO ANIMAL CARE AND USE IN THE PROPOSED PROJECT; IF THE RESEARCH PLAN SHOULD REQUIRE REVISION, I WILL INFORM THE IACUC. I AGREE TO ABIDE BY THE PROVISIONS OF THE GUIDE FOR THE CARE AND USE OF LABORATORY ANIMALS. I WILL PERMIT EMERGENCY VETERINARY CARE TO ANIMALS SHOWING EVIDENCE OF PAIN OR ILLNESS IF NOT THE DESIRED EFFECT OF THE ABOVE APPROVED TECHNIQUES. I UNDERSTAND THAT I MUST OBTAIN REAPPROVAL ANNUALLY.

Melissa E. Trego, OD _____ March 27, 2006
Principal Investigator Date

PROTOCOL APPROVAL

Veterinarian approval: Yes ____ No ____ _____
Signature Date

IACUC Chairperson approval: Yes ____ No ____ _____
Signature Date

Attachment to Protocol # A-MT0505-00
Narrative:

The purpose of this protocol is to establish animal procedures at PCO for the next 3-year period. The animals associated with this protocol will be accounted for regardless of whether or not they will be used in an actual experiment.

RATIONALE **for using mouse models:** Mice have typical mammalian retinas that are well characterized anatomically and physiologically. Various mouse retinal proteins are well studied and their primary structures are determined. Of the non-human mammalian species, the mouse genome is best elucidated, as shown in the particular protein of interest, αA-crystallin (see BLAST attachment). Mice are fast breeders and produce sufficient amounts of tissue, allowing reliable statistical analysis of results. Mice can be easily adapted to darkness or to light before collecting retinas or conducting electrophysiological studies. Models for expression of various retinal proteins in mice have been successfully used in the past and are well documented. Mouse transgenic services are widely available. Published protocols are also widely available.

MOUSE TAILS CLIPPING FOR ISOLATION OF DNA (minor **Code A** procedure). This common technique is described in many protocols, for example, a laboratory manual, "Manipulating the Mouse Embryo" by B. Hogan et al., Cold Spring Harbor Laboratories Press, 1994, pp. 296-298. Mice of age 3 weeks will be labeled with a small identification ear tag number (National Band and Tag Co., Newport, KY). A small piece (~ **3-5** mm long) of the tip of the tail (wiped with 70% ethanol just before the cutting) will be clipped using a sterile razor blade wiped with ethanol. Some protocols use 0.5ml/L Isoflurane for anesthesia, but young mice such as we are going to use, do not experience pain/distress during this minor procedure so the tail clipping for 3-weeks without anesthesia is widely used and commonly accepted. Short-term minor bleeding after the tail clipping is common and no special further treatment is required, however, before the animals are put back into the cage, the bleeding will be stopped by pressing on and holding with an aseptic glove at the end of the tail until the clot is completely formed. Tail clipping will be performed for each mouse once **at the age of 3 weeks, when this procedure is painless for the animals.**

BREEDING procedure. Strains: **MICE of the same genetic backgrounds** will be used (**129Sv**). **Breeding will be necessary to maintain the homozygous transgenic lines and possible breeding between the nontransgenic (control) mice with the homozygous α-crystallin knock-out mice may occur, depending on the experimental results** (i.e. if there is a big difference between the results of the control with the knockout mouse, it may be also beneficial to examine hemizygous progeny between the control and knockout). Between 20 and 30 breeding pairs will be used yearly on the average - the exact number depends on the frequency and viability of the transgenic progeny. **Housing**: PCO, 4 floor, S424E and quarantine rooms. **How often**: once every 6 months to maintain the lines. **Estimated quantity of offsprings**: up to 500-600 mice, depending on the statistical requirements (to be determined experimentally) in 20-25 small cages (19x20x13cm)/year, total of up to 1800 for the whole 3-year project. **Number of mice per small cage (19x20x13 cm)**: 4 each - Each cage will house one nontransgenic heterozygous male and 1-3 homozygous females or one pair of homozygous female and male. When pregnant, each female will be housed in a separate cage. In 3 weeks after birth, progeny mice will be tagged, and DNA isolated from small pieces of their tails for genotyping. Immediately after tagging and tail clipping females and males from the progeny will be housed in separate cages, 4 mice per cage until used in experiment or for further breeding as described above. **Typically, after one year, males and females will by replaced with the fresh breeding pairs from the progeny, and used in experiments (euthanized for subsequent tissue harvesting).**

TYPE OR PRINT CLEARLY — PLEASE FILL IN EVERY BLANK OR MARK "NA"

PENNSYLVANIA COLLEGE OF OPTOMETRY
INSTITUTIONAL ANIMAL CARE AND USE COMMITTEE (IACUC)
APPLICATION FOR IACUC APPROVAL

PROTOCOL # A-MT0603

Principal Investigator*:MELISSA E. TREGO _____ Degree: OD _____

Address: PCO 8360 OLD YORK ROAD, ELKINS PARK___Dept: RESEARCH Phone: 215-780-1427_____

Emergency Contact: MELISSA TREGO, ALEXANDER DIZHOOR _____Phone: 267-735-9657 (MET)

Project Title: ALPHA CRYSTALLINS AND RETINAL PROTECTION AGAINST LIGHT DAMAGE & OXIDATIVE STRESS _____

Co-Investigators*:			**Technicians*:**		
Name	Dept	Phone	Name	Dept	Phone
Alexander Dizhoor	Research	1468	_____	_____	_____
Pierrette Dayhaw-Barker	BasicSci	1257	_____	_____	_____
_____	_____	_____	_____	_____	_____
_____	_____	_____	_____	_____	_____

** **Please supply C.V.'s and/or proof of experience and qualifications with aspects in protocol.**

II. RESEARCH CATEGORIES

Major Categories of Research Use: Please check as applicable. Please attach a narrative describing the detailed purpose of the animal use, the risks to the animals and handlers, the experimental design, and the benefits occurred by the research. If an application for funding exists that includes the above, it may be substituted for the narrative attachment.

A. X Euthanize and harvest tissue (detail method euthanasia)
B. ____ Immunization/Antibody Production (include antigen, adjutant use, route of immunization, method of obtaining blood as well as volume & frequency)
C. ____ Physiologic Measurements (provide detailed descriptions)
D. ____ Dietary Manipulations (food or water restriction, special diets, provide details on parameters, monitoring and justify)
E. ____ Pharmacology/Toxicology (materials used. dose, route of administration, frequency, duration, endpoint)
F. ____ Behavioral Studies (provide detailed description)
G. ____ Trauma (provide a detailed description)
H. ____ Oncology/Tumor Transplantation (provide information on origin, passage, adventitious pathogen testing [MAP], biohazard potential, endpoint)
I. ____ Sampling (tissue/substances amount, frequency, method, etc.)
J. ____ Dosing (agent, dose, route of administration, frequency, duration)
K. ____ Breeding Colony (justify need)
L. ____ Biohazardous /Infectious Agents (Describe the nature of hazard and personnel safety precautions)
M. ____ Chronic or Prolonged Restraint (provide justification for restraint, a description of the device and duration of the restraint)
N. ____ Surgery
  _____ Survival Surgery
  _____ Non-Survival Surgery
  _____ Multiple Major Survival Surgery: species_____ (Same animal surviving two or more surgeries) Provide adequate justification for need.
O. _____ Specialized Housing/Husbandry (contact Veterinary Resources, and describe arrangements)

II. FUNDING SOURCE*

CURRENT OR ANTICIPATED
_____X___ NIH - K08 RESEARCH TRAINING GRANT
_____PHS
_____NSF
_____State Funds
_____Departmental/Internal Funds
_____Other External Funds (specify): _____

* Should match project budgetary information

III. ANIMAL USAGE

Species/Strain	SOURCE	Weight	Age	Sex	(# PER YEAR) YR1	YR2	YR3	Census
MICE:129Sv:CryA1	NIH	15-35 g	0-12 months	M and F	max. 75	75	50	~20-25
MICE:129Sv	Alexander Dizhoor, PhD Charles River or Teconic, Inc.	15-35 g	0-12 months	M and F	max. 75	75	50	~20-25

If additional species/strains are being requested, include on an additional page

Are animals to be housed individually or in groups? Individually and in groups (Male mice and lactating females will be housed individually)

Justify species and number of animals to be used: At the present time, the 129Sv:CryA1 line is not available by commercial vendor (only available through the NIH). Additionally, it is the only animal species available with the alpha-crystallin gene knockout. Approximately 75 animals per year should be sufficient for the statistical analysis of the morphological and physiological changes which occur in the retinal cells of the knockout mice for the first two years. This number is expected to decrease to 50 in the third year. It is estimated that of those 75 animals, approximately 20 will be utilized for breeding, while the remaining 55 will be used for experimentation and harvesting of tissue. Additionally, approximately 75 animals per year should be sufficient for the use as controls in comparison with the knockout α-crystallin mice for the first two years. It is estimated that of those 75 animals, approximately 20 will be utilized for breeding, while the remaining 55 will be used for experimentation and harvesting of tissue and used as controls. It is estimated at this time that no more than ~20-25 animals will be housed for breeding at any given time.

Does the procedure have the potential to involve momentary pain, distress, or discomfort without the use of anesthetics, analgesics, or tranquilizers? __X__Yes ___No

If yes, what anesthesia will be used: Ketamine (IP), Xylazine (IP)

Justify: For isolation of mice retinal pigment epithelium (RPE) and retinas, mice will be euthanized by IP injection of 210 mg/kg ketamine/21 mg/kg xylazine followed by decapitation, after which eyes will be enucleated for subsequent RPE cell isolation. (For details please see attached narrative).

RESTRAINT METHODS, INCLUDING GENERAL ANESTHESIA FOR PROCEDURES:

SPECIES & #	PHYSICAL	CHEMICAL	DESCRIPTION (drug name, dose, route; for physical restraint--duration and frequency)
1 Mice		X	210mg/kg ketamine (IP, IM) and 21 mg/kg xylazine (IP,IM) once

IV. SURGERY

Survival Surgery*

A. Procedure _____ Species_____
B. Anesthesia _____
C. Building & Room Number where surgery will take place _____
D. Person performing survival surgery _____
E. Describe Post-Operative Care (e.g., supportive fluids, analgesics, antibiotics, other drugs & frequency of observation) _____
_____
F. Person(s) providing & recording post-operative care _____

*Describe in detail the surgery, aseptic procedures & post-operative care in the NARRATIVE section.

Non-Survival Surgery

A. Procedure _____ Species_____
B. Anesthesia _____
C. Method of Euthanasia _____
D. Building & Room Number where surgery will take place _____
E. Person(s) performing non-survival surgery _____

V. LOCATIONS OF ANIMAL USAGE*

Please list all locations where Animal Procedures will be performed & check the appropriate blank. It is preferred, when possible, procedures should be performed in the CMC Procedure Rooms. These areas will be inspected, randomly, on a semiannual basis.

	Building	Floor/Room #	LABORATORY	ANIMAL FACILITIES PROCEDURE ROOM	TYPE OF PROCEDURE
1.	PCO, South Wing	4/S418-423	S418-S423	X	Euthanasia, Harvesting

Animals may not be housed in an investigator's laboratory for more than 24 hours unless specifically approved by the IACUC. Submit documentation for this approval with this application.*

VI. BIOHAZARD INFORMATION

Infectious agents, radioactive substances, toxic chemicals/chemical carcinogens, recombinant DNA and ionizing and non-ionizing radiation to be used in animal protocols MUST BE reviewed and approved by the PCO Biosafety and/or Nuclear Radiation Committee(s) PRIOR TO submission to the IACUC.

Please indicate the general biohazard being used **in-vivo**:

Infectious Agents_____ Radioactive Substances_____ Toxic Chemicals/ Chemical Carcinogens_____ Recombinant DNA_____

Ionizing and Non-ionizing radiation _____

Name of Agent _____

Please provide:
A) BSL level (1, 2 or 3) for infectious agents _____
B) Concentration _____
C) Route of administration _____

D) Duration of exposure _____
E) Room location where agent is administered _____
F) Location of animal housing post exposure _____
G) Length of time animals will be kept following exposure _____
H) Method of animal disposal _____

Are there risks from biohazardous materials or their metabolic products to: (Circle Y/N)

Yes (No) Investigators using agents
Yes (No) Animal Care Personnel
Yes (No) Other Personnel (Maintenance, employees, or visitors to animal care center)

If hazardous agents are to be used, approval from the appropriate committees is required.

VII. TRAINING OF RESEARCH PERSONNEL

Describe your experience and training in the care and use of laboratory animals. Be specific about training courses.

Within the past year, have you and/or your personnel (scientists, students, and technicians) attended continuing education programs concerning the care and utilization of laboratory animals in biomedical research? Yes _X_ No ___
Describe the nature of the education programs/courses that were attended within the past year.

- Traveled to the laboratory of Dan Gibbs, PhD and David Williams, PhD at the UCSD School of Medicine in La Jolla, CA to observe and participate in the proper isolation of mouse RPE.
- Course: Occupational Health and Safety in the Laboratory Workshop; January 4, 2006 by Dr. Jean Marie Pagani

A training CD titled, "Training in Basic Biomethodology for Laboratory Mice" has been viewed (see attachement)

Have taken the following on-line training provided by LATA:

5.) The Humane Care & Use of Laboratory Animals
6.) The Humane Care & Use of the Laboratory Mouse
7.) Anesthesia & Analgesia of Rodents
8.) Occupational Health and Safety with Laboratory Animals

Attended a hands-on training session with the CCMC (Animal facility orientation)

Will attend a hands-on training session with the CCMC (Mouse handling procedures)

If no, when do you and/or your personnel plan on attending such a course?

VIII. AREA OF RESPONSIBILITY

The Animal Care Coordinator is responsible for maintaining programs of laboratory animal care, including animal procurement, husbandry, disease control and prevention, humane treatment and adequate veterinary care under the supervision of a doctor of veterinary medicine.

The Principal Investigator is responsible for all aspects of the research protocol including post-operative monitoring and care, research-related complications, and humane treatment by investigative personnel.

The Principal Investigator is responsible for making daily checks of their animals and for euthanizing animals in distress. In the event that euthanasia or other intervention is necessary for humane reasons, the investigator will be consulted whenever possible. However, if the investigator is unavailable, it is the responsibility of the Institution or it agent(s), including the attending veterinarian, animal care staff, or IACUC members, to use whatever means is required to relieve the animal's pain or distress. This may range from mild tranquilization to relieve anxiety to euthanasia for insufferable pain. Death as an endpoint of convenience is not acceptable.

ASSURANCE OF COMPLIANCE WITH PUBLIC HEALTH SERVICE POLICY ON HUMANE CARE AND USE OF LABORATORY ANIMALS

The Pennsylvania College of Optometry assures that professionally acceptable standards governing the care, treatment, and use of animals, including appropriate use of anesthetic, analgesic, tranquilizing drugs, prior to, during, and following actual research, teaching, testing, surgery, or experimentation were followed.

The institution adheres to the standards and regulations under the Animal Welfare Act. There are no exceptions.

I have considered alternatives to animal use in these procedures and could find none.

LIST METHODS AND SOURCES USED TO CONSIDER ALTERNATIVES:

_____ Animal Welfare Information Center

X __ Literature Search

_____ Biological Abstracts

_____ Current Research Information Center

_____ Index Medicus

X __ Other (Please specify) Database Search _____

DATABASE LITERATURE SEARCH

Identify the services (computer databases, literature searches, etc.) that were used to obtain information on alternatives to painful procedures, use of live animals and prevention of unnecessary duplication of research.

A MINIMUM OF TWO DATABASES MUST BE USED.

Please check below the databases and your search strategy or key words. (Refer to instructions for examples.)

DATE OF SEARCH: March 27, 2006 _____

DATABASES: MEDLINE__X__; AGRICOLA____; EMBASE____; PSYCHINFO____; OTHER__X (Google Scholar)__

STRATEGY OR KEY WORDS: mouse retinal explants + mouse retinal pigment epithelium isolation + RNA isolation + protein isolation + histological changes in mouse tissue

Please include the literature reference used to consider alternatives to animal use:

DO NOT EXIST

RINCIPAL INVESTIGATOR'S ACKNOWLEDGMENT OR RESPONSIBILITY

certify that the activities described in this form do not unnecessarily duplicate previous experiments.

certify the above protocol will be conducted in compliance with the Federal, State, and local policies and regulations. I also knowledge full responsibility for knowledge of and compliance with all applicable standards governing radioactive or ohazardous materials involved in my project. I understand that compliance with these policies is a prerequisite for purchasing d housing animals, and for the use of animals in research and teaching at professional schools and colleges.

THE INFORMATION GIVEN ABOVE IS A COMPLETE AND ACCURATE SUMMARY OF PROCEDURES PERTAINING TO ANIMAL CARE AND USE IN THE PROPOSED PROJECT; IF THE RESEARCH PLAN SHOULD REQUIRE REVISION, I WILL INFORM THE IACUC. I AGREE TO ABIDE BY THE PROVISIONS OF THE GUIDE FOR THE CARE AND USE OF LABORATORY ANIMALS. I WILL PERMIT EMERGENCY VETERINARY CARE TO ANIMALS SHOWING EVIDENCE OF PAIN OR ILLNESS IF NOT THE DESIRED EFFECT OF THE ABOVE APPROVED TECHNIQUES. I UNDERSTAND THAT I MUST OBTAIN REAPPROVAL ANNUALLY.

Melissa E. Trego, OD _____ March 27, 2006
Principal Investigator Date

PROTOCOL APPROVAL

Veterinarian approval: Yes ____ No ____ _____
Signature Date

IACUC Chairperson approval: Yes ____ No ____ _____
Signature Date

Attachment to Protocol #A-MT0603
Narrative:

The purpose of this attachment is to establish animal procedures at PCO for the next 3-year period. The animals associated with this protocol will be accounted for regardless of whether or not they will be used in an actual experiment.

EUTHANASIA AND MOUSE RETINAL PIGMENT EPITHELIAL (RPE) CELL HARVESTING.

Primary cultures of RPE from both wild-type and αA-crystallin knock out mice in 129SVE or B6 b genetic background will be harvested as described by Gibbs and Williams 2003 (see attached publications for further detail). Briefly, intact eyes will be removed quickly from 10-14 day old mice after euthanasia and decapitation (the age of the mice used for RPE isolation is very critical to the success of this particular procedure). Prior to decapitation, mice will be anesthesized with high IP doses of ketamine/xylazine (10/21 mg/kg, respectively). Lots containing 10 eyes each will be washed, treated enzymatically with Dispase and then carefully dissected by removing the anterior cornea, lens, capsule and associated iris pigmented epithelium. Remaining posterior eyecups will contain loosely attached neural retina, easily removed from RPE preventing apical surface damage, and provide clean isolation of the intact underlying RPE. This procedure optimizes the use of animals, since both RPE and neural retina can be isolated separately and then each used for future experiments. After numerous washes and centrifugation, cells will be cultured for 7 to 10 days until confluent colonies are present. These primary RPE cells will maintain their pigmentation and hexagonal morphology of *in vivo* RPE. Cultured primary RPE will be used for baseline expression of α-crystallins in the mouse RPE and for future blue light exposure experiments, and oxidative stressor exposure (*t*-BOOH and H_2O_2) experiments. **To perform successful RPE isolation, 10 retinas/RPE layers are required per isolation. The total number of mice is (@ 2 retinas/mouse) 5 mice X 40 assays X 1 transgenic lines and 1 control lines = 400 for the entire 3-year project.**

IACUC USE ONLY

Protocol Number	
Submission Date	
Approval Date	
Expiration Date	

PENNSYLVANIA COLLEGE OF OPTOMETRY
INSTITUTIONAL ANIMAL CARE AND USE COMMITTEE (IACUC)
APPLICATION FOR IACUC APPROVAL

Project Title:	Alpha (α) – Crystallin Proteins as Potential Protectors Against Continuous Visible Blue Light Exposure

Principal Investigator*: Melissa E. Trego Degree: OD, PhD (Candidate)

Dept: Research Email: mtrego@pco.edu Phone: x3455 Emergency Phone: 267.735.9657

Co-Investigators*:			**Technicians*:**		
Name	Dept	Phone	Name	Dept	Phone
Alexander Dizhoor	Research	1468	Michael Coulton	Research	
Pierrette Dayhaw-Barker	Basic Sciences	1257	Tressa Larson	Optometry	

Please attach C.V.'s (on file)

Emergency Contact: Melissa E. Trego Phone: 267.735.9657

Review Status:	Is this a new submission?	**Yes**	Is this a 3-year resubmission?	**No**

Funding Source: Should match project budgetary information)	**No external funding**	Current?	
		Pending?	

GENERAL INFORMATION

A. Goals and /or Benefits

In a short paragraph, describe the goals and anticipated benefits in terms that can be understood by a layperson without a scientific background.

My ultimate goal for this experiment is to determine if the presence of alpha-crystallin (a structural protein), protects the retina against damage caused by continuous visible light. Alpha-crystallin is a protein which was thought to only reside in the lens, protecting it from a lifetime worth of light exposure. Since the lens does not have a blood supply nor is capable of fixing broken proteins, the alpha-crystallin proteins actually help maintain the clarity of the lens by grabbing onto those broken proteins and making sure that they do not team up with other broken proteins to change the clarity of the lens, therefore affecting clear vision. Recently alpha-crystallins have been found in a number of other tissues (mostly tissues that cannot easily repair themselves) such as the brain, heart, kidneys and the retina. Why are they in the retina? What is their role? My hypothesis is that these crystallins will exhibit a protective effect in the retina, very similar to their role in the lens. However, the stressors that the retina encounters on a daily basis will be different from those stressors of the lens. The retina of the eye is also exposed to a lifetime of light, however this light is visible (or blue light in the spectrum) and in addition to light exposure, there is a very

stressed environment from normal aging metabolic processes of surrounding tissues. This experiment will contain mice that do have the alpha-crystallin protein (Pigment Controls (WT 129Sv) and Non-Pigmented Controls (BALB/cByJ) and those that do not have the alpha-crystallin protein (experimental – Knock-out mice). Both sets of mice will be exposed to continuous blue light and then their eyes will be examined for any changes in retinal structure or protein expression. It is expected that those mice which lack the alpha-crystallin protein will show greater damage than those who do have this protein. Ultimately, if alpha crystallins do exhibit potential protection and defense against environmental stressors, future therapeutic strategies could be implemented which may help to preserve vision in such eye disease such as Age-Related Macular Degeneration. Retinitis Pigmentosa, Lebers Congenital Neuropathy, etc..

B. Description of Proposed Research

Describe the experimental design. Provide more specific details regarding the procedures that will be performed, include treatment groups and appropriate controls, and the endpoint of the experiment. Please note that death as an endpoint is not acceptable. You may use time-lines and/or flowcharts.

Please see FLOWCHART 1 and attached NARRATIVE for proposed research.

C. Animal Usage

Species and Strain	Source	Age and/or Weight	Sex	#per year			Total # of Animals
				YR1	YR2	YR3	
Mice: 129Sv (Control)	**CMC**	**15-35 grams**	**M or F**	**100**	**100**	**100**	**300**
Mice: 129Sv:CryA1 (Experimental)	**CMC**	**15-35 grams**	**M or F**	**100**	**100**	**100**	**300**
Mice: BALB/cByJ (Albino) - Control	**Jackson Laboratories**	**15-35 grams**	**M or F**	**80**	**0**	**0**	**60**

- Are animals to be housed individually or in groups? Groups
- Species Justification (Provide separate justification for each species listed on the protocol. Why must you use the species you have requested?)

Rational for using mouse models: Mice have typical mammalian retinas that are well characterized anatomically and physiologically. Various mouse retinal proteins are well studied and their primary structures are determined. Of the non-human mammalian species, the mouse genome is the best elucidated. Mice are fast breeders and produce sufficient amount of tissue, allowing reliable statistical analysis of results. Mice can be easily adapted to darkness or to light before collecting retinas or conducting electrophysiological studies. Models for expression of various retinal proteins in mice have been successfully used in the past and are well documented. At the present moment, 129Sv:CryA1 line is the only animal species available with the alpha-crystallin gene knock-out. Based on the experimental design and hypothesis that alpha-crystallins provide protection against various stressors, comparing the knock-out line with controls (or those who have the gene) will give a direct correlation between the presence of absence of alpha-crystallins and their potential role in protection.

- Animal Numbers (What is the scientific justification for the number of animals to be used? Describe the experimental groups and the number of animals per group. Table/flow chart may be used.)

Please refer to Tables 1 and 2. As shown in table 1, in order to examine the mice, both histological and for

expression of protein, two mice will be used per day of exposure/per strain; this would yield **4 eyes** for tissue analysis of each strain (1 eye for protein; 1 eye for histology from each mouse). After the designated day of exposure, one mouse will be euthanized and tissue harvested immediately, the second mouse will be returned to normal lighting conditions and analyzed at 10-days post exposure. Control animals will include pigmented (129Sv) and non-pigmented mice (albino; BALB/cByJ). In order to achieve minimal statistical significance, the experiment must be repeated **three** independent times. The request for each independent experiment and use of animals can be seen in **Table 1**. Examination of tissue will be examined initially at 2 time points; immediate post-exposure and at 10 days post-exposure. Total number of animals requested can be seen in **Table 2** – this amount will allow the experiment to be repeated 3 times, with the option of repeating it a fourth time (if necessary). Total for three independent runs include **64** – an additional **20%** is requested for a possible fourth run/human error/ equipment malfunction/animal anatomical anomaly etc. However, if there is no need to repeat the experiment a fourth time or the procedure becomes redundant, the animals will not be used – all animals will be accounted for regardless.

D. Locations of Animal Usage*

Please list all locations where Animal Procedures will be performed & check the appropriate blank. It is preferred, when possible, procedures should be performed in the CMC Procedure Rooms. These areas will be inspected, randomly, on a semiannual basis.

	Floor/Room #	LABORATORY	ANIMAL FACILITIES PROCEDURE ROOM	TYPE OF PROCEDURE
1.	South Wing, Basement, Room #	S17	X	Blue light exposure, post-blue light exposure housing
2.	South Wing, 4th Floor, S418-423	S418-423	X	Euthanasia/Tissue harvesting
3.				

***Animals may not be housed in an investigator's laboratory for more than 24 hours unless specifically approved by the IACUC. Submit documentation for this approval with this application.**

II. SPECIFIC PROCEDURES

Please check the procedures to be used in this protocol and provide detailed information in the appropriate section.

Check (X)		Procedure
X	1	Anesthesia
	2	Behavioral Studies
	3	Blood Collection
	4	Breeding Colony
	5	Biohazard Information
	6	Chronic or Prolonged Restraint
	7	Dietary Manipulations
X	8	Dosing – drugs or other substances
X	9	Euthanasia
	10	Immunization/Antibody Production
	11	Oncology/Tumor Transplantation

X	12	Physiologic Measurements – **ERG**
X	13	Special Housing/Husbandry Procedures
X	14	Tissue Harvest (removal of tissue from dead animals)
X	15	Use of Transgenic Animals
X	16	Other Procedures – **Visible Blue Light Exposure**
	Appendix A	Surgery

1. Anesthesia and Sedation Used in Non-surgical Procedures

Procedure	Agent	Dose (mg/kg)	Route	Frequency
ERG	**Ketamine/ Xylazine**	**150/10**	**IP or IM**	**Pre and Post Exposure (Day 0 and Day 10)**

2. Behavior Studies

Provide detailed description.

N/A

3. Blood Collection N/A

Method	Frequency/Interval	Volume per withdrawal	Anesthesia/Sedation

4. Breeding Colony

Justify need.

N/A

5. **Biohazard Information** (The use of biohazardous materials requires the approval of the Biosafety Committee and/or Radiation Safety Committee. Please provide documentation of approval with this application.) **N/A**

Please indicate the general biohazard being used **in-vivo** and complete the table for each agent:

___ Infectious Agents
___ Radioactive Substances
___ Hazardous Chemicals/Carcinogens/Toxins
___ Ionizing and Non-ionizing radiation
___ Recombinant DNA

Agent	Risk	Containment Method	Disposal Method

Do any of the hazards identified above pose a risk to humans through direct or indirect contact with the animal or its bedding? If yes, explain how the risk will be controlled.

N/A

6. Chronic or Prolonged Restraint

Provide justification for restraint, a description of the device and duration of the restraint.

N/A

7. Dietary Manipulations

a. Food or water restriction? ____ Yes ____ No

If yes, justify and indicate the duration, frequency and possible outcomes.

N/A

b. Special diets? ____ Yes ____ No

If yes, provide details of the composition of the special diet, who will prepare the diet, how often will the animals be fed, and what are the consequences of the diet change.

8. Dosing – Drug and Other Agents (excluding anesthetics, sedatives, and antigens for antibody production)

Agent (drug)	Dose (mg/kg)	Route	Frequency	Duration
Atropine Sulfate	1 drop in both eyes	Instillation in eyes	1 drop in both eyes	Drops work for 7 days
Tropicamide (0.5% or 1%)	1 drop in both eyes	Instillation in eyes	1 drop in both eyes	3hrs
Phenylephrine 2.5%)	1 drop in both eyes	Instillation in eyes	1 drop in both eyes	3hrs
Systane	1 drop in both eyes – as needed	Instillation in eyes	1 drop in both eyes	3-4hrs

9. Euthanasia

Species/Strain	Primary procedure*	Dose (mg/kg) or % gas	Agent	Route	Volume
Mice:129Sv	Tissue harvest	To effect	CO_2	Inhalation	To effect
Mice:129Sv:CryA1	Tissue harvest	To effect	CO_2	Inhalation	To effect
Mice: BALB/cByJ	Tissue harvest	To effect	CO_2	Inhalation	To effect

(*Primary procedure: e.g., overdose, cervical dislocation, decapitation, exsanguinations).

Describe how death is confirmed for carbon dioxide asphyxiation.

Primary procedure will include carbon dioxide asphyxiation then followed with cervical dislocation.

10. Use and/or Production of Monoclonal or Polyclonal Antibodies

a. Will you use animals to produce antibodies? ____ Yes ____ No

If yes, justify and provide information on the antigen, adjuvant, dose per site, route of administration, volume per site, number of boosters, and the frequency of boosters.

N/A

b. Will you be purchasing antibodies to be used in animals from a commercial source? ___ Yes ___ No
c. Will you use Complete Freund's Adjuvant? ____ Yes ____ N0
If yes, justify its use.

11. Oncology/Tumor Transplantation

Provide information on origin, passage, adventitious pathogen testing, biohazard potential, and determination of endpoint. How will you evaluate pain/distress in these animals? How will you alleviate those conditions?

N/A

12. Physiologic Measurements

Provide detailed descriptions (include frequency and duration of measurements).

ERG recordings done at pre-exposure (day 0), immediate exposure, and 10 days post-exposure. Please see ERG NARRATIVE for detailed description.

13. **Special Housing/Husbandry Procedures** Describe arrangements and contact the CCMC.

Please see attached NARRATIVE.

14. Tissue Harvest (removal of tissue from dead animals)

Tissues/Organs/Body Fluids being harvested include:	**Eyes (whole eyes, only fresh retina/only fresh RPE) for histology and protein analysis**
What method of euthanasia will you be using?	**CO_2 inhalation followed by cervical dislocation**

15. Use of Transgenic Animals

The use of transgenic animals requires the approval of the Institutional Biosafety Committee (IBC). Please submit the approval letter with this application.

Source of transgenic mice:	Transgenic mice (129Sv:CryA1) were originally obtained from Eric Wawrousek at the National Eye Institute (NEI) of the National Institute of Health (NIH) – mice are now bred in the CMC **(Protocol #: A-MT0505-00)**
Describe method of genotyping to sample the DNA from these animals.	Tail clipping with subsequent PCR analysis (see Narrative)

16. Other Procedures (Describe)

Visible blue exposure (see NARRATIVE)

Appendix A: Surgery (Attach if applicable.)

II. SEARCH FOR ALTERNATIVES

Federal regulations require a literature search for alternatives to the **use** of animals and for **painful/distressful** procedures. The search should include **"replacing"** the species requested with one lower on the phylogenetic scale, **"reducing"** the number of animals requested and **"refining"** by using less stressful procedures. You must use a minimum of two databases. Search dates must be within the past six months. Attach the search results. – **There are no alternatives for this mouse model**

Check (X)	Databases or other sources Consulted	Date of Search	Years covered by search	Keywords/strategies used in search

	Agricola			
	Biosis/Life Science			
	Embase			
	Current Research Information System (CRIS)			
	Medline			
	Toxline			
	Altweb http://altwebjhsph.edu			
	Animal Welfare Information Center http://agclass.nal.usda.gov/altrntvs/index.htm			
	Center for Animal Alternatives, University of California at Davis http://www.vetmed.ucdavis.edu/Animal_Alternatives/main.htm http://www.vetmed.ucdavis.edu/Animal_Alternatives/micegrid.htm			
	Norwegian Reference Centre for Laboratory Animal Sciences and Alternatives http://oslovet.veths.no			
X	Other: (Specify) – PubMed, Google Scholar	5/23/2007		Alpha A-crystallin knock-out, blue light damage + mouse, alpha-crystallins + retinal degeneration

IV. TRAINING OF RESEARCH PERSONNEL

Describe the experience and training in the care and use of laboratory animals for all research personnel listed on this protocol. Be specific about training courses.

- Traveled to laboratory of Dan Gibbs, PhD and David Williams, PhD at the UCSD School of Medicine in La Jolla, CA to observe and participate in the proper isolation of mouse RPE
- Took Occupational Health and Safety in the Laboratory Workshop on January 4, 2006 by Dr. Jean Marie Pagani
- Viewed CD, "Training in Basic Biomethodology for Laboratory Mice Successfully completed online training provided by LATA including: Humane Care and Use of Laboratory Animals, Humane Care and Use of the Laboratory Mouse, Anesthesia & Analgesia of Rodents, Occupational Health and Safety with Laboratory Animals
- Attended hands-on training session with CCMC for animal facility orientation and mouse handling procedures

Describe the nature of the education programs/courses that were attended within the past year.

Annual IACUC Training – 7/18/2007
IACUC Occupational Health and Safety Training – 2/21/2007
Annual IACUC Training – 6/27/2006

V. INVESTIGATOR ASSURANCE

- I certify that the information provided in this application is complete and accurate and consistent with any proposal(s) submitted to external funding agencies.

- I certify to abide by PHS Policy, USDA regulation, the Guide for the Care and Use of Laboratory Animals, all federal regulations, and the policies of the Pennsylvania College of Optometry's Institutional Animal Care and Use Committee (IACUC).

- I will notify the IACUC in writing of any changes in this protocol and will await IACUC approval before proceeding with animal research.
- I understand that I must obtain reapproval annually.
- I will permit emergency veterinary intervention, including euthanasia, for animals exhibiting pain, distress, or illness. An effort to contact me or my representative (the animal emergency contact identified on page 1) will be made prior to any emergency treatment.
- I will report at once to the IACUC any adverse events.
- I certify that all personnel performing any procedures on animals, including myself, have been or will be trained in humane and scientifically acceptable procedures for animal handling, procedural techniques, administration of anesthesia, analgesia, and euthanasia to be used in this project.
- I assure that all personnel, including myself, will follow the recommendations of the Occupational Health and Safety Program. In addition, I will ensure that all personnel have appropriate training including, but not limited to, biosafety principles and techniques, chemical safety, accidental spills, and the proper handling of all hazardous materials and waste management.
- I understand it is my responsibility as the Principal Investigator to ensure that all individuals listed on the protocol have read and understand the procedures. I assume full responsibility for compliance with all regulations and policies.
- I certify that this protocol does not unnecessarily duplicate previous experiments.

?I Signature **Date**

PROTOCOL APPROVAL

/eterinarian approval	Yes	No	Signature	Date
ACUC Chairperson ıpproval	Yes	No	Signature	Date

Attachment to Protocol:

The purpose of this protocol is to establish animal procedures at PCO for the next 3-year period. The animals associated with this protocol will be accounted for regardless of whether or not they will be used in an actual experiment.

MOUSE TAILS CLIPPING FOR ISOLATION OF DNA (minor **Code A** procedure). This common technique is described in many protocols, for example, a laboratory manual, "Manipulating the Mouse Embryo" by B. Hogan et al., Cold Spring Harbor Laboratories Press, 1994, pp. 296-298. Mice of age 3 weeks will be labeled with a small identification ear tag number (National Band and Tag Co., Newport, KY). A small piece (~ **3-5** mm long) of the tip of the tail (wiped with 70% ethanol just before the cutting) will be clipped using a sterile razor blade wiped with ethanol. Some protocols use 0.5ml/L Isoflurane for anesthesia, but young mice such as we are going to use, do not experience pain/distress during this minor procedure so the tail clipping for 3-weeks without anesthesia is widely used and commonly accepted

practice. Short-term minor bleeding after the tail clipping is common and no special further treatment is required, however, before the animals are put back into the cage, the bleeding will be stopped by pressing on and holding with an aseptic glove at the end of the tail until the clot is completely formed. Tail clipping will be performed for each mouse once **at the age of 3 weeks, when this procedure is painless for the animals.**

BLUE LIGHT EXPERIMENTS (Please refer to FLOWCHART 1 for illustrative detail). Twenty-eight non-transgenic mice (14 of 129Sv and 14 of BALB/cByJ) and fourteen αA-crystallin knock-out mice (129Sv:CryA1) will be exposed to blue light (400-480nm) at energy levels that do not produce immediate tissue response for periods of 24 - 168 hrs (1 – 7 days) to assess the location and degree of retinal damage (Seiler et al., 2000, Davies et al., 2001, Ham et al., 1980, Farrer et al., 1970). This exposure mimicks the blue light hazard function (BLHF Fig 1). The blue light apparatus caging consists of 6 mounted, stainless steel fluorescent light holders bolted together, creating an enclosed box open at both ends. Each stainless steel mount holds 2, 48" fluorescent bulbs (Philips Natural Sunshine, 40 watts; T12, Philips Lighting Company, Somerset, NJ, USA), therefore there are 4 on top, 2 on both sides and 4 on the bottom for a total of 12 lights. The apparatus holds 6 individual stainless steel cages measuring 5"Hx6"Wx11"L . Wavelength and irradiance of the exposure will be regulated by spectral filters as previously described (Schutt et al., 2000). Caging temperature will be kept low by using fans to circulate air through the whole apparatus and individual cages. The radiant exposure produced by the 12 Phillips fluorescent tubes is filtered by blue gel filter material (Lee #197 Zenith Blue) that is wrapped around the caging inside the boxed fluorescent tubes (Figure 2). This arrangement results in a net spectral exposure shown in figure 2 which is a close approximation of the BLHF, but which includes a small long wavelength window which has been seen typically in other experiments and is not considered to be significant to the photic damage outcomes. As constructed, this apparatus is nearly identical to that of Seiler et al , 2000 and did produce an illumination level (590 lux) in the same range as that research group. Mice will be dark-adapted for 12-16 hours in a standard cage supplied with food and water. Before exposure, mice will undergo ERG readings for initial assessment of visual function (please see description below). During ERG recordings, mice pupils will be dilated once with 1% atropine sulfate, which will keep the pupils fully open for maximum exposure for 7 days. Animals will not be sedated with standard anesthesia for blue light exposure experiments. This treatment does not comply with the Guide For the Care and Use of Laboratory Animals (NRC 1996) for light period, but then this is the purpose of the study, namely to produce the well known effect of retinal degeneration due to constant light. Previous studies have examined continuous blue light exposure up to freely moving, unsedated animals (Seiler et al., 2000, Noell et al., 1966, Rapp and Williams, 1979). However, I will closely monitor the mice at least twice a day for any behavioral evidence of pain and distress and will institute sedation if this becomes an issue. Photophobia can be encountered in typical bright, full-spectrum light; but with the blue light restriction, there is a natural dimming of the perceived brightness which lowers the chance of photophobia in the animals. After light exposure, some animals will be euthanized immediately and tissue will be harvested. Mice not euthanized immediately will be returned to normally lighted cages and euthanasia will occur at 10 days post-exposure.

EUTHANASIA AND RETINA HARVESTING. Mice will be adapted to darkness before ERG recordings and some cases also before organ/tissue harvesting. For the dark adaptation, standard cages containing 4 mice each, provided with food and water will be kept for 6-12 hours in light-sealed ventilated room. Mice will be euthanized under the infrared illumination by CO_2 inhalation followed by cervical dislocation. Eyes will be removed from freshly euthanized animals either immediately after designated post-exposure (1, 2, 3, 4 days, etc.) or at 10 days post-exposure. From each animal, one eye will be fixed in 4% paraformaldelhyde for future histological analysis and the other eye will have the retina and RPE harvested for future protein expression. For protein analysis, the neural retina and RPE cells will be homogenized in RIPA protein lysis buffer and total protein concentrations will be standardized based on Pierce's BCA™ Protein Assay kit determination. Homogenates will be assayed for their change in α-crystallin (αA- or αB-) activity with respect to a housekeeping protein, actin. Indicies of reactive oxygen species generation, including protein oxidation, DNA damage and lipid peroxidation, will be evaluated as described in previous studies (Jarrett and Boulton, 2005; Davies et al., 2001; Boulton and Dayhaw-Barker 2001).

ELECTRORETIONGRAM (ERG) (recordings from the mice (approx. 50/year)). **This procedure will be used to evaluate the impact of crystallin knockout on retinal function. The ERG will be done prior to light exposure and at post-exposure, right before the euthanasia and tissue harvesting. No additional animals need to be purchased.** ERG will register functional changes in the retinas of the α-crystallin knock out mice. The ERG recordings will follow standard widely known non-surgical procedure. The animals will be **sedated with 150 mg/kg ketamine (IP) and 10 mg/kg xylazine (IP) for the duration of recordings (approx. 1.5 hour),** in order to minimize discomfort from application of electrodes on their cornea, eyelid and skin and to prevent movements during the recordings. They will be given atropine, tropicamide or phenylephrine eye drops 10 min. to fully dilate their eyes before the recordings start, and their eyes will be kept moist with methylcellulose-containing eye drops (Systane). Normothermia will be maintained by electronic warming pad. A small contact electrode will be applied to the cornea of the sedated mouse with a drop of water in it to serve as the active electrode. A stainless steel "ground" electrode will be place in the animal's mouth. **After the ERG recordings mice will be sacrificed by CO2 inhalation or ketamine/xylazine overdose and cervical dislocation for tissue** harvesting as described above.

ADVERSE EVENT REPORT

All serious and unexpected adverse events must be reported within 24 hours. Please obtain the PI signature and submit to the IACUC Chairman.

Reported by (name): Melissa E. Trego, OD
Date Reported: Monday, July 16, 2007 at 1430

IACUC Protocol Number	**Project Title**
A-MT0705	Alpha Crystallin Proteins as Potential Protectors Against Continuous Blue Light Exposure

Principal Investigator

Name (Last, First)	Degree	Phone #	Fax #	E-Mail Address
Trego, Melissa E.	OD	X3455	215.780.1464	mtrego@pco.edu

DESCRIPTION OF EVENT

1. Type of Event:	2. Location of Event: S17C	3. Date and Time of Event:
X Initial ☐ Follow-up		Monday July 16, 2007 at 1400

4. Provide a brief narrative of the event, problem, or complaint including steps or actions taken to resolve the issue including any protocol amendment(s)-attach additional pages if necessary.

As per the protocol, ERGs were to be performed pre, interim and post blue light exposure. Calculations were done to create a cocktail of both ketamine and xylazine to anesthetize the animals. Measured amounts to be administered were originally ranged from 0.08 – 0.1ml of the combined cocktail. The first animal (N123) was given the specified dose and a successful ERG was performed. A second animal (N116) was given a specified dose (same as N123) and had an adverse reaction to the anesthesia and failed to survive. Initially I felt it might be an adverse reaction, so I went ahead and administered a lesser dose (0.08ml) to a third animal (N119) and that animal also failed to survive. I ceased the experiment and re-checked my original calculations and found that due to a mathematical error, I was off by a power of ten. My original calculations called for ~0.09ml per mouse and the new calculations only required 0.01mL per mouse of the combined cocktail. Unsure as to proceed, I contacted Jim Wood and informed him of the situation and calculation error. He recommended that I contact Dr. Gwen Talham and inform her of the situation as well. I spoke with Gwen and discussed my error and we agreed on the second calculation of administering 0.02ml of combined cocktail. I rang Jim Wood again to inform him on my conversation with Gwen and he stated that there was no way a mouse will go down with such a small amount. I tried to administer the new volume on a fourth animal (N117) and after 40 minutes, the animal had no reaction to the anesthesia. At that point, I made the decision to cease the administration of the anesthesia until I can sit down with Gwen in person (at our IACUC training session on July 18, 2007) to review my calculations and to discuss possible dilutions of the ketamine and xylazine. Due to PhD time constraints, I forfeited having pre-ERGs for my first trial of blue light exposure to WT animals, but will perform pre-ERGs, interim and post-ERGs on remaining trials once all calculations and dilutions have been sorted.

Reporting Person Signature	Print Name	Date

Principal Investigator Assurance
I have reviewed the contents of this report and certify that the information provided is complete and accurate to the best of my knowledge.

Principal Investigator Signature	Print Name	Date

IACUC Chairman Signature	Date

Form #22 12/00
Institutional Review Board
Pennsylvania College of Optometry
(215) 780-1417
Fax (215) 780-1325

REQUEST FOR REVIEW OF EXEMPT RESEARCH

Note: Exploration of sensitive topics does not qualify for exemption.

	DATE		**01/30/2007**
Principal Investigator (PI)	(Last) TREGO (First) MELISSA (Credentials) OD, PhD(c)		
PI Status	[**X**] PCO Faculty/Staff [ ] Other:		
Faculty/Staff Sponsor	Dr. Felix Barker, Dr. Pierrette Dayhaw-Barker, and Dr. Alex Dizhoor		
Division / Department	**Research**		
PI's Address/Box	**S418**	Phone #	**X3455**
E-mail address	**mtrego@pco.edu**	FAX #	
Person Responsible for Paperwork	**Melissa E. Trego**	*Phone #*	**2677359657**
E-mail address	**mtrego@pco.edu**		
Protocol Title (must match the NIH/Sponsor title)	**Alpha Crystallins and Retinal Protection Against Light Damage & Oxidative Stress**		
Key Words	1. Alpha-crystallins 2. Retinal Pigment Epithelium (RPE) 3. Retina		
Research Site(s)	**Pennsylvania College of Optometry, 8360 Old York Road, Elkins Park, PA 19027 – Rooms S418, S418A, S418B**		
Funding Source (include pending)	**Pennsylvania College of Optometry**		
Does this research involve cancer?	[**X**] No [ ] Yes		

Define any abbreviations and use simple language throughout the application.

1. Designate the category that qualifies this proposal for exemption (see following page), and justify this designation by responding to the questions below each category. ***All text boxes will expand.***

Category # 4
1.

2.

CATEGORIES OF RESEARCH THAT QUALIFY FOR EXEMPTION

§46.101(b) Unless otherwise required by Department or Agency heads, research activities in which the only involvement of human subjects will be in one or more of the following categories are ***exempt*** from this policy:

CATEGORY 1

Research conducted in established or commonly accepted educational settings, involving normal educational practices, such as (i) research on regular and special education instructional strategies, or (ii) research on the effectiveness of or the comparison among instructional techniques, curricula, or classroom management methods.

1. Educational research protocols are exempt providing **all** of the following conditions are met:
   a. All of the research is conducted in a commonly accepted educational setting (e.g., public school).
   b. The research involves normal educational practices (e.g., comparison of instructional techniques).
   c. The study procedures do not represent a significant deviation in time or effort requirements from those educational practices already existent at the study site.
   d. The study procedures involve no increase in the level of risk or discomfort attendant in normal, routine educational practices.
   e. The study procedures do not involve sensitive subjects (e.g., sex education).
   f. Provisions are made to ensure the existence of a non-coercive environment for those students who choose not to participate.
   g. The school or other institution grants written approval for the research to be conducted.
2. **Information Required for Justification**:
   a. Is research part of the commonly accepted educational setting at the research site listed on page one?
   b. Describe the research in relation to (i) and/or (ii) above.
3. **NOTE**: *Educational projects that do not meet the above-listed conditions are not exempt and must, therefore, be submitted for IRB review using the IRB Application for Non-therapeutic Research and will be reviewed by either the expedited or full board method.*

CATEGORY 2

Research involving the use of educational tests (cognitive, diagnostic, aptitude, achievement), survey procedures, interview procedures or observation of public behavior, ***unless***: (i) information obtained is recorded in such a manner that human subjects can be identified, directly or through identifiers linked to the subjects; ***and*** (ii) any disclosure of the human subjects' responses outside the research could reasonably place the subjects at risk of criminal or civil liability or be damaging to the subjects' financial standing, employability, or reputation.

1. **Information Required for Justification**:
   a. Describe the type of educational activity.
   b. State how the information will be recorded to assure that it is ***impossible*** for the investigator to link the data to any individual subject as required in (i), ***and*** assure that there are no risks to subjects as described in item (ii).
2. **NOTE**: *Sensitive survey research is **not** exempt. A sensitive survey is one that deals with sensitive or highly personal aspects of the subject's behavior, life experiences, or attitudes. Examples include chemical substance abuse, sexual activity or attitudes, sexual abuse, criminal behavior, sensitive demographic data, detailed health history, etc. The principal determination of sensitivity is whether or not the survey research presents a potential risk to the subject in terms of possible precipitation of a negative emotional reaction. An additional risk to the subject in terms of possible precipitation of a negative emotional reaction. An additional risk consideration is, of course, whether or not there is a risk associated with a breach of confidentiality should one occur. With respect to potential psychological risk associated with a survey, the presence or absence of subject identifiers is not necessarily a consideration since the risk may be primarily associated with the sensitive nature of the survey as opposed to being dependent upon confidentiality. Subject identifiers do, however, become a factor when confidentiality is an issue.*
3. **NOTE**: *When children are involved as subjects in research using survey or interview procedures, the research is **not** exempt. The IRB Application for Non-therapeutic Research must be submitted.*
4. **NOTE**: *When children are involved as subjects in research using observation techniques, the research is **not** exempt if the investigator participates in the activities being observed. The IRB Application for Non-therapeutic Research must be submitted.*
5. **NOTE**: *Observation research involving sensitive aspects of a subject's behavior is **not** exempt. The IRB Application for Non-therapeutic Research must be submitted.*

CATEGORY 3

Research involving the use of educational tests (cognitive, diagnostic, aptitude, achievement), survey procedures, interview procedures, or observation of public behavior that is not exempt under paragraph (b)(2) of this section, if:
(i) the human subjects are elected or appointed public officials or candidates for public office; or (ii) Federal statute(s) require(s) without exception that the confidentiality of the personally identifiable information will be maintained throughout the research and thereafter.

1. **Information Required for Justification**:
   a. State the type of test to be used in the research activity.
   b. Discuss how the research qualifies for exemption based on item (i) or (ii).

CATEGORY 4
Research involving the collection or study of existing data, documents, records, pathological specimens, or diagnostic specimens, if these sources are publicly available ***or*** if the information is recorded by the investigator in such a manner that subjects **cannot** be identified, directly or through identifiers linked to the subjects.

1. **Information Required for Justification**:
   a. State: ***type*** of and **source(s)** from which the data/specimens will be collected, and ***if they are publicly available***.
   b. Confirm that the materials are "existing," and discuss the method that will be used to record the data to assure that individual subjects ***cannot be linked*** to the research activity. State whether the data or specimens involve the existence of code numbers that can be linked to the individual.
2. **NOTE**: *The information must be existing and, therefore, precludes use of any data obtained prospectively.*
3. **NOTE**: *Examples of publicly available information include a driver's license or court records.*

CATEGORY 5
Research and demonstration projects which are conducted by or subject to the approval of Department or Agency heads, and which are designed to study, evaluate, or otherwise examine: (i) Public benefit or service programs; (ii) procedures for obtaining benefits or services under those programs; (iii) possible changes in or alternatives to those programs or procedures; or (iv) possible changes in methods or levels of payment for benefits or services under those programs.

1. **Information Required for Justification**:
   a. Is this research subject to approval of Department or Agency heads?
   b. Discuss the purpose of the research and discuss how it qualifies for exemption based on item (i), (ii), (iii), or (iv).

CATEGORY 6
Taste and food quality evaluation and consumer acceptance studies, (i) if wholesome foods without additives are consumed or (ii) if a food is consumed that contains a food ingredient at or below the level and for a use found to be safe, or agricultural chemical or environmental contaminant at or below the level found to be safe, by the Food and Drug Administration or approved by the Environmental Protection Agency or the Food Safety and Inspection Service
of the U.S. Department of Agriculture.

1. **Information Required for Justification**:
   a. Explain the purpose of the research.
   b. Discuss how the research qualifies for exemption based on item (i) or (ii).

2. Describe the research (background, objectives, and description of how the research will be conducted) in simple language.

My research project involves examining the expression of alpha-crystallins in the retinal pigment epithelium (RPE) and neural retina of both humans and mice. Alpha-crystallins, a set of molecular chaperone proteins, were once though to only be expressed the lens, however they have also been found to be expressed in a number of other tissues including the retina/RPE in both humans and mice. My intent will be to examine the change in expression of these crystallins when the human RPE/retinae are exposed to a number of environmental stressors including oxidative and light induced. This research will provide a greater understanding into the molecular mechanisms involved in retinal eye disease with regards to environmental stressors.

3. State the approximate number of subjects, existing records, or specimens required for valid statistical analysis. **~18-20 donor eyes**
4. State the age range of the subjects, or the age range of subjects whose data or specimens will be collected. **0-99 yrs**

Indicate special or vulnerable classes, if any, that will participate in the research:

[ ] Pregnant Women [ ] Cognitively Impaired [ ] Children * [ ] Prisoners*

*Note: Research cannot be exempt when the population includes prisoners or when children are the subjects of:
- survey or interview procedures, or
- an observation(s) in which the investigator participates in the observed activities.

5. Will there be equal representation of: Genders [ ] Yes [X] No Racial/ethnic groups [ ] Yes [X] No

If no for either of above, please explain.

The main goal to is to receive human eye tissue in any age range. It is not important for this particular study to examine any changes in expression in gender or ethnicity.

6. Specify risks and benefits to the subjects and/or society.

Risks: There will be no risks to the subjects since the eyes will be received post-mortem.

Benefits: The benefits will be a greater insight into the molecular mechanisms involved in retinal degenerations and eye disease.

Applicable to all Categories except Category 4

7. Describe recruitment procedures. *(Attach advertisements, flyers, telephone and verbal consent, cover letters, etc. for approval.)*

N/A

8. **Discuss the consent process.**

N/A

To receive waiver of consent, the research **must** meet the following four criteria established by 45CFR46.116(d)(1-4). **Please explain (below each statement) how your research meets these criteria.**

1. The research involves no more than minimal risk* to the subjects

2. The waiver or alteration will not adversely affect the rights and welfare of the subjects;

3. The research could not practicably be carried out without the waiver or alteration; **AND**

4. Whenever appropriate, the subjects will be provided with additional pertinent information after participation.

Submit the following:

[X] Formal research protocol including any questionnaires, surveys, telephone scripts, etc.

When applicable:

[ ] Complete grant application, with budget (when project is funded). Block out confidential salary information and total dollar amount.

[ ] Consent form, information sheet, brochure, and/or letter, script for verbal consent (when applicable).

[ ] Recruitment materials, e.g., flyers, advertisements, telephone script, letters, etc.

* **Note: Minimal risk** means that the probability and magnitude of harm or discomfort anticipated in the research are not greater in and of themselves than those ordinarily encountered in daily life or during the performance of routine physical or psychological examinations or tests.

Pennsylvania College of Optometry
8360 Old York Road Elkins Park, PA 19027-1598

General Information
(215) 780-1400

INSTITUTIONAL ANIMAL CARE AND USE COMMITTEE

CERTIFICATE OF APPROVAL FOR A PROJECT INVOLVING ANIMALS

June 4, 2007

Melissa Trego, OD
Pennsylvania College of Optometry
8360 Old York Road
Elkins Park, PA 19027

Dear Dr. Trego:

The Institutional Animal Care and Use Committee (IACUC) has reviewed the involvement of animals in your proposed study entitled:

Alpha-Crystallin Proteins as Potential Protectors Against Continuous Blue Light Exposure
A-MT0705

I am pleased to inform you that this study was approved on May 31, 2007.

This approval expires on May 31, 2010 unless suspended or terminated earlier by action of the IACUC. Please be reminded that you are required to submit the form, *Request for Continuing Review* to the Research Office at least month before the anniversary of this approval. At the conclusion of this project, or one month prior to the expiration of the approval, please complete and submit the form, *Termination of Research.*

Any proposed change in the protocol must be submitted to the IACUC for review and approval before the proposed change can be implemented. Please complete the form *Request for Approval of Changes* to protocol for this purpose.

Sincerely,

Pierrette Dayhaw-Barker Ph.D.

Pierrette Dayhaw-Barker, PhD
Acting Chairperson, IACUC

Shaping the Future of Vision Care

Pennsylvania College of Optometry
8360 Old York Road Elkins Park, PA 19027-1598

INSTITUTIONAL ANIMAL CARE AND USE COMMITTEE CERTIFICATE OF APPROVAL FOR A PROJECT INVOLVING ANIMALS

July 31, 2007

Melissa Trego, PhD
Pennsylvania College of Optometry
8360 Old York Road
Elkins Park, PA 19027

Dear Dr.Trego:

The Institutional Animal Care and Use Committee (IACUC) has reviewed the protocol change involving animals in your proposed study entitled:

Alpha Crystallins Proteins as Potential Protectors Against Continuous Blue Light Exposure
A-MT0705

I am pleased to inform you that the following protocol change to this study were approved on July 31, 2007:

- Addition of Michael Coulton as a technician.
- Revised anesthetic dose to be used for the ERG procedure.
- Addition of methylcellulose-containing eye drops during ERG procedure

This approval expires on May 31, 2010 unless suspended or terminated earlier by action of the IACUC. Please be reminded that you are required to submit the form, *Request for Continuing Annual Review* to the Research Office at least one month before the anniversary of this approval. At the conclusion of this project, or one month prior to the expiration of the approval, please complete and submit the form, *Termination of Research*.

Any proposed change in the protocol must be submitted to the IACUC for review and approval before the proposed change can be implemented. Please complete the form *Request for Approval of Changes to Protocol* for this purpose.

Sincerely,

Pierrette Dayhaw-Barker Ph.D

Pierrette Dayhaw-Barker, PhD
Acting Chairperson, IACUC

Shaping the Future of Vision Care

Pennsylvania College of Optometry
8360 Old York Road Elkins Park, PA 19027-1598

INSTITUTIONAL ANIMAL CARE AND USE COMMITTEE CERTIFICATE OF APPROVAL FOR A PROJECT INVOLVING ANIMALS

August 9, 2007

Melissa Trego, OD
Pennsylvania College of Optometry
8360 Old York Road
Elkins Park, PA 19027

Dear Dr. Trego:

The Institutional Animal Care and Use Committee (IACUC) has reviewed the addition of personnel who will work with animals in your proposed study entitled:

Alpha-Crystallin Proteins as Potential Protectors Against Continuous Blue Light Exposure
A-MT0705

I am pleased to inform you that the addition of Tressa Larson as a technician to this study was approved on 08/09/07. James Wood, CCMC, provided Facility Orientation and Species-Specific Training for Mice on 08/09/07.

This approval expires on May 31, 2010 unless suspended or terminated earlier by action of the IACUC. Please be reminded that you are required to submit the form, *Request for Continuing Annual Review* to the Research Office at least one month before the anniversary of this approval. At the conclusion of this project, or one month prior to the expiration of the approval, please complete and submit the form, *Termination of Research*.

Any proposed change in the protocol must be submitted to the IACUC for review and approval before the proposed change can be implemented. Please complete the form *Request for Approval of Changes to Protocol* for this purpose.

Sincerely,

Pierrette Dayhaw-Barker, Ph.D

Pierr
Actin Pierrette Dayhaw-Barker, PhD

Shaping the Future of Vision Care

Pennsylvania College of Optometry
8360 Old York Road Elkins Park, PA 19027-1598

INSTITUTIONAL ANIMAL CARE AND USE COMMITTEE CERTIFICATE OF APPROVAL FOR A PROJECT INVOLVING ANIMALS

September 7, 2007

Melissa Trego, OD
Pennsylvania College of Optometry
8360 Old York Road
Elkins Park, PA 19027

Dear Dr. Trego:

The Institutional Animal Care and Use Committee (IACUC) has reviewed the involvement of animals in your proposed study entitled:

Alpha-Crystallin Proteins as Potential Protectors Against Continuous Blue Light Exposure
A-MT0705

I am pleased to inform you that the following protocol changes to this study were approved on September 7, 2007:

- Addition of another strain of mice (Balb/cByJ)
- Addition of a control group that will NOT be exposed to blue light, but will undergo ERGs at day 0 and day 10 post blue-light exposure.

This approval expires on May 31, 2010 unless suspended or terminated earlier by action of the IACUC. Please be reminded that you are required to submit the form, *Request for Continuing Annual Review* to the Research Office at least one month before the anniversary of this approval. At the conclusion of this project, or one month prior to the expiration of the approval, please complete and submit the form, *Termination of Research*.

Any proposed change in the protocol must be submitted to the IACUC for review and approval before the proposed change can be implemented. Please complete the form *Request for Approval of Changes to Protocol* for this purpose.

Sincerely,

Pierrette Dayhaw-Barker, PhD
Acting Chairperson, IACUC

Shaping the Future of Vision Care

Pennsylvania College of Optometry
8360 Old York Road Elkins Park, PA 19027-1598

General Information
(215) 780-1400
www.pco.edu

INSTITUTIONAL ANIMAL CARE AND USE COMMITTEE

CERTIFICATE OF APPROVAL FOR A PROJECT INVOLVING ANIMALS

March 5, 2008

Melissa Trego, OD
Pennsylvania College of Optometry
8360 Old York Road
Elkins Park, PA 19027

Dear Dr. Trego:

The Institutional Animal Care and Use Committee (IACUC) has reviewed the *Request for Continuing Annual Review of Research Involving Laboratory Animals involvement of Animals* for the study:

Alpha Crystallins and Retinal Protection against
Light Damage and Oxidative Stress
A-MT0603-02

I am pleased to inform you that re-approval of this study was granted on March 5, 2008.

This approval expires on March 16, 2009 unless suspended or terminated earlier by action of the IACUC. Please be reminded that you are required to submit the form, *Request for Continuing Review* to the Research Office at least month before the anniversary of this approval. At the conclusion of this project, or one month prior to the expiration of the approval, please complete and submit the form, *Termination of Research*.

Any proposed change in the protocol must be submitted to the IACUC for review and approval before the proposed change can be implemented. Please complete the form *Request for Approval of Changes* to protocol for this purpose.

Sincerely,

Pierrette Dayhaw-Barker, PhD
Acting Chairperson, IACUC

Shaping the Future of Vision Care

Pennsylvania College of Optometry
8360 Old York Road Elkins Park, PA 19027-1598

General Information
(215) 780-1400
www.pco.edu

INSTITUTIONAL ANIMAL CARE AND USE COMMITTEE

CERTIFICATE OF APPROVAL FOR A PROJECT INVOLVING ANIMALS

May 21, 2008

Melissa Trego, OD
Pennsylvania College of Optometry
8360 Old York Road
Elkins Park, PA 19027

Dear Dr. Trego

The Institutional Animal Care and Use Committee (IACUC) has reviewed the *Request for Continuing Annual Review of Research Involving Laboratory Animals involvement of Animals* for the study:

Alpha-Crystallin Proteins as Potential Protectors Against Continuous Blue Light Exposure
A-MT0705-01

I am pleased to inform you that re-approval of this study was granted on May 12, 2008.

This approval expires on May 31, 2010 unless suspended or terminated earlier by action of the IACUC. Please be reminded that you are required to submit the form, *Request for Continuing Review* to the Research Office at least month before the anniversary of this approval. At the conclusion of this project, or one month prior to the expiration of the approval, please complete and submit the form, *Termination of Research*.

Any proposed change in the protocol must be submitted to the IACUC for review and approval before the proposed change can be implemented. Please complete the form *Request for Approval of Changes* to protocol for this purpose.

Sincerely,

Pierrette Dayhaw-Barker, PhD
Acting Chairperson, IACUC

Shaping the Future of Vision Care

Pennsylvania College of Optometry
8360 Old York Road Elkins Park, PA 19027-1598

General Information
(215) 780-1400
www.pco.edu

INSTITUTIONAL ANIMAL CARE AND USE COMMITTEE

CERTIFICATE OF APPROVAL FOR A PROJECT INVOLVING ANIMALS

May 30, 2008

Melissa Trego, OD
Pennsylvania College of Optometry
8360 Old York Road
Elkins Park, PA 19027

Dear Dr. Trego

The Institutional Animal Care and Use Committee (IACUC) has reviewed the involvement of animals in your proposed study entitled:

Establish and Maintain a Breeding Colony for the 129Sv: CryA1 gene line
A-MT0505-03

I am pleased to inform you that this study was approved on May 21, 2008.

This approval expires on May 21, 2011 unless suspended or terminated earlier by action of the IACUC. Please be reminded that you are required to submit the form, *Request for Continuing Review* to the Research Office at least month before the anniversary of this approval. At the conclusion of this project, or one month prior to the expiration of the approval, please complete and submit the form, *Termination of Research*.

Any proposed change in the protocol must be submitted to the IACUC for review and approval before the proposed change can be implemented. Please complete the form *Request for Approval of Changes* to protocol for this purpose.

Sincerely,

Pierrette Dayhaw-Barker

Pierrette Dayhaw-Barker, PhD
Acting Chairperson, IACUC

Shaping the Future of Vision Care

Appendix 2

Table 1. Summary Statistics for Outcome Measures for WT and αA-K/O Mice:

A-frequency AMPLITUDE										
Type	Time	N Obs	N	Mean	Std Dev	Minimum	Lower Quartile	Median	Upper Quartile	Maximum
KO	Pre	21	21	129.71	35.57	83.00	101.00	128.00	161.00	204.00
	After	21	21	96.38	31.49	60.50	68.00	92.00	118.00	172.50
	Post	21	21	59.86	22.95	25.00	44.00	53.00	73.50	110.50
WT	Pre	21	21	144.62	37.94	86.00	118.00	142.50	161.00	226.00
	After	21	21	103.02	33.04	32.50	82.00	99.50	118.00	168.50
	Post	21	21	96.52	40.25	29.00	63.00	95.00	134.00	179.00

B-frequency AMPLITUDE										
Type	Time	N Obs	N	Mean	Std Dev	Minimum	Lower Quartile	Median	Upper Quartile	Maximum
KO	Pre	21	21	265.93	87.77	160.00	191.50	248.50	346.50	407.00
	After	21	21	176.40	61.66	109.00	121.50	158.50	211.00	296.50
	Post	21	21	126.64	35.46	78.50	101.50	119.00	158.00	199.00
WT	Pre	21	21	298.29	101.57	155.00	199.00	298.50	367.00	453.50
	After	21	21	179.36	60.37	63.00	144.00	178.00	211.50	285.50
	Post	21	21	153.98	59.52	54.00	125.00	147.00	201.50	265.50

A-frequency latency										
Type	Time	N Obs	N	Mean	Std Dev	Minimum	Lower Quartile	Median	Upper Quartile	Maximum
KO	Pre	21	21	22.98	3.74	14.00	21.00	23.00	25.00	29.50
	After	21	21	22.62	4.70	13.00	19.50	23.00	26.50	29.50
	Post	21	21	21.24	2.65	15.50	20.00	21.00	22.50	26.00
WT	Pre	21	21	22.02	3.24	16.00	20.00	22.00	24.00	29.00
	After	21	21	23.52	4.06	16.50	20.50	23.50	25.50	31.50
	Post	21	21	23.12	5.50	14.50	19.50	24.00	26.00	33.50

B-frequency latency										
Type	Time	N Obs	N	Mean	Std Dev	Minimum	Lower Quartile	Median	Upper Quartile	Maximum
KO	Pre	21	21	116.26	18.26	87.50	100.00	117.50	129.00	157.50
	After	21	21	112.95	16.16	82.50	105.00	110.00	122.50	147.50
	Post	21	21	114.43	19.77	82.50	100.00	107.50	134.00	147.50
WT	Pre	21	21	111.21	13.31	92.50	100.00	112.50	120.00	140.00
	After	21	21	107.19	18.99	70.00	97.50	105.00	122.50	135.00
	Post	21	21	105.88	12.52	77.50	100.00	107.50	115.00	120.00

Table 2. Normality Statistics for Outcome Measures WT and K/O Combined

Time	the normality test statistic, Aamp	the normality test statistic, Alatency	the normality test statistic, Bamp	the normality test statistic, Blatency
Pre	0.95284	0.98718	0.91567	0.96608
After	0.96202	0.98704	0.95675	0.98729
Post	0.91854	0.96722	0.97009	0.97648

As is indicated above, the normality statistics are well-above 0.90, indicating near normality of our outcome measures.

Histograms Over Time

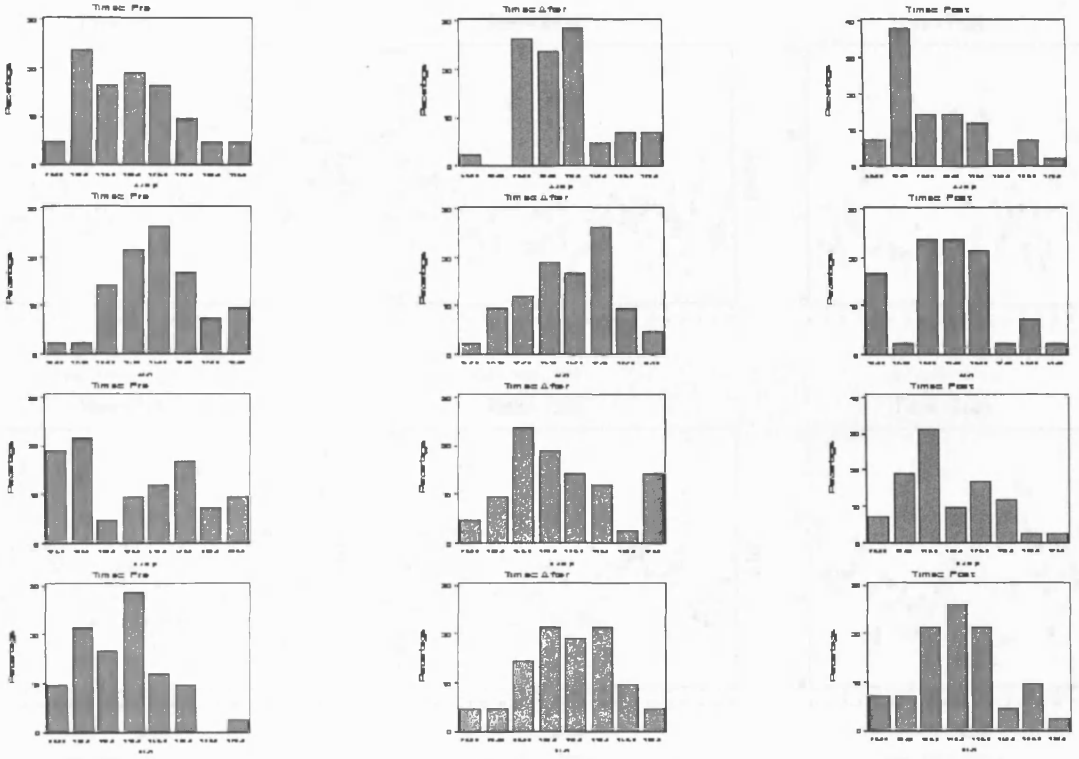

As indicated above it appears we have near normality in our outcome measures at each timepoint with possibly the exception of the B-amplitude at baseline, but overall there does not appear to be any substantial deviation from near normality. (***Columns shown from left to right are pre, immediate and post-exposure, respectively; rows going from top to bottom are a-wave, a-latency, b-wave, b-latency)***

Assessing the Reproducibility of the Left and Right Eye Measures:

Below shows the two measures per mice over the three repeated measures on the four outcomes of interest. Blue are the right side measures and the red are the left side measures. Proximity of the red and blue marks within mice shows the reproducibility of the measures on the two sides.

Reproducibility over Time pt 1

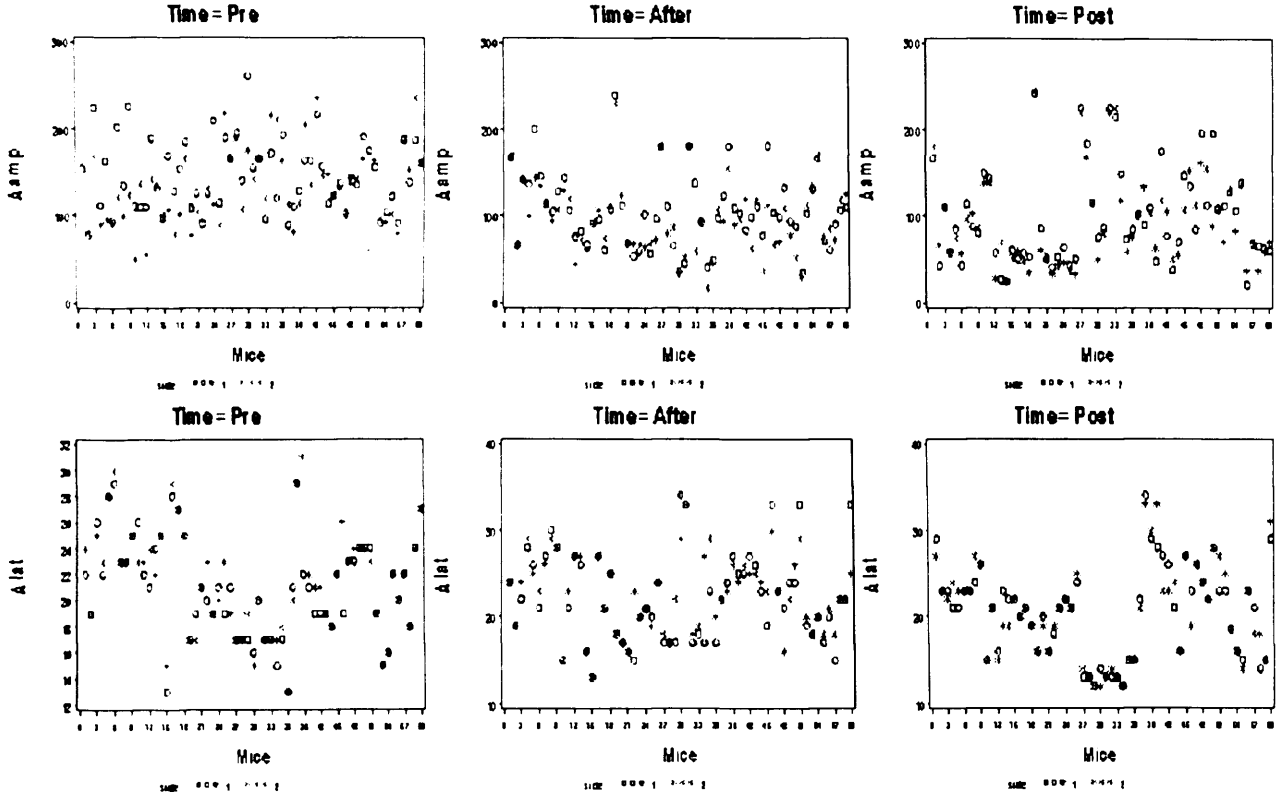

Reproducibility over Time pt2

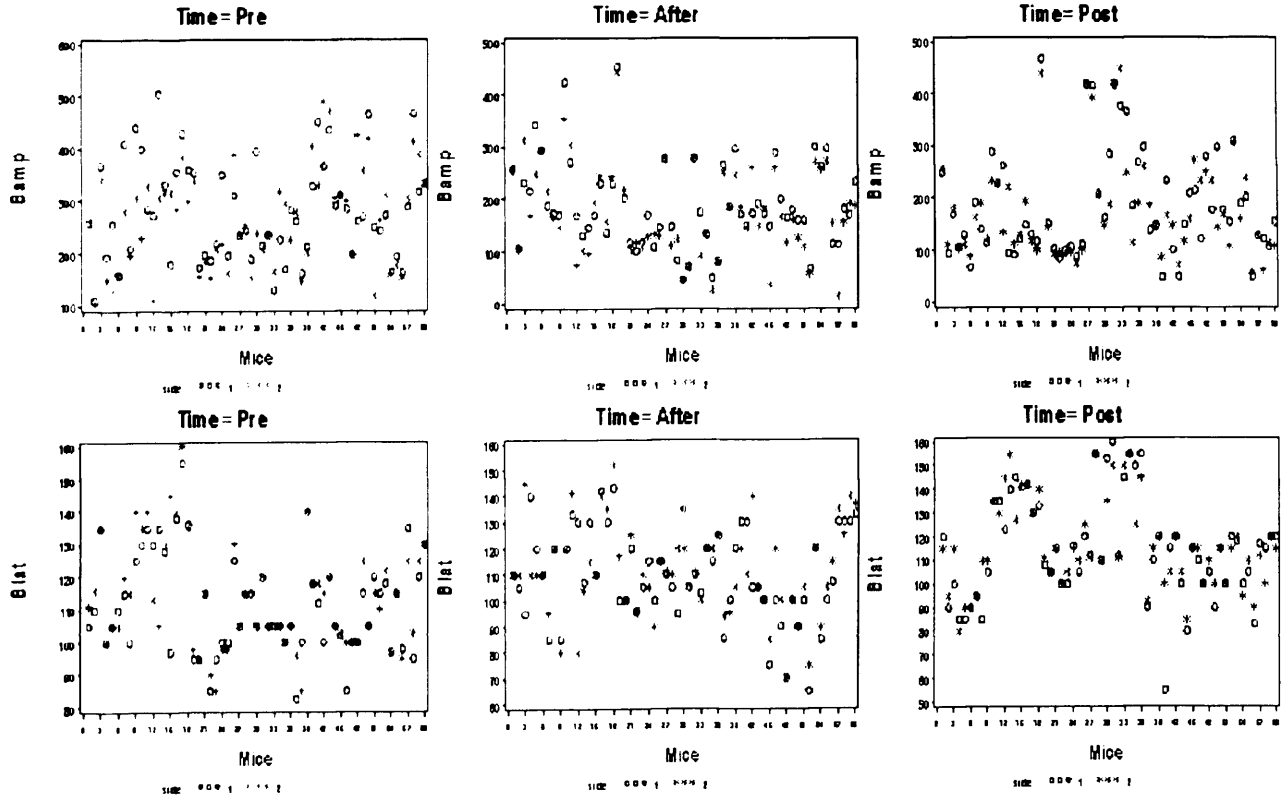

Intra-class correlation coefficient (ICC) takes on values between 0 and l and is near 1 when difference between pairs is small compared to the differences between mice. Ranges or ICC usually fall into these rule of thumb breakdowns:

- Poor agreement = Less than 0.20
- Fair agreement = 0.20 to 0.40
- Moderate agreement = 0.40 to 0.60
- Good agreement = 0.60 to 0.80
- Very good agreement = 0.80 to 1.00

Table 1. Intraclass correlation coefficient for the Pre Measures:

ITEM	ICC	RHO	VARID	VARE	Lower Bound	Upper Bound
Aamp	0.55696	0.55696	1044.38	830.77	0.35587	0.70904
Alat	0.88254	0.88254	13.84	1.84	0.81131	0.92802
Bamp	0.66899	0.66899	6106.18	3021.22	0.50250	0.78786
Blat	0.81064	0.81064	198.85	46.45	0.70270	0.88222

Table 2. Intraclass correlation coefficient for the At Exposure Measures:

ITEM	ICC	RHO	VARID	VARE	Lower Bound	Upper Bound
Aamp	0.84132	0.84132	1514.30	285.608	0.74844	0.90194
Alat	0.83870	0.83870	19.06	3.667	0.74449	0.90026
Bamp	0.88297	0.88297	6440.11	853.580	0.81198	0.92830
Blat	0.70653	0.70653	221.91	92.177	0.55387	0.81342

Table 3. Intraclass correlation coefficient for the Post Measures:

ITEM	ICC	RHO	VARID	VARE	Lower Bound	Upper Bound
Aamp	0.89762	0.89762	2632.05	300.19	0.83474	0.93746
Alat	0.94289	0.94289	26.14	1.58	0.90644	0.96543
Bamp	0.86759	0.86759	8448.08	1289.34	0.78832	0.91861
Blat	0.87747	0.87747	364.38	50.88	0.80349	0.92484

Appendix 3

Ear Tag	Trial #1	Ear Tag	Trial #2
N629	Day 0 - Immediate	N623	Day 1 - 10d Post
N628	Day 1 - Immediate	N621	Day 3 - 10d Post
N626	Day 3 - Immediate	N619	Day 5 - 10d Post
N625	Day 5 - Immediate	N617	Day 7 - 10d Post
N624	Day 7 - Immediate	No ET	Day 0 - 10d Post
N622	Day 1 - 10d Post		
N620	Day 3 - 10d Post		
N618	Day 5 - 10d Post		
N616	Day 7 - 10d Post		

A3.1 Ear tag key for both trials BALB/cBYJ mice.

Ear Tag	Trial #1	Ear Tag	Trial #2	Ear Tag	Trial #3
N131	Day 1 – Immediate	N146	Day 1 - Immediate	N149	Day 1 - Immediate
N819	Day 2 – Immediate	N145	Day 2 - Immediate	N151	Day 2 - Immediate
N127	Day 3 – Immediate	N142	Day 3 - Immediate	N162	Day 3 - Immediate
N817	Day 4 – Immediate	N148	Day 4 - Immediate	N155	Day 4 - Immediate
N125	Day 5 – Immediate	N821	Day 5 - Immediate	N157	Day 5 - Immediate
N816	Day 6 – Immediate	N135	Day 6 - Immediate	N159	Day 6 - Immediate
N123	Day 7 – Immediate	N132	Day 7 - Immediate	N163	Day 7 - Immediate
N130	Day 1 - 10d Post	N147	Day 1 - 10d Post	N150	Day 1 - 10d Post
N818	Day 2 - 10d Post	N144	Day 2 - 10d Post	N152	Day 2 - 10d Post
N122	Day 3 - 10d Post	N143	Day 3 - 10d Post	N154	Day 3 - 10d Post
N121	Day 4 - 10d Post	N823	Day 4 - 10d Post	N156	Day 4 - 10d Post
N120	Day 5 - 10d Post	N822	Day 5 - 10d Post	N158	Day 5 - 10d Post
N118	Day 6 - 10d Post	N820	Day 6 - 10d Post	N164	Day 6 - 10d Post
N117	Day 7 - 10d Post	N133	Day 7 - 10d Post	N867	Day 7 - 10d Post
No ET	Day 0 – Ctrl	N824	Day 0 - Ctrl	N866	Day 0 - Ctrl

Ear Tag	Trial #4
N172	Day 1 - 10d Post
N171	Day 2 - 10d Post
N170	Day 3 - 10d Post
N169	Day 4 - 10d Post
N168	Day 5 - 10d Post
N167	Day 6 - 10d Post
N166	Day 7 - 10d Post
N173	Day 0 - Ctrl

A3.2 Ear tag key for all trials of Wild-Type mice.

Ear Tag	Trial #1	Ear Tag	Trial #2	Ear Tag	Trial #3
N517	Day 1 - Immediate	N554	Day 1 – Immediate	N579	Day 1 - Immediate
N520	Day 2 - Immediate	N552	Day 2 – Immediate	N577	Day 2 - Immediate
N522	Day 3 - Immediate	N550	Day 3 – Immediate	N575	Day 3 - Immediate
N524	Day 4 - Immediate	N548	Day 4 – Immediate	N573	Day 4 - Immediate
N526	Day 5 - Immediate	N546	Day 5 – Immediate	N571	Day 5 - Immediate
N516	Day 6 - Immediate	N544	Day 6 – Immediate	N569	Day 6 - Immediate
N530	Day 7 - Immediate	N542	Day 7 – Immediate	N567	Day 7 - Immediate
N518	Day 1 - 10d Post	N553	Day 1 - 10d Post	N578	Day 1 - 10d Post
N521	Day 2 - 10d Post	N551	Day 2 - 10d Post	N576	Day 2 - 10d Post
N523	Day 3 - 10d Post	N549	Day 3 - 10d Post	N574	Day 3 - 10d Post
N525	Day 4 - 10d Post	N547	Day 4 - 10d Post	N572	Day 4 - 10d Post
N528	Day 5 - 10d Post	N545	Day 5 - 10d Post	N570	Day 5 - 10d Post
N529	Day 6 - 10d Post	N543	Day 6 - 10d Post	N568	Day 6 - 10d Post
N531	Day 7 - 10d Post	N541	Day 7 - 10d Post	N566	Day 7 - 10d Post
No ET	K/O Ctrl; Day 0	N555	K/O Ctrl; Day 0	DEAD	K/O Ctrl; Day 0
No ET	W/T Ctrl; Day 0	N556	W/T Ctrl; Day 0	N580	W/T Ctrl; Day 0

A3.3 Ear tag key for all trials of αA-crystallin Knock-out mice.

Parameters	Values/Yes/No	*Comments/Problems*
Maximum Temperature/Humidity (Time)		
Minimum Temperature/Humidity		
Average Temperature/Humidity		
Signs/symptoms of pain or distress		
Anterior segment abnormalities		
Food/H2O		
Emptied A/C H2O bucket		
Reset temperature monitor (Time)		
Rotate Cages		
Total number of mice		
Number of cages		

A3.4 Standard check-off sheet for exposed mice (filled out twice a day).